Genetic and molecular analysis of *Solanum* disease resistance genes

Robert Peter James Heal

The Sainsbury Laboratory, Norwich

March 2024

This thesis has been submitted to the University of East Anglia
for the degree of Doctor of Philosophy

Abstract

Plants encode intracellular nucleotide-binding leucine-rich repeat (NLR) receptors which recognise pathogen effectors and trigger an immune response. In this thesis, NLR-mediated immunity is investigated in several contexts, namely, resistance to phloem-limited pathogens, non-host resistance, and the ability of the same NLRs to recognise multiple pathogens.

In Chapter 3, a resistance gene against potato leafroll virus (PLRV) was cloned. This gene, *Rl$_{adg}$*, encodes a Bs4-like TIR-NLR that recognises a serine protease which is essential for viral replication. Rl$_{adg}$ is the first NLR that has been found to confer resistance to a phloem-limited pathogen. PLRV belongs to the *Polerovirus* genus, which contains many economically important viruses that cause significant yield losses in various crop species. We found that Rl$_{adg}$ is capable of broad-spectrum recognition of poleroviruses and explored its potential to elevate resistance to these viruses.

In Chapter 4, the basis of non-host resistance to *Phytophthora infestans* in the wild potato relative *Solanum americanum* was explored. *S. americanum* is the source of two late blight resistance genes, *Rpi-amr1* and *Rpi-amr3*, that confer strong resistance against multiple *P. infestans* isolates. Here, *Rpi-amr5*, a paralogue of *Rpi-amr1*, was also found to confer resistance to *P. infestans*. Interestingly, in another accession, we identified an *Rpi-amr5* allele (named *Rpc2*) which also confers strong resistance to *Phytophthora capsici*, which infects tomato and pepper. Two *P. infestans* effectors and three *P. capsici* effectors are recognised by both NLRs. It is currently unclear why *Rpi-amr5* does not confer resistance to *P. capsici*. In Chapter 5, we characterized several other resistance genes to *P. capsici*. While they remain uncloned, there is potential for identifying additional *Rpc* genes and making *Rpc*-gene stacks to reduce the economic impact of *P. capsici*.

Table of contents

List of tables

List of Figures

List of appendices

List of abbreviations

ADR1 (activated disease resistance 1)

ANIP1 (AvrPi9-interacting protein 1)

APAF1 (apoptotic protease-activating factor 1)

ATR1/2/5 (*Arabidopsis thaliana* recognised 1/2/5)

Avr-gene (avirulence gene)

BAK1 (BRI1-associated receptor kinase 1)

BMYV (beet mild yellowing virus)

BRI1 (brassinosteroid insensitive 1)

BSL (BRI1-suppressor-like)

CaBYV (cucurbit aphid-borne yellows virus)

CaMV (cauliflower mosaic virus)

CAR1 (CEL-activated resistance 1)

CARD (caspase activation and recruitment domain)

Cas9 (CRISPR associated protein 9)

CAZymes (carbohydrate-active enzymes)

CC (coiled-coil)

CC-NLR (coiled-coil NLR)

CCR1 (*Cochliobolus carbonum* race 1)

CED-4 (cell death protein 4)

CER (controlled environment room)

CLRDV (cotton leafroll dwarf virus)

CoIP (co-immunoprecipitation assay)

CP (coat protein)

CpCSV (chickpea chlorotic stunt virus)

CRISPR (clustered regularly interspaced short palindromic repeats)

CTD (C-terminal domain)

CVEV (citrus vein enation virus)

DBD (DNA-binding domain)

Diglig (digestion and ligation)

dpi (days post-infiltration)

EDS1 (enhanced disease susceptibility 1)

EF1α (elongation factor 1α)

ELR (elicitin response)

ETI (effector-triggered immunity)

ETS (effector-triggered susceptibility)

GEV-1 (grapevine enamovirus-1)

HMA (heavy metal-associated)

Hpa (*Hyaloperonospora arabidopsidis)*

HR (hypersensitive response)

IP (immunoprecipitation)

LB (lysogeny broth)

LDDT (local distance difference test)

LRR (leucine-rich repeat)

MAPK (mitogen activated protein kinases)

MAX (*Magnaporthe* Avrs and ToxB-like)

MEP1 (*Magnaporthe* effector protein 1)

MLA3 (mildew locus a 3)

mlo (mildew locus o)

MS (Murashige and Skoog)

MYDV (maize yellow dwarf virus)

NAD (nicotinamide adenine dinucleotide)

NADPH (nicotinamide adenine dinucleotide phosphate)

NB (nucleotide binding)

NHR (non-host resistance)

NLR (nucleotide-binding leucine-rich repeat)

NLR-ID (NLR integrated-domain)

Nos (nopaline synthase)

NRC (NLR required for cell death)

NRG1 (N requirement gene 1)

NTD (N-terminal domain)

Ocs (octopine synthase)

OD (optical density)

PAD4 (phytoalexin deficient 4)

PAGE (polyacrylamide gel electrophoresis)

PAM (protospacer-adjacent motif)

PAMP (pathogen associated molecular patterns)

PBL (PBS1-like)

PCN (potato cyst nematode)

PEMV-1 (pea enation mosaic virus-1)

PEN (penetration-gene)

PERU (Pep-13 receptor unit)

PeVYV (pepper vein yellows virus)

PIBP1 (PigmR-interacting and blast resistance protein 1)

PICI1 (PigmR-interacting and chitin-induced protein 1)

PLRV (potato leafroll virus)

PopMV (poplar mosaic virus)

PPV (plum pox virus)

PRR (pattern-recognition receptors)

PTI (PAMP-triggered immunity)

PVX (potato virus X)

PVY (potato virus Y)

Pwl2 (pathogenicity toward weeping lovegrass 2)

R-gene (resistance-gene)

REL (responsive to elicitins)

RenSeq (resistance gene enrichment sequencing)

RGA4 (R-gene analog 4)

RGA5 (R-gene analog 5)

RIN4 (RPM1 interacting protein 4)

RLK (receptor-like kinase)

RLM3 (resistance to *Leptosphaeria maculans* 3)

RLP (receptor-like protein)

ROQ1 (recognition of XOPQ 1)

ROS (reactive oxygen species)

Rpc- (Resistance to *Phytophthora capsici*)

Rpi- (Resistance to *Phytophthora infestans*)

RPM1 (resistance to *Pseudomonas syringae pv maculicola* 1)

RPO1 (resistance to poleroviruses 1)

RPP1/2/5/8 (resistance to *Peronospora parasitica* 1/2/5/8)

RPS2/4/5 (resistance to *Pseudomonas syringae* 2/4/5)

RPW8-NLR (Resistance to powdery mildew 8 NLR)

RRS1-R (resistance to *Ralstonia solanacearum* 1)

RSA (rye-sucrose agar)

RTF (restricted taxonomic functionality)

SAG101 (senescence-associated gene 101)

SDS (sodium dodecyl sulphate)

SeMV (sesbania mosaic virus)

SERKs (somatic embryogenesis receptor-like kinases)

SNC1 (suppressor of NPR1-1 constitutive 1)

SOBIR-1 (suppressor of bir1-1)

SS15 (sprysec15)

TAL (Transcription activator-like)

TIR (toll, interleukin-1 receptor domain)

TIR-NLR (toll, interleukin-1 receptor NLR)

TMV (tobacco mosaic virus)

TRV (tobacco rattle virus)

TuMV (turnip mosaic virus)

TuYV (turnip yellows virus)

TV2 (tobacco virus 2)

v/v (volume/volume)

VIGS (virus-induced gene silencing)

Vpg (viral protein genome-linked)

w/v (weight/volume)

WRR (white-rust resistance)

WT (wild-type)

WYDV (wheat yellow dwarf virus)

ZAR1 (hopz-activated resistance 1)

ZRK (zed1-related kinases)

Acknowledgements

I express my sincere gratitude to Professor Jonathan Jones for providing the opportunity to study in his group. I appreciate all your guidance, advice, and opportunities. I have learnt a lot over the last five years and I feel that I have developed greatly during this period thanks to your mentorship.

Thank you to my supervisory team members Dr. Sanu Arora, Dr. Matthew Moscou, Dr. Kamil Witek and Dr. Xiao Lin for their guidance and support. I'd also like to thank Dr. Sebastian Fairhead who was fantastic to discuss science, politics, and many other topics with, he is sadly missed.

Thank you to all the Jones lab members for their support and feedback. I would like to thank Agnieszka Witek, Agnieszka Alexander, Hee-Kyung Ahn, and Maheen Alam for their wonderful friendship, advice, and expertise.

I would also like to thank the past and current PhD students in the JJ lab: Joanna Feehan, Bruno Ngou, Lila Grandgeorge, Sophie Johnson, Camille-Madeleine Szymansky, and Yordan Dolaptchiev for sharing fantastic discussions and providing a great environment to work in. I have had the pleasure to work with many interns and students who contributed to the data presented in this thesis. Thank you to Jesus Sanchez Pardo-Echevarria, Maria López Martin, Andrea Carolina Olave Achury, Fatma Yuksel, and Li Long. I would especially like to thank Maria Sindalovskaya for her incredible support and for providing feedback on this thesis.

Thank you to the TSL community and especially the support teams. In particular: Matthew Smoker, Jodie Foster, and Aleksandra Wawryk-Khamdavong, who have provided invaluable tissue culture and transformation support. Also, Sarah Perkins, Justine Smith, Timothy Wells, and Matt Castle, who have grown thousands of plants for me.

I would also like to thank Dr Colwyn Thomas, for introducing me to plant science, and providing fantastic support and advice over the last eight years. Also thank you to Dr. Jacob Malone and Dr. Richard Little who gave me my first opportunities to experience research.

Finally, I would like to thank all my family without whom none of this would be possible.

Chapter 1: General introduction

1.1 – Molecular plant microbe interactions

1.1.1 – Tackling biotic stresses in agriculture

In 2050, the global population is expected to reach 9 billion. As of 2020, 9.3% of the global population is undernourished and the rate of childhood stunting is at 22% (World Health Organization, 2022). To improve the nutrition of the current population and meet the needs of future population food production must be increased. To enhance food production, various factors could be addressed including biotic and abiotic stresses, poor farming practices and conflicts.

Plant pathogens contribute to large yield losses in many crops, with estimates of losses in potato, maize, soybean, wheat and rice ranging from 17% to 30% (Savary et al., 2019). Plant pathogens can also lead to severe social consequences. The most infamous example is the Irish potato famine in the 1840s, which was in part caused by the potato late blight pathogen, *Phytophthora infestans.* This famine led to the death of 750,000 people and the displacement of one million people (Zadoks, 2008). The emergence of pandemic plant pathogens is more likely with a developing global plant trade, the use of genetically homogenous monocultures, and climate change which will alter the dynamics of overwintering and spread of insect vectors (Bebber et al., 2013, Brasier, 2008, Jones, 2021).

The challenge of mitigating the impact of plant pathogens can, in part, be tackled using crop improvement including genetics. By understanding plant-pathogen interactions, crops can be modified and engineered to elevate innate immunity and ensure this has longevity and durability.

1.1.2 – A general model for molecular plant pathogen interactions

Plant pathogens encompass a diverse range of organisms including viruses, fungi, oomycetes, bacteria, insects, and nematodes. Plant immunity is non-adaptive and dependent on perception of pathogens. Unlike mammals, plants lack mobile immune cells; each cell must be capable of recognising pathogens and activating an immune response (Jones and Dangl, 2006, Ngou et al., 2022a).

The canonical model of the plant immune system was proposed by Jones and Dangl (2006). In this 'zig-zag-zig' model plants activate PAMP-triggered immunity (PTI) upon detection of apoplastic pathogen-associated molecular patterns (PAMPs) by pattern-recognition receptors (PRRs). Cell surface-bound PRRs include the receptor like-proteins (RLPs) and receptor-like kinases (RLKs). PTI is a robust defence system which involves activation of NADPH oxidases, calcium channels, and mitogen activated protein kinases (MAPKs). Action of these proteins causes calcium influx, ROS (reactive oxygen species) burst, callose deposition and stomatal closure. These PTI-derived cellular changes result in a hostile environment which restricts pathogen growth. To enable colonisation, pathogens suppress PTI using effector proteins secreted into the host apoplast and cytoplasm. This is known as effector-triggered susceptibility (ETS). In turn, plants have evolved receptors to recognise pathogen effectors and activate effector-triggered immunity (ETI). ETI activation often results in programmed cell death known as a hypersensitive response (HR) (Jones and Dangl, 2006, Ngou et al., 2022a).

Since the zig-zag-zig model was conceptualised, PTI and ETI have been treated as two distinct layers of immunity rather than two layers of perception. However, this model has been re-evaluated and crosstalk and mutual potentiation of ETI and PTI has been demonstrated. To produce a complete immune response, activation of both intracellular and cell-surface immune receptors is required. Activation of intracellular receptors potentiate the cell surface receptor responses and the HR induced by ETI is enhanced by detection at the cell surface (Ngou et al., 2021, Yuan et al., 2021). Supporting the link between PTI and ETI, it has recently been demonstrated that the helper NLR NRG1 (discussed in 1.1.4 and 1.1.6) requires cell-surface signalling for activation (Feehan et al., 2023).

1.1.3 – Plant *Resistance*-genes (*R*-genes) often encode intracellular immune receptors

It has long been known that strong plant disease resistance can be simply inherited as a monogenic trait. Using flax and the rust fungus *Melampsora lini*, Flor (1942) demonstrated a gene-for-gene model of disease resistance where for each host *Resistance* gene (*R*-gene), there is a corresponding pathogen *Avirulence* (*Avr*) gene. In his study, both *R*-gene and *Avr*-gene were shown to be semidominant.

Numerous *R*-genes have been cloned, many of which encode NLR (nucleotide-binding, leucine-rich repeat) proteins. Plant NLRs can be classified into three groups according to their N-terminal domain; 'Toll, interleukin-1 receptor' (TIR-NLR), 'Coiled-coil' (CC-NLR) or 'Resistance to powdery mildew 8' (RPW8-NLR). NLRs within all three groups possess a central NB-ARC domain and a C-terminal LRR domain (Ngou et al., 2022a). These domains have canonical functions, which are adhered to by most, but not all, NLRs. The leucine-rich repeat (LRR) domain contains repeats of an LxxLxL motif and generally serves as the site of pathogen recognition. LRRs also have a role in negative regulation of NLR immunity: intramolecular interactions hold the receptor in a closed, inactive state, while effector binding causes a conformational change which relaxes this regulation and activates the NLR via the NB-ARC domain (Faustin et al., 2007, Takken et al., 2006). The central NB-ARC domain, is a nucleotide-binding (NB) domain with homology to human APAF1 (APOPTOTIC PROTEASE-ACTIVATING FACTOR 1) and *Caenorhabditis elegans* CED-4 (CELL DEATH PROTEIN 4) (van der Biezen and Jones, 1998). The NB-ARC domain facilitates oligomerization through ATPase activity by exchanging ADP for ATP (Tameling et al., 2006). Together with the N-terminal domain, NB-ARC-driven oligomerization can produce a resistosome structure. The N-terminal CC or TIR domains function as signalling or 'executer' domains. In general, the N-terminal domain correlates with the phylogenetic group in which an NLR is found, TIR-NLR, RPW8-NLR and CC-NLR form distinct phylogenetic clades (Kourelis et al., 2021). The role of the CC domain varies between NLRs. In recent resistosome models, the CC-domains form ion channels that function in the cell death response (Adachi et al., 2019, Wang et al., 2019a). Other CC-NLRs do not oligomerise but activate signalling 'helper' NLRs (Ahn et al., 2023, Contreras et al., 2023c). CC domains can also function in signalling by activating transcription factors. The rice RRM (RNA recognition motif) protein PIBP1 (PigmR-INTERACTING and BLAST RESISTANCE PROTEIN 1), activates defence gene expression upon binding to the CC domain of the NLR PigmR (Zhai et al., 2019). TIR-domains of TIR-NLRs have been shown to have NADase activity. Upon activation, these NLRs produce small molecules which function in downstream signalling to helper NLRs (Huang et al., 2022, Jia et al., 2023).

Non-canonical NLR domains also exist, many of these are known as integrated domains, or NLR-ID (Cesari et al., 2014). NLR-IDs are very diverse and can include domains with homology to WRKY transcription factors, kinases and BED zinc finger domains. In some species NLR-IDs are absent, however Sarris et al. (2016) found that, on average, they constitute 10% of the NLR complement in flowering plants. NLR-IDs are often used as decoys of effector targets, as discussed later in this chapter (1.1.5).

1.1.4 – Many sensor NLRs require 'helper' NLRs to activate immunity

Most CC-NLRs and TIR-NLRs act as sensors to initiate an immune response after effector detection. While some of these are 'functional singletons', many NLRs require additional 'helper' NLRs to activate immunity. There are two main categories of helper NLRs defined so far: RPW8-NLRs and the NRC class of NLR.

RPW8-NLRs work in conjunction with the lipase-like proteins ENHANCED DISEASE SUSCEPTIBILITY 1 (EDS1), PHYTOALEXIN DEFICIENT 4 (PAD4) and SENESCENCE-ASSOCIATED GENE 101 (SAG101). The most characterised RPW8-NLR helpers are N REQUIREMENT GENE 1 (NRG1) and ACTIVATED DISEASE RESISTANCE 1 (ADR1). NRG1 was first characterised as an NLR required for the *N* gene to confer resistance to tobacco mosaic virus (TMV) in *Nicotiana benthamiana* (Peart et al., 2005). The role of the ADR1 family in immune signalling was first characterised in *A. thaliana* (Bonardi et al., 2011). The co-occurrence of RPW8-NLRs with TIR-NLRs, and their role in signalling from TIR-NLR sensors has been well studied (Collier et al., 2011, Castel et al., 2019).

The NLR REQUIRED FOR CELL DEATH (NRC) clade of NLRs mediate signalling downstream of NRC-dependent CC-NLRs. Unlike other helper NLRs, there is often partial genetic redundancy between NRCs. This has been described as an 'NLR network'. NRCs are found across the Asterids. The NRC clade has greatly expanded within the Lamiids, particularly the Solanaceae (Huang et al., 2023, Sakai et al., 2023). The mechanism of NRC activation and downstream activation of cell death is discussed later in this chapter (1.1.6).

1.1.5 – Plant sensor NLRs perceive pathogens through a variety of mechanisms

Despite the shared architecture of plant NLRs, effector perception can occur through a range of mechanisms. The most common is by direct interaction of an NLR with the corresponding effector. One well characterised example is the interaction of the *Hyaloperonospora arabidopsidis* (*Hpa*) effector ATR1 (ARABIDOPSIS THALIANA RECOGNISED 1) with the TIR-NLR RPP1 (RESISTANCE TO PERONOSPORA PARASITICA 1) from *A. thaliana* (Krasileva et al., 2010). ATR1 makes contact with both the LRRs and a C-terminal jelly roll/Ig-like domain (C-JID) domain of RPP1 resulting in activation of the NLR (Ma et al., 2020). While less frequent, other studies have reported that pathogen effectors can interact directly with CC or TIR domains. The TIR domain of the NLR N directly binds to the TMV p50 helicase domain (Burch-Smith et al., 2007). Rpi-blb1 binds to *P. infestans* effector IPI-O1 through its CC domain (Chen et al., 2012).

Some NLRs recognise their cognate effector indirectly. In some instances, this can be explained by the guard model. A classic example of the guard model involves the *Arabidopsis* protein RIN4 and the NLRs RPM1 and RPS2. RIN4 (RPM1 INTERACTING PROTEIN 4) is guarded by the NLRs RPM1 (RESISTANCE TO PSEUDOMONAS SYRINGAE PV MACULICOLA 1) and RPS2 (RESISTANCE TO PSEUDOMONAS SYRINGAE 2). RPS2 and RPM1 detect changes in their guardee RIN4 and activate an immune response. Secretion of the *Pseudomonas* effectors AvrRpm1 and AvrB leads to the phosphorylation of RIN4. RPM1 interacts with RIN4 and can detect this phosphorylation, activating defence (Mackey et al., 2002). Similarly, RPS2 detects the cleavage of RIN4 by the cysteine protease action of the effector AvrRpt2 (Axtell and Staskawicz, 2003, Mackey et al., 2003).

Other NLRs operate through integrated decoy systems. These NLRs are often found in genetically linked pairs. One NLR has an integrated domain that acts as a bait, the other NLR detects binding of an effector to this integrated domain and participates in immune signalling. An example of this is the *A. thaliana* NLRs RPS4 (RESISTANCE TO PSEUDOMONAS SYRINGAE 4) and RRS1-R (RESISTANCE TO RALSTONIA SOLANACEARUM 1). This pair of head-to-head orientated genes encode TIR-NLRs which together confer resistance to *Pseudomonas syringae*, *Ralstonia solanacearum* and *Colletotrichum higginsianum*. Using a WRKY domain integrated into RRS1-R, the pair recognises PopP2 from *R. solanacearum,* AvrRps4 from *P. syringae* and an unknown effector from *C. higginsianum* (Sarris et al., 2015). Many other paired NLRs with integrated domains have been identified including the *O. sativa* Pik-1/Pik-2 CC-NLR pair, which recognise the *Magnaporthe oryzae* effector AVR-pik using a heavy metal-associated domain (HMA) domain integrated into Pik-1 (Białas et al., 2021). RGA4/RGA5 (R-GENE ANALOG 4/ R-GENE ANALOG 5), also from *O. sativa*, recognise AVR-Pia and AVR1-CO39 from *M. oryzae*. Like Pik-1, RGA5 contains an integrated HMA protein (Cesari et al., 2013).

While the CC/TIR, NB-ARC and LRR domains are typically present, the absence of these domains does not preclude function. The yellow stripe rust resistance gene *YrSP,* found in wheat (*Triticum aestivum*), is truncated and most of its LRR domain is absent (Marchal et al., 2018). Similarly, TN2 from *A. thaliana* has been shown to have an immune function despite the absence of LRRs (Zhao et al., 2015). Another example is the TIR-NB protein RLM3 (RESISTANCE TO LEPTOSPHAERIA MACULANS 3) in *A. thaliana*, which was identified as a *R*-gene to the necrotrophic fungus *Leptosphaeria maculans*. *RLM3* also confers resistance to *Botrytis cinerea*, *Alternaria brassicicola* and *Alternaria brassicae* (Staal et al., 2008).

1.1.6 – NLR activation, oligomerization and signalling

The mechanism of effector detection and downstream signalling varies between NLR classes. However, a common feature is oligomerization. It is predicted that plant NLRs have suppressive intramolecular domain interactions which are adjusted upon activation. Like mammalian NLRs, many plant NLRs have been shown to form higher order oligomers upon activation (Ahn et al., 2023, Ma et al., 2020, Martin et al., 2020, Wang et al., 2019a, Wang et al., 2019b, Zhao et al., 2022).

ZAR1 (HOPZ-ACTIVATED RESISTANCE 1) was the first oligomerised NLR structure to be published. In its resting state ZAR1 is monomeric and interacts with ZRK (ZED1-RELATED KINASES) pseudokinases. Using the ZRK pseudokinases, ZAR1 indirectly detects modification of PBL (PBS1-LIKE) kinases by *Pseudomonas* effectors (Wang et al., 2015a, Lewis et al., 2013, Martel et al., 2020, Schultink et al., 2019). Upon activation, monomers oligomerise into a pentameric resistosome. The ZAR1 oligomer has been shown to function as a plasma membrane calcium-permeable channel. An influx of Ca^{2+} correlates with timing of secretion of *P. syringae* effectors by the type-III secretion system, prior to subsequent loss of plasma membrane integrity and ROS production (Bi et al., 2021).

Following the publication of the ZAR1 resistosome structure, several other NLR resistosome structures have been elucidated. The *N. benthamiana* TIR-NLR ROQ1 (RECOGNITION OF XOPQ 1) oligomerises into a tetramer upon activation caused by binding of XopQ. The NLR and effector are found in a 1:1 ratio within the structure. This conformational change leads to the exposure of the NADase active site, hypothesised to induce helper NLR activation (Martin et al., 2020). The structure of the RPP1 TIR-NLR resembles that of ROQ1. The activated NLR forms a tetrameric oligomer where four ATR1 effector molecules are bound, its oligomerization is also required for NADase activity (Ma et al., 2020). The *Triticum monococcum* CC-NLR Sr35 oligomerises into a pentameric structure upon direct interaction with the wheat stem rust (*Puccinia graminis f. sp. tritici*) effector AvrSr35 (Zhao et al., 2022). The N-terminal amino acids (amino acid 1-20) of the CC-NLRs ZAR1, Sr35 and NRC are essential for immune function, but not resistosome assembly. Mutant alleles of Sr35 lacking these amino acids are able to oligomerise and associate with the membrane, but cannot mediate HR (Zhao et al., 2022).

Similar to ZAR1, helper NLRs NRG1 and ADR1 form resistosomes that may function as Ca^{2+} channels (Jacob et al., 2021). In *Arabidopsis*, the lipase-like protein EDS1 forms heterodimers with either PAD4 or SAG101. EDS1-SAG101 functions as a receptor, binding small molecules produced by TIR domains of sensor NLRs. This results in enhanced association of EDS1-SAG101 with NRG1. The resulting EDS1-SAG101-NRG1 complex may invoke transcriptional reprogramming and cell death by Ca^{2+} channel activity. While the activation of NRG1 by an intracellular sensor NLR leads to formation of the EDS1-SAG101-NRG1 complex, the oligomerization of this heterotrimer requires the activation of cell surface immunity (Feehan et al., 2023). The molecular basis of this is currently unknown.

Considering that both sensor TIR-NLRs, and their corresponding helper RPW8-NLRs, form oligomers upon activation, the question arises as to whether NRC helpers and their corresponding CC-NLR sensors do the same. Ahn et al. (2023) and Contreras et al. (2023c) found that the sensors Rpi-amr1, Rpi-amr3 and Rx remain as monomers upon activation. Instead, the corresponding NRC oligomerises into a complex which was initially hypothesised to be a pentamer. The interaction between the sensor and helper is hypothesised to be transient and could function by the helper monitoring the sensor for an effector-dependent conformational change (Huang et al., 2023).

Recently, Muniyandi et al. (2023) and Liu et al. (2023) conducted structural analysis of various forms of NRC protein. Muniyandi et al. (2023) found that in its resting state, NRC2 has intermolecular interactions between monomers and forms a homodimer. They predict that the activated sensor NLR disrupts this homodimer, producing primed monomers which can subsequently oligomerize. Liu et al. (2023) found that NRC4 D478V, an autoactive NRC4 mutant, forms a hexameric resistosome in *N. benthamiana*. This resistosome facilitates the influx of Ca^{2+} into the cell, which precedes the cell death response. The authors also identified a dodecameric form, where 12 NRC4 protomers form a dumbbell-shaped structure resembling two stacked hexamers. In this structure, the CC domains are buried in the centre of the dodecamer, preventing cell death response. The authors propose that this is an inactive form that contributes to the regulation of the NRC4 response, like the mouse NLRC4 protein where an oligomer variant buries the active caspase activation and recruitment domain (CARD) at the centre (Tenthorey et al., 2017). This structure is intriguing but seems to conflict the proposed inactive homodimer form of NRC2, and the gain in oligomeric state previously observed upon activation of the NRC class of protein (Muniyandi et al., 2023, Ahn et al., 2023).

These NRC structural analyses highlight the diversity of structural changes involved in plant NLR activation and signalling. Most notably, the inactive forms are different, while inactive NRC2 is a dimer, ZAR1 and Sr35 are monomeric. The integration of effectors also varies, with ROQ1 and RPP1 integrating their elicitors into the resistosome, while characterised RPW8-NLR and NRC oligomers do not contain the sensor NLR or effector. Another common feature is association with the plasma membrane and function as a Ca^{2+} channel.

Other CC-NLRs promote immunity by alternative mechanisms, including the protection of host susceptibility factors. The rice NLR PigmR functions by preventing effector-mediated degradation of PICI1 (PigmR-INTERACTING AND CHITIN-INDUCED PROTEIN 1), a host deubiquitinase protein. PICI1 stabilizes methionine synthetases promoting their role in immunity. The blast fungus effector AvrPi9 inhibits PTI by degrading PICI1., PigmR can prevent this, possibly functioning via binding competition (Zhai et al., 2022). A similar model has been proposed for the rice NLR Pi9, the blast effector AvrPi9 and AVRPI9-INTERACTING PROTEIN 1 (ANIP1). ANIP1 is a host protein which negatively regulates resistance against *M. oryzae*, it can be bound by both Pi9 and AvrPi9. AvrPi9 inhibits the degradation of ANIP1 leading to inhibition of immunity. When Pi9 is present, AvrPi9 promotes the dissociation of Pi9 from ANIP1. The release of Pi9 could lead to the activation of the NLR and ETI (Shi et al., 2023). For both PigmR and Pi9, it is unclear if the immune output is solely due to protection of the host target, or if conventional signalling by the NLR also influences this.

1.1.7 – Effectors manipulate the host to promote infection

Effectors can be broadly divided into two groups: those secreted into the apoplast and those secreted into the host cells. Distinguishing apoplastic effectors from other apoplastic molecules such as PAMPs is complicated. In this thesis, apoplastic effectors are defined as molecules secreted into the apoplast which manipulate the host and produce favourable conditions for the pathogen. One of the most well studied systems in plant immunity is the interaction between tomato and the *Cladosporium fulvum* leaf mold fungus. The cell surface immune receptors Cf-2, Cf-4 and Cf-9 activate immunity upon detection of the *C. fulvum* apoplastic effectors AVR2, AVR4 and AVR9.

The second group of effectors, the cytoplasmic effectors, are, as previously discussed, often recognised by NLR proteins. Cytoplasmic effectors promote colonisation of host tissue through a variety of mechanisms. Well characterised examples include the *P. infestans* effectors AVR1 and AVR2. AVR1 prevents the deposition of callose by targeting the Sec5 component of the exocyst complex, which is required for vesicle trafficking (Du et al., 2015b). AVR2 interacts with the BRI1-SUPPRESSOR-LIKE (BSL) family. The resulting up-regulation of the brassinosteroid pathways impairs immune signalling, therefore promoting virulence (Turnbull et al., 2019).

The conventional assumption is that individual effectors are disposable and can be lost with little cost to virulence (Kvitko et al., 2009, Zheng et al., 2014, Thordal-Christensen et al., 2018). This loss would enable evasion of recognition and result in the 'breaking' of an *R*-gene. This is supported by the presence/absence of some effectors between strains, which has been reported for the *P. infestans* effector AVR2 and the *Puccinia graminis f. sp. tritici* effector AvrSr50 (Chen et al., 2017, Gilroy et al., 2011). Other pathogen strains evade resistance by reducing the expression of recognised effectors. The *P. infestans* strain EC1 is the only identified strain virulent against *Rpi-vnt1* genotypes, EC1 has reduced expression of *AVRvnt1* relative to other strains (Pais et al., 2018). The apparent disposability of effectors conflicts with the evidence of their specialised function. While the loss of an effector may have little impact upon the ability of an individual strain to cause disease, within a population this may not be the case. Yan et al. (2023) demonstrated that while an *M. oryzae* strain lacking the effector Mep1 (MAGNAPORTHE EFFECTOR PROTEIN 1) is still able to cause disease, at a population level the strain had a significant disadvantage and was driven to extinction within three generations. This suggests that instead of losing a recognised effector, other strategies may be preferable to evade resistance. One such strategy is the suppression of specific NLRs, which is discussed later in this chapter (1.1.8). This also highlights one of the driving forces behind frequency-dependent selection, also discussed later in the chapter (1.2.2).

The effector repertoire of a pathogen is important in determining its host range. Many plant species have convergently evolved recognition of effectors. For example, the phylogenetically distinct NLRs R2 (from *Solanum demissum*) and Rpi-mcq1 (from *Solanum mochiquense*) both recognise the *P. infestans* effector AVR2 (Aguilera-Galvez et al., 2018). The barley NLR MLA3 (MILDEW LOCUS A 3) and an unknown weeping lovegrass *R*-gene convergently evolved recognition of the *M. oryzae* effector Pwl2 (PATHOGENICITY TOWARD WEEPING LOVEGRASS 2) (Brabham et al., 2023). Convergent evolution for recognition in the apoplast has also been reported. The *Phytophthora* PAMP Pep13 is recognised by the potato LRR-RLK PERU (PEP-13 RECEPTOR UNIT) and a distinct unidentified receptor in

parsley (Torres Ascurra et al., 2023). The *Phytophthora* apoplastic elicitor INF1 is recognised by both REL (RESPONSIVE TO ELICITINS) from *N. benthamiana* and ELR (ELICITIN RESPONSE) from potato, both are LRR-RLPs (Du et al., 2015a, Chen et al., 2023). The diverse recognition of these molecules and their retention despite selective pressure from multiple host species suggests that their function is non-dispensable and required either for virulence or basic pathogen growth and development.

1.1.8 – Perception of pathogen effectors does not always result in resistance

With the advance in quality and quantity of published plant and pathogen genomes, a screening approach utilizing libraries of effectors has enabled quicker identification of immune receptors and their cognate effectors. However, this 'effectoromics' approach comes with a major limitation. Although recognition genes can be rapidly identified, often their recognition does not correlate with resistance. Several factors contribute to this discrepancy.

One reason for recognition without resistance is immune suppression. Although a single effector may be recognised, other effectors can suppress the immune response. Immune suppression can occur through various mechanisms, including the suppression of sensor NLRs or helper NLRs, or by interference of signalling cascades and secondary messengers (Wu and Derevnina, 2023). The *P. infestans* effector IPI-04 binds to the CC domain of the *S. bulbocastanum* sensor Rpi-blb1/RB, preventing IPI-01- (AVRblb1-) dependent HR. It has been speculated that this binding could prevent oligomerization of Rpi-blb1 and the subsequent immune response (Wu and Derevnina, 2023, Chen et al., 2012, Karki et al., 2021). Derevnina et al. (2021) identified two effectors that have convergently evolved to suppress NRC helper NLRs, one from *P. infestans* and one from the potato cyst nematode (PCN). The PCN effector, SPRYSEC15 (SS15) achieves this by directly binding to the NB-ARC domain of the NRC preventing its activation (Contreras et al., 2023a). Inter- and intra-species variation for evasion of suppression does exist for many of these examples (Karki et al., 2021). Suppression activity of some pathogens is evidently broader and stronger than others. *Albugo candida* is capable of strong suppression of immunity, its infection of *A. thaliana* allows co-infection by additional avirulent and non-adapted microbes including downy mildews and *P. infestans* (Cooper et al., 2008, Prince et al., 2017).

When distinguishing recognition from resistance, another factor to consider is the quantitative and dosage-dependent nature of disease resistance. For example, transgenic barley carrying the *MLA3* gene can resist *M. oryzae*, but only when multiple copies are present. The strength of resistance increases with higher copy number, a single copy alone is insufficient for effective resistance (Brabham et al., 2023). This finding suggests that while pathogen recognition is required for resistance, the downstream signalling is quantitative, resulting in variable resistance levels. This may be a common feature among NLRs, it also suggests that multiple NLRs with weak recognitions could be stacked to confer a visible phenotype. Another example of the quantitative nature of NLR-mediated resistance is the *A. thaliana* NLR SNC1 (SUPPRESSOR OF NPR1-1 CONSTITUTIVE 1). SNC1 recognises the *P. syringae* effector AvrPtoB. However, plants carrying SNC1 can still support growth of *Pseudomonas* strains carrying *AvrPtoB*. Only a slight increase in bacterial growth can be observed in *snc1* knock out lines, indicating that while SNC1 activates immunity, it does so quantitatively (Wang et al., 2023d).

The importance of the context of recognition and the subsequent immune response can be seen in the artificial evolution of Rx, an NLR which confers resistance to potato virus X (PVX) in potato. Through mutation of the Rx LRRs, recognition can be extended to additional PVX strains and the more distantly related poplar mosaic virus (PopMV). PopMV recognition does not result in resistance, instead, a trailing necrosis phenotype is observed. This was attributed to the response being ‘too slow’ to prevent viral spread (Farnham and Baulcombe, 2006). While such gain-of-function mutations may occur spontaneously in nature, alleles conferring an insufficient response may be selected against. Stepwise evolution towards a superior allele is possible. This was artificially demonstrated by Harris et al. (2013) where the same Rx variant was further mutated to increase its sensitivity. These sensitised alleles confer resistance to PopMV. Reduced fitness cost associated with such alleles would decrease selection against them, facilitating their expansion within a population.

1.2 – Immune receptor variation and durability

1.2.1 – NLR-encoding loci are hotspots for genetic variation

The abundance of plant pathogens and the large array of effectors has resulted in extensive diversity in both the number and nucleotide diversity of intracellular immune receptors, between and within species. Considering that NLR loci are hotspots for genetic variation, exploring the mechanisms behind the generation and maintenance of this variation is intriguing.

In angiosperms, the normalised number of NLRs relative to the total predicted protein number count ranges from 0 to 3.266% (Ngou et al., 2022b). Many expansions and contractions are lineage-specific; for instance, TIR-NLRs are absent from monocots, while CC-NLRs are expanded in the Solanaceae (Seo et al., 2016, Tarr and Alexander, 2009). Interestingly, reduced NLR number does not correspond with a compensatory increase in the number of PRRs. Instead, there is a concerted expansion and contraction of NLR numbers alongside cell-surface immune receptor numbers (Ngou et al., 2022b). Many plant lifestyles are correlated with extremes in immune receptor number. Trees and grasses generally appear to have much larger receptor repertoires, although there are exceptions to this. The drought tolerant resurrection grass *Oropeteum thomaeum*, atypically for Poales species, has few immune receptors. Aquatic, carnivorous and parasitic plants have few NLRs and some species have lost NLR signalling pathways altogether (Baggs et al., 2020, Ngou et al., 2022b). How lifestyle has shaped the immune receptor repertoire is unclear, but it could be related to exposure to genetically diverse pathogens. Grasses typically grow densely and are exposed to rusts and blast which undergo sexual reproduction and somatic hybridisation, leading to the emergence of novel strains (Li et al., 2019, Stukenbrock, 2016). In contrast, aquatic species are submerged and have limited exposure to these pathogens (Liu et al., 2021). Parasitic and carnivorous plants have simplified root systems with fewer entry points to pathogens. Conceivably, these factors could influence immune receptor repertoires.

Within species, there is extensive diversity in NLR-encoding genes between haplotypes. This can exist as allelic variation, presence-absence polymorphism and copy number variation. The NLR diversity, or pan-NLR-ome, of several species have been studied. Van de Weyer et al. (2019) found that among 64 *A. thaliana* accessions, the ‘core-NLRome’ (defined as those found in at least 52 accessions) constitutes around 23% of the total number of NLRs. Conversely, the ‘cloud NLRs’ which are found in fewer than 12 accessions make up 13% of NLRs. This finding demonstrates that while there is a significant diversity of NLRs within the

species, many are conserved and could be maintained under selection. Another important finding was that despite the wide geographical distribution of these accessions, NLR diversity saturated far below the total number of sampled accessions. Similar observations were reported by Sutherland et al. (2023).

Van de Weyer et al. (2019) proposed that biotrophic pathogens are the driving force behind NLR diversity. In *A. thaliana*, the most diverse NLR orthogroups have members which are implicated in resistance to these pathogens, including *Hpa*, *A. candida* and *Pseudomonas spp*. Clustering of *R*-genes that confer resistance to single pathogens is most extreme in the development of *R*-gene allelic series. Examples of this include the *MLA* locus in barley, the *Pm3* locus in wheat, the *L* locus in flax and the *Rpp13* locus in *Arabidopsis*. Within these allelic series, variants are highly similar, but confer resistance to different strains of the respective pathogen. This variation is often extensive, there are 19 distinct and functional alleles of *RPP13*, 23 alleles of *MLA*, and 17 alleles of *Pm3* (Ellis et al., 1999, Bittner-Eddy et al., 2000, Bourras et al., 2015, Bourras et al., 2019). Within the *MLA* and *Pm3* allelic series, sites of diversifying selection are located on the exposed concave surface of LRRs, indicating selection for novel variants (Seeholzer et al., 2010, Bhullar et al., 2010, Cao et al., 2023), as noted nearly 30 years ago for RLPs (Parniske et al., 1997). The elicitors of these NLRs are often structurally similar despite sometimes having low sequence identity (Bourras et al., 2019, Lu et al., 2016). This highlights the constraints that pathogens face when escaping recognition. Effectors possess some non-variable features, perhaps to maintain certain functions within the host or to ensure correct translocation (Cao et al., 2023). Moreover, an allelic series may be advantageous because, at the population level, a plant species has broader recognition capacity than a single individual, a single allele can recognise only one effector (Brown and Tellier, 2011, Dangl and Jones, 2001).

1.2.2 – Pathogen-host interactions drive changes in *R*-gene repertoires

An *R*-gene conferring strong resistance within a plant population imposes high selective pressure on pathogens to lose or mutate the corresponding effector. Where effectors confer a virulence function, development of novel alleles or changes in expression may instead occur. The pressure on both hosts and pathogens has led to two theories, the molecular arms race and trench warfare models. The arms race model proposes that *R*-genes will undergo recurrent directional selection, meaning new *R*-genes are selected as older ones are broken. This would result in an iterative process of diversification causing the birth and death of *R*-genes (Saur et al., 2021, Michelmore and Meyers, 1998). The molecular arms race is compatible with plant

breeding and agriculture. However, fixation of new alleles and loss of others is not supported in natural populations where alleles conferring resistance and susceptibility have co-existed for millions of years (Stahl et al., 1999, Terauchi and Yoshida, 2010). The trench warfare model offers an alternative. The model proposes that variation in *R*-gene loci is maintained through epidemics causing cyclical gain and loss of *R*-gene alleles and their corresponding effectors (Stahl et al., 1999). This is negative frequency-dependent selection, a form of balancing selection. Bakker et al. (2006) found evidence of balancing selection on around one third of NLR-encoding genes across 96 *A. thaliana* accessions.

The fitness cost to the pathogen upon losing effectors supports the trench warfare model. Whether maintaining a resistant haplotype confers a fitness cost to the plant has been debated, this has been presented as an explanation as to why many *R*-genes are not fixed. Several *A. thaliana* NLRs have been used to model this relationship between relative fitness under lack of disease and the benefit of maintaining them. *Rpm1* and *Rps5* confer a pleiotropic effect, there is a 5-10% cost to fitness in their natural presence-absence polymorphism (Tian et al., 2003, Karasov et al., 2014). Instead, other *R*-genes, including *Rps2*, exists as two haplotypes of resistant or susceptible alleles, neither conferring a greater cost to fitness (MacQueen et al., 2016). Haplotype diversity maintained by balancing selection results in the recognition capacity within a species being far greater than within one sampled individual, in contrast to the monocultures used in agriculture.

Balancing selection maintains genetic diversity while counteracting genetic drift and the reduced genetic diversity associated with inbreeding. Balancing selection is pervasive over long periods and through speciation. By studying the speciation of two inbreeding *Capsella* species (*Capsella rubella* and *Capsella orientalis*) from the outbreeding species *Capsella grandiflora*, Koenig et al. (2019) observed a general reduction in genetic diversity. However, some NLR and RLP/RLK loci were found to have maintained greater diversity. Notably, balancing selection is affected by domestication. Gladieux et al. (2022) report that while balancing selection is active in both landrace and modern rice NLR loci, it is more prevalent in landrace accessions. This is consistent with the greater diversity within these varieties.

The limitation of most studies of population dynamics in plant immunity is the assumption of a simple gene-for-gene interaction. However, resistance is polygenic. Plants must detect, signal, and execute a response, at each step the pathogen acts to evade or suppress. This is further complicated by multiple effector recognition by some receptors, suppression by plant pathogens, and the fact that single *R*-genes can confer resistance to multiple pathogens. For example, *Rpi-amr3* confers resistance to *Phytophthora infestans*, *Phytophthora parasitica* and

Phytophthora palmivora. Thus, which pathogen exerts greatest selection pressure on the host cannot be determined. Similarly, NLRs that have convergently evolved recognition of an effector complicate conclusions based on the diversity and evidence of selection exerted on the effector.

1.2.3 – Durable disease resistance and non-host resistance

As previously discussed, *R*-genes can be 'broken' or overcome by changes in the pathogen effector repertoire. This is often observed in agriculture and is contrasted by natural populations where some resistance is durable for many years. However, other deployed *R*-genes remain durable for many years. It is often unclear what makes some resistances durable. Durability could be due to the recognition of multiple effectors, the recognition of an effector essential for virulence, or where the loss of the effector is too costly for the pathogen to persist within a population.

For any plant species, most pathogens cannot cause infection. This non-host resistance (NHR) is considered to be broader and more durable than host-resistance (Lee et al., 2016, Vega-Arreguin et al., 2017, Zimnoch-Guzowska et al., 2003, Strugala et al., 2015, Nürnberger and Lipka, 2005). Many definitions of NHR exist. Strictly defined, NHR is the situation when no isolates of a given pathogen can infect any accession of a species (Lee et al., 2016, Schulze-Lefert and Panstruga, 2011, Panstruga and Moscou, 2020). Less stringent definitions allow non-host species to contain a few susceptible accessions, in these cases NHR components may be mutated (Strugala et al., 2015). NHR does not always confer complete incompatibility, instead a range of outcomes are possible. Bettgenhaeuser et al. (2014) reviewed outcomes of NHR to rust pathogens which included (i) physical incompatibility (ii) entry without haustoria formation (iii) infection without sporulation but with the presence of small pustules. These instances can be defined as NHR as infection cannot progress further. In the context of this thesis NHR is defined broadly as when the majority of members of a species are resistant to the majority of strains of a pathogen (Cevik et al., 2019).

Given that plant and pathogen species coevolve, Niks and Marcel (2009) proposed that a spectrum of host to non-host exists. Intermediate species are either developing incompatibility or becoming hosts. This raises questions about how NHR is established, how mechanisms of NHR change through evolution, and whether the mechanisms involved in NHR are the same as those involved in race-specific resistance.

At large evolutionary distance between hosts and non-hosts, NHR is caused by physical incompatibility between non-adapted pathogens and non-hosts. Pre-invasion defence consists of physical barriers preventing pathogen adhesion and penetration as well as metabolic barriers providing antimicrobial defence (Lee et al., 2017). *A. thaliana* prevents barley powdery mildew infection through the action of proteins encoded by *PENETRATION* genes (*PEN1*, *PEN2* and *PEN3*). These genes encode a syntaxin vesicle targeting protein, a glucosyltransferase, and an ABC transporter, respectively. Upon infection, these proteins trigger release of cell wall precursors, antimicrobial compounds and toxic aglycons preventing further spread of the pathogen (Lipka et al., 2008). Some loss-of-susceptibility *R*-genes confer phenotypes similar to metabolic or physical incompatibility. These *R*-genes lack a strong immune response and act by preventing essential virulence function (Kourelis and van der Hoorn, 2018). The maize *HM1* gene encodes a reductase which detoxifies the HC toxin produced by *Cochliobolus carbonum* race 1 (CCR1) (Johal and Briggs, 1992). This non-receptor *R*-gene is found in several other grass species and is responsible for monogenic non-host resistance in barley to CCR1 (Sindhu et al., 2008). This class of NHR may be more common than reported and mistaken for physical incompatibility due to the lack of an immune response.

As evolutionary distance between hosts and non-hosts decreases, the role of immune receptors and ETI is greater (Schulze-Lefert and Panstruga, 2011, Lee et al., 2017). Receptors involved in NHR may be conserved and maintained within a species, rather than under diversifying selection. Evidence for such receptors does exist (Schulze-Lefert and Panstruga, 2011, Cevik et al., 2019). At greater evolutionary distance, non-hosts would be expected to lose these genes as barriers to infection evolve. This would allow the receptor repertoire to remain adaptive to recognition of other pathogens. Conservation of *R*-genes between species demonstrates the durability of these resistances across long evolutionary periods, contrasting the classical model of unstable gene-for-gene interactions.

Many studies have demonstrated that NHR shares mechanisms with race-specific resistance. Vega-Arreguin et al. (2017) managed to compromise *Nicotiana tabacum* and *Nicotiana edwardsonii* non-host resistance to *Phytophthora capsici* by silencing the *I2* NLR family showing the role of NLRs in this NHR. Gilbert et al. (2018) and Bettgenhaeuser et al. (2018) demonstrated that *Brachypodium distachyon* resistance to non-adapted wheat stripe rust is simply inherited and caused by *R*-genes including NLRs. Laflamme et al. (2020) demonstrated that 95% of *P. syringae* strains contain effectors that can be recognised via the CAR1 (CEL-ACTIVATED RESISTANCE 1) and ZAR1 NLRs in the *Arabidopsis thaliana* accession Col-0. The authors also suggest that as few as 8 NLRs provide resistance to all *P. syringae* strains

which are unable to infect Col-0. *A. thaliana*'s NHR to *A. candida race Ac2V* is mediated primarily through activation of NLRs. Mutations in *EDS1* result in loss of resistance to multiple races of *A. candida* indicating that TIR-NLRs are responsible for resistance. Subsequently, multiple *WRR* (*WHITE RUST RESISTANCE*) genes have been cloned from *Arabidopsis* through transgressive segregation and map-based cloning (Cevik et al., 2019, Borhan et al., 2008).

In wheat, the resistance genes *Pm3b*/*Pm3c*/*Pm3D* confer race-specific resistance to wheat powdery mildew but contribute to NHR to non-adapted mildews which infect rye and a wild grass (*Dactylis glomerata*) (Bourras et al., 2019). In this instance, non-host resistance directly overlaps with host resistance. The authors suggest that plant breeders should maintain race-specific resistance to host pathogens in order to prevent emergence of new virulent pathogens from non-adapted pools. These novel strains could easily emerge through hybridisation (Bourras et al., 2019, Menardo et al., 2016). These studies demonstrate NHR often involves the same recognition-dependent mechanisms as race-specific resistance. Conceivably, durable receptor-mediated resistance in non-hosts could be transferred between species as gene stacks.

NHR may also happen due to the inability of the pathogens' effector repertoire to successfully enhance susceptibility in the non-host species. This was demonstrated by McLellan et al. (2022) who found that while *P. infestans* effectors can interact with their target potato proteins, the orthologues from *A. thaliana* are not targeted. This is supported by the finding that *A. candida* infection of *Arabidopsis* supports the colonisation by *P. infestans*. *Arabidopsis* is a non-host of *P. infestans*, *A. candida* can suppress this immunity. Incompatibility between pathogen suppressor molecules and their host suppression targets has been demonstrated on smaller evolutionary timescales. Oh et al. (2023) and Derevnina et al. (2021) demonstrate that the *P. infestans* effector PITG_15278 is able to suppress the *Solanum bulbocastanum* NLR *Rpi-blb2*, but not the orthologue from *Capsicum annuum*, a non-host to *P. infestans*.

While NHR was previously hypothesised to occur due to mechanisms distinct from host resistance, it has become increasingly clear that host and non-host resistance overlap. The distinction between host/non-host resistance is often based on the context rather than mechanism, similar to previous classifications such as monogenic/polygenic, vertical/horizontal or partial/complete resistance (Parlevliet and Zadoks, 1977). When NHR is caused by stacking of *R*-genes, the polygenic nature might disturb the frequency-dependent selection of gene-for-gene interactions in favour of the plant. Pathogens must mutate multiple avirulence genes to overcome resistance.

Given the evidence that NHR often occurs due to the same classes of *R*-gene as host resistance, several questions emerge: how do these two become distinct? Are components of NHR fixed within the species, or do they remain polymorphic and under balancing selection? Dissecting the identity and distribution of NHR components will allow these questions to be answered.

1.2.4 – Deploying *R*-genes using modern breeding techniques

By developing our understanding of the genetic and molecular basis of resistance, we can improve resistance in crop species. This can be achieved through breeding, transgenic and gene-editing approaches. Crucially, the deployment of *R*-genes should be in a context that ensures durability. In principle, the route to durable genetic resistance has been long known. Parlevliet and Zadoks (1977) instruct that there are two approaches to assure diverse and stable resistance to pathogens in crops. In the first scenario, all plants in a population carry several *R*-genes but each plant carries a different combination. In the second scenario, all plants carry the same *R*-genes, but in a combination that confers near complete resistance. With the development of modern breeding techniques this is achievable.

The speed and power of plant resistance breeding has greatly improved with the advent of genome sequencing and positional mapping. After identifying the position of *R*-genes, breeders can select for lines carrying known resistance loci and combine these into 'pyramids' to try to ensure durability (Mundt, 2018). While breeders can improve the power of selection using resistance-linked markers, this approach is limited by linkage-drag of negative traits from landraces or wild relatives. Additionally, genes which map to the same locus but are located on different haplotypes cannot be combined. Resistance breeding is further complicated by polyploidy, self-incompatibility and inbreeding depression which can result in low genetic gains. This is exacerbated in species where more complex breeding programmes are required, including biennials.

Transgenic approaches greatly expand the capacity to exploit available variation. The GM method facilitates the movement of *R*-genes (and other genes) into crops from plants beyond breeding barriers. The *Solanum stoloniferum R*-gene Ry_{sto}, is a prime example of this. Ry_{sto} was identified as a *R*-gene to potato virus Y (PVY). Grech-Baran et al. (2022) reported that Ry_{sto} recognises a diverse array of potyvirus coat proteins including turnip mosaic virus (TuMV). Through transgenic approaches Ry_{sto} could elevate TuMV resistance in *Brassica* species. Genetic modification would also facilitate the deployment of durable *R*-gene stacks.

R-gene stacking has been used to develop late blight resistant potato and stem rust resistant wheat. Ghislain et al. (2019) improved the African potato variety Victoria by addition of three *R*-genes: *Rpi-blb1*, *Rpi-blb2* and *Rpi-vnt1*. Together these genes confer strong resistance to a wide range of *P. infestans* strains. Varieties generated showed greatly reduced disease symptoms and no morphological differences to the untransformed variety. Similarly, Luo et al. (2021) transferred five stem rust resistance genes (*Sr22*, *Sr35*, *Sr45*, *Sr50* and *Sr55*) into the bread wheat cultivar Fielder. The 5R transgenic lines were highly resistant and showed no pleiotropic effects. These examples demonstrate the potential of gene stacking, and how this can be achieved with no growth-defence trade-off. Discovery of the recognised effectors also enables rapid screening and validation of these lines, ensuring functionality of each gene on a T-DNA. The limitation to developing durable resistance through gene stacking will be the rate of *R*-gene identification and the policies regulating use of the method.

1.2.5 – Deploying *R*-genes – Overcoming restricted taxonomic functionality

One consideration when deploying *R*-genes is that their function may differ between genetic backgrounds or when transferred between species. Many *R*-genes can be transferred across large evolutionary distances, for example, the barley CC-NLR MLA which confers resistance to barley powdery mildew in transgenic *A. thaliana* (Maekawa et al., 2012). For other NLRs, function can be reduced or completely absent. This phenomenon is known as restricted taxonomic functionality (RTF). RTF was first described by Tai et al. (1999) who observed that the *Bs2* gene from pepper can confer resistance to *Xanthomonas campestris pv. vesicatoria* in transgenic tomato, but not *Arabidopsis*, turnip, cucumber or broccoli. *Bs2* encodes an NRC-dependent NLR, and its lack of function is likely due to the absence of the *NRC* clade in Brassicaceae and Cucurbitaceae. Differences between NRC repertoire also exist across shorter evolutionary distances. Lüdke et al. (2023) demonstrated that within Solanaceae species, lineage-specific subfunctionalization of NRCs has occurred. The tomato NLRs Hero and MeR1, which recognise cyst and root-knot nematodes, are dependent on NRC6. NRC6 is absent from *S. tuberosum* and *N. benthamiana* preventing function of either sensor in these species (Sobczak et al., 2005, Ernst et al., 2002). Similar RTF exists for the sensor Rpi-blb2, which is supported by the tomato *NRC3* allele, but not the *N. benthamiana* allele (Huang et al., 2023). In these instances, the coevolution of NLRs within species appears to have resulted in incompatibility of sensors with orthologues of their native helpers. This occurs with sequence divergence, gene duplication/loss and neofunctionalization.

RTF of TIR-NLRs also occurs. TIR-NLRs are absent from monocots which have undergone convergent loss of the TIR-NLR signalling components including EDS1, PAD4 and the helper NLR NRG1 (Baggs et al., 2020). The absence of these genes provides a clear reason why the transfer of TIR-NLR function into monocots has not been successfully demonstrated. These instances highlight the importance of understanding the molecular mechanisms of NLR mediated immunity in plants, and the assaying of individual *R*-genes before transferring stacks of *R*-genes between plant species.

1.3 – Plant viruses and the *Polerovirus* family

This thesis describes the molecular and genetic basis of resistance to three plant pathogens. In Chapter 3 resistance to potato leafroll virus (PLRV) in *Solanum tuberosum ssp. andigena* was investigated and the resistance gene *Rl$_{adg}$* was cloned. The basis of PLRV recognition by Rl$_{adg}$ was investigated. By understanding the mechanism and function of this resistance, the potential for broad application of polerovirus resistance was discovered.

1.3.1 – Consequence and control of poleroviruses

Plant viruses are a complex polyphyletic group which have interactions not only with their primary plant hosts, but with alternative hosts and vectors which include nematodes, arthropods, oomycetes, fungi and protists (Lefeuvre et al., 2019, Tamada and Kondo, 2013, Andika et al., 2017, Andret-Link et al., 2004). They range from being plant host-specific to broad range, and from highly symptomatic to apparent symptomless infection.

Polerovirus is a genus of plant-infecting viruses within the *Solemoviridae* (formerly *Luteoviridae*) family which infect several economically important food crops including wheat, maize, barley, and potato. Poleroviruses have a positive sense ssRNA genome with a shared architecture containing five major ORFs (ORF0-ORF5). ORF0 encodes P0, a suppressor of RNA silencing. The ORF1-2 region encodes replicase-associated proteins including the P1 protein and a P1-P2 fusion produced by a -1 ribosomal frameshift. The product of ORF4 is a movement protein which enables cell-to-cell movement of the viral RNA. ORF3 and ORF5 encode two components of the coat protein (CP). ORF5 is produced by a readthrough of the ORF3 stop codon.

Poleroviruses are phloem-limited and are transmitted via an aphid vector which becomes infected in a circulative, non-persistent manner. These viruses only replicate in the plant host phloem, not in the insect vector (Macleod et al., 2023). The *Polerovirus* type species is potato leafroll virus (PLRV), one of the most important viral pathogens of potato. PLRV infection can result in yield loss of 50-80% and reduced tuber quality through the appearance of net-necrosis (Kondrák et al., 2020, Carneiro et al., 2017). While primary infection may produce only mild symptoms, shoots from infected tubers can be stunted and discoloured. Co-infection with other viruses can also produce more severe symptoms. This is believed to be due to the loss of phloem-restriction, which has been observed during co-infection with potato virus A (Hameed et al., 2014, Jingwei et al., 2013, Barker, 1987, Savenkov and Valkonen, 2001).

Persistent infection of vegetative tissue by plant viruses is more important in potato than other species. Many viruses are not seed-transmitted but are carried in tubers. They can rapidly build up across multiple rounds of propagation resulting in higher viral load and more severe symptoms. Consequently, the viral titres in seed potatoes are tightly regulated (Carneiro et al., 2017, Mondal et al., 2017). Currently, most poleroviruses are controlled by targeting the insect vector, *Myzus persicae*, with broad-spectrum insecticides. Insecticide resistance and climate change are likely to exacerbate the impact of *M. persicae*-vectored viruses. Warmer winters may result in earlier aphid flight as well as the build-up of the vector on alternative hosts prior to emergence of the crop (Hemming et al., 2022). The control of insect vectors has been further limited by the advancing regulation surrounding chemicals. In 2018, the European Union passed a ban on the outdoor use of neonicotinoids due to the adverse impact on pollinating insects (Bass and Field, 2018). In combination with elevated resistance to other insecticides, this could mean increased viral infection where previous control was successful. Elevating immunity of crop varieties would provide a chemical-free solution to plant viruses.

1.3.2 – Resistance to poleroviruses is limited

Many NLR-encoding genes that confer resistance to viruses have been identified. However, no cloned *R*-genes against poleroviruses have been reported. The elusiveness of dominant, major gene resistance is not specific to PLRV. While genes conferring resistance to turnip yellows virus (TuYV) have been reported in *Brassica rapa*, *Brassica oleracea* and *Brassica napus*, these genes are partially dominant and do not exhibit major effects (Greer et al., 2021, Hackenberg et al., 2020, Juergens et al., 2010, Macleod et al., 2023).

Notably, poleroviruses are phloem-limited pathogens. It is unclear whether conventional NLR-mediated ETI functions in the phloem. However, NLR transcripts in phloem procambium and companion cells have been reported (Tang et al., 2023). Poleroviruses move between the sieve elements, companion cells and vascular parenchyma cells (Esau and Hoefert, 1972, Shepardson et al., 1980). Given this, NLR-mediated resistance to these pathogens is conceivable.

While several sources of PLRV resistance have been identified, their use is limited due to linkage to negative traits, or because of a complex genetic basis. Resistance to TuYV and PLRV was reported in *Nicotiana glutinosa*. This trait is monogenic and segregates in a 3:1 manner in a biparental cross. Expression of the PLRV P0 protein was found to elicit a response

in the resistant *N. glutinosa* accession. This *R*-gene was named *RPO1* (*RESISTANCE TO POLEROVIRUSES 1*) but its successful cloning has not been reported (Wang et al., 2015b, Wang et al., 2023c). If cloned, *RPO1* could only be used in *S. tuberosum* by a transgenic approach, whereas resistance from potato could be defined as cisgenic or used in conventional breeding. To be considered cisgenic, the transferred gene must be one that could also be introduced through conventional breeding. This is considered important as the result closely mimics traditional breeding, potentially making it more acceptable for regulatory and public approval.

1.3.3 – An Andean potato landrace is highly resistant to PLRV

Through extensive screening, three *S. tuberosum ssp. andigena* landraces with high levels of heritable resistance were discovered. These accessions, LOP-868, HUA-332 and OCH-7643 are highly resistant, and viral titres remain low upon graft inoculation with PLRV-infected plants (Mihovilovich et al., 2007). Using a dihaploid mapping population, Velasquez et al. (2007) discovered that resistance in this accession is mediated by a single major locus. This *R*-gene, named Rl_{adg}, was mapped to the long arm of Chromosome 5. In the annotated potato reference genome, this locus contains many NLR encoding genes (Jupe et al., 2012, Kuang et al., 2005). The use of Rl_{adg} is currently limited by complex tetraploid genetics and the lack of a perfect marker. The progeny resulting from crosses between LOP-868 and other potato cultivars show large variation in tuber yield, size and appearance (Carneiro et al., 2017). The identification of the Rl_{adg} gene would simplify its deployment in breeding and facilitate its use in transgenics.

1.4 – *Phytophthora* - The plant destroyer

In Chapter 4 and Chapter 5, non-host resistance to *P. infestans* and host resistance to *P. capsici* was investigated. Two resistance genes were cloned, and the connection between resistance to these pathogens is discussed.

1.4.1 – The *Phytophthora* genus contains several highly virulent pathogens

Phytophthora species are filamentous oomycetes found within the *Stramenopilia* clade of the kingdom *Chromista* (Beakes et al., 2012, Brasier et al., 2022). The name *Phytophthora* is derived from the Greek for "plant destroyer". The genus is well-known due to its extensive economic impact, being responsible for billions of dollars in control and prevention costs each year (Haverkort et al., 2009). *P. infestans*, the potato and tomato late blight pathogen, was one of the causative agents of the food crisis in the 1840s known as the European potato failure. In Ireland, this resulted in an estimated 750,000 deaths and the displacement of over one million people (Brasier et al., 2022, Zadoks, 2008, Yoshida et al., 2013). Unlike *P. infestans,* which primarily infects tomato and potato, *P. capsici* has a far broader host range, affecting numerous species within the Solanaceae and Cucurbitaceae families across both field and greenhouse conditions, and it can lead to complete crop losses (Sanogo and Ji, 2012, Saltos et al., 2022). *P. capsici* strains also show high genetic diversity compared to the largely clonal populations typical of *P. infestans*, which may relate to the broad range when compared to *P. infestans* which is more specialised and primarily infects potato and tomato (Quesada-Ocampo et al., 2011, Lamour et al., 2012a).

Phytophthora species are hemibiotrophic pathogens. Infection is initiated by the release of single-celled motile zoospores from egg-shaped sporangia. Released zoospores move toward plant tissue and encyst before forming hyphae which penetrate the host. After penetration, the hyphae grow into the host cell and establish an intracellular infection structure. Hyphae move extracellularly and form complex structures known as haustoria through invagination of the host cell (Fawke et al., 2015). Haustoria enable the oomycete to gain proximity to the host plasma membrane and are the sites of secretion of proteins into the host cells. Secreted proteins include effectors, proteases, cell wall degrading enzymes and carbohydrate-active enzymes (CAZymes) (Wang et al., 2018, Wang et al., 2021). After successfully colonising the host, more sporangia are produced. The necrotrophic phase of *Phytophthora* is associated with devastating symptoms, including rotting of the leaf, stem, root, crown or fruit (Fawke et al., 2015). Although both *P. infestans* and *P. capsici* feature a hemibiotrophic lifestyle, they have distinct features, most notably the balance between the biotrophic and necrotrophic phases. *P.*

infestans generally has a biotrophic phase of at least two days, for certain strains, this phase is extended beyond seven days (Vega-Sánchez et al., 2000, Fry, 2008). In contrast, *P. capsici* transitions into a necrotrophic phase after just 24 hours (Jupe et al., 2013b).

Phytophthora are sexual organisms, although the nature of this varies between species. Some are homothallic and can self-fertilise, others are heterothallic and require cross fertilization between different mating types (Brasier et al., 2022). The sexual nature of *Phytophthora* allows for the emergence of new strains through intraspecific and interspecific hybridization. Reshuffling of virulence factors and effectors can lead to breakdown of resistance (Brasier, 2001). Some *Phytophthora* species can also produce oospores or chlamydospores, hardy cells that are able to survive in adverse conditions. These cells enable *Phytophthora* to survive in soil throughout winter and emerge in the following season (Lamour and Hausbeck, 2000).

P. capsici is notable for its rapid adaptation to new hosts and its ability to overcome fungicides. This may be aided by the pathogen's ability to undergo rapid loss of heterozygosity during mitosis. This allows *P. capsici* to fix alleles rapidly, bypassing meiosis and chromosome segregation. Rapid loss of heterozygosity has also been associated with switching from mating type A1 to A2 (Lamour et al., 2012a, Hu et al., 2013). It is unclear how widespread this feature is in oomycetes, but similar observations have been reported in *Phytophthora ramorum* (Vercauteren et al., 2011).

1.4.2 – Effectors and virulence of *Phytophthora spp.*

Like other oomycete and fungal pathogens, *Phytophthora* can be recognised by plants at the cell surface. *P. infestans* apoplastic molecules include INF1 and Pep13/25, which are recognised by the cell-surface immune receptors ELR and PERU respectively (Torres Ascurra et al., 2023, Du et al., 2015a). PERU and ELR both provide only moderate resistance to *P. infestans*.

Many cytoplasmic effectors from *Phytophthora* species have been characterised. Most characterised *Phytophthora* effectors have both an RXLR (Arg-X-Leu-Arg) and an EER motif, as well as a signal peptide. Effectors are secreted across the haustoria and translocate into the host cells by clathrin-mediated endocytosis (Whisson et al., 2007, Gilroy et al., 2011, Wang et al., 2018, Wang et al., 2023b). The exact function of the RXLR motif is unknown. The motif is cleaved from the effector prior to secretion and does not play a direct role in the secretion process, but it could be the site of cleavage before secretion (Wawra et al., 2017).

Within the *P. infestans* reference genome, there are 563 predicted RXLR effectors (Haas et al., 2009, Vleeshouwers et al., 2011).

Several oomycete effectors have been found to lack these motifs. For example, the *Hpa* effectors ATR2 and ATR5, which are recognised by the *A. thaliana* NLRs RPP2 and RPP5, both lack an RXLR motif. Instead, ATR5 features a GRVR (Gly-Arg-Val-Arg) motif, while ATR2 has a GHVR (Gly-His-Val-Arg) motif (Bailey et al., 2011, Kim et al., 2023). Similar non-RXLR effectors are also present in *Phytophthora*. Wood et al. (2020) found that in *P. infestans*, *P. parasitica* and *P. capsici*, there are many effectors which lack either, or both, RXLR and EER motifs. It remains unclear whether these non-RXLR oomycete effectors follow the same secretion and uptake pathways (Wang et al., 2023a). Many of these effectors still contain other conserved folds including the WY and LWY domains, two distinct α-helical protein folds which have been implicated in immune suppression (Zhang et al., 2019, He et al., 2019, Kim et al., 2023).

While known for its historic importance, *P. infestans* remains a devastating plant pathogen. Major gene resistance to *P. infestans* has been a goal for potato breeders for many years. Classical breeding temporarily achieved this by introducing eleven *R*-genes from *S. demissum* into potato. These genes, named *R1-R11* are well characterised and mapped. In addition to *S. demissum*, *Rpi* genes from *S. bulbocastanum* (*Rpi-blb1*, *Rpi-blb2*), *S. berthaultii* (R_{ber}), *S. chacoense* (*Rpi-chc1*) and *S. venturii* (*Rpi-vnt1*) have been identified and bred into commercial potato cultivars. Despite this success, resistance-breaking strains have evolved for many *Rpi* genes, primarily due to single gene deployment and the nature of the fast-evolving pathogen (Vleeshouwers et al., 2011). All these examples use resistance from other hosts of *P. infestans*, non-host resistance could provide a more durable alternative. Wild *Solanum* species to which *P. infestans* is non-adapted are a reservoir of untapped resistance.

1.4.3 – *Solanum americanum* is a non-host to *P. infestans*

To reduce the impact of *P. infestans*, scientists have utilised several wild potato species and more distantly related wild relatives. Potato and its tuber-forming relatives collectively comprise the section *Petota*, which includes over 100 species (Ovchinnikova et al., 2011). Among *Petota* species, *Solanum venturii*, *Solanum bulbocastanum* and *Solanum chacoense* have been studied for resistance to *P. infestans* (Foster et al., 2009, Monino-Lopez et al., 2021, van der Vossen et al., 2005). Species outside of *Petota* are also known to be highly resistant to *P. infestans*. The black nightshade group, also known as the *Morella* clade, comprises 76

species centred in distribution within the tropical Andes (Särkinen et al., 2015). Among these species, the diploid *Solanum americanum* and its hexaploid relative *Solanum nigrum* are both considered non-hosts to *P. infestans* (Colon et al., 1992). *S. americanum* is particularly promising for mapping novel *Rpi* genes due to its diploid, inbreeding nature and broad geographic distribution.

S. americanum has been the source of two major *Rpi* genes, *Rpi-amr1* and *Rpi-amr3*, which confer recognition of the *P. infestans* RXLR effectors AVRamr1 (PITG_07569) and AVRamr3 (PITG_21190). Both are very broad spectrum, and no resistance-breaking strain has been identified for *Rpi-amr1*. While first identified in *S. americanum*, highly similar alleles are also found in *S. nigrum* (Lin et al., 2022, Lin et al., 2020). In recent years, the availability of genomic resources for *S. americanum* has increased substantially. Lin et al. (2023) published the complete genome sequences for four *S. americanum* accessions and characterised the recognition capacity of 52 *S. americanum* accessions against 315 *P. infestans* effectors. Although some of these accessions are susceptible in detached leaf assays, all display field resistance and recognise multiple effectors. This resistance may be quantitative and could be masked in laboratory infection assays, where artificially high inoculum concentrations and pathogen-favourable conditions – such as moderate temperature and high humidity – are applied. These experiments are more suited to detecting qualitative resistance and may not fully represent field conditions, under which *S. americanum* consistently remains resistant.

Using this effectoromics data, three additional *R*-genes against *P. infestans* were cloned from *S. americanum*; *Rpi-amr4*, *R04373* and *R02860* which confer recognition of PITG_22825, PITG_04373 and PITG_02860 respectively. Of these three receptors, a resistance phenotype was confirmed for *Rpi-amr4*. Additional uncloned resistance exists within *S. americanum*; for instance, two resistant accessions (SP2275 and SP3370) do not respond to either AVRamr1, AVRamr3 and AVRamr4.

Cloning additional *Rpi* genes from black nightshades, including *S. americanum*, offers a double benefit. Firstly, new *Rpi* genes will facilitate the development of durable resistance to *P. infestans* in commercial potato and reduce the economic and ecological cost of controlling late blight through application of chemicals. Secondly, we will gain further insights into the mechanism of non-host resistance and determine whether the durability of these *R*-genes is due to the nature of the recognised molecules or is simply due to the stacking of multiple *R*-genes.

1.4.4 – There are no reported *R*-genes against *P. capsici*

Unlike *P. infestans*, characterised resistance to *P. capsici* is limited. *P. capsici* is a very broad range pathogen which infects pepper, tomato, and several cucurbit species. *P. capsici* infects seedlings, leaves, stems, and fruit and can cause 100% yield loss (Sanogo et al., 2022). Currently, *P. capsici* management relies on improving drainage and reducing irrigation. These practices aim to reduce the spread of the pathogen by creating less optimal conditions (Lamour et al., 2012b, Lamour and Hausbeck, 2002). Chemical control is ineffective due to the rapid development of insensitivity, facilitated by the high genetic diversity of this pathogen (Barchenger et al., 2018). Genetic diversity and genome plasticity of *P. capsici* is a result of high outcrossing rates and rapid changes in heterozygosity (Hu et al., 2013). The thick-walled oospores produced by the pathogen are able to persist between seasons in soil. This means that infection can be difficult to remove, and the infecting individuals are genetically diverse due to mating (Bi et al., 2014, Lamour and Hausbeck, 2002, Sanogo et al., 2022). Like *P. infestans*, *P. capsici* has a suite of RXLR effectors used to manipulate host species (Thilliez et al., 2019, Li et al., 2020). There are currently no published *Rpc*- (*RESISTANCE TO PHYTOPHTHORA CAPSICI*) genes.

1.5 – Aims of this thesis

The aim of this thesis is to investigate and understand the basis of resistance to three economically important pathogens of Solanaceae species. In doing so, the diversity and breadth of their recognition was defined and the potential for the deployment of these *R*-genes was investigated.

Chapter 3 describes the cloning and characterisation of Rl_{adg}. This *R*-gene confers strong major gene resistance to potato leafroll virus, a pathogen for which resistance has eluded breeders and molecular geneticists for several decades. Rl_{adg} encodes a TIR-NLR which recognises the serine protease domain of the PLRV protein P1, most likely in a direct manner. Rl_{adg} is also capable of recognising a diverse range of poleroviruses including turnip yellows virus and beet mild yellowing virus. Rl_{adg} could be applied to elevate resistance to these pathogens.

In Chapter 4, novel resistance to *P. infestans* in *S. americanum* accession was investigated. This gene, named *Rpi-amr5*, was mapped to the *Rpi-amr1* cluster and identified as a paralogue of this previously characterised *R*-gene. Additionally, resistance to *P. capsici* in another *S. americanum* accession was mapped and cloned. This gene, named *Rpc2*, was found to be an allele of *Rpi-amr5* which can mediate resistance to both *P. infestans* and *P. capsici.* Both alleles recognise *P. infestans* and *P. capsici* effectors, but only one (*Rpc2*) confers resistance to *P. capsici*. We hypothesise that that is due to an effector capable of suppressing *Rpi-amr5* but not *Rpc2*.

In Chapter 5, additional resistance to *P. capsici* was investigated. Another resistant *S. americanum* accession was found to contain novel resistance. This gene, named *Rpc1,* was mapped to a cluster of NLR-encoding genes on Chromosome 10. Using VIGS, resistance was demonstrated to be due to an orthologue of *Rpi-chc1*. However, no gene in this family confers resistance to *P. capsici* in an *N. benthamiana* transient assay.

Chapter 2: Materials and methods

2.1 – Bacterial strains

2.1.1 – Growth and transformation of *Escherichia coli*

For molecular cloning in *Escherichia coli*, two strains were used: Invitrogen One Shot™ Top10 (ThermoFisher Scientific: C404010), and NEB® Stable (New England Biolabs: C3040H). Strains were transformed, recovered and cultures grown according to the manufacturer's instructions.

Transformed *E. coli* was plated onto lysogeny broth (LB) media containing the appropriate selection antibiotics. Where applicable, blue/white colony selection was performed by spreading 4 µl of 1 M isopropyl β-D-1-thiogalactopyranoside (IPTG) and 40 µl of 60 mg/ ml 5-bromo-4-chloro-3-indolyl β-D-galactopyranoside (X-Gal) onto the plate 20 minutes prior to plating of bacteria. After overnight growth at 37 °C, single colonies were selected for subsequent applications.

2.1.2 – Growth and transformation of *Agrobacterium tumefaciens*

For plant transformation and transient expression assays, two *Agrobacterium tumefaciens* strains were used. Agl1 was used in all *Solanum* transformations, and GV3101(PMP90) was used for all *A. thaliana* transformations. For transient expression assays, either GV3101(PMP90) or Agl1 were used. The Agl1 strain was used for vectors carrying NptII bacterial selection, and GV3101(PMP90) was used for vectors carrying AmpR. Cultures were grown at 28 °C in LB media containing rifampicin and additional antibiotics determined by the plasmid-carried selection marker (concentrations of antibiotics are indicated in Table 2.1).

For transformation of these non-commercial *A. tumefaciens* strains, 50 µl of cells (~5 x 10^8) were transformed in 0.1 cm cuvettes using a micropulser (BioRad) with settings recommended by the manufacturer. Bacteria was resuspended in 400 µl LB and incubated at 28 °C for 2 hours. After incubation, 40 µl of culture was plated onto selective media and incubated for 48 hours at 28 °C. Once visible, single colonies were selected for downstream applications.

For long-term storage of *A. tumefaciens* strains, glycerol stocks were generated. 10 ml cultures were pelleted by centrifugation and resuspended in 1.5 ml of 20% glycerol. The stocks were snap-frozen in liquid nitrogen and stored at -80 °C until required.

2.2 - Oomycete strains

2.2.1 – *Phytophthora infestans*

In this project, two *P. infestans* strains were used. For infection of *S. lycopersicum*, the strain 90128 was used, and in all other instances, the strain 88069 was used. Both strains were maintained at 17 °C on rye-sucrose agar (RSA) media. To induce zoospore release, 14-day-old plates were flooded with cold water and left at 4 °C for at least 1 hour. The concentration of the zoospore suspension was measured using a haemocytometer before dilution to the appropriate concentration (as indicated in figure legends).

2.2.2 – *Phytophthora capsici*

For all *P. capsici* infection assays, the strain LT1534 was used. *P. capsici* was maintained on plates of V8 media in a 25 °C incubator. To induce zoospore release, 10-day-old plates were flooded with cold water and incubated at 4 °C for 1 hour, then at room temperature for 1 hour. After measuring the concentration of zoospores using a haemocytometer, the suspension was diluted to 10,000 spores ml^{-1}. This concentration was used for all *P. capsici* infection assays.

2.3 - Viral material

2.3.1 – Potato leafroll virus (PLRV)

Two clones of potato leafroll virus were available. PLRV-Puc18, was provided by Professor Michael Taliansky (James Hutton Institute) and used as a template for PLRV ORF cloning. The second clone, PLRV-Hutton, was used for *N. tabacum* infection experiments (Cowan et al., 2023).

2.3.2 – Beet mild yellowing virus (BMYV) and turnip yellows virus (TuYV)

An infectious clone of TuYV was used for *N. tabacum* infection assays. The TuYV clone was produced and supplied courtesy of Professor John Walsh (University of Warwick). Transient expression of the TuYV clone was performed using a transformed *Agrobacterium* strain.

BMYV infection of *Arabidopsis thaliana* was performed by transfer of aphids from infected sugar beet material. Infected sugar beet was provided by the BBRO (British Beet Research Organisation).

2.3.3 – Viral genomic resources

Viral genomes used in this project are all publicly available and were obtained through GenBank. The PLRV genomes used as listed in Appendix 1, additional polerovirus genomes used are listed in Appendix 2. Enamovirus reference sequences are listed in Appendix 3.

2.4 - Plant material

2.4.1 – Conditions for growth of *Solanum species*

All *Solanum* species using in this project (*S. americanum*, *S. tuberosum*, *S. lycopersicum*, *S. villosum*, *S. scabrum*, and *S. nigrum*) were grown in glasshouse conditions. Plants were grown in the same conditions for all applications - detached leaf assays, seed bulking, crossing etc.

2.4.2 – *Solanum tuberosum*

In most *S. tuberosum* assays, the potato cultivar Maris Piper was used. Stable transformation was performed following the previously described methods (Witek et al., 2016). For each transformed construct, at least thirty independent transgenic lines were phenotyped before a minimum of two lines were retained for further characterisation.

For the cloning of Rl_{adg}, described in Chapter 4, The PLRV-resistant *S. tuberosum ssp. andigena* accession LOP-868 was used. In addition to this accession, DNA extractions from PLRV-resistant accessions HUA-332 and OCH-7643 were available; as well as DNA from 153 dihaploids (34 susceptible and 119 resistant). These materials were supplied by Hannele Lindqvist-Kreuze (International Potato Center, Peru).

2.4.3 – *Solanum lycopersicum*

In *S. lycopersicum* assays, the cultivar Moneymaker was used. Transgenic plants were generated following the previously published protocol (Fillatti et al., 1987).

2.4.4 – Collections of wild *Solanum spp.*

Collections of *Solanum americanum, Solanum nigrum, Solanum villosum and Solanum scabrum* were used in this project. The 52 *S. americanum* accessions were collected from a variety of seed banks and were previously described in publications (Witek et al., 2016, Witek et al., 2021, Lin et al., 2023). The major accessions used in this study are SP1102, SP2271, SP2275 and SP2308. Nine *S. villosum*, thirty-three *S. nigrum* and four *S. scabrum* accessions were also used. *S. nigrum* accessions were described previously (Lin et al., 2022). The *S. villosum* and *S. scabrum* accessions are described in Appendix 4 and Appendix 5.

S. americanum transformation was performed following the method described by Lin et al. (2023). For each transformation, thirty independent transgenic lines were initially phenotyped before a minimum of two lines were retained for further characterisation.

2.4.5 – *Nicotiana tabacum* and *Nicotiana benthamiana*

N. benthamiana and *N. tabacum* lines were sown and grown in a controlled environment room (CER) with conditions maintained at 22 °C, 45-65% relative humidity, and 16-hours of light per day. *N. benthamiana* lines included the *nrc234* mutant (Witek et al., 2021), an *eds1* mutant (Schultink et al., 2017), and a wild-type line. The wild-type *N. tabacum* used in this study is *N. tabacum cv.* Petit Gerard. Transgenic *N. tabacum* was produced following the protocols described by (Clemente, 2006).

2.4.6 – *Arabidopsis thaliana*

The *A. thaliana* accession Col-0 was used as the background for the transgenics in this thesis. Plants grown for genotyping and selection were sown on compost and grown in a CER in short-day conditions, with 10 hours of light and 14 hours of dark. The CER was maintained at a temperature of 20 °C and 70% relative humidity. For seed collection, plants were moved to long-day conditions of 16 hours of light and 8 hours of dark, at 20 °C and 70% relative humidity.

2.4.7 – Plant genomics resources

Whole-genome assemblies used in this project are all previously published. They include assemblies of four *S. americanum* genomes (Lin et al., 2023), two *S. nigrum* genomes (Wu et al., 2023, Lee et al., 2023) and forty-seven *S. tuberosum* genomes (Wu et al., 2023, Hardigan et al., 2016).

Sixteen SMRT RenSeq datasets generated from *S. americanum* accessions are previously published (Witek et al., 2016, Witek et al., 2021, Lin et al., 2023). During this project, additional SMRT RenSeq datasets were generated for *S. tuberosum* landrace LOP-868, *S. americanum* accession SP2297, and *S. villosum* accessions SP3057, SP3059 and SP3065.

2.5 – General chemicals, antibodies and media

2.5.1 – Liquid and solid lysogeny broth (LB) media

Growth of *E. coli* and *A. tumefaciens* was performed in LB media, composed of 1% (w/v) tryptone, 1% (w/v) sodium chloride and 0.5% (w/v) yeast extract in water. For liquid media, the total volume was autoclaved without agar. For solid media, 1.5% (w/v) agar was added prior to autoclaving. For bacterial selection, the media was cooled before the addition of antibiotics.

2.5.2 – Rye-sucrose agar (RSA)

RSA media was used for the maintenance of *P. infestans* strains. Dry rye grains (6%, w/v) were soaked in a 1/40 dilution of 10% chlorite (thin bleach) for four minutes before being rinsed thoroughly in water. Sieved grains were left covered in water overnight to germinate. The next day, grains were ground and transferred to a Duran bottle and mixed with water to near final volume before being heated for 3 hours at 50 °C. The mixture was then filtered through a sieve before addition of sucrose (2%, w/v), water and agar (1.5%, w/v). The final volume was autoclaved before use.

2.5.3 – V8 juice agar

V8 juice agar was used for the maintenance of *P. capsici*. V8 juice agar was composed of 10% (v/v) V8 juice, 0.1% (v/w) calcium carbonate, 0.0065% (w/v) β-sitosterol and 1.5% (w/v) agar. Before use the mixture was autoclaved.

2.5.4 – Murashige and Skoog media (1/2 MS)

For plant tissue culture, ½ Murashige and Skoog (MS) media was used. Media was prepared by autoclaving 0.22% (w/v) MS salts, 0.5% sucrose (w/v) and 1% (w/v) agar in water.

2.5.5 – Antibiotics

Several antibiotics were used for bacterial and plant selection. Stock and working concentrations are listed in Table 2.1. Antibiotic stock solutions were filter-sterilised (0.3 μm) and stored at -20 °C, except for rifampicin which was stored at 4 °C.

Table 2.1. Antibiotic stock and working concentrations used in this project.

Antibiotic	**Stock concentration (mg ml^{-1})**	**Working concentration (μg ml^{-1})**	
		E. coli	***A. tumefaciens***
Carbenicillin	100 (dissolved in water)	100	100
Gentamycin	10 (dissolved in water)	-	20
Kanamycin	50 (dissolved in water)	50	50
Rifampicin	10 (dissolved in methanol)	-	50
Spectinomycin	100 (dissolved in water)	50	50

2.6 – Molecular Biology methods

2.6.1 – Genomic DNA extraction from plants

Two DNA extraction methods were used depending on the end use. DNA used in sequencing library preparation was extracted using the QIAGEN DNeasy Plant Mini Kit according to the manufacturer's instructions.

DNA extraction for marker screening was performed using a modified CTAB extraction protocol. Leaf tissue (approximately 300 mg) was crushed in liquid nitrogen and mixed with CTAB extraction buffer (2% w/v CTAB, 100 mM Tris-HCl, 20 mM EDTA, 1.4 M NaCl, 1% v/v BME, 1% w/v PVP) before incubation for 1 hour at 65 °C. Chloroform was added in a 1:1 ratio before vortexing and centrifugation for 20 minutes at 6,000 rpm. The supernatant was treated with RNase A (ThermoFisher Scientific: R1253) for 1 hour at 37 °C before chloroform extraction was repeated. Isopropanol (0.8X volume) was used to precipitate DNA from the extracted aqueous phase, the mixture was incubated for 10 minutes at -20 °C. Precipitated DNA was dissolved in 0.1X TE after centrifugation and removal of supernatant.

2.6.2 – Polymerase chain reaction

Polymerase chain reaction (PCR) was used to amplify DNA for use in molecular cloning, or in genetic marker analysis. Oligonucleotides used in PCR were synthesised by Sigma-Aldrich or IDT. Oligonucleotides were resuspended in water and diluted to 100 µM before storage at -20 °C. For all PCR reactions, annealing temperatures were determined using tools to predict melting temperatures (T_m) built into Geneious Prime (Geneious Prime 2023.1.2 https://www.geneious.com). Elongation times were determined based on the target length and the polymerase manufacturer's advice. Different polymerases were used for specific purposes, as detailed below.

When amplifying DNA for molecular cloning, high-fidelity polymerases were used. For Golden Gate, KAPA HiFi HotStart ReadyMix (Roche: KK2601) was used. For USER cloning, KAPA HiFi HotStart Uracil+ReadyMix (Roche: KK2801) was used. Reaction components and conditions were determined according to the manufacturer's instructions, target products and primer design. Marker screening and colony PCR were performed using NEB Taq Polymerase (New England Biolabs: M0273S) and the standard PCR buffer provided. Thermocycler conditions used for each polymerase are shown in Table 2.2, and Table 2.3.

When cloning large fragments from complex *R*-gene clusters, nested PCR was used. Primers flanking the target were used in an initial PCR. Size-verified product (diluted 1 into 200 µl water) was then used as a template for amplifying the target fragment.

Table 2.2. Thermocycling conditions for KAPA Uracil or KAPA HiFi readymix PCRs.

Reaction step	Temperature °C	Time
Denaturation	98	5 minutes
25 cycles	98	30 seconds
	Annealing temperature determined using predicted T_m	30 seconds
	72	1 minute per kb
Final extension	72	10 minutes
Hold	16	-

Table 2.3. Thermocycling conditions for NEB Taq polymerase.

Reaction step	Temperature °C	Time
Denaturation	95	5 minutes
30 cycles	95	30 seconds
	Determined using predicted T_m	30 seconds
	68	1 minute per kb
Final extension	68	5 minutes
Hold	16	-

2.6.3 – Agarose gel electrophoresis

To visualise DNA, agarose gel electrophoresis was used. Gels used contained 1% (w/v) agarose, ethidium bromide (0.5 µg/ml) and TAE (40 mM Tris-acetate pH 8.0, 1 mM ethylenediaminetetraacetic acid). Prior to loading, DNA was mixed with an NEB Gel Loading Dye (New England Biolabs: B7024S). To identify the sizes of DNA, the 1 kb Plus DNA Ladder (New England Biolabs: N3200S) was run alongside samples. Electrophoresis was performed in TAE buffer at 100 V before visualisation under UV light.

2.6.4 – Purification of DNA from an agarose gel

All DNA fragments used in molecular cloning were purified from agarose gels. The DNA bands of interest were cut from the gel after electrophoresis, with care taken to minimise exposure to UV light. Isolation of DNA from these fragments was performed using Machery-Nagel™ Nucleospin™ Gel and PCR Clean-up kits following the manufacturer's instructions.

2.6.5 – Gene synthesis

Where no template DNA was available for PCR, gene synthesis was used. Synthesis was performed by Twist Biosciences. Required DNA sequences were retrieved from published sequences available on Genbank or published reference genomes. Sequences were 'domesticated' to remove BbsI and BsaI sites (see 2.6.7) and Golden Gate compatible overhangs were added to the sequence to allow direct cloning into appropriate vectors.

2.6.6 – Golden Gate cloning

Through Golden Gate assembly, multiple modules can be assembled into an acceptor vector simultaneously using type II restriction endonucleases and T4 DNA ligase. Distinct 4 bp overhangs were designed at junctions to ensure correct assembly. The digestion and ligation (diglig) reaction contained 5 U of either BsaI-HF® (New England Biolabs: R3733S) or BbsI-HF® (New England Biolabs: R3539S), 400 U T4 DNA Ligase (New England Biolabs: M0202S), 1.5 µl T4 ligase buffer, 1X bovine serum albumin (New England Biolabs: B9000S). For each reaction, 100 ng of acceptor vector was included, insert DNA was included in a 2:1 molar ratio of insert: acceptor.

Water was added to a total volume of 20 µl. The diglig reaction was as follows: 20 cycles of 3 minutes at 37 °C and 4 minutes at 16 °C following incubation periods of 5 minutes and 30 seconds at 50 °C, 5 minutes at 80 °C and 20 minutes at 16 °C. The reaction was performed in a thermocycler. After completion, 1 µl of the reaction was used for the transformation of *E. coli*.

2.6.7 – Domestication, domain swaps and point mutation

For successful Golden Gate cloning, inserts must lack BsaI and BbsI sites. Where these sites are present, 'domestication' was performed to remove them. To domesticate sequences, single nucleotides were changed to abolish recognition without altering the amino acid sequence. These changes were incorporated through the fusion of multiple PCR products in the diglig reaction. In cases where many sites are present in a gene, level-minus-1 plasmids were used to clone these fragments before level-0 assembly. Where domain swaps or point mutations were made, a similar approach was taken to alter a single base or join two fragments together.

2.6.8 – USER Cloning

In some instances, USER cloning was applied to circumvent the need for gene domestication. USER cloning enables single or multiple-fragment ligation independent of restriction sites within cloning targets. 10 µl ligation reactions contained 30 ng KAPA-uracil PCR products, 30 ng linearised USER compatible vectors, 1 µl Cutsmart® buffer, 400 U T4 DNA Ligase (New England Biolabs: M0202S) and 1 U USER® Enzyme (New England Biolabs: M5505S). Ligation mixtures were incubated at 37 °C for 30 minutes and at room temperature for 90 minutes. 2.5 µl of the ligation reaction was used for the transformation of chemically competent *E. coli*.

pICSLUS0004_OD was used as the USER acceptor vector to express genes under the CaMV *35S* promoter and *A. tumefaciens Ocs* terminator. The custom USER vector pICSLUS0005_OD was generated to express candidates under *S. americanum NRC4a* regulatory elements (cloned from SP1102). The backbone used in this custom vector was derived from pICSL86900_OD.

When cloning large fragments (> 5 Kb) by USER, single insert cloning was attempted. When unsuccessful, USER-FUSION was performed. An overlap of 11 bp starting with adenine and ending with thymine was selected approximately in the middle of the gene. Primers were designed as specified by (Geu-Flores et al., 2007), with the eleventh base (thymine) being replaced with uracil. The two PCRs were then added into a single ligation reaction.

2.6.9 – USER vector linearisation

For the successful application of USER cloning, linearised vectors must be used. USER-compatible vectors (2.5 µg) were linearised by digestion using 25 U PacI (New England Biolabs: R0547S) in 1x Cutsmart® buffer (25 µl total volume) for 2 hours at 37 °C. Next, 20 U Nt.BbvCI (New England Biolabs: R0632S) was added and the reaction was incubated for another 2 hours at 37 °C. After the incubation, the enzymes were deactivated by incubation at 80 °C for 20 minutes. Digested plasmid was run on a 1% agarose gel, the linearised band was purified using the method described in 2.6.4.

2.6.10 – Plasmid screening, purification, and validation

To enable the isolation of individual ligation events, USER and Golden Gate ligation reactions were transformed into *E. coli* and as described in 2.1.1. Colonies were screened by PCR using NEB Taq polymerase and the conditions described in 2.6.2. The primer pairs were designed to span a junction between the backbone and insert. Positive colonies were used to inoculate 10 ml liquid LB cultures that were grown overnight at 37 °C. Plasmid purification was performed using the Machery-Nagel™ Nucleospin™ Mini kit for plasmid DNA, following the low-copy protocol.

To confirm that assembled plasmids contained all inserts, restriction digestion was performed. Digestion reactions were performed according to the enzyme used and the manufacturer's instructions. Generally, 200 ng of DNA is used as input and digested DNA was visualised by gel electrophoresis after 1 hour of incubation with the appropriate enzyme.

If the digested plasmid size appeared to be correct, the insert sequence was validated through the Sanger sequencing service by Genewiz. Pre-mixed reactions of 500 ng DNA and 2.5 uM primer in molecular biology-grade water were prepared. Results were visualised in Geneious Prime. The resulting basecalling and quality scores were used to determine mutations or SNPs in amplified or cloned DNA.

2.6.11 – RNA extraction and cDNA synthesis

RNA extraction and cDNA synthesis were used to prepare samples for cDNA RenSeq libraries or as a template for PCR. RNA was extracted using the QIAGEN RNeasy Plant Mini Kit and quality was assessed through gel electrophoresis. DNase treatment was performed using the TURBO DNA-free™ Kit (ThermoFisher Scientific: AM1907) following the stringent protocol. First-strand cDNA synthesis was performed using the Superscript™ IV Reverse Transcriptase (ThermoFisher Scientific: 18090010) protocol. For comparative analysis of expression by PCR, the first-strand synthesis reaction was used directly as a template. For the generation of sequencing libraries, second-strand synthesis was performed.

Second-strand cDNA synthesis was performed following the protocol described by Bjornson et al. (2020). The single-strand cDNA was mixed with 1x *E. coli* ligase buffer, 1x additive (20 mM Tris-HCl, 1 mM $MgCl_2$), 0.05 U/µl RNase H (ThermoFisher Scientific: EN0201), 0.4 U *E. coli* DNA Polymerase I (New England Biolabs: M0209S), 0.1 U/µl *E. coli* DNA Ligase (New England Biolabs: M0205S) and 0.2 mM dNTPs. The second-strand synthesis reaction

was performed as follows: 2.5 hours at 16 °C before addition of 20 U Exonuclease I (New England Biolabs: M0293S) and incubation at 37 °C for 30 minutes. Next, the reaction mixture was combined with 5 µl 0.5 M EDTA (pH 8.0) and 1 µl (10 mg/ml) RNase A (ThermoFisher Scientific: R1253) and incubated at 37 °C for 30 minutes. Double-stranded cDNA was cleaned using 1X AMPure XP Beads (Beckman Coulter: A63881) and sheared using Covaris S2 following the microTUBE protocol for 1 kb fragment sizes with the treatment time reduced to 7 seconds.

2.6.12 – Enrichment library preparation

Input for the DNA shearing was prepared using the Zymo Genomic DNA Clean & Concentrator-10 kit (Zymo Research: D4010). Both short and long fragment enrichment libraries were prepared according to the published RenSeq protocol (Witek et al., 2016). Modifications from this protocol were used for generating Illumina libraries: Covaris shearing (as described by the manufacturer), size selection through AMPure beads (increased from 0.4X to 1.0X) and PCR extension times (reduced to one minute).

Enrichment for NLR encoding genes was performed using the V4 RenSeq bait library (Witek et al., 2021, Seong et al., 2020). For SMRT RenSeq library preparation, 700 ng of enriched library was used as an input for the SMRTbell Prep Kit 3.0 (Pacific Biosciences: 102-182-700). The generated libraries were sequenced on a PacBio v3 SMRT cell at the Earlham Institute.

Illumina RenSeq libraries generated in the *Rl_{adg}* project were sequenced using the MiSeq 250 bp paired-end sequencing platform at the Earlham Institute. Illumina RenSeq libraries generated to identify *Rpi-amr5* and *Rpc2* were sequenced by Novogene using the MiSeq 250 bp paired-end platform. cDNA enrichment libraries were sequenced using the HiSeq 250 platform by Novogene.

2.6.13 – Targeted gDNA enrichment using Xdrop

Targeted gDNA enrichment of the *Rpi-amr3* locus in *S. americanum* (accession SP1102) and the *Rl_{adg}* locus in *S. tuberosum* (accession LOP-868) was carried out using the Xdrop technique developed by Samplix (Samplix ApS, https://samplix.com/). This method isolates individual DNA molecules using target-specific primers and flow cytometry. High molecular weight gDNA was extracted from leaf tissue following the protocol in section 2.6.1, with two modifications: 5 g of leaf tissue was used instead of 300 mg, and gDNA was precipitated by

spooling onto a glass rod to minimise shearing rather than using centrifugation. DNA length was compared with linear lambda phage DNA on a 2% agarose gel, extracts exceeding 50 Kb were used as input for Xdrop.

All enrichments using this technique were performed by Samplix using probe primers designed at TSL. These primers targeted short sequences (80-120 bp) located near the regions of interest. Enriched samples were sequenced on the Nanopore platform, and reads were assembled using the Flye assembler. Assemblies were manually investigated to identify contigs containing target amplicons and known sequences (Kolmogorov et al., 2019).

2.7 – Bioinformatic methods

2.7.1 – Assembly and annotation of SMRT RenSeq libraries

SMRT RenSeq datasets produced in this project were assembled using software built into Geneious Prime. Reads with less than 80% homology to any RenSeq bait were removed (by BLAST homology search). The remaining reads were trimmed by 200 nt to stringently remove multiplexing adapters. *De novo* assembly was performed using customised settings - maximum mismatches of 1% per read, 1% gaps per read (maximum 3 bp) and a maximum ambiguity setting of 16. These stringent settings aimed to prevent the collapse of paralogues that can be observed during the assembly of large and highly repetitive NLR families. After assembly, filtering was applied to remove any contigs composed of fewer than 20 reads. The remaining contigs were trimmed at regions where fewer than five reads provided support.

Once assembly was completed, the annotation of NLR-encoding genes was performed using NLR-parser (Steuernagel et al., 2015). NB-ARC lists generated by NLR-parser were used in tree construction to determine the phylogenetic relationship between candidates and previously cloned NLRs. Gene models were manually annotated using cDNA RenSeq reads that were mapped to SMRT RenSeq assemblies (as described below).

2.7.2 – Illumina RenSeq mapping and candidate *R*-gene identification

Bulked segregant analysis was performed using previously described methods (Jupe et al., 2013a, Andolfo et al., 2014, Witek et al., 2016). In short, Illumina RenSeq reads were mapped against the assembly using BWA before polymorphisms were identified using Samtools mpileup. The resulting output was used to filter for contigs with allele ratios expected within each parental and bulk group.

In Chapter 3, for identification of Rl_{adg}-linked contigs, detection of near absence from bulk susceptible data was performed. This was detected by searching for reduced coverage of mapped reads from the bulk susceptible dataset but maintained coverage in the bulk resistant dataset. This filtering was performed following the read mapping described above. SAM files were inspected and the number of reads from each read group mapping to each contig counted using tools built into The Sainsbury Laboratory (TSL) customised Galaxy platform. Data was initially filtered to ensure at least 100 reads from the bulk resistant and LOP-868 groups were mapped, and then to retain only contigs showing duplex dosage in LOP-868 data and absence in the bulk susceptible data.

After identifying resistance-linked contigs by either approach described above, candidates were further filtered by the presence of motifs identified using NLR-parser, and when available, by using cDNA RenSeq to determine whether the candidates are expressed. To detect expression, cDNA RenSeq reads were mapped using HISAT spliced aligner under standard settings (Kim et al., 2015). BAM files were visualised using IGV to define expression and identify splice variants.

2.7.3 – Phylogenetic tree construction

All phylogenetic trees shown were constructed in Geneious Prime. Alignments were produced using ClustalW. Trees were generated using the Neighbour-Joining method following the Jukes-Cantor genetic distance model. For each branch point, bootstrap values were calculated following 1,000 iterations. Unless otherwise stated, phylogenies of NLRs were produced using NB-ARC sequences identified by NLR parser.

A library of previously characterised NLRs was used to show the relatedness of candidates to NLRs from other studies. *Capsicum*, *Nicotiana* and *Solanum* NLRs were extracted from the sequences compiled by (Kourelis et al., 2021).

2.7.4 – Design of CRISPR sgRNAs

To knock out candidate genes, Cas9-compatible guide RNAs were designed using the software built into Geneious Prime. Guides were generated (PAM = NGG) with a maximum of 3 mismatches allowed against a reference dataset (either whole genome or SMRT RenSeq, depending on the accession used). Once generated, these guides were filtered to select guides with the fewest off-target hits, and the greatest activity score (Doench et al., 2016). Two guides were selected for each CRISPR construct.

Constructs were designed using the same components as Lin et al. (2023). Guide sequences were cloned into level-1 vectors with U6-26 promoters (pICSL90002). Level-2 constructs were assembled containing *35S:NPTII:Nos* (pICSL11055, position-1), *AtUbi10:Cas9(with_introns):rbcS-E9t* (pICSL11197, position-2), guide RNAs (positions -3, -4, -5, -6) and an endlinker (pICH41822). pICSL4723__OD was used as an acceptor.

2.7.5 – Design of VIGS fragments for cluster-wide and paralogue-specific silencing

To test candidate *R*-genes, virus-induced gene silencing (VIGS) was used. To identify sequences suitable for VIGS, candidate CDS sequences were aligned using ClustalW and manually inspected. To silence whole clusters, highly conserved regions of NB-ARC-encoding sequence were used. These fragments were relatively large (between 200 and 300 bp). To silence individual paralogues, the least conserved regions were identified. These regions were generally shorter (between 60 and 150 bp) and found within the LRR-encoding region. A conservative approach was used to define off-target silencing: the candidate region was divided into 21-mer sequences, off-target hits were defined as those where fewer than 2 SNPs were present within these 21-mer sequences (i.e. $\geq$90.5% identity).

2.8 – Plant biology methods

2.8.1 – Preparation of *A. tumefaciens* for transient expression assays

Agrobacterium strains were struck out onto LB agar plates which contained the appropriate antibiotics, plates were incubated at 28 °C for 36-48 hours. Cells were scraped from plates and resuspended in the infiltration buffer ($MgCl_2$-MES, pH 5.6). A dilution (1 in 20) of cells was used to measure the OD_{600} in a spectrophotometer. Next, the original suspensions were

diluted to the concentrations required for each experiment and combined as required (concentrations used are indicated in figure legends). Prior to the infiltration, acetosyringone (500 μM) was added to each *Agrobacterium* suspension.

2.8.2 – *Agrobacterium* infiltration for hypersensitive response assays

Agrobacterium suspensions were prepared as described in 2.8.1. For HR assays, leaves were spot-infiltrated with *Agrobacterium* suspensions. When multiple infiltrations on a single leaf were performed, care was taken to avoid overlapping infiltration. For HR assays in *N. benthamiana*, *N. tabacum*, *S. americanum,* and *S. villosum*, expanded leaves were selected from plants that were between five and six weeks old. Leaves were infiltrated using 1 ml needleless syringes. Plants were left for 3-5 days for cell death to develop.

For successful transient expression in *S. tuberosum*, plants were propagated in tissue culture, and rooted in 1% MS media for two weeks before being moved to compost. After another two weeks, leaves were infiltrated as described above.

2.8.3 – Transient assays to test *Rpi* and *Rpc* gene candidates in *N. benthamiana*

To test candidate *Rpi* and *Rpc* genes, transient expression was performed prior to infection of *N. benthamiana* leaves. *Agrobacterium* suspensions were prepared as described in 2.8.1. When *N. benthamiana* plants were between five and six weeks old, infiltration of whole leaves was performed. Leaves were left for 24 hours before being removed and drop-inoculated as described in 2.8.6.

2.8.4 – *N. benthamiana in planta* split luciferase assay

To assay for *in planta* association between NLRs and their cognate effectors, a split luciferase assay approach was taken. NLR proteins were tagged with a C-terminal fragment of luciferase (pICSL50048), effectors were tagged with an N-terminal luciferase fragment (pICSL50047). Using Golden Gate, CDS sequences were cloned into the pICSL86922 vector which contains the CaMV *35S* promoter and *Ocs* terminator. *Agrobacterium* strains carrying these constructs were spot-infiltrated into an *N. benthamiana* mutant line where cell death would be abolished. When TIR-NLRs were used in this assay, *eds1* KO lines were used, for NRC-dependent CC-NLRs, the *nrc234* line was used.

Two days after co-infiltration, leaves were removed for imaging. Immediately before imaging, 100 mM sodium citrate buffer containing 0.4 mM luciferin was infiltrated into the leaf. Luminescence was visualised using the Nightowl II LB 983 In vivo imaging system and the Winlight software (Berthold Technologies, Germany). As a control for TIR-NLR interaction, the *S. stoloniferum* NLR Ry_{sto} and the potato virus Y coat protein were used (Grech-Baran et al., 2019, Grech-Baran et al., 2022). For CC-NLRs, the *S. americanum* NLR Rpi-amr3 and Avramr3 were used as a control (Witek et al., 2016, Lin et al., 2022).

2.8.5 – Virus-induced gene silencing (VIGS) of *S. americanum* and *S. villosum*

Gene fragments, designed as described in 2.7.5, were cloned into a BsaI-compatible TRV2 vector (Duggan et al., 2021). VIGS of *S. americanum* was performed by vacuum infiltration of seedlings between 2-5 days post-germination. *Agrobacterium* suspensions of TRV1 and TRV2 (containing the silencing target fragment) were mixed in a 1:1 ratio to a final OD_{600} of 0.3. Before infiltration, acetosyringone (500 μM) and Silwet-L77 (0.1 μl/ ml) were added.

Seedlings were transferred from compost into the *Agrobacterium* suspension, a vacuum was applied for one minute, before being released. Vacuum infiltration was repeated two more times. Seedlings were then moved into compost and grown in a CER at 17 °C for 7 days before being transferred to glasshouse conditions. When plants were five weeks old, leaves were selected and drop-inoculated as described in 2.8.6. To confirm the efficacy of gene silencing, a fragment from the gene encoding the magnesium-chelatase subunit ChIH was used. Silencing of this gene results in tissue bleaching, acting as a marker for successful silencing.

2.8.6 – Detached leaf assays of *Solanum* and *Nicotiana* species

Detached leaf assays were used to assess the resistance of *Solanum* and *Nicotiana* species to *P. infestans* and *P. capsici*. Fully expanded leaves from five- to six-week-old plants were placed onto damp paper lining 500 cm^2 square culture dishes. From a suspension of induced zoospores (induced as described above), 10 μl droplets were pipetted onto each leaf. For *P. infestans* infection, trays were incubated at 17 °C for 5-10 days until susceptible controls showed infection. For *P. capsici* infection, trays were incubated at 25 °C for 2-4 days until susceptible controls showed infection.

2.8.7 – *N. tabacum* infection using polerovirus infectious clones

Infectious clones of PLRV and TuYV were used to assay resistance in transgenic *N. tabacum* lines. For each plant, a whole leaf was infiltrated with a 0.3 OD_{600} suspension of *Agrobacterium.* After 2 weeks, 1 cm leaf discs were taken from the three leaves above the infiltration site. cDNA from this tissue was generated (as described in 2.6.11) and tested for presence of the virus by PCR. Primers used to amplify each virus and a housekeeping gene are shown in Table 2.4.

2.8.8 – Testing *A. thaliana* for resistance to BMYV

Arabidopsis thaliana transgenic lines were tested for resistance to BMYV using an aphid infestation assay. *A. thaliana* seeds were germinated on soil and plants grown for 5 weeks in short-day conditions to prevent bolting. At the five-week stage, aphids were transferred from sugar beet infected with BMYV. For each plant, five aphids were transferred to a single leaf and were contained within a clip cage. After 10 days, the caged leaves were removed and discarded. Plants were grown for a further five days, before samples were harvested (15 days post-aphid transfer). Additional samples were taken at weekly intervals. Samples were processed and tested as described in 2.6.11 and 2.8.7 using oligonucleotides shown in Table 2.4. Maintenance and transfer of aphid colonies was performed by the John Innes Centre Insectary team.

Table 2.4. Oligonucleotides used to detect infection by poleroviruses. Oligonucleotide pairs were designed to amplify either PLRV, BMYV, or TuYV. Additional pairs were designed to amplify the control genes from *Arabidopsis thaliana* and *Nicotiana tabacum*.

ID	Oligonucleotide sequence (5' to 3')	Target and annealing temperature
BMYV_F	GAAGAAGACGACCACGTAGGCAAACGC	BMYV movement protein ORF
BMYV_R	GTAATCCCGAACTTGTTGATAGTTGATGAAAGGGC	412 bp expected size. 65 °C annealing temperature.
PLRV_F	GGTGGTGTACAACAACCAAGAAGGCGAA	PLRV movement protein ORF
PLRV_R	GTAATTTGGAACTTGTTGACGTAGGACTGGAGG	378 bp expected size. 65 °C annealing temperature.
TuYV_F	GAAGACGACCACGGAGGCAAGCAC	TuYV movement protein ORF
TuYV_R	GTGATCCCGAATTTGTTGATAGTTGAGGAAAGGGA	409 bp expected size. 65 °C annealing temperature
AtEF1α_F	CAGGCTGATTGTGCTGTCCTTA	*Arabidopsis thaliana EF1α.*
AtEF1α_R	GTTGTATCCGACCTTCTTCAGG	231 bp cDNA product, 324 bp gDNA product. 53 °C annealing temperature.
RH_797	GAAAAGACGGATGTGTTTGGCTATG	*Nicotiana tabacum SERK3.*
RH_798	TCATCTTGGCCCCGACAATTC	432 bp product. 59 °C annealing temperature.

Chapter 3: Broad-spectrum polerovirus resistance is conferred by an *S. tuberosum* TIR-NLR immune receptor

3.1 – Introduction

Poleroviruses, which belong to the family *Solemoviridae*, are RNA viruses that infect many crop species and cause significant yield losses. The control of poleroviruses is mostly achieved by spraying broad-spectrum insecticides that decrease the population of the aphid vector (Macleod et al., 2023, Mondal et al., 2017). Among the economically important poleroviruses, the type species – potato leafroll virus (PLRV) – causes stunting and net-necrosis in tubers. Co-infection with other viruses increases infection severity, resulting in greater viral titre and more severe symptoms (Barker, 1987, Savenkov and Valkonen, 2001). Other poleroviruses infect important crops including oilseed rape (*Brassica napus subsp. napus*) and sugar beet (*Beta vulgaris var. saccarifera*). These viruses include turnip yellows virus (TuYV) and beet mild yellowing virus (BMYV) (Macleod et al., 2023).

Currently, there are no cloned resistance genes to PLRV or any other poleroviruses. Furthermore, no NLRs have been reported to detect phloem-limited pathogens. This chapter details the mapping, identification and cloning of Rl_{adg}, an *R*-gene that was reported to confer strong resistance to PLRV in an Andean landrace of potato (*Solanum tuberosum ssp. andigena*) (Velasquez et al., 2007, Mihovilovich et al., 2007). Previously mapped to an NLR-rich region on Chromosome 5, I report here that Rl_{adg} is an orthologue of *Bs4*, the *Solanum lycopersicum* gene that confers resistance to bacterial spot disease. The encoded TIR-NLR recognises a serine protease in PLRV and other tested poleroviruses. Since Rl_{adg} confers broad-spectrum recognition of these viruses, we explored its potential to elevate resistance in *Brassica* species.

3.2 – Results

3.2.1 – Two classes of NLR-encoding gene co-segregate with *Rl*$_{adg}$ in a dihaploid population

Most potato varieties are susceptible to PLRV. However, after screening 2500 potato accessions, Mihovilovich et al. (2007) identified strong resistance to PLRV in a landrace named LOP-868. Using dihaploid genetics, PLRV resistance, designated *Rl*$_{adg}$, was mapped to the long arm of Chromosome 5. In annotated reference genomes, this region contains the *R1* and *Bs4* clusters – two large groups of *R*-genes.

To identify *Rl*$_{adg}$, SMRT RenSeq was used to assemble the NLR repertoire of LOP-868. In this assembly, 27 *R1* orthologues, and 17 *Bs4* orthologues were identified (Fig. 3.1a, Fig. 3.1b). To identify alleles present in the resistant haplotype, bulked segregant analysis was used. Illumina RenSeq was performed on bulked resistant and susceptible groups. Each bulk contained DNA from 30 plants phenotyped by Velasquez et al. (2007) (Fig. 3.1a). To identify resistance-linked NLRs, reads from these datasets were mapped to the LOP-868 SMRT RenSeq assembly. *Rl*$_{adg}$ candidates were identified by filtering for contigs with the read coverage depleted in the susceptible dataset but maintained in the resistant dataset. Candidates included three *Bs4* orthologues and eight *R1* orthologues. Expression of each candidate was determined using cDNA RenSeq, performed on leaf tissue from LOP-868. These data demonstrated the expression of three *Bs4* orthologues and six *R1* orthologues (Table. 3.1) (Fig. 3.1a). These genes were selected for further testing.

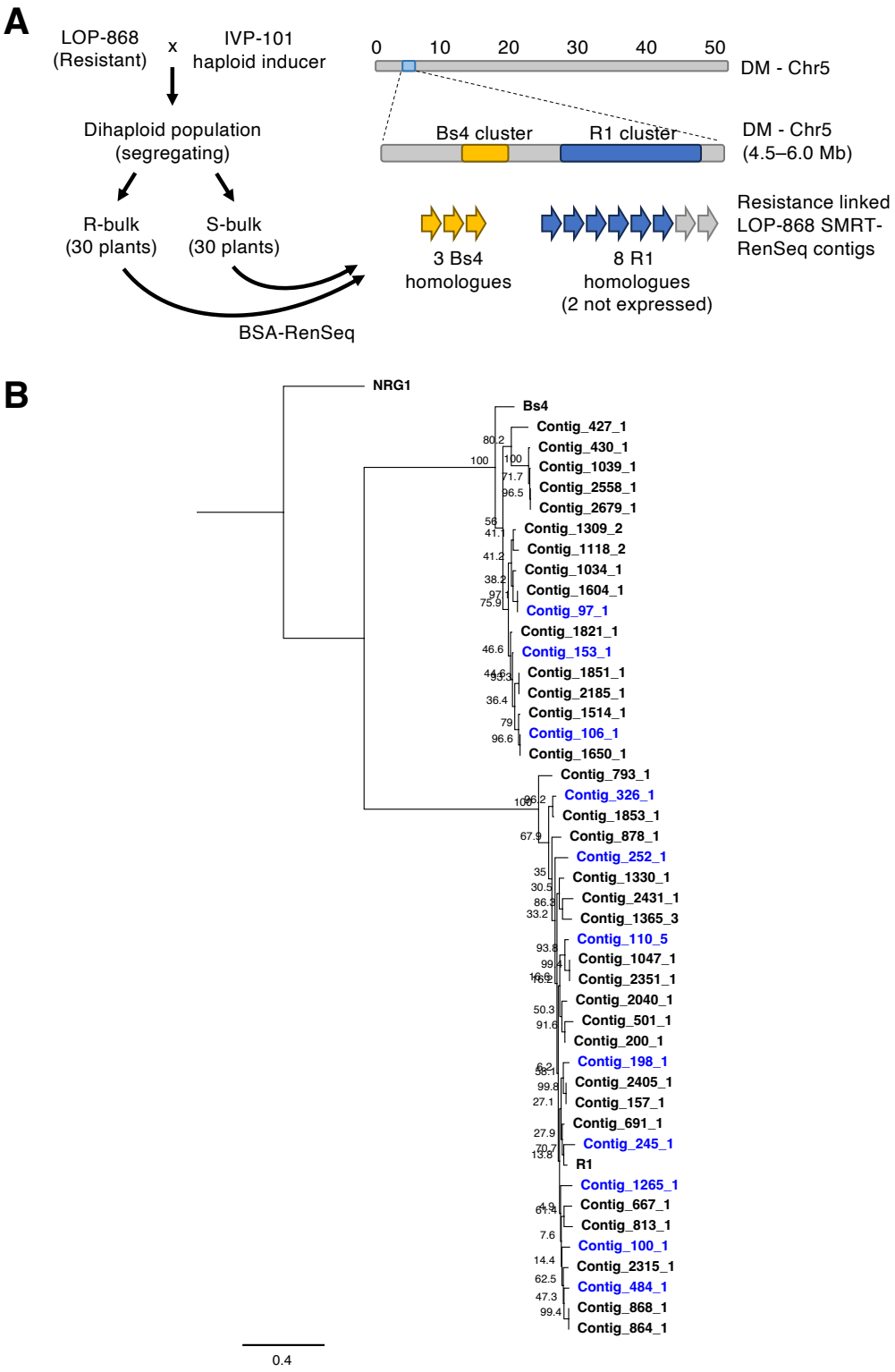

Figure 3.1. *Rl*$_{adg}$ maps to the *R1* and *Bs4* gene clusters on Chromosome 5. (**A**) *Rl*$_{adg}$ was mapped to the *R1* and *Bs4* *R*-gene clusters on Chromosome 5 using a dihaploid population previously characterised by Velasquez et al. (2007). LOP-868 was crossed to IVP-101 and the PLRV resistance of resulting progeny was characterised. 30 resistant and 30 susceptible dihaploids were bulked into separate Illumina RenSeq libraries. Bulked segregant analysis was used to identify *R1* and *Bs4* orthologues present on the resistant haplotype of LOP-868. *Rl*$_{adg}$ candidates include three expressed *Bs4* orthologues and six expressed *R1* orthologues.

Expression was defined using cDNA RenSeq data generated from LOP-868 leaf tissue. **(B)** Two classes of NLR co-segregate with Rl_{adg}. The figure shows a phylogenetic tree constructed using the amino acid sequences of all R1 and Bs4 NLRs in LOP-868. 17 Bs4-like and 27 R1-like NLRs were identified in the LOP-868 SMRT RenSeq data. Indicated in blue, 11 NLRs are found on the resistant haplotypes, this was determined using bulked segregant RenSeq. Support for branches within the tree are indicated as a percentage determined from 1000 iterations.

Table 3.1. *Rl_{adg}* is a *Bs4* orthologue. *Rl_{adg}* maps to the *R1* and *Bs4 R*-gene clusters on Chromosome 5. Of the 11 NLRs identified on the resistant haplotypes of LOP-868, 8 were tested as *Rl_{adg}* candidates. The ID, gene family assignment and expression in LOP-868 (determined using cDNA RenSeq of LOP-868) is shown. Cloned candidates were tested in *N. tabacum* by co-expression with the PLRV P1-P2 region, NLR_97_1 conferred gain of cell death in this assay.

NLR_ID	Homologous to	Expression in LOP-868	HR with P1-P2
NLR_100_1	R1	Yes	**No**
NLR_110_1	R1	Yes	**No**
NLR_198_1	R1	Yes	**No**
NLR_245_1	R1	**No**	-
NLR_252_1	R1	Yes	**No**
NLR_326_1	R1	Yes	**No**
NLR_484_1	R1	Yes	**No**
NLR_1265_1	R1	**No**	-
NLR_97_1	Bs4	Yes	**Yes**
NLR_106_1	Bs4	Yes	**Uncloned**
NLR_151_1	Bs4	Yes	**No**

3.2.2 – Independent capture sequencing of the *Bs4* haplotype supports the approach used to identify the *Rl$_{adg}$* haplotype

Using bulked segregant analysis, the NLR alleles mapped to the LOP-868 haplotypes were identified. To confirm that this approach identified paralogues on the same haplotype, the *Bs4* haplotype was investigated using the Xdrop technique developed by Samplix (Samplix ApS, https://samplix.com/). This approach utilises a microfluidics system to isolate individual molecules of DNA which are then selected using target-specific primers and flow cytometry. This technique was used to selectively enrich the *Bs4* haplotype associated with *Rl$_{adg}$*, to assemble the entire cluster, and to verify the linkage of candidates.

To validate the Samplix technique using a positive control, the *Rpi-amr3* cluster from *S. americanum* was used as a model. In the reference accession SP1102, the 140 Kb *Rpi-amr3* cluster contains 16 paralogues. Five sets of oligonucleotides were designed at approximately 30 Kb intervals to ensure enrichment across the whole cluster (Fig. 3.2a). Separate enrichment reactions were performed for each primer pair, resulting in enriched DNA, which was sequenced by Oxford Nanopore. For all targets combined, 3.8 Gb of data were produced. From these data, de-novo assembly was performed using the Flye assembler (Kolmogorov et al., 2019). Contigs were manually aligned, and a 230 Kb sequence was assembled. This assembly completely covers the *Rpi-amr3* cluster with greater than 99% accuracy relative to a whole genome assembly (Fig. 3.2a).

Next, this enrichment technique was applied to the *Bs4* haplotype of LOP-868 to test whether *NLR_97_1*, *NLR_106_1* and *NLR_153_1* are located on the same haplotype and not linked to other *Bs4* orthologues. A primer set was designed to enrich DNA containing *NLR_97_1*. Assembly of 1.2 Gb data from this enrichment produced a sequence containing both *NLR_97_1* and *NLR_153_1*; each NLR was 100% identical to the sequence produced from SMRT RenSeq (Fig. 3.2b). Surprisingly, *NLR_106_1* is not included in this contig. No additional *Bs4* orthologues were found in this assembled sequence.

The Xdrop technique allows for the selective enrichment of NLR clusters. It could be applied to clone more *R*-genes through selective enrichment of regions using resistance-linked genetic markers.

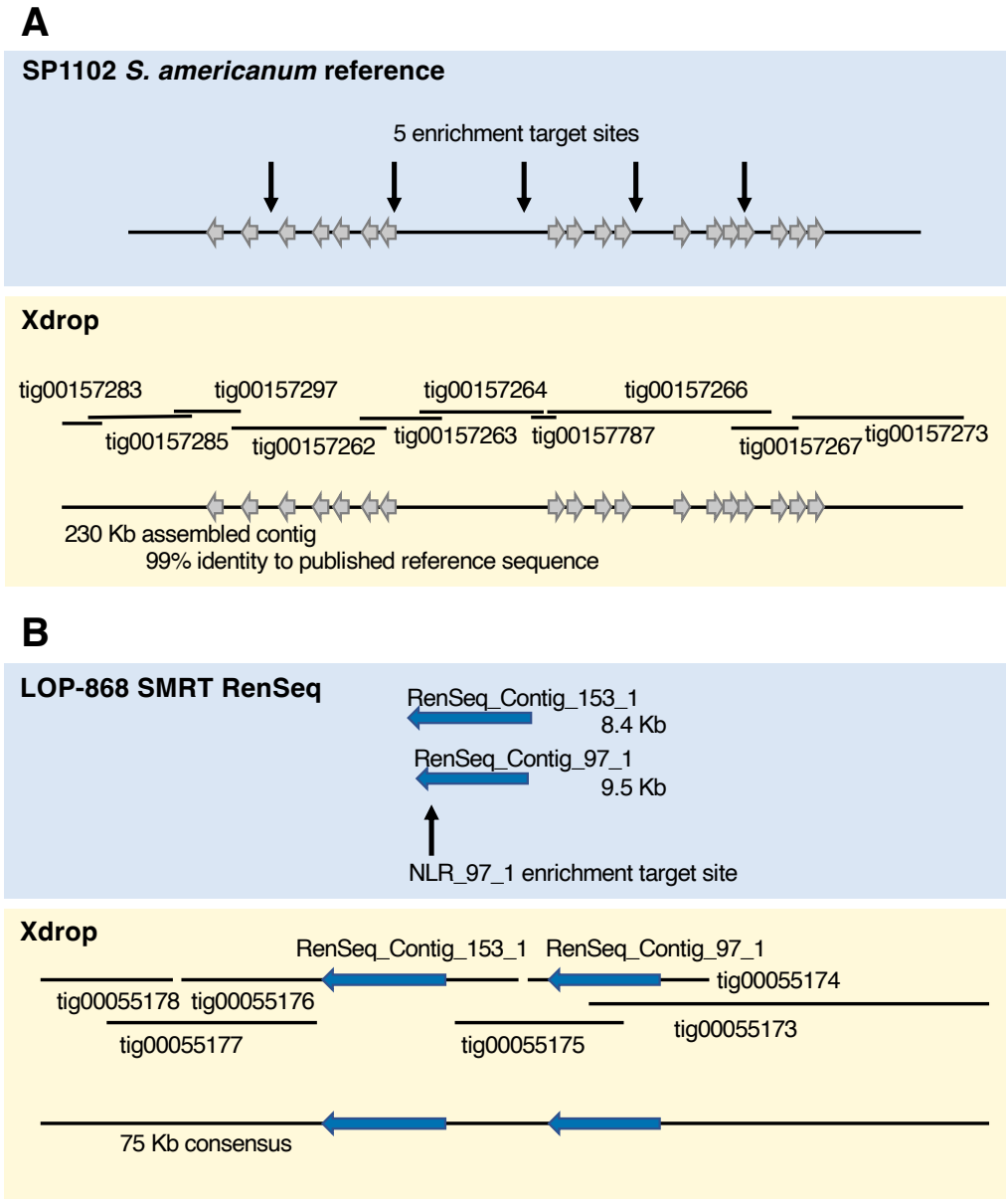

Figure 3.2. Xdrop enables assembly of the *Rpi-amr3* cluster and part of the LOP-868 *Bs4* haplotype. (A) The Xdrop technique was used to assemble the *Rpi-amr3* cluster from the *S. americanum* SP1102. For *Rpi-amr3*, the genome of SP1102 (which carries *Rpi-amr3*) was used as a reference to assess the technique. This cluster contains 18 NLR-encoding genes which are indicated using grey arrows. Five separate enrichment reactions were performed, the position of targets used to select DNA molecules are indicated. Enriched DNA was sequenced using Oxford Nanopore, 3.8 Gb of data was generated. Subsequent assembly produced several contigs which were then aligned to completely assemble the *Rpi-amr3* cluster. This assembly has greater than 99% identity to the published SP1102 reference genome. **(B)** Xdrop was applied to the resistance-linked *Bs4* haplotype of LOP-868. *NLR_97_1* was used as the target for enrichment. Enriched DNA was sequenced using Oxford Nanopore, 1.2 Gb of data was generated. A 75 Kb contig was produced containing both *NLR_97_1* and *NLR_153_1*, confirming their linkage. *NLR_106_1* was not assembled in this contig.

3.2.3 – Expression of the PLRV P1-P2 genomic region elicits HR in LOP-868

Nine NLRs were identified as candidates for *Rl*$_{adg}$. To facilitate rapid testing of these candidates, *Agrobacterium*-mediated transient expression was used to identify the elicitor from PLRV. Within the PLRV genome, there are several major proteins; a suppressor of RNA silencing (P0), a viral proteinase (P1), a fusion protein produced by a -1 ribosomal frameshift from the P1 ORF (P1-P2), the Rap1 protein and a movement protein (MP). At the 3' end of the genome, ORFs encode a two-part coat protein (CP). These two proteins are produced by the occasional readthrough of the stop codon in the shorter ORF (Fig. 3.3a).

Each of these ORFs were amplified from a PLRV cDNA clone and cloned into a CaMV *35S* expression vector. These constructs were designed to produce either P0, the P1-P2 region (encompassing Rap1, P1 and the P1-P2 fusion protein), the MP, or the CP (Fig. 3.3a). To identify the recognised protein, these constructs were transiently expressed in the leaves of LOP-868 and the potato cultivar Maris Piper. Expression of the *35S:P1-P2* construct in LOP-868 resulted in strong HR after 3 days. No response was observed for any other PLRV ORF in LOP-868, or the PLRV susceptible cultivar Maris Piper (Fig. 3.3b). Either P1, the P1-P2 fusion protein, or Rap1 is the elicitor of Rl$_{adg}$. This finding allowed the rapid testing of *Rl*$_{adg}$ candidates by co-expression with the P1-P2 region.

3.2.4 – A single *Bs4* orthologue confers PLRV recognition in *N. tabacum*

From bulked segregant analysis, 9 NLRs were identified as *Rl*$_{adg}$ candidates. ORFs which were defined using cDNA RenSeq, were cloned into a CaMV *35S* expression vector. All six *R1* orthologues and two *Bs4* orthologues were successfully cloned. The *Rl*$_{adg}$ candidates were co-expressed with the PLRV P1-P2 region in *Nicotiana tabacum*. No cell death was observed for any *R1* homologue (Fig. 3.4). Co-expression of *P1-P2* with one *Bs4* orthologue (*NLR_97_1*) resulted in HR (Fig. 3.5a). *NLR_97_1* is hereafter referred to as *Rl*$_{adg}$. *Rl*$_{adg}$ is a four-exon gene which encodes a 1,123 amino acid TIR-NLR, sharing 79.8% amino acid identity to Bs4 (Fig. 3.5b).

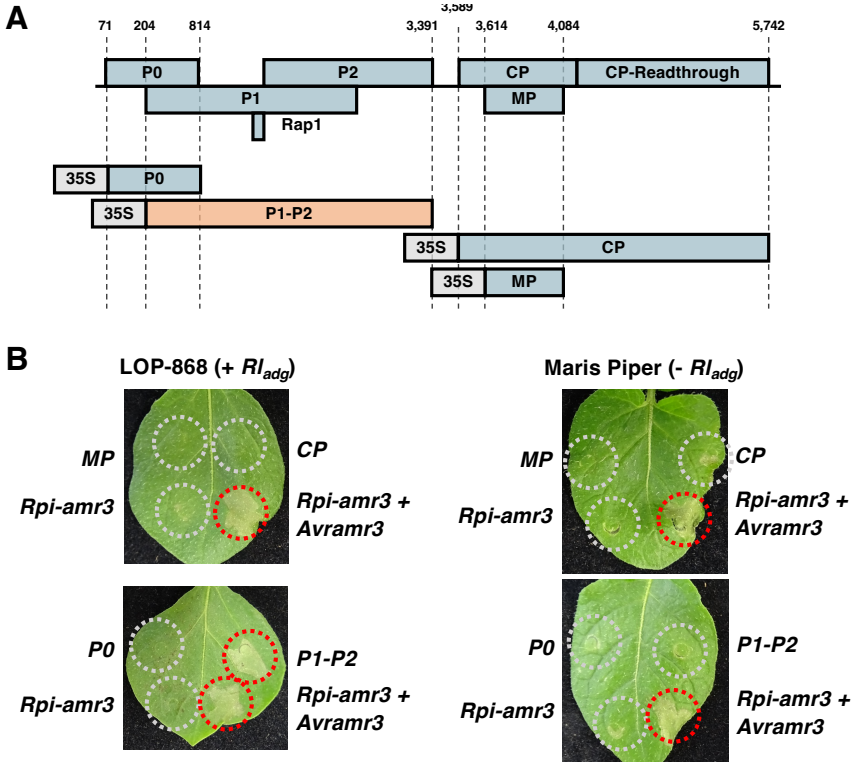

Figure 3.3. Transient expression of the PLRV P1-P2 genomic region elicits HR in LOP-868. (A) To identify the elicitor of Rl_{adg}, the PLRV genome was divided into four constructs expressing the P0, P1-P2, CP and MP genomic regions. Each region was cloned into a binary vector with a CaMV *35S* promoter and *Ocs* terminator. The defined boundaries within the PLRV genome (Genbank accession ID: KP090166.1) are indicated. Expression of the P1-P2 construct (indicated in red) in LOP-868 results in HR. **(B)** These constructs were transiently expressed in leaves of LOP-868 (which carries *Rl_{adg}*), and potato cultivar Maris Piper (which lacks *Rl_{adg}*). Expression of the P1-P2 region results in *Rl_{adg}*-dependent HR. *Agrobacterium* was diluted to 0.1 OD_{600} before infiltration. Photographs were taken at 3 dpi.

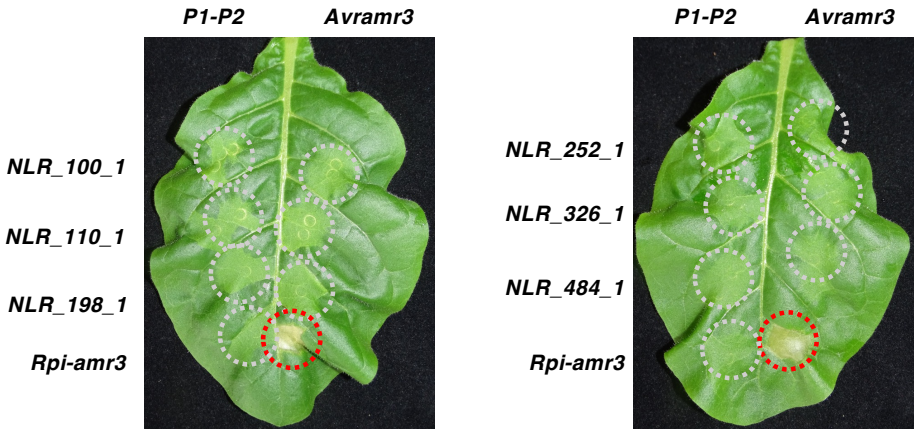

Figure 3.4. No *Rl_{adg}* candidates with homology to *R1* trigger HR upon co-expression with PLRV P1-P2. Eight *R1* homologues are linked to resistance in LOP-868, six show expression in cDNA RenSeq data. These six candidates were cloned and tested by co-expression with the PLRV P1-P2 genomic region in *N. tabacum* leaves. No HR was observed for any of these infiltrations. Avramr3 and Rpi-amr3 was used as controls. Each *Agrobacterium* strain was infiltrated at an OD_{600} of 0.3. Pictures were taken 3 dpi.

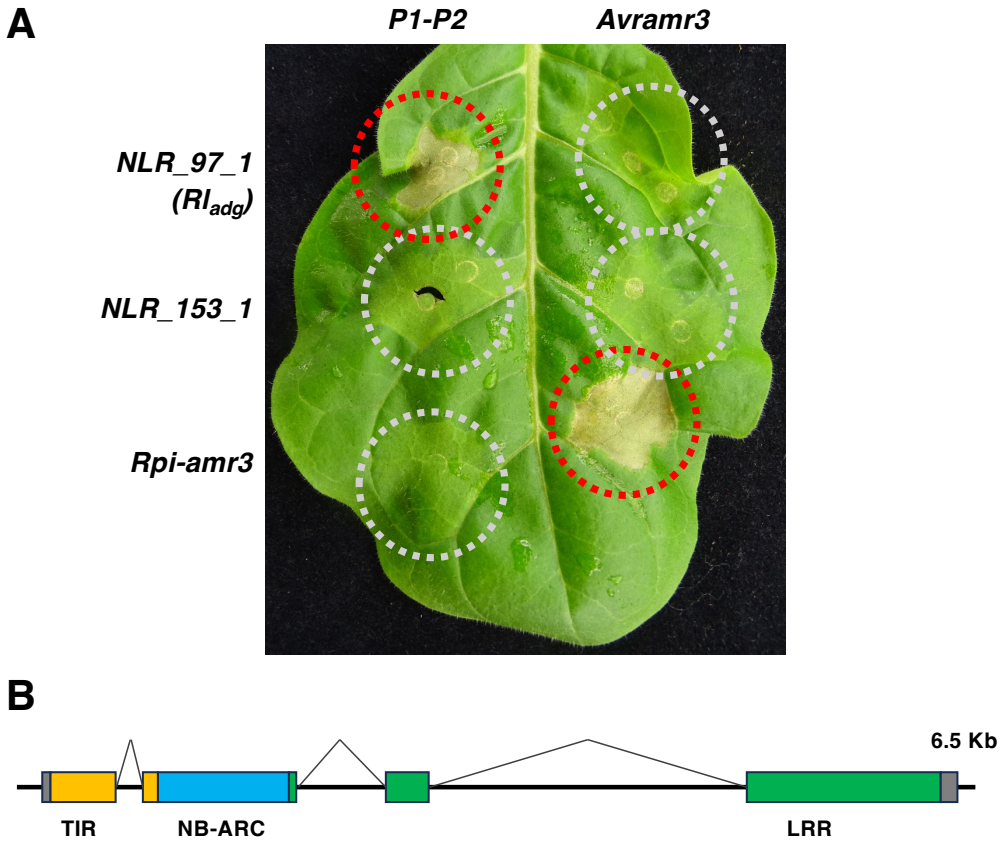

Figure 3.5. *Rl*$_{adg}$ is a four-exon *Bs4* orthologue which encodes a TIR-NLR. (A) Two resistance-linked *Bs4* homologues were successfully cloned from LOP-868, one remains uncloned. Transient expression of NLR_97_1 with P1-P2 in *N. tabacum* leaves results in HR. No cell death was observed when NLR_97_1 was co-expressed with Avramr3, or when another Bs4 homologue (NLR_153_1) or Rpi-amr3 were expressed with PLRV P1-P2. Photographs were taken at 3 dpi. Each *Agrobacterium* strain was infiltrated at an OD_{600} of 0.3. **(B)** *Rl*$_{adg}$ (NLR_97_1) encodes a 1,123 amino acid TIR-NLR with 79.8% identity to Bs4. The region encoding the TIR domain is indicated in yellow, the NB-ARC in blue, the LRRs in green. 5' and 3' UTRs are indicated in grey. Intron and exon boundaries were determined using cDNA RenSeq data generated from LOP-868 leaf tissue, no evidence of alternative splicing was found.

To confirm the identity of *Rl*$_{adg}$, two other PLRV-resistant potato landrace accessions (OCH-7643 and HUA-332) were sequenced using Illumina RenSeq, to identify alleles of *Rl*$_{adg}$. Both accessions carry alleles that are highly similar to the characterised LOP-868 *Rl*$_{adg}$. Within a phylogeny of *Rl*$_{adg}$ orthologues, produced using publicly available genome data, the LOP-868, OCH-7643 and HUA-332 alleles cluster closely together. As these two accessions are not available, they cannot be tested by transient expression of the Rl$_{adg}$ elicitor. This sequence similarity suggests that resistance is probably due to *Rl*$_{adg}$ (Fig. 3.6).

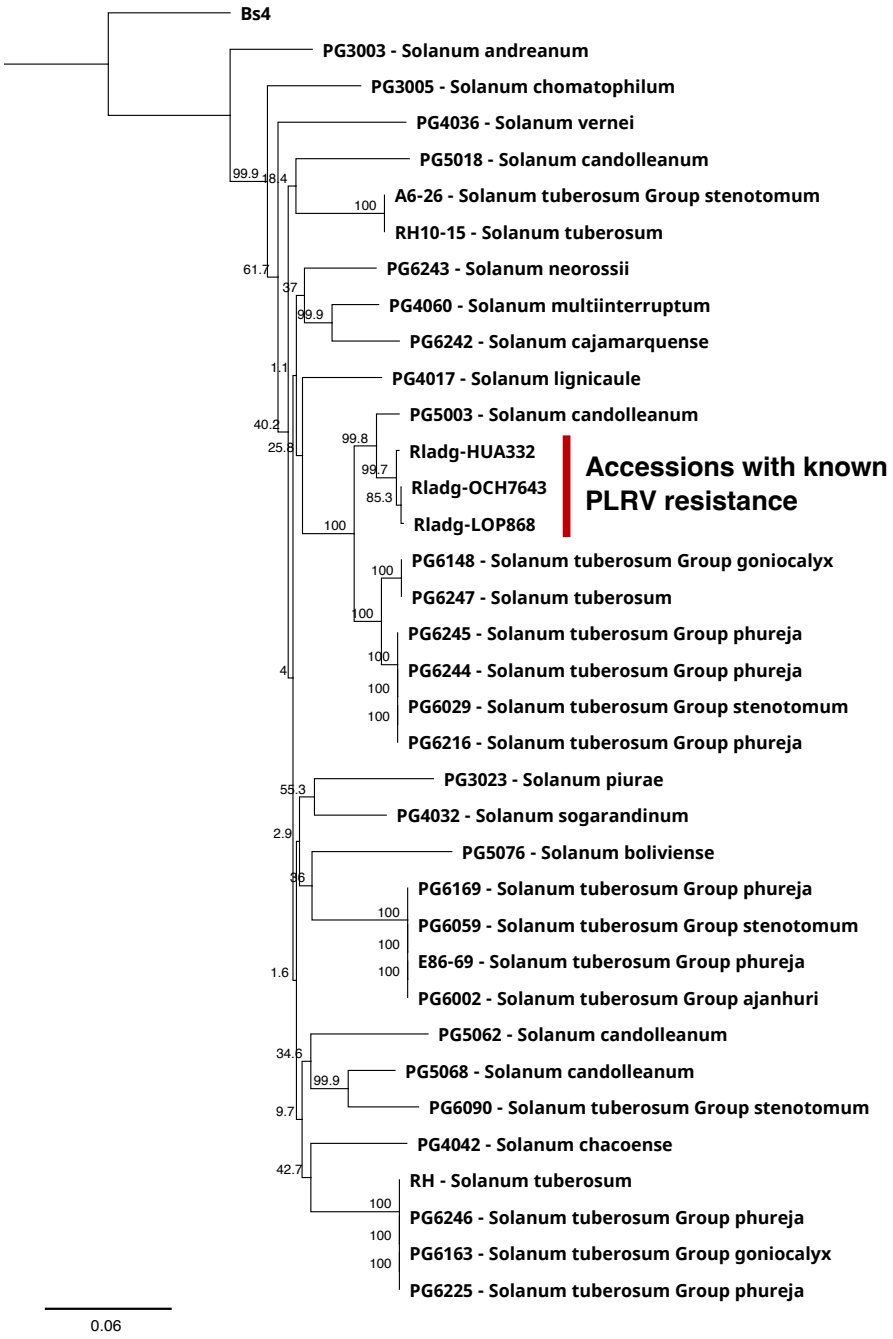

Figure 3.6. *Rl*$_{adg}$ alleles in three PLRV resistant accessions are closely related. Phylogenetic tree constructed using *Rl*$_{adg}$ orthologues from wild and cultivated potato genomes. Illumina RenSeq was performed on two additional accessions (OCH-7643 and HUA-332) which are resistant to PLRV. The *Rl*$_{adg}$ alleles in these accessions were identified by mapping Illumina RenSeq datasets to the LOP-868 SMRT RenSeq assembly. Identified alleles are highly similar to the *Rl*$_{adg}$ allele from LOP-868 (Indicated as Rladg-LOP868). These data provided complete coverage of *Rl*$_{adg}$ in HUA-332, but incomplete coverage of the OCH-7643 allele (66 bases lack mapped reads). The sequenced regions of both alleles are highly similar to the LOP-868 reference. The most closely related *Bs4* homologue from other wild and landrace potato varieties were identified using BLAST and are represented in the phylogenetic tree. Alleles from accessions with known resistance cluster together. Branches within the tree have a percentage support across 1000 iterations indicated.

3.2.5 – Rl_{adg} recognises the serine protease domain of P1

The P1-P2 genomic region encodes three proteins; P1, Rap1 and the P1-P2 fusion protein (Fig. 3.7a). To identify which of these proteins is recognised by Rl_{adg}, the P1-P2 construct was truncated to remove either P1 or the P2 ORF. Mutation of the Rap1 start codon was also performed. Transient expression in *N. tabacum* demonstrates that the P1 protein alone is sufficient to induce HR upon co-expression with *Rl_{adg}* (Fig. 3.7b).

P1 is a polyprotein which self-cleaves into three proteins. This processing is performed by the central domain, a serine protease. P1 products include an N-terminal domain (NTD) of unknown function, the serine protease, and the C-terminal domain (CTD) which acts as a Vpg protein, which caps the RNA viral genome (Fig. 3.8a). To identify which of these proteins are recognised by Rl_{adg}, further truncation was performed. Three constructs were designed to express these domains under the CaMV *35S* promoter. Co-expression of *Rl_{adg}* with the protease resulted in HR in *N. tabacum*, while neither NTD nor CTD elicited a response (Fig. 3.8b). In this assay, NLR_153_1 did not respond to the protease, indicating that the HR is specific to Rl_{adg}.

3.2.6 – PLRV recognition by Rl_{adg} does not require protease enzymatic activity

Dissection of the PLRV P1 protein revealed the protease domain as the elicitor of Rl_{adg}. To test whether this recognition is dependent on protease activity, a non-functional variant was produced. Serine proteases contain an HDS (His254, Asp286, Ser353) catalytic triad which is required for proteolytic activity. Mutation of any of these residues abolishes the function of the PLRV P1 protease (Sadowy et al., 2001). To determine whether Rl_{adg} recognises the protease indirectly, through cleavage of a host protein, a H254L-D286A-S353A protease mutant (hereafter named HDS mutant) was produced (Fig. 3.8a). Co-expression of the HDS mutant with *Rl_{adg}* results in strong cell death which is equivalent to the functional protease (Fig. 3.8c). This indicates that protease activity is not required for recognition. Recognition is more likely to be through direct association, rather than recognition of a cleaved host target or a guarded protein.

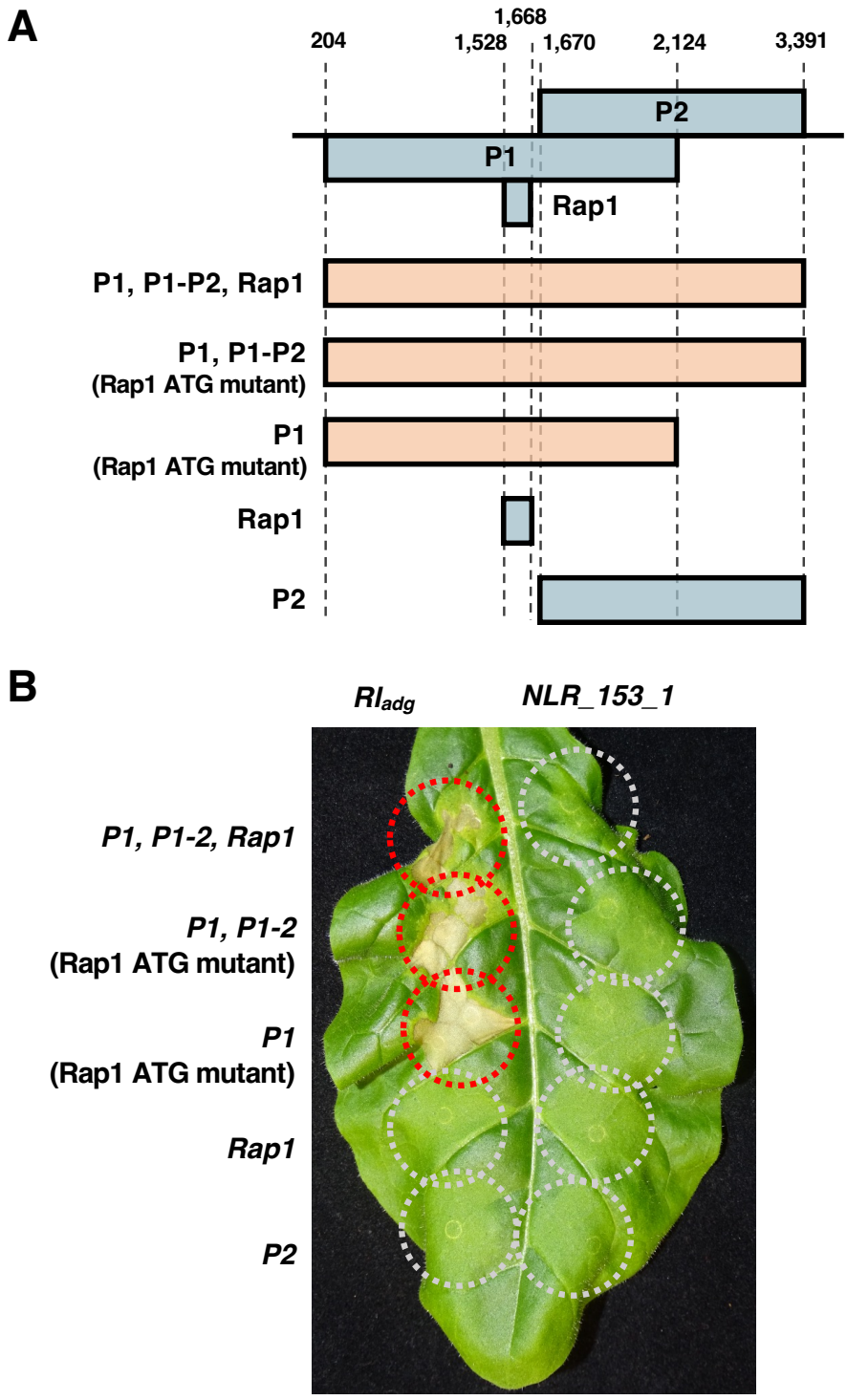

Figure 3.7. The elicitor of Rl_{adg} is encoded within the P1 ORF. (A) The P1-P2 genomic region encodes three proteins: P1, a P1-P2 fusion protein and Rap1. Truncated constructs and start-codon mutants were used to dissect which of these proteins is recognised by Rl_{adg}. The relative position of these ORFs within the PLRV reference genome (Genbank accession ID: KP090166.1) is indicated. Truncations which elicit an Rl_{adg}-dependent response in *N. tabacum* are indicated in red. **(B)** Co-expression of these constructs with Rl_{adg} in *N. tabacum* demonstrated that the Rap1 and P2 are not required for Rl_{adg}-dependent cell death. P1 alone is sufficient. Each *Agrobacterium* strain was infiltrated at an OD_{600} of 0.3. Pictures were taken 3 dpi.

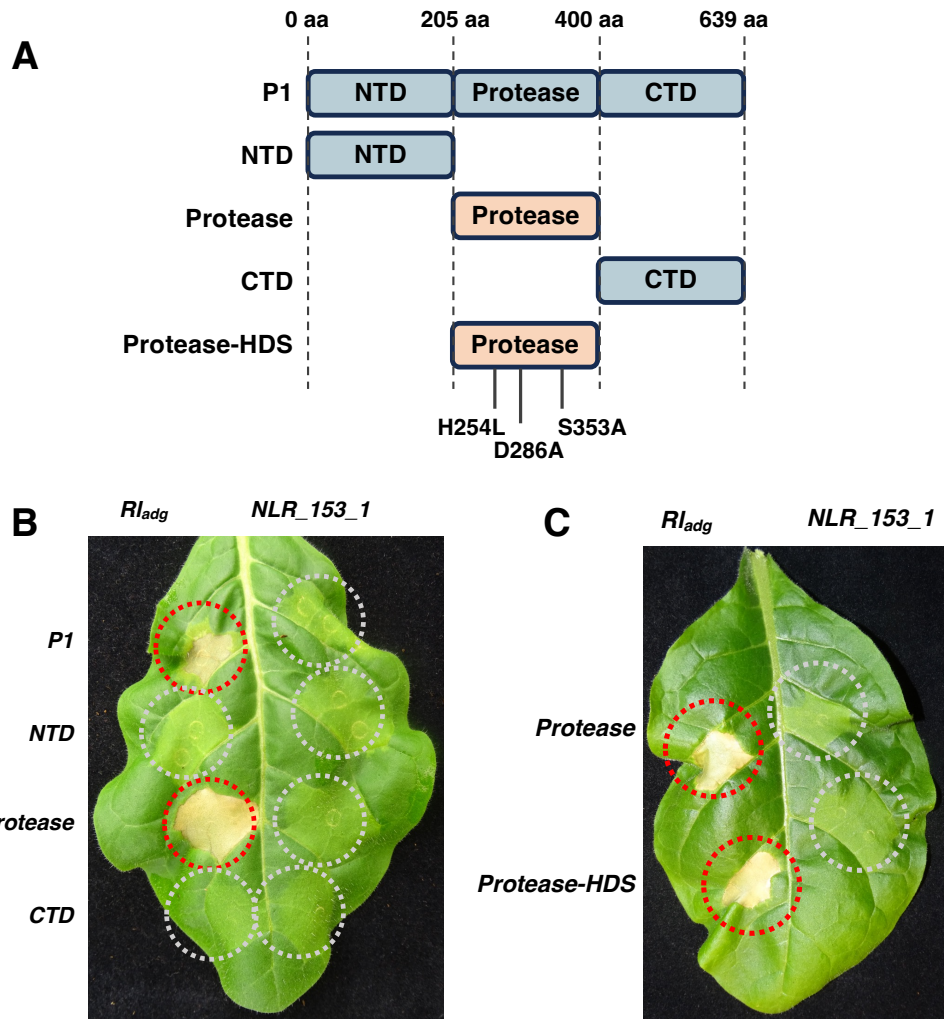

Figure 3.8. Rl_{adg} recognises the protease domain of P1, independent of its activity. **(A)** P1 is a polyprotein which self-cleaves through serine protease action. Once cleaved, P1 produces three fragments: an N-terminal domain (NTD), a serine protease and a C-terminal domain (CTD) which functions as the Vpg protein. The *P1* ORF was truncated into three constructs expressing these proteins individually. Another construct where the serine protease is mutated at the HDS catalytic triad was also produced (indicated as Protease-HDS). Modified amino acids are indicated, these are replicated from Sadowy et al. (2001). The protease domain, and the HDS mutant variant (both indicated in red) elicit an Rl_{adg}-dependent response in *N. tabacum*. **(B)** The P1-protease is sufficient to activate HR when co-expressed with Rl_{adg}, no cell death was observed for either the NTD or CTD fragments. Each *Agrobacterium* strain was infiltrated at an OD_{600} of 0.3. Pictures were taken 3 dpi. **(C)** The HDS catalytic triad mutant protease elicits cell death when co-expressed with Rl_{adg}, this is equivalent to HR when Rl_{adg} is co-expressed with the functional protease. *Agrobacterium* suspensions were infiltrated at an OD_{600} of 0.3, leaves were photographed at 3 dpi.

3.2.6 – *Rl_{adg}* confers PLRV protease recognition in transgenic potato and tobacco

To confirm that *Rl_{adg}* alone is sufficient for recognition of the PLRV protease, transgenic *S. tuberosum* and *N. tabacum* were generated. Constructs containing the *Rl_{adg}* ORF under either its native promoter, or the CaMV *35S* promoter, were transformed into *S. tuberosum*. Transgenic *35S:Rl_{adg} N. tabacum* lines were also produced. Consistent with the transient expression assays, expression of the PLRV protease in the transgenic *N. tabacum* lines is sufficient to trigger HR (Fig. 3.9a). Similarly, the gain of recognition was observed in transgenic potato plants with both native and CaMV *35S*-driven constructs (Fig. 3.9b). These experiments demonstrate that delivery of a single NLR is sufficient to reconstitute the LOP-868 HR phenotype in *S. tuberosum* and *N. tabacum*.

Agroinfiltration of an infectious PLRV cDNA clone into leaves of *35S:Rl_{adg} N. tabacum* lines is also able to activate HR. At 10 days post-infiltration cell death was observed in the transgenic lines, but not in the wild-type control (Fig. 3.9c). While we can see a clear differential in immune response of these lines, we could not test for restricted viral spread as systemic infection of wild-type *N. tabacum* could not be achieved using this cDNA clone.

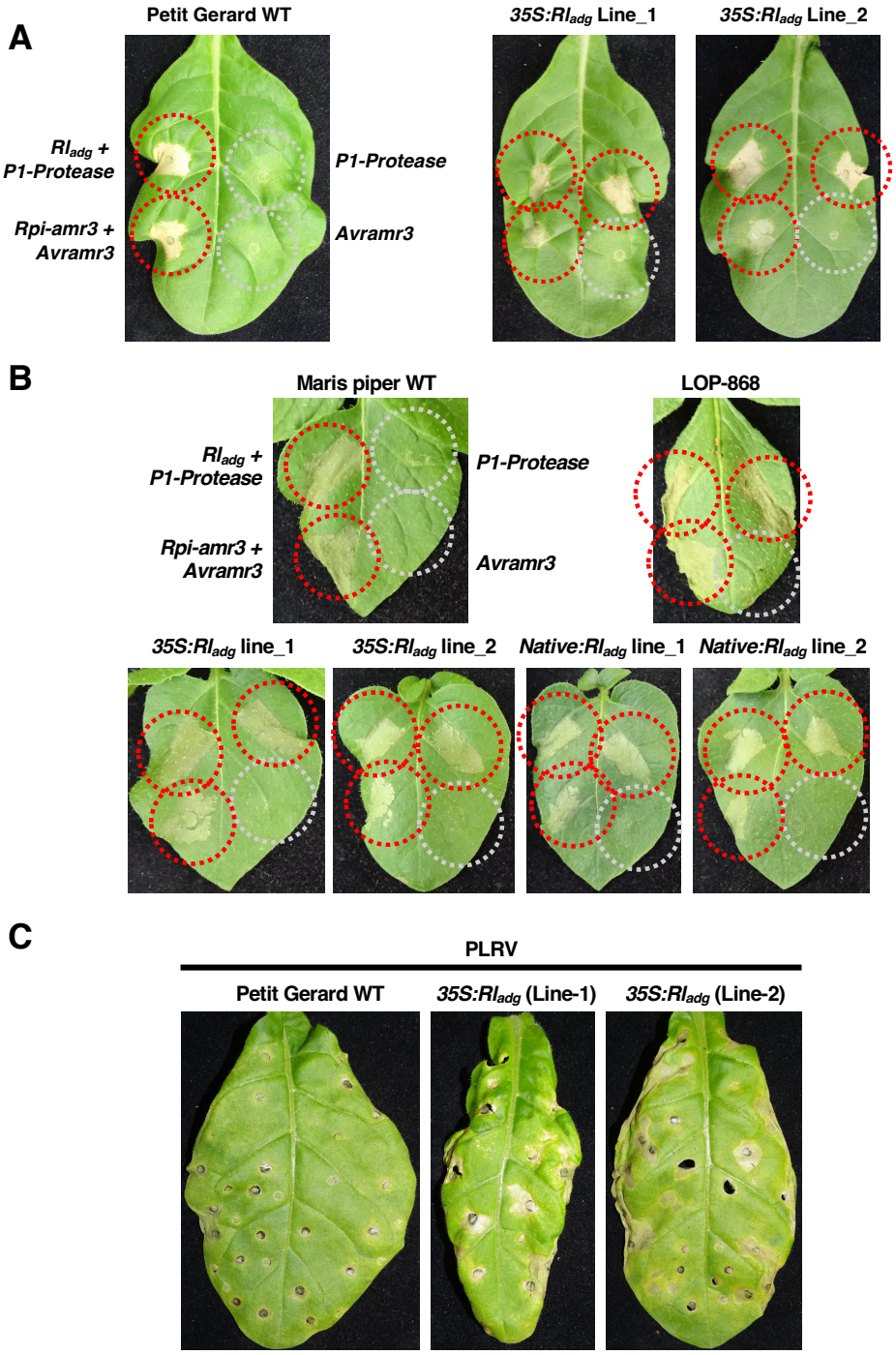

Figure 3.9. *Rl*$_{adg}$ confers PLRV recognition in transgenic *N. tabacum* and *S. tuberosum*. **(A)** Expression of the PLRV serine protease causes HR in *N. tabacum* expressing *35S:Rl*$_{adg}$. *Agrobacterium* strains were infiltrated at 0.3 OD_{600}. Photographs were taken at 3 dpi. **(B)** Transgenic *S. tuberosum* (cultivar Maris Piper) expressing *Rl*$_{adg}$ under either CaMV *35S* promoter or native regulatory elements from LOP-868 (defined from 1.5 Kb before the start codon, to 0.6 Kb after the stop codon) recognise the PLRV protease. In the untransformed control, HR is only observed after transient co-expression of the protease with Rl_{adg}. *Agrobacterium* strains were infiltrated at an OD_{600} of 0.1, images were taken at 2 dpi. **(C)** Expression of an infectious cDNA clone of PLRV results in some cell death in *35S:Rl*$_{adg}$ *N. tabacum* lines. WT *N. tabacum* does not respond strongly to PLRV expression. *Agrobacterium* was infiltrated at 0.3 OD_{600}. Photographs were taken at 10 dpi.

3.2.7 – *Rl_{adg}* confers recognition of a diverse set of poleroviruses

Many NLRs recognise elicitor structures that are conserved between pathogens, and recognition of these orthologues can translate into resistance. For example, the *S. stoloniferum* TIR-NLR Ry_{sto} recognises the coat protein from potato virus Y (PVY) and several other potyviruses (Grech-Baran et al., 2019, Grech-Baran et al., 2022). Orthologues of PLRV P1 are found in many solemoviruses, and the serine proteases within the family are known to adopt a chymotrypsin-like fold (Mann and Sanfaçon, 2019). Alphafold was used to predict the structures of the proteases from PLRV and nine other poleroviruses. The models generated are predicted to be high quality, with LDDT (local distance difference test) scores above 80 for most positions within the model (Fig. 3.10a). Since there is currently no available structure for any polerovirus serine protease, these models were evaluated by comparing them to the characterised structure of the sesbania mosaic virus (SeMV) serine protease (Gayathri et al., 2006). SeMV, a member of the *Sobemovirus* genus, shares classification within the *Solemovirus* family, similar to poleroviruses. The structures predicted for the polerovirus proteases are highly similar to each other, and the SeMV protease (Fig. 3.10b, Fig. 3.10c). All protease models share the same chymotrypsin-like fold as the SeMV protease. This similarity is remarkable, especially considering the low sequence similarity between these proteases (between 40.6% and 82.6% relative to PLRV) (Fig. 3.11a, Fig. 3.11b). The similarity between these structures was quantified using DALI (Holm et al., 2023): pairwise z-scores between all polerovirus proteases were high (above 20), indicating strong similarity (Fig. 3.11c).

These nine polerovirus proteases were synthesised and tested by co-expression with *Rl_{adg}* in *N. tabacum*. Remarkably, strong Rl_{adg}-dependent HR was observed for all nine proteases (Fig. 3.11d). The diversity of the recognised poleroviruses is far greater than the variation between sequenced PLRV strains. The 22 published PLRV strains have proteases with at least 97.4% amino acid identity relative to the PLRV protease which was used in transient expression assays (Fig. 3.12). The ten polerovirus proteases which elicit a response via Rl_{adg} share between 40.6% and 82.6% amino acid identity to the PLRV protease (Fig. 3.11a) (Fig. 3.11b). Given this, it can be hypothesised that Rl_{adg} is likely to recognise all published PLRV strains and remain durable in the field.

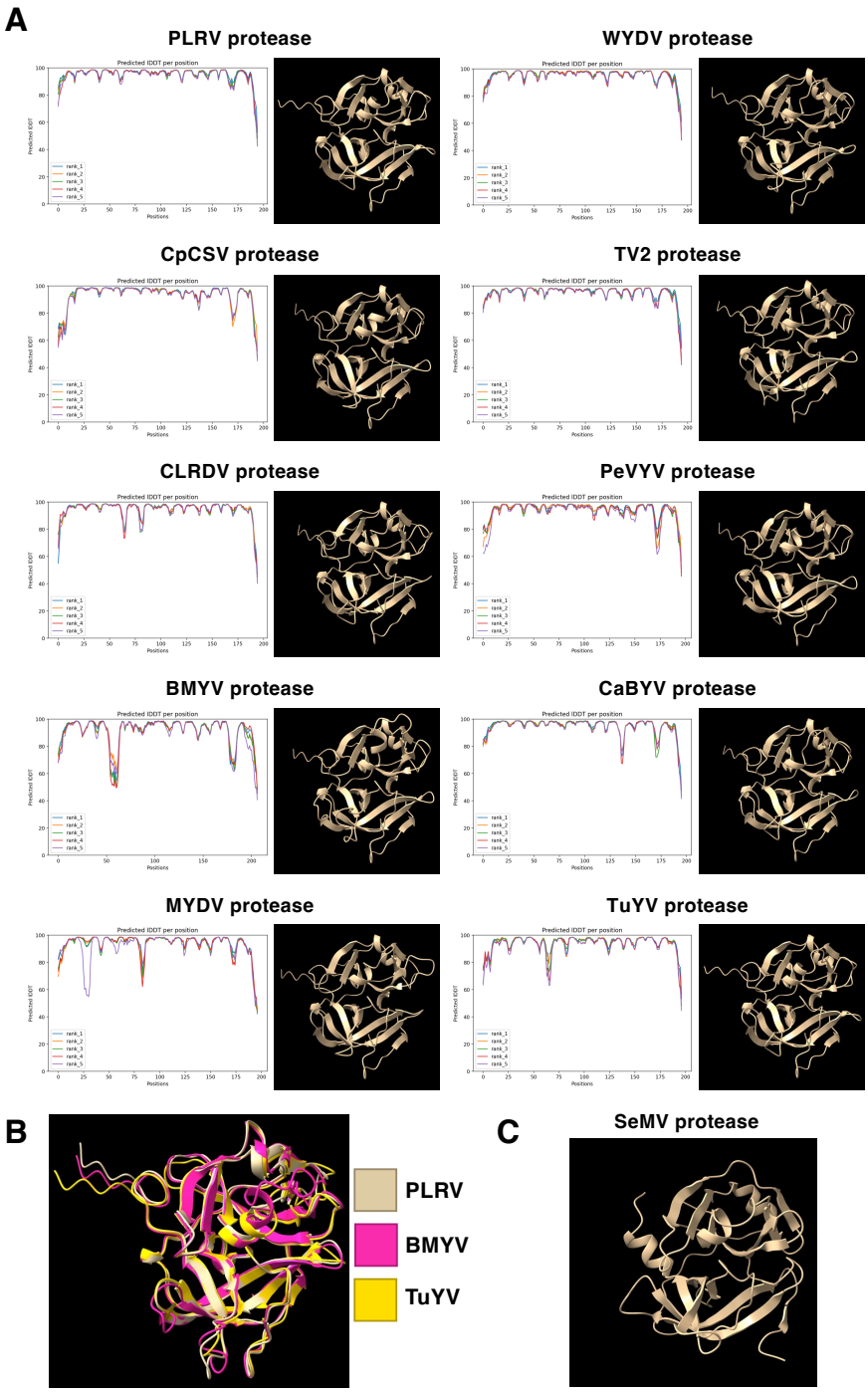

Figure 3.10. Polerovirus protease predicted structures share a conserved fold. (A) Alphafold was used to predict structures for each of the polerovirus proteases recognised by Rl_{adg}. For each model, the LDDT score at each position is shown. All proteases share a similar predicted structure, suggesting that they fold in a similar manner to the PLRV protease. **(B)** An overlayed representation of the PLRV, TuYV and BMYV structures demonstrates that the proteases share a similar fold. **(C)** The most closely related protease with an experimentally derived structure is the sobemovirus SeMV which forms a chymotrypsin-like fold similar to the predicted polerovirus protease structures.

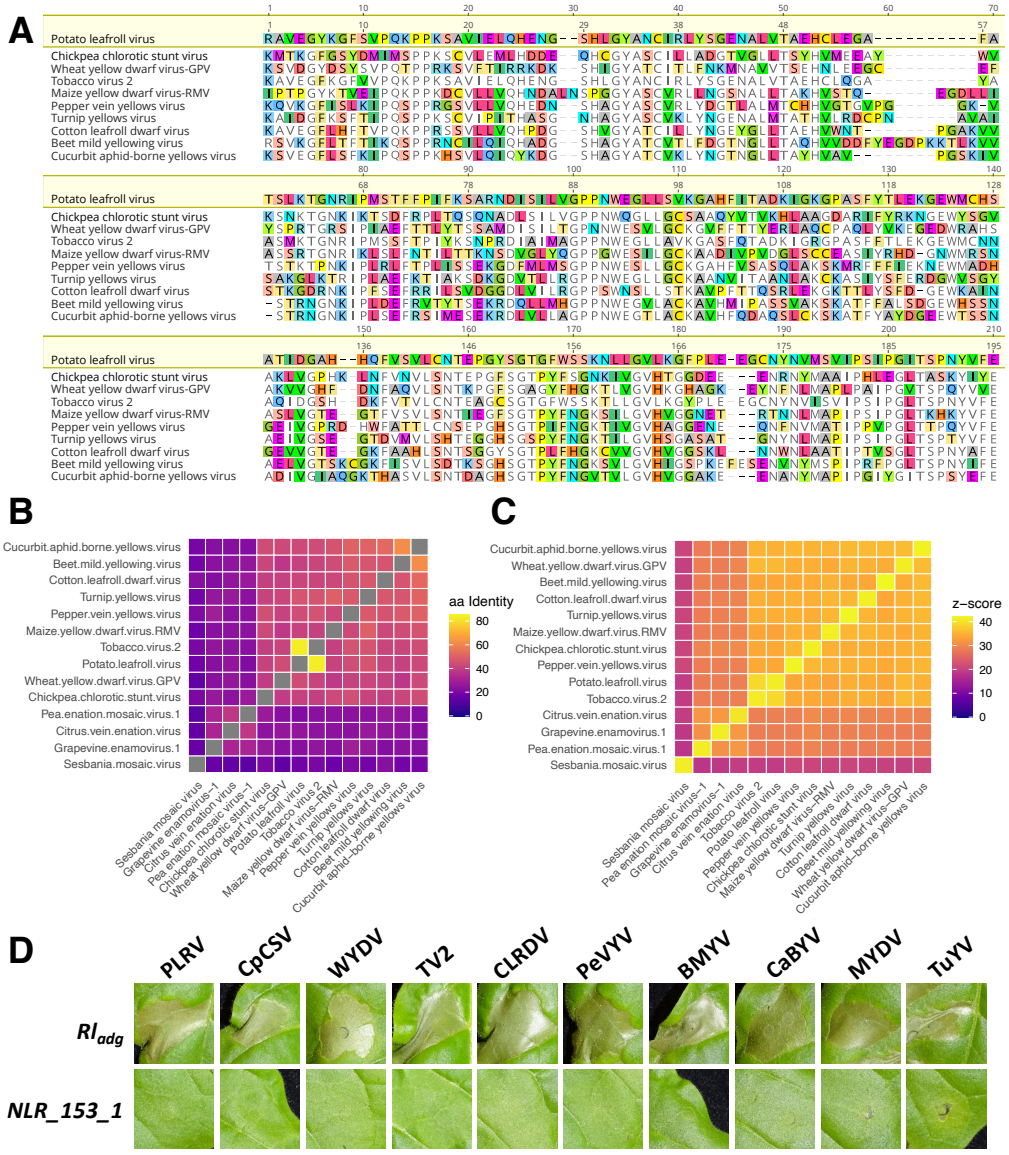

Figure 3.11. Rl_{adg} recognises multiple polerovirus proteases despite their diverse amino acid sequences. (A) Alignment of the amino acid sequence of the tested polerovirus proteases with the PLRV protease. Very few residues are conserved between all proteases. In each sequence, polymorphisms relative to the PLRV reference are highlighted. **(B)** Polerovirus proteases have low sequence identity to each other and enamoviruses. The amino acid identity between a selection of polerovirus and enamovirus proteases is represented as a heatmap. Polerovirus proteases tested against Rl_{adg} share low sequence identity compared to the PLRV protease, ranging between 40.6% and 82.6%. **(C)** Alphafold was used to predict the structures of these polerovirus and enamovirus proteases. Despite sharing low amino acid identity, they share very similar predicted structures. Pairwise comparison between proteases from these poleroviruses and enamoviruses was performed using DALI. The closest experimentally validated protease, from SeMV, was also included. Pairwise z-scores are represented as a heatmap. z-scores above 20 indicate strong similarity between two proteins. **(D)** Rl_{adg} recognises nine polerovirus proteases in addition to the PLRV protease. Transient co-expression of Rl_{adg} and polerovirus proteases was performed in *N. tabacum* leaves. The non-functional paralogue NLR_153_1 was used as a negative control. *Agrobacterium* strains were infiltrated at an OD_{600} of 0.3, leaves were photographed at 3 dpi.

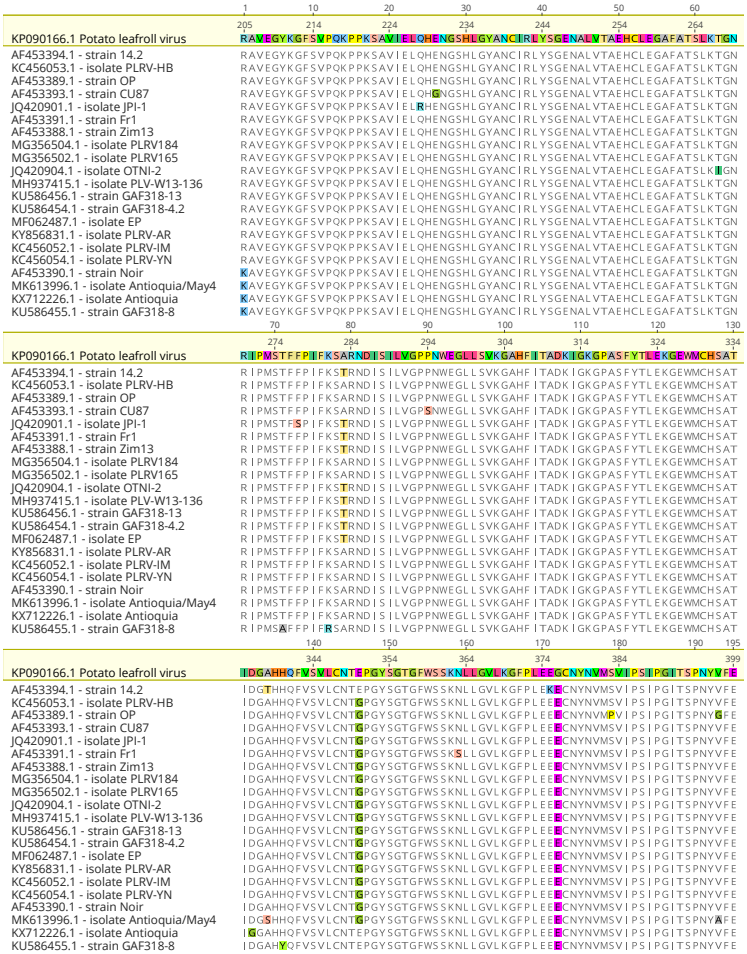

Figure 3.12. The P1 protease is highly conserved within published PLRV isolates. The P1 protease is found in all 22 published PLRV strains. Alignment of the amino acid sequences shows that this protein is highly similar between different strains. The strain used to identify and characterise Rl_{adg} is included (Genbank accession ID: KP090166.1). Polymorphisms between the reference strain and each protease are highlighted.

To determine the limit of recognition, Rl_{adg} was tested against three proteases from the *Enamovirus* genus. Enamoviruses share a similar genome structure to poleroviruses and produce a self-cleaving P1 protein. However, these proteases share lower sequence similarity with the PLRV protease (between 20 and 25%) (Fig. 3.11b) (Fig. 3.13c). The structures of three enamovirus proteases (citrus vein enation virus (CVEV), grapevine enamovirus-1 (GEV-1) or pea enation mosaic virus-1 (PEMV-1)) were predicted using Alphafold. The predicted structures are similar to those of polerovirus proteases (Fig. 3.13a, Fig. 3.13b). Recognition of these three proteases by Rl_{adg} was tested in *N. tabacum* leaves, however, no cell death was observed (Fig. 3.14). This suggests that the sequence, or fold, in polerovirus proteases which is recognised by Rl_{adg}, is not conserved outside of the *Polerovirus* genus. The tested enamovirus proteases are too diverged from polerovirus proteases to be recognised by Rl_{adg}.

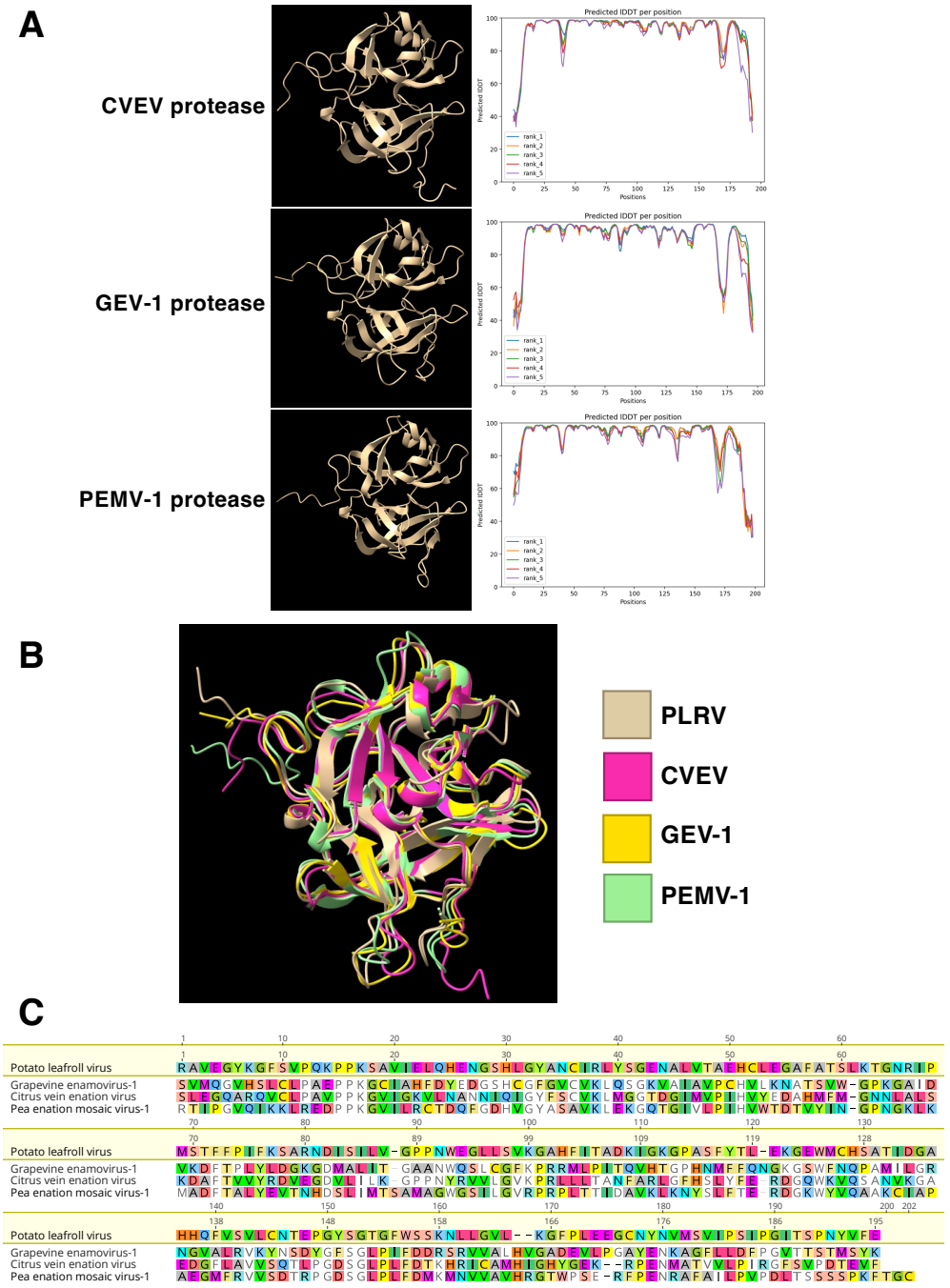

Figure 3.13. Enamovirus serine proteases have similar predicted structures to the PLRV protease despite low amino acid identity. (A) Alphafold models were generated for three enamovirus proteases: citrus vein enation virus (CVEV), grapevine enamovirus-1 (GEV-1) and pea enation mosaic virus-1 (PEMV-1). The quality of the prediction was assessed by the LDDT score for each position within the sequence. **(B)** An overlayed representation of the predicted structures suggests a highly similar fold to the PLRV protease, this is supported by the pairwise z-scores calculated using DALI (Fig. 3.11c). **(C)** Enamovirus proteases tested for recognition by Rl_{adg} show little sequence similarity to the PLRV protease (between 20 and 25% amino acid identity). Alignment of the amino acid sequence of the three tested enamovirus proteases with the PLRV protease that is recognised by Rl_{adg}. Polymorphisms between the enamovirus proteases and PLRV-protease are highlighted.

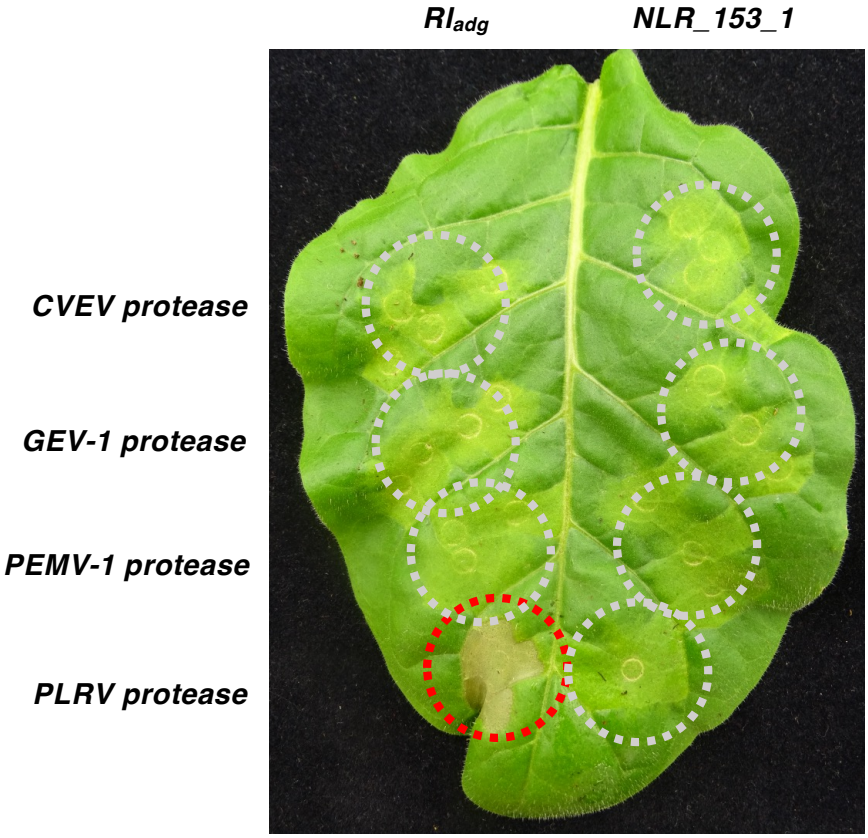

Figure 3.14. Rl_{adg} recognition does not extend to enamovirus proteases. In *N. tabacum* transient assays, Rl_{adg} does not activate HR when co-expressed with the proteases from CVEV, GEV-1, or PEMV-1. Co-expression of Rl_{adg} with the PLRV protease results in clear cell death. *Agrobacterium* strains were infiltrated at 0.3 OD_{600}. Pictures were taken 3 dpi.

3.2.8 – *Rl_{adg}* confers resistance to TuYV in transgenic *N. tabacum*

Transient co-expression of *Rl_{adg}* with many polerovirus proteases results in HR in *N. tabacum*. As Rl_{adg} appears to function in *N. tabacum,* transgenic lines were used to test whether the recognition of these poleroviruses translates into recognition of the virus during infection. *35S:Rl_{adg}* transgenic lines were infiltrated with an agrobacterium strain expressing an infectious clone of TuYV. Strong cell death was observed in these leaves indicating that recognition of the isolated protease also correlates with recognition of the virus during infection (Fig. 3.15). However, systemic movement of TuYV beyond the infiltrated tissue could not be detected in wild-type plants. This suggests that while the infectious clone does produce the virus, systemic infection cannot be achieved. This result indicates that *Rl_{adg}* could be used to elevate resistance to TuYV, and possibly other poleroviruses.

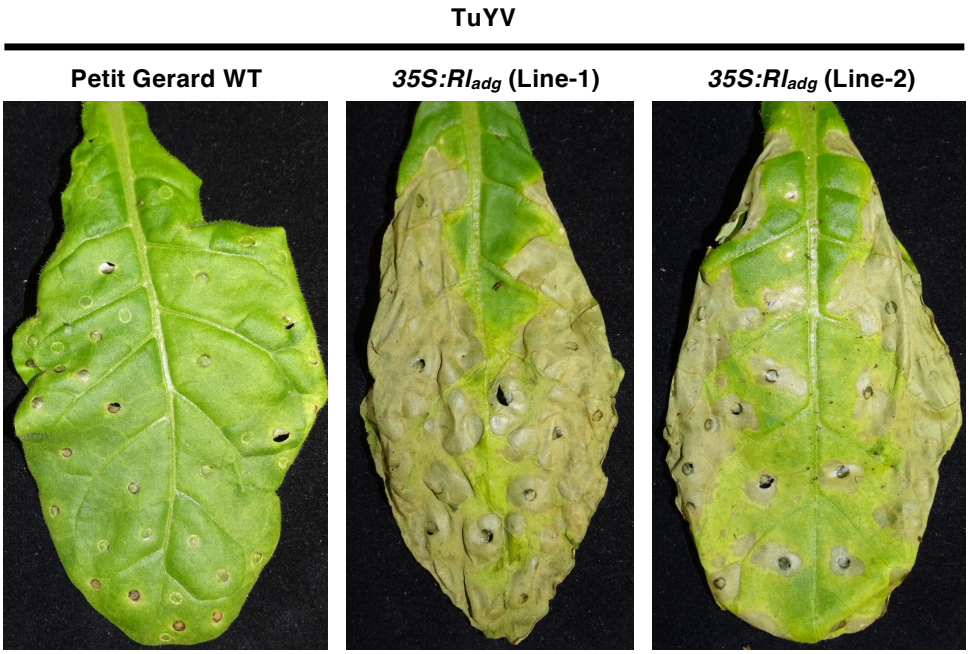

Figure 3.15. *Rl_{adg}* confers resistance to TuYV delivered by an infectious cDNA clone. *Rl_{adg}* confers resistance to TuYV in *N. tabacum*. Whole leaves of *N. tabacum* stably expressing Rl_{adg} were infiltrated with an *Agrobacterium* strain carrying an infectious clone of TuYV. Infiltration was performed using an *Agrobacterium* suspension with an OD_{600} of 0.3, leaves were imaged at 10 dpi.

3.2.9 – Rl_{adg} activation in a *Brassica* species results in a hypersensitive response

Rl_{adg} recognises several important viruses of Brassicaceae species, including TuYV and BMYV. For *Rl_{adg}* to confer resistance to these viruses in Brassicaceae species, the NLR must not only recognise the viral proteases but be compatible with TIR-NLR signalling pathways in Brassicaceae.

To confirm that Rl_{adg} can function in Brassicaceae, a transient expression HR assay was performed. As *A. thaliana* is not amenable to agroinfiltration, a turnip variety (cultivar Just Right) was used. Just Right was previously shown to respond to *Agrobacterium*-mediated delivery of the *Pseudomonas syringae* effector AVRrps4 (Sohn et al., 2009). After co-expression of Rl_{adg} with the PLRV protease, HR could be observed. This cell death was comparable to the response triggered by the recognition of the *A. candida* effector CCG28 by *A. thaliana* TIR-NLR WRR4 (Fig 3.16). This approach verifies that the TIR-NLR Rl_{adg} is able to function with the signalling components of at least one *Brassica* species.

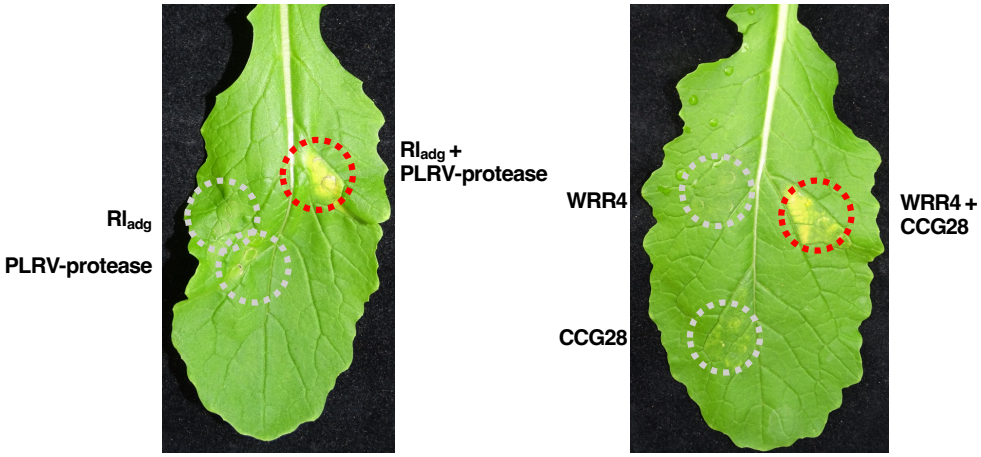

Figure 3.16. *Rl_{adg}* functions in *Brassica rapa subsp. rapa* cultivar Just Right. To test the functionality of Rl_{adg} in a *Brassica* species, the agroinfiltration-amenable turnip variety Just Right was used. Co-expression of Rl_{adg} with the PLRV protease resulted in cell death equivalent to the positive control of the *A. thaliana* TIR-NLR, WRR4, co-expressed with *A. candida* effector CCG28. *Agrobacterium* strains were infiltrated at 0.3 OD_{600}. Photographs were taken at 7 dpi.

3.2.10 – BMYV resistance was not observed in a preliminary *A. thaliana* experiment

A. thaliana was chosen as the system to test BMYV resistance conferred by *Rl_{adg}*. BMYV is a relatively broad-range virus, causing disease in oilseed rape and sugar beet, it is also capable of infecting *A. thaliana*. *A. thaliana* accession Col-0 was transformed with a T-DNA containing *Rl_{adg}* expressed under the CaMV *35S* promoter. Several primary transgenic lines were recovered and tested for expression of *Rl_{adg}*. Of these, two high-expressing transformants were selected, bred to the T3 generation and non-segregating populations were identified. To assay resistance conferred by *Rl_{adg}*, wild-type and transgenic *Arabidopsis* lines were infested with aphids carrying BMYV. After incubation for 15 days, BMYV infection of each plant was tested. PCR was performed using cDNA as a template and resulting bands were compared to an uninfected control. Most plants, both wild-type and transgenic, showed clear bands corresponding to BMYV (Fig. 3.17). There is no clear indication of elevated resistance to BMYV in these transgenic lines. In future experiments, additional transgenic lines expressing *Rl_{adg}* will be generated and resistance to other poleroviruses, such as TuYV, will be tested. The function of *Rl_{adg}* in the transgenic lines could also be validated using another approach, such as delivery of the protease via the *Pseudomonas syringae* pv. *tomato* DC3000D36E strain (Wei et al., 2015).

If *Rl_{adg}* does confer resistance to TuYV and BMYV, this gene could be delivered to various crop species including oilseed rape and sugar beet enhancing resistance to these viruses.

Testing of Rl_{adg} in Brassicaceae is ongoing but currently the performance of Rl_{adg} when challenged against aphid-vectored TuYV or BMYV remains unclear. However, in transgenic tobacco, expression of Rl_{adg} confers strong HR upon expression of a TuYV infectious clone. While systemic infection was not detected in the wild-type plants, this recognition is likely to translate into resistance in other species.

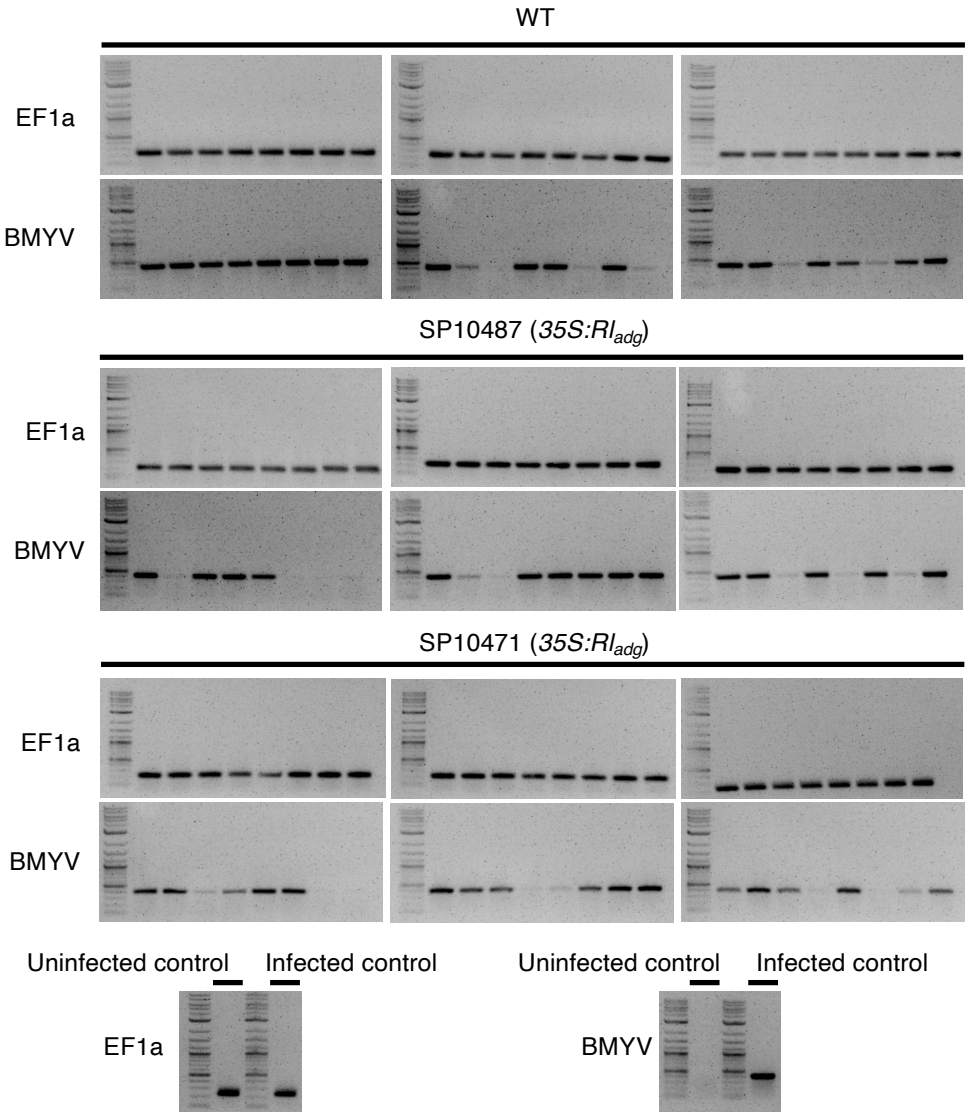

Figure 3.17. In a preliminary assay, Rl_{adg} did not confer resistance to BMYV in transgenic *Arabidopsis thaliana*. *35S:*Rl_{adg} *Arabidopsis* lines do not show a reduced rate of infection by BMYV. For each line, 24 plants were grown in short day conditions for five weeks before transfer of aphids from BMYV-infected sugar beet plants. Five aphids were placed onto each plant and covered with clip cages. After 10 days the colonized leaf and clip cages were removed. Samples from each plant were harvested 15 days after aphid infestation. After RNA extraction and cDNA synthesis, PCR was performed and imaged as above. BMYV-specific primers were used to determine presence of the virus in sampled tissue. EF1a-specific primers were used to assess cDNA quality. Uninfected and infected controls are also shown.

3.2.11 – Upon interaction with polerovirus proteases, Rl_{adg} forms higher-order complexes

Rl_{adg} can recognise multiple polerovirus proteases which have diverse amino acid sequences. Recognition by Rl_{adg} is independent of protease function, as the HDS catalytic triad mutant still activates Rl_{adg}. This suggests that recognition does not require a cleaved intermediate or guarded protein; instead, it suggests that Rl_{adg} directly associates with these proteases. To test the association between Rl_{adg} and its elicitors, a co-immunoprecipitation (CoIP) assay was performed. The FLAG-tagged Rl_{adg} was co-expressed with Myc-tagged effectors in the *eds1* knockout *N. tabacum* line where HR is abolished. Immunoprecipitated Rl_{adg} was analysed using SDS-PAGE. The association between Rl_{adg} and the PLRV protease, but not between Rl_{adg} and the N-terminal P1 fragment was observed. Similarly, Rl_{adg} associates with the HDS protease mutant and the TuYV and BMYV proteases (Fig. 3.18a).

To support the CoIP assay and the conclusion that Rl_{adg} and the PLRV protease associate *in planta*, a split luciferase assay was performed. Rl_{adg} tagged with the C-terminal luciferase fragment was co-expressed with the three P1 fragments tagged with the N-terminal luciferase fragment. Expression was performed in the *eds1* knock out *Nicotiana benthamiana* line. Clear luminescence was observed upon co-expression of the protease domain with Rl_{adg}, but not with the CTD or NTD (Fig. 3.18b). Together, the split luciferase and CoIP assays suggest that Rl_{adg} recognises polerovirus proteases through direct interaction *in planta*. Consistent with the HR observed when using the HDS protease mutant, this supports a model where the recognition is direct rather than through an intermediate protein.

Next, non-denaturing native-PAGE was used to detect a change in the oligomeric state of Rl_{adg} upon protease detection. After co-expression of Rl_{adg} with PLRV protease in *eds1 N. tabacum*, a higher-order Rl_{adg} oligomer can be detected. As expected, this is not observed when expressed with the N-terminal P1 fragment, or with the PVY coat protein (Fig. 3.18c). Like ROQ1 and RPP1, Rl_{adg} appears to transit from a monomeric to an oligomeric form upon activation. It remains unclear whether this resistosome is a tetramer and whether the effector is integrated into the structure, like in ROQ1 and RPP1 resistosomes. The CoIP and native-PAGE experiments were performed with postdoctoral researcher Dr He Zhao.

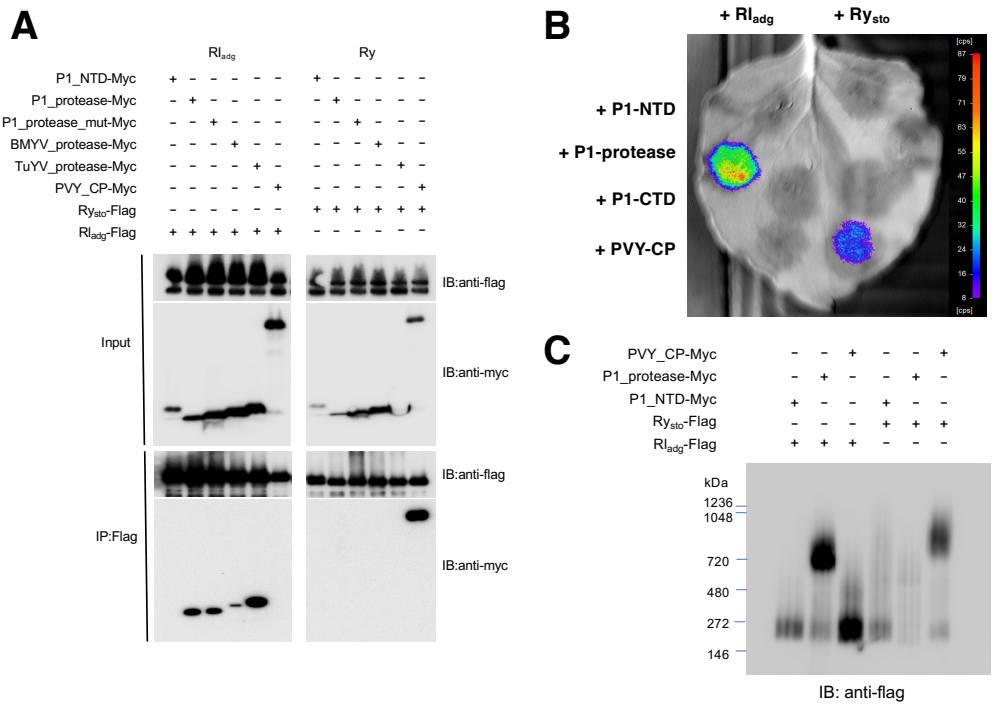

Figure 3.18. Rl_{adg} associates with polerovirus proteases *in planta*. (A) A co-immunoprecipitation assay was used to test for *in planta* association between NLRs and effectors. The PLRV, TuYV and BMYV proteases co-precipitate with Rl_{adg}, as does the HDS mutant protease. Neither the P1-NTD, or the PVY coat protein co-precipitate with Rl_{adg}. Ry_{sto}, which pulls down PVY coat protein, was used as a control. Samples were prepared from agroinfiltrated leaves of the *eds1 N. benthamiana* line. *Agrobacterium* strains were infiltrated at an OD_{600} of 0.5_{600}. Samples were harvested at 3 dpi. **(B)** An *in planta* split luciferase assay demonstrates association between Rl_{adg} and protease domain of P1. No signal was observed when Rl_{adg} was co-expressed with the P1-CTD, P1-NTD, or for the PVY CP. Co-expression of Ry_{sto} with the PVY CP was used as a positive control. This assay was performed in the *eds1 N. benthamiana* line. The NLRs were tagged with a C-terminal luciferase fragment, effectors with an N-terminal luciferase fragment. *Agrobacterium* strains were infiltrated at 0.2 OD_{600}. Leaves were imaged at 2 dpi. **(C)** Rl_{adg} forms a higher order oligomer when co-expressed with the P1 protease domain. FLAG-tagged NLRs were co-expressed with Myc-tagged elicitors in the *N. benthamiana eds1* line. *Agrobacterium* strains were infiltrated at an OD_{600} of 0.5. Samples harvested at 3 dpi were used to detect changes in oligomeric state. Samples were run on a blue native gel before blotting. **Experiments in panels A and C were performed by postdoctoral researcher Dr He Zhao.**

3.3 – Discussion

3.3.1 – Rl_{adg} is a TIR-NLR which confers resistance to the phloem-limited PLRV

Genetic resistance to PLRV is limited. The only reported instance of a single major *R*-gene against PLRV is *Rl*$_{adg}$ in potato accession LOP-868. Since Velasquez et al. (2007) positioned *Rl*$_{adg}$ at an NLR-rich region on Chromosome 5, it was hypothesised that *Rl*$_{adg}$ belongs to either the *R1*, or *Bs4*, gene clusters and encodes an NLR protein. In this chapter, *Rl*$_{adg}$ was identified using resistance gene enrichment sequencing coupled with bulked segregant analysis and PacBio sequencing. *Rl*$_{adg}$ is a *Bs4* orthologue which encodes a TIR-NLR intracellular immune receptor.

Rl_{adg} is the first characterised NLR that confers resistance to a phloem-limited pathogen. This demonstrates that plants can respond to infection within the vasculature through NLR-mediated resistance. NLRs which recognise and respond to other phloem-limited pathogens may exist. There are many economically important phloem-limited pathogens where little resistance has been identified, notably, Citrus greening disease (*Candidatus Liberibacter spp*) and various *Phytoplasma* species. It is intriguing why *R*-genes for these pathogens have not been identified. Resistance to phloem-limited pathogens may be quite costly in the event of mis-regulation or incomplete resistance. Even weak autoactivity in these tissues could significantly reduce fitness when compared to non-vascular tissue. Similarly, partial resistance in the vasculature may confer a greater fitness cost to the host than a biotrophic infection.

Interestingly, response to the P1 protease in LOP-868 can be seen across the leaf. This suggests that *Rl*$_{adg}$ is not exclusively expressed in vascular cells. *Rl*$_{adg}$ should confer resistance to PLRV upon co-infection with other viruses, which enable PLRV to move out of the vasculature (Barker, 1987, Savenkov and Valkonen, 2001).

Although these results show that *Rl*$_{adg}$ enables strong recognition of several poleroviruses, it has not been confirmed that *Rl*$_{adg}$ can prevent the spread of these viruses. Previous studies have suggested that PLRV can systemically infect *Nicotiana* species upon transient expression in leaf tissue (Nurkiyanova et al., 2000, Cowan et al., 2023); however, we were unable to detect the virus outside the infiltrated tissue. Typically, polerovirus colonisation relies on aphid vectors, which deliver the virus directly to the phloem. Our inoculation method may be limited by the virus's ability to reach the phloem from cells transiently expressing the viral clone. Since poleroviruses are adapted to colonise only phloem tissue, this movement may be restricted. Alternative approaches could include grafting transgenic plants onto susceptible

plants carrying the virus or using aphids carrying the virus to initiate infection. Other methods, such as coinfection of PLRV with other viruses to aid movement into the phloem, could also be investigated, although this would significantly complicate the experiment.

3.3.2 – Rl_{adg} recognises a range of polerovirus proteases

Several NLRs, such as Ry_{sto}, recognise effectors from multiple different viruses (Grech-Baran et al., 2022). In many instances, this may be through recognition of a conserved structure. Using Alphafold, the PLRV protease structure was predicted. The produced model is similar to the published structure of the protease from SeMV (Gayathri et al., 2006). The same fold was predicted in the models of proteases from other poleroviruses and enamoviruses. The recognition capacity of Rl_{adg} against a panel of proteases was tested. Surprisingly, all tested polerovirus proteases are recognised despite their highly diverse amino acid sequences. This recognition does not extend to the tested enamoviruses. This characterisation of *Rl_{adg}* draws parallels to the PVY *R*-gene *Ry_{sto}*, cloned from *S. stoloniferum*. Both genes encode TIR-NLRs which recognise a range of viruses through association with a conserved structural feature. Ry_{sto} recognises the coat proteins from at least 10 viruses and was demonstrated to elevate resistance to turnip mosaic virus (TuMV) and plum pox virus (PPV). Similarly, Rl_{adg} recognises many poleroviruses including TuYV and BMYV.

By observing this breadth of recognition, it could be predicted that *Rl_{adg}* will be durable when deployed in commercial potato varieties, as PLRV strains show little variation. This is also supported by the fact that the protease is strictly required for polerovirus replication and virus maturation so it cannot be simply lost to evade resistance. *Rl_{adg}* could be used to engineer resistance to BMYV and TuYV. *N. tabacum* transgenic lines carrying *35S:Rl_{adg}* respond strongly to agroinfiltration of an infectious TuYV clone. Given that Rl_{adg} is an unpaired TIR-NLR, it is predicted to not require NRC helpers or another *S. tuberosum*-specific NLR. Rl_{adg} confers protease-specific cell death in a *Brassica* species showing that the function of this NLR is not restricted to Solanaceae. It has not yet been demonstrated that *Rl_{adg}* can confer resistance to BMYV or TuYV in a *Brassica* species. In a preliminary assay, BMYV resistance of two transgenic *A. thaliana* lines appeared to be indistinguishable from untransformed Col-0. Additional transgenic lines will be tested for BMYV resistance. Also, resistance to TuYV in these lines will be tested as the interaction between Rl_{adg} and the TuYV protease appears to be stronger than with the BMYV protease (discussed further in 3.3.3). If proven to be effective, *Rl_{adg}* could perform an invaluable role in combatting poleroviruses in multiple economically important crop species.

3.3.3 – Rl_{adg} functions through direct recognition of the serine protease structure

Rl_{adg} functions through recognition of the PLRV serine protease. By testing a catalytic mutant of the PLRV protease, recognition was found to be independent of protease function. Co-immunoprecipitation and native-PAGE experiments demonstrate that Rl_{adg} activation occurs upon association with the protease. Rl_{adg} appears to directly recognise the viral protease and oligomerise to activate the immune response.

Despite having similar predicted structures, no cell death was observed when Rl_{adg} was co-expressed with proteases from enamoviruses. The more distantly related enamovirus proteases may not be recognised due to subtle differences in protein structure or the sequence within the site recognised by Rl_{adg}. Structural analysis of the interaction between Rl_{adg} to the PLRV protease could enable the engineering of Rl_{adg} to extend its recognition. Amino acids within the binding site of Rl_{adg} could be modified to confer recognition of enamovirus proteases, following the principles demonstrated with Pikp-1, and Sr50 (Maidment et al., 2023, Tamborski et al., 2022). This approach could also steer the optimisation of recognition of each polerovirus protease, enabling the strongest binding possible.

Engineering of Rl_{adg} would begin with identifying the amino acids involved in the interaction between the NLR and the recognised proteases, as well as the specific surface regions on the protease that are recognised. Interaction sites could be predicted using tools like Alphafold Multimer or directly characterised with experimental techniques such as cryo-electron microscopy. Once identified, these interacting residues would be confirmed by mutating them and testing for loss of recognition of the PLRV protease. With this characterisation complete, recognised and unrecognised proteases could be compared to form hypotheses about why the enamovirus proteases are not recognised and what modifications to Rl_{adg} might facilitate this interaction. Importantly, if Rl_{adg} can be modified to recognise enamoviruses, it would be essential to confirm that this recognition confers actual resistance to these pathogens.

This approach could be taken to expand the recognition of many NLRs. For example, the tomato TIR-NLR Bs4, which recognises the TAL (Transcription activator-like) effectors AvrBs3, AvrBs4, HAX3 and HAX4 in transient expression assays. These effectors contain a DNA-binding domain (DBD) with repeats of 34 amino acids. The effectors HAX2 and AvrHah1 are not recognised, possibly due to their DBD having repeats of 35 amino acids rather than 34. Despite Bs4 recognising AvrBs3 in transient expression assays, resistance to

Xanthomonas strains carrying AvrBs3 is weaker compared to strains with AvrBs4 (Schornack et al., 2004, Kay et al., 2005, Schornack et al., 2005, Schwartz et al., 2017). The direct interaction mechanism for Bs4 has not been demonstrated. However, if proven, the NLR could be engineered to enhance interaction with AvrBs3, which may result in stronger resistance. Similarly, engineering of Bs4 could enable recognition of HAX2 or AvrHah1.

In a preliminary test, transgenic *A. thaliana* expressing Rl_{adg} does not appear to have elevated resistance to BMYV. While the experiments are ongoing and only two transgenic events have been tested, the recognition of BMYV may not translate into resistance. Association of Rl_{adg} with the BMYV protease may be sufficient for HR, but insufficient for resistance. This hypothesis is supported by the CoIP assay (Fig 3.18a), where association with the BMYV protease appears to be weaker than for the PLRV protease, despite having a stronger input band than either the PLRV protease or TuYV protease. Actual binding strength could also be investigated further through *in vitro* binding and calorimetry assays.

We focused on using Rl_{adg} to enhance resistance to TuYV and BMYV. However, Rl_{adg} could also be used to elevate resistance to poleroviruses in several monocot species. Maize yellow dwarf virus, wheat yellow dwarf virus and sugarcane yellow leaf virus infect maize, wheat, and sugarcane respectively. Rl_{adg} recognises the maize and wheat polerovirus proteases in *N. tabacum* transient co-expression assays. To establish function in monocots, a golden gate, multigene transfer would likely be needed to transfer the Rl_{adg} with the EDS1/PAD4/SAG101 signalling pathway including NRG1 and/or ADR1.

In summary, Rl_{adg} was identified as a *Bs4* orthologue that encodes a TIR-NLR capable of broad-spectrum recognition of poleroviruses. Rl_{adg} could prove to be valuable in developing resistance in several plant families. While not tested biochemically, structural prediction led us to hypothesise that Rl_{adg} recognises a broadly conserved protease structure.

Chapter 4: A complex resistance gene locus from *Solanum americanum* confers resistance to multiple *Phytophthora* species

4.1 – Introduction

The genus *Phytophthora* contains many economically important plant pathogens. The most well-known is *Phytophthora infestans*, the causative agent of potato and tomato late blight. Resistance to *P. infestans* has been extensively explored, with nearly 50 *Resistance to Phytophthora infestans* (*Rpi*) genes cloned (Paluchowska et al., 2022). In contrast, there are no reported *R*-genes against *Phytophthora capsici*, which causes fruit, root, crown and stem rot in many *Solanum* and *Cucurbit* species.

Solanum americanum is a wild diploid species which is considered to be a non-host to *P. infestans* (Colon et al., 1992). This resistance has been well studied and several *Rpi-amr* genes and their elicitors have been cloned. The strongest are *Rpi-amr1* and *Rpi-amr3*, which encode NLRs that recognise the effectors AVRamr1 and AVRamr3 (Witek et al., 2016, Witek et al., 2021, Lin et al., 2020, Lin et al., 2022). More recently, the presence-absence of effector recognition across 52 accessions of *S. americanum* was characterised and several "*non-amr1,3*" *R*-genes were identified (Lin et al., 2023). The study of non-host resistance (NHR) to *P. infestans* in *S. americanum* has been supported by extensive genomic data including four high-quality reference genomes, and short-read whole genome sequencing of 52 accessions (Lin et al., 2023).

In this chapter, a novel *Rpi* gene named *Rpi-amr5* was cloned and characterised. *Rpi-amr5* is a paralogue of *Rpi-amr1* and functions through the recognition of two *P. infestans* effectors. Interestingly, we cloned an *Rpi-amr5* allele (named *Rpc2*) from another accession, which also confers strong resistance to *Phytophthora capsici*. The differences between these two alleles and their recognition of *P. capsici* effectors provide insight into the molecular mechanisms behind resistance to these oomycete pathogens.

4.2 – Results

4.2.1 – *Rpi-amr5* from *S. americanum* accession SP2275 maps to the *Rpi-amr1* cluster

S. americanum is a non-host to *P. infestans*. All tested accessions resist *P. infestans* in the field; however, five are susceptible in detached leaf assays where conditions are optimised for pathogen growth. These assays mask quantitative resistance, enabling the study of qualitative *R*-genes. Using this approach, *Rpi-amr1* and *Rpi-amr3* were cloned from the *S. americanum* accessions SP2273 and SP1102, respectively, and their cognate effectors, AVRamr1 and AVRamr3, were subsequently discovered.

Novel *P. infestans* resistance was identified by screening resistant *S. americanum* accessions for lack of response to these two effectors. Two resistant accessions (SP2275 and SP3370) lack recognition of AVRamr1 or AVRamr3 and thus must contain novel *R*-genes (Fig. 4.1a, Fig. 4.1b). Both lines were crossed to a susceptible accession (SP2271) yielding resistant F1s. Small F2 populations (~200 plants) derived from each F1 plant were phenotyped, and 3:1 (resistant: susceptible) segregation ratios were observed. To identify NLR-encoding genes linked to resistance in SP2275, 24 susceptible and 16 resistant segregants were used in bulked segregant sequencing (Fig. 4.1c). Separately, bulks of 35 susceptible and 24 resistant segregants derived from the SP3370 F2 were also sequenced.

Through bulked segregant analysis, resistance in both SP2275 and SP3370 was mapped to the *Rpi-amr1* locus on the short arm of Chromosome 11. SMRT RenSeq assemblies were used to compare the *Rpi-amr1* haplotypes of SP2275 and SP3370. All complete genes share 100% identity between these accessions (Fig 4.2a); therefore, resistance in SP2275 and SP3370 is most likely identical. As a high-quality SP2275 genome is published (Lin et al., 2023), resistance in this accession was prioritised and subsequently named *Rpi-amr5*.

Using NLR-parser (Steuernagel et al., 2015), 16 paralogues within the *Rpi-amr1* cluster of SP2275 were identified. Paralogues belong to two sub-clusters: one previously identified by Witek et al. (2021) and a second cluster located closer to the top of the chromosome (Fig. 4.1c). Gene models and expression levels of candidates were defined using cDNA RenSeq reads mapped to the SP2275 whole genome assembly. Of the sixteen genes in the cluster, four are expressed and encode complete NLRs that have all canonical domains (Table. 4.1). Using BLAST and a phylogenetic approach, these SP2275 genes were named according to homology to NLRs in accession SP2273, where the Rpi-amr1 cluster was first characterised (Witek et

al., 2021). The *Rpi*-amr1e paralogue, which confers resistance in SP2273, is non-functional in both SP2275 and SP3370 due to a frameshift leading to a premature stop codon (Fig. 4.2b).

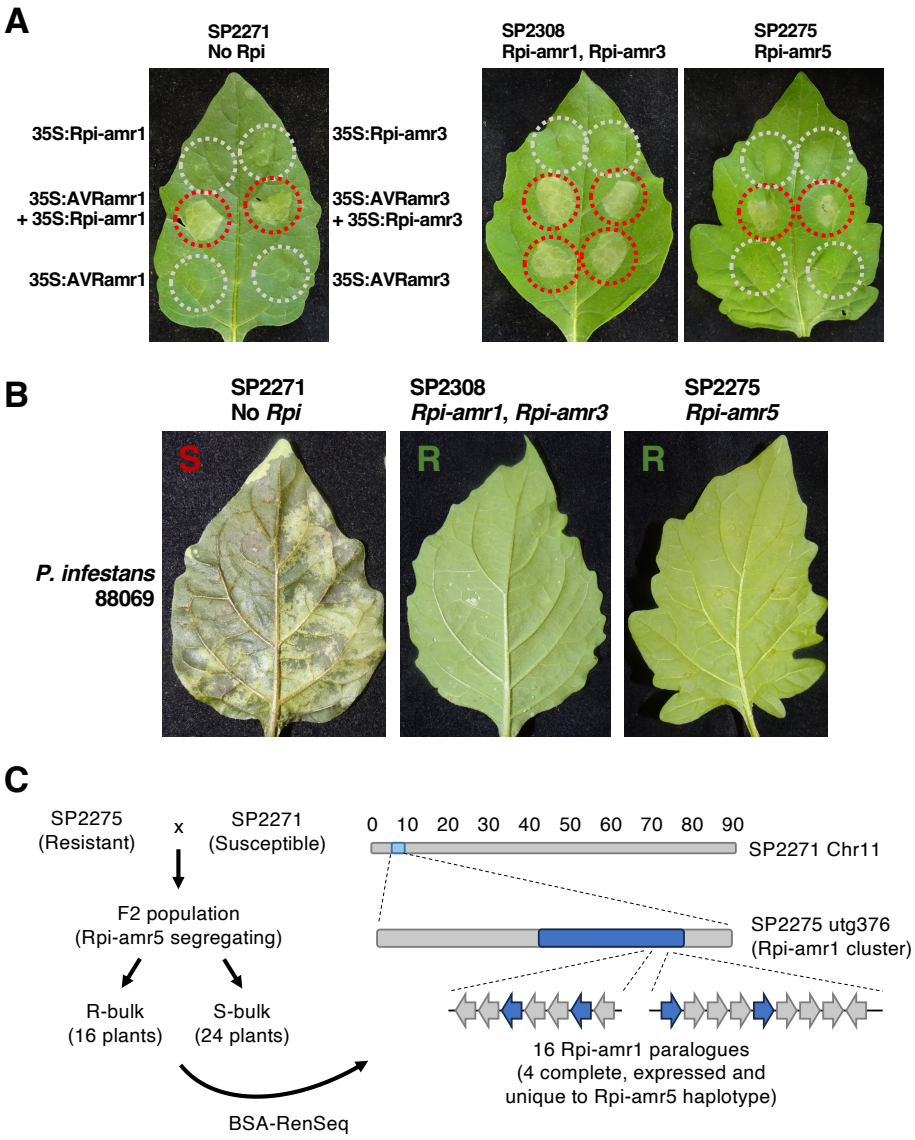

Figure 4.1. *Rpi-amr5* maps to the *Rpi-amr1* cluster but confers novel resistance to *P. infestans*. (A) *S. americanum* accession SP2275 does not respond to AVRamr1 or AVRamr3. Transient expression of these effectors in SP2275 does not result in cell death. The susceptible reference accession SP2271 was used as a negative control, SP2308 which carries both *Rpi-amr1* and *Rpi-amr3* was used as a positive control. *Agrobacterium* strains were infiltrated at an OD_{600} of 0.5, photographs were taken at 3 dpi. **(B)** SP2275 is highly resistant to *P. infestans*. The resistant accession SP2308 and susceptible accession SP2271 were used as controls. Leaves were imaged 5 days post-inoculation with *P. infestans* strain 88069 (10 µl drops at 20,000 spores ml^{-1}). **(C)** SP2275 was crossed to SP2271 and an F2 population was phenotyped. The 24 most susceptible and 16 most resistant plants were used for bulked segregant RenSeq analysis. *Rpi-amr5* was mapped to the *Rpi-amr1* cluster on Chromosome 11, which contains 16 paralogues in SP2275. NLR encoding genes are represented with arrows, *Rpi-amr5* candidates are indicated in blue. *Rpi-amr1* is non-functional in SP2275 due to a premature stop.

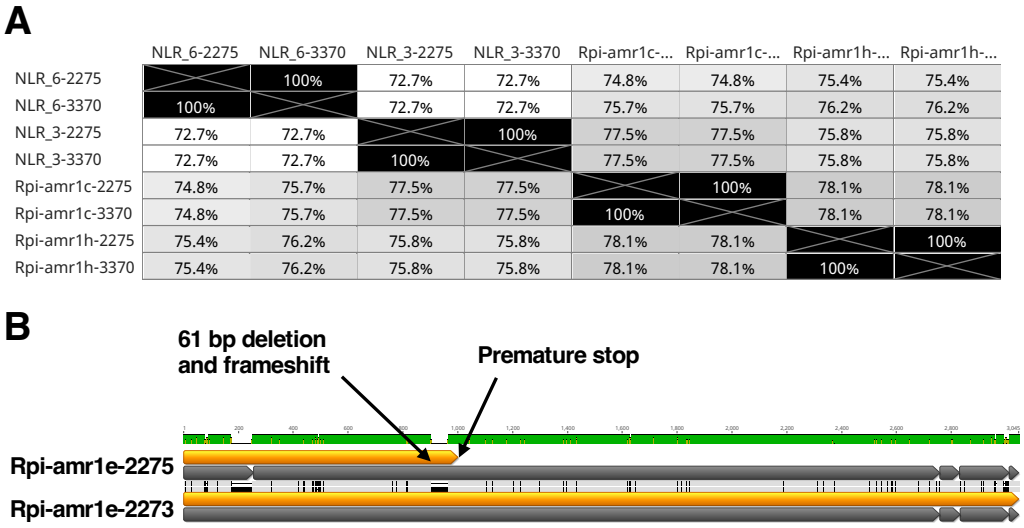

Figure 4.2. *Rpi-amr5* candidates are identical in SP2275 and SP3370 and do not include the *Rpi-amr1e* paralogue. (A) SP2275 and SP3370 both contain novel resistance to *P. infestans.* The complete NLR-encoding genes within the resistance-linked *Rpi-amr1* cluster were compared. All complete NLRs within this cluster are identical between accessions, this is represented by a heatmap of the percent identity of aligned amino acid sequences. Resistance to *P. infestans* in SP3370 and SP2275 is due to the same gene. **(B)** Resistance in SP2275 is not due to *Rpi-amr1*. The *Rpi-amr1e* paralogue, which is responsible for resistance in SP2273, is non-functional in SP2275 due to a frameshift and premature stop. The position of this stop is indicated in the alignment. The CDS of each allele is shown, grey bars indicate the position of exons and orange bars the CDS.

Table 4.1. Four NLR encoding genes were identified as *Rpi-amr5* candidates. *Rpi-amr5* maps to the *Rpi-amr1* cluster on Chromosome 11. Of the 16 paralogues identified in the SP2275 reference genome, four are candidates for *Rpi-amr5*. The ID, expression (determined using cDNA RenSeq of SP2275) and homology to the characterised *Rpi-amr1* cluster (from SP2273) is shown. Filtered candidates were tested in transient *N. benthamiana* assays, the result is shown.

NLR_ID	Rpi-amr1 homologue	Expression in SP2275	Candidate notes	Transient assay result
NLR_1		Expressed	**Premature stop**	**-**
NLR_2		**No expression**	-	**-**
NLR_3		Expressed	-	**No resistance**
NLR_4		**No expression**	-	-
NLR_5		**No expression**	-	-
NLR_6		Expressed	-	**No resistance**
NLR_7		Expressed	**Frameshift mutation**	-
NLR_8		Expressed	**Partial – No CC domain**	-
NLR_9	Rpi-amr1h	Expressed	**-**	**Autoactive**
NLR_10	Rpi-amr1f	Expressed	**Partial – No CC domain**	-
NLR_11	Rpi-amr1e	Expressed	**Frameshift mutation**	-
NLR_12	Rpi-amr1d	Expressed	**Found in non-amr5 accession**	-
NLR_13	Rpi-amr1c	Expressed	**-**	**Autoactive**
NLR_14		Expressed	**Incomplete**	-
NLR_15		Expressed	**Partial – incomplete NB-ARC, no LRRs**	-
NLR_16	Rpi-amr1a	Expressed	**Found in non-amr5 accession**	-

4.2.2 – VIGS and CRISPR define the paralogue that confers *Rpi-amr5* function

To test the function of the four *Rpi-amr5* candidates, open reading frames were amplified from SP2275 gDNA and cloned into expression vectors under the CaMV *35S* promoter. After *Agrobacterium*-mediated transient expression in *Nicotiana benthamiana*, elevated resistance to *P. infestans* was tested. Two candidates conferred no visible resistance in this assay (Fig. 4.3a). Expression of the other two candidates resulted in constitutive activity and pathogen-independent cell death (Fig. 4.3b). To assay these candidates more effectively, a loss-of-function TRV-based VIGS approach was used.

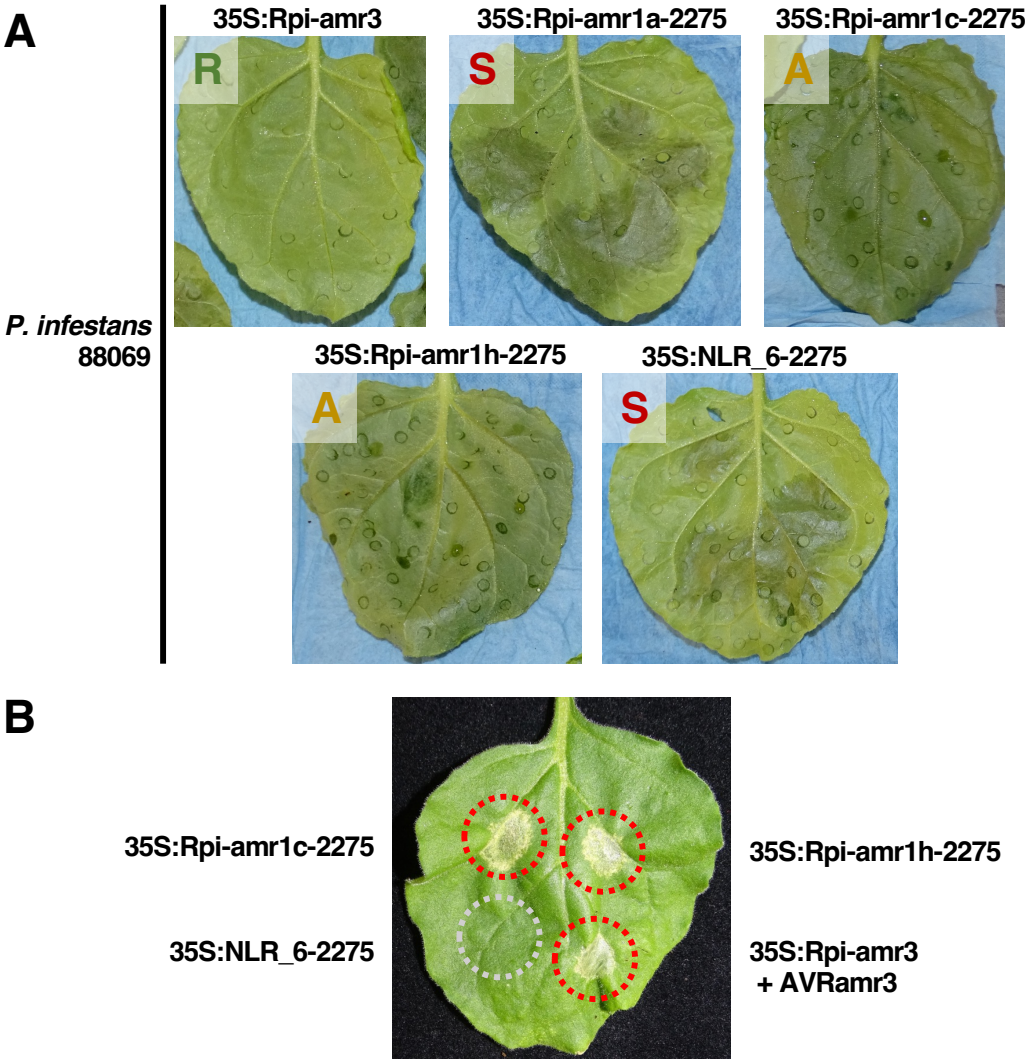

Figure 4.3. Two *Rpi-amr5* candidates are constitutively active in *N. benthamiana* transient assays. (A) *Rpi-amr5* candidates were initially tested in *N. benthamiana* transient assays. *Rpi-amr1a-2275*, which is also found in accessions lacking *Rpi-amr5*, was used as a negative control, *Rpi-amr3* was used as a positive control. *NLR_6-2275* conferred no elevated resistance (indicated as S – susceptible). Expression of *Rpi-amr1c-2275* and *Rpi-amr1h-2275* paralogues caused a wilted phenotype (indicated as A – autoactive). Agroinfiltration was performed at 0.2 OD_{600}. At 2 dpi, leaves were detached and *P. infestans* (strain 88069) inoculation was performed (10 µl drops at 20,000 spores ml^{-1}). Leaves were photographed at 6 days post-inoculation. **(B)** Transient expression of *Rpi-amr1c-2275* and *Rpi-amr1h-2275* in *N. benthamiana* results in strong HR indicating constitutive activity. *N. benthamiana* infiltrations were performed using *Agrobacterium* suspensions at 0.2 OD_{600}, leaves were imaged at 4 dpi.

To silence the entire cluster, a fragment from the NB-ARC encoding region of the *Rpi-amr1h* paralogue was cloned into TRV2, as this sequence is highly conserved between all members of this cluster. Individual paralogues were silenced by targeting LRR-encoding regions (Fig. 4.4a). Whole-cluster silencing resulted in complete susceptibility, and silencing the *Rpi-amr1c* paralogue produced a similar susceptible phenotype (Fig. 4.4b). *Rpi-amr1c-2275*, hereafter named *Rpi-amr5*, was stably transformed into susceptible accession SP2271 and found to confer late blight resistance in primary transformants (Fig. 4.5a). Using CRISPR/Cas9 mutagenesis, *Rpi-amr5* was knocked out in SP2275 resulting in elevated susceptibility relative to wild-type accession (Fig. 4.5b). *Rpi-amr5* is a four-exon *Rpi-amr1* paralogue which encodes a CC-NLR immune receptor (Fig 4.5c).

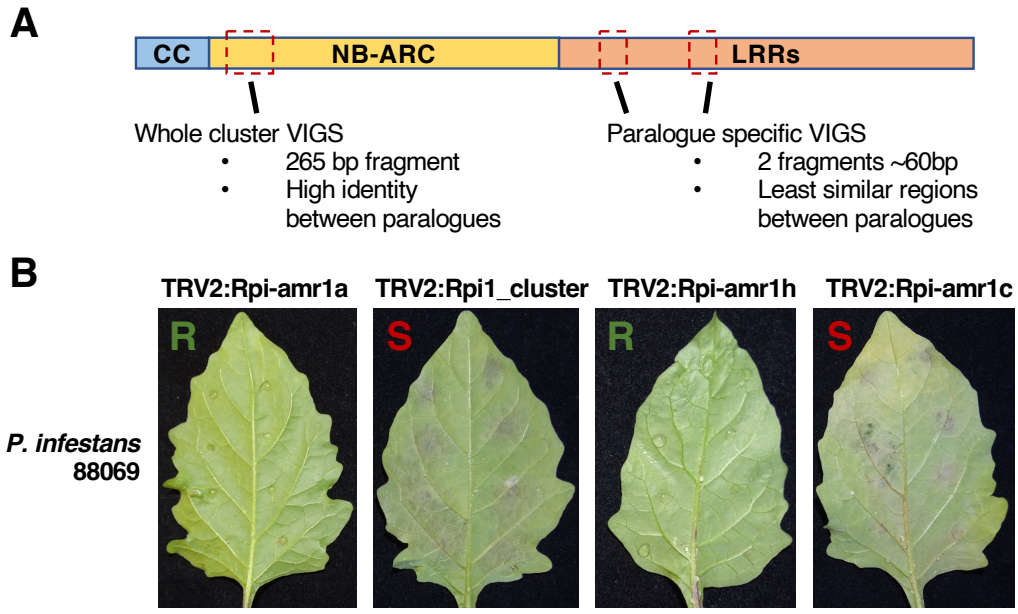

Figure 4.4. VIGS reveals *Rpi-amr5* as a paralogue of *Rpi-amr1*. (A) *Rpi-amr5* candidates were tested using VIGS. Whole-cluster silencing was performed using a fragment from the NB-ARC encoding region of the *Rpi-amr1h* paralogue. Paralogue-specific silencing was performed using constructs containing two LRR-encoding fragments fused together. **(B)** Silencing of the *Rpi-amr1* cluster and the *Rpi-amr1c* paralogue compromised resistance in SP2275, silencing of *Rpi-amr1a* or *Rpi-amr1h* did not affect resistance. Leaves were inoculated with 10 µl drops of *P. infestans* (strain 88069) spores at a concentration of 20,000 spores ml^{-1}. Leaves were photographed at 5 days post-inoculation.

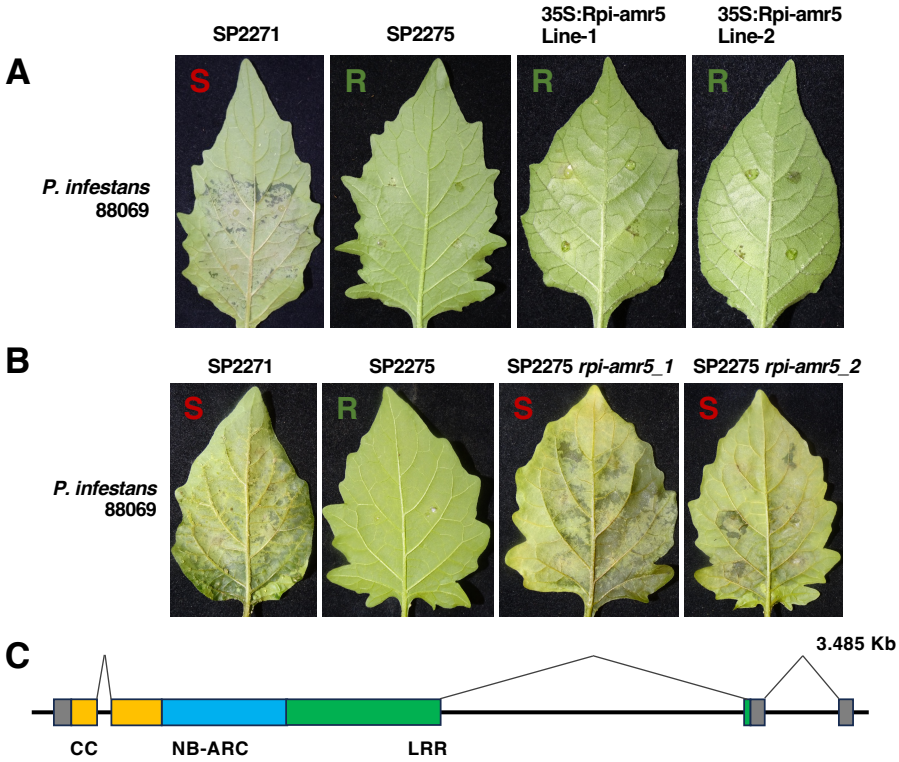

Figure 4.5. *Rpi-amr5* encodes a CC-NLR and is a paralogue of *Rpi-amr1*. (A) Overexpression of *Rpi-amr5* (*Rpi-amr1c-2275*) from SP2275 elevates resistance in the susceptible accession SP2271. Constructs containing a T-DNA of *35S:Rpi-amr5* were stably transformed into SP2271. Leaves were inoculated with 10 µl drops of *P. infestans* strain 88069, at a concentration of 20,000 spores ml^{-1}, and imaged at 5 days post-inoculation. Two independent primary transgenic events are shown. **(B)** CRISPR knock out of *Rpi-amr5* in SP2275 greatly reduces resistance to *P. infestans*, resistance was equivalent to the susceptible accession SP2271. Leaves were inoculated with 10 µl drops at 20,000 spores ml^{-1} and imaged at 10 days post-inoculation. *P. infestans* strain 88069 was used. Two independent biallelic mutants are shown. **(C)** *Rpi-amr5* is a four-exon gene which encodes an 897 amino acid CC-NLR with 74.1% identity to Rpi-amr1. Intron and exon structure was determined using cDNA RenSeq data generated from SP2275 leaf tissue, no evidence of alternative splicing was found. The region encoding the CC domain is indicated in yellow, the NB-ARC in blue and the LRR in green. 5' and 3' UTRs are indicated in grey.

4.2.3 – Screening *S. americanum* diversity for *P. capsici* resistance reveals *Rpc2* in SP2308

While *S. americanum* carries genes for resistance to *P. infestans* and *Ralstonia solanacearum* (Witek et al., 2016, Moon et al., 2021), resistance to *P. capsici* has not been previously investigated. The 52 *S. americanum* accessions were screened for resistance to *P. capsici* and two accessions were found to be highly resistant. One resistant accession, SP2308 (Fig. 4.6a), was crossed with the susceptible accession SP2271. An F2 population of 200 plants segregated in a 3:1 ratio (resistant: susceptible), indicating that a single gene is responsible for the resistant phenotype. This gene was named *RESISTANCE TO PHYTOPHTHORA CAPSICI 2* (*Rpc2*). Resistance in the other accession (SP1102) is investigated further in Chapter 5.

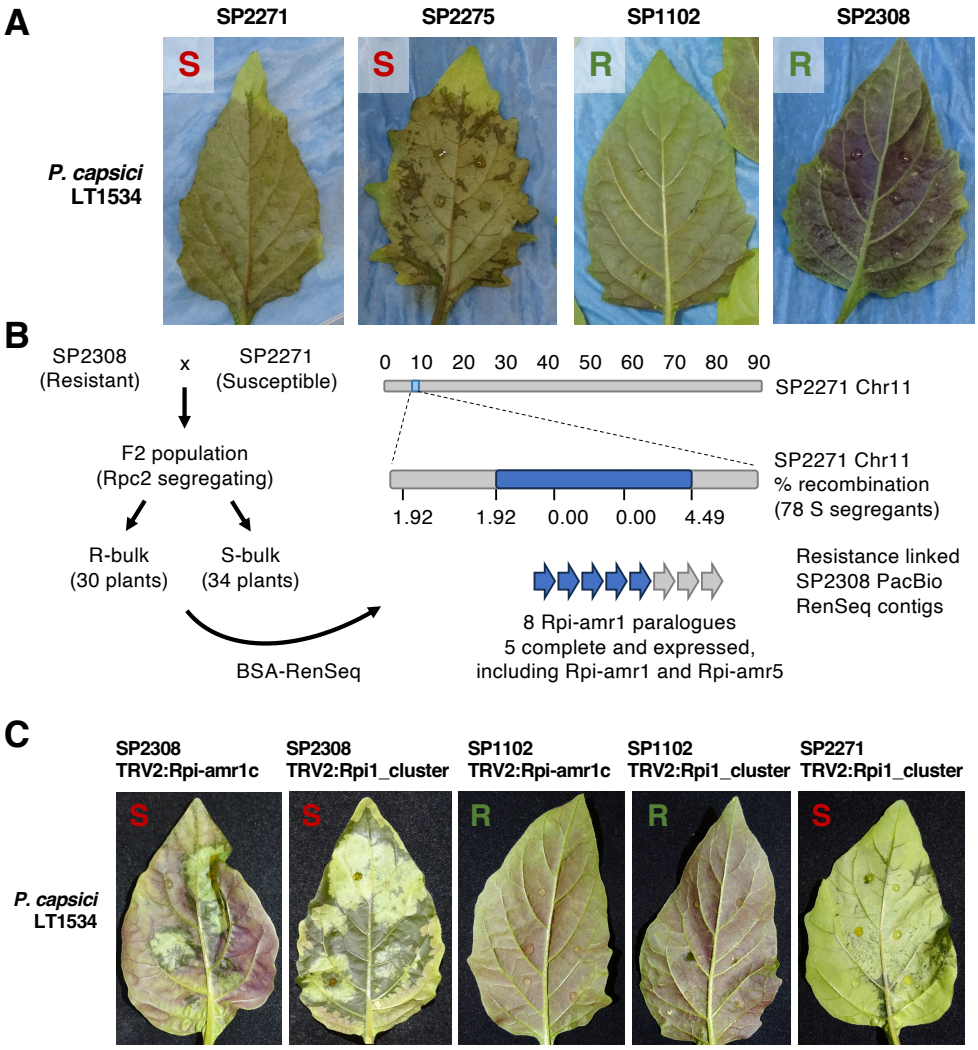

Figure 4.6. *Rpc2*, which confers resistance to *P. capsici*, maps to the *Rpi-amr1*/*Rpi-amr5* cluster in SP2308 and silencing of *Rpi-amr1c-2308* compromises resistance. (A) *S. americanum* accessions SP1102 and SP2308 are highly resistant to *P. capsici*, SP2271 and SP2275 are susceptible. Leaves were imaged 3 days post-inoculation with *P. capsici* strain LT1534 (10 µl drops at 10,000 spores ml^{-1}). **(B)** SP2308 was crossed to SP2271 and an F2 population was phenotyped, the 34 most susceptible and 30 most resistant plants were used for bulked segregant analysis. Using the SP2271 reference genome, *Rpc2* was mapped to the *Rpi-amr1* cluster on Chromosome 11. Fine mapping in an expanded population of 78 susceptible segregants was performed, percentage recombination rates are indicated. Eight NLR-encoding genes within this interval were identified in the SP2308 SMRT RenSeq assembly, the five complete candidates are indicated in blue. Both *Rpi-amr1* and *Rpi-amr5* are complete in SP2308. **(C)** VIGS was performed to silence candidates in SP2308. Silencing of either the whole cluster, or the *Rpi-amr5* paralogue (*Rpi-amr1c*) compromised resistance, neither silencing construct affected resistance in SP1102. Leaves were inoculated with 10 µl drops of *P. capsici* strain LT1534 at a concentration of 20,000 spores ml^{-1} and imaged at 3 days post-inoculation.

4.2.4 – *Rpc2* maps to the *Rpi-amr1*/*Rpi-amr5* cluster

From the phenotyped F2 population, bulks of 34 susceptible and 30 resistant plants were used for short-read RenSeq. Using bulked segregant analysis, *Rpc2* was mapped to the *Rpi-amr1*/*Rpi-amr5* cluster. Fine mapping performed on 78 susceptible segregants identified a mapping interval of 508 Kb (Fig. 4.6b). Using PacBio RenSeq on SP2308, 8 NLR-encoding genes within the interval were identified. Three of these are pseudogenes, lacking canonical NLR domains or showing no clear ORF. The remaining five genes, which included novel alleles of *Rpi-amr1* and *Rpi-amr5*, were subsequently tested as *Rpc2* candidates (Fig. 4.6b) (Table 4.2).

Table 4.2. Five NLR encoding genes were identified as *Rpc2* candidates. Using bulked segregant analysis, *Rpc2* was mapped to the *Rpi-amr1*/*Rpi-amr5* cluster on Chromosome 11. Of the eight paralogues identified within the *Rpc2* mapping interval, five were identified as candidates. The ID and homology to the characterised *Rpi-amr1* cluster is shown. Candidates encoding complete NLRs were tested in transient *N. benthamiana* assays, the result is shown.

NLR_ID	Rpi-amr1 homologue	Candidate notes	Transient assay result
NLR_1	Rpi-amr1h	-	**No resistance**
NLR_2	Rpi-amr1g	-	**No resistance**
NLR_3	Rpi-amr1e	-	**No resistance**
NLR_4	-	**Pseudogenised, 5 Kb insertion into NB-ARC**	-
NLR_5	Rpi-amr1c	-	**Autoactive**
NLR_6	-	**Incomplete NB-ARC**	-
NLR_7	Rpi-amr1a	-	**Autoactive**
NLR_8	-	**No clear ORF**	-

4.2.5 – *Rpc2* is an allele of *Rpi-amr5*

In *N. benthamiana* transient assays, three candidates (including an allele of *Rpi-amr1*) did not confer resistance to *P. capsici*. The other two NLRs (including an allele of *Rpi-amr5*) were found to be constitutively active in *N. benthamiana* (Fig. 4.7). Therefore, VIGS was used to test functionality of the candidates in the native accession. Whole-cluster silencing resulted in susceptibility, and a similar phenotype was observed upon specific silencing of the *Rpi-amr5* gene (*Rpi-amr1c-2308*) (Fig. 4.6c). CRISPR-induced mutation of *Rpi-amr1c-2308* in SP2308 also resulted in susceptibility to *P. capsici* (Fig. 4.8a). Moreover, when *Rpi-amr1c-2308* was

transformed into susceptible *S. americanum,* resistance to both *P. capsici*, and *P. infestans* was observed in primary transformants (Fig. 4.8b, Fig. 4.8c). These experiments demonstrate that *Rpc2* is an allele of *Rpi-amr5*. These alleles are highly similar and encode NLRs with 97.4% amino acid identity (Fig. 4.8d). *Rpi-amr5* and *Rpc2* confer resistance to *P. infestans* in SP2275 and SP2308, respectively, but only *Rpc2* is capable of conferring resistance to *P. capsici*.

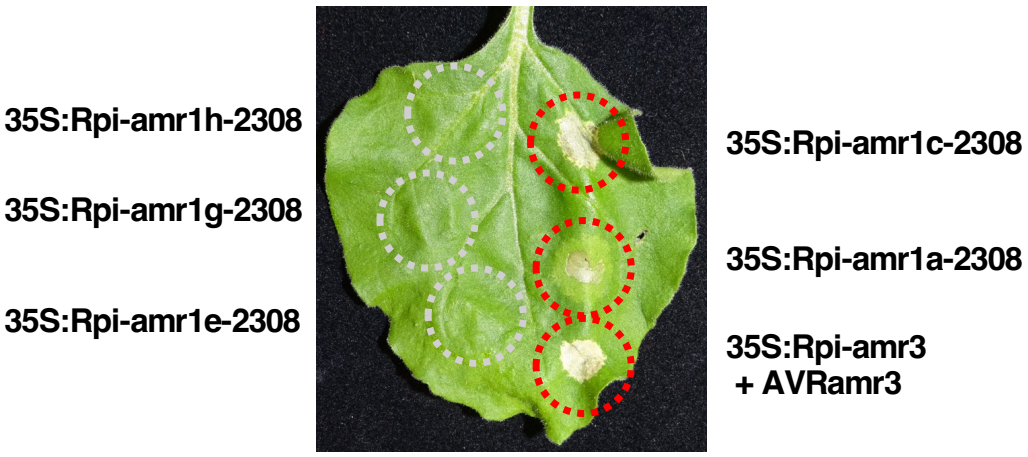

Figure 4.7. Two *Rpc2* candidates are constitutively active in *N. benthamiana*. Five *Rpc2* candidates were identified and cloned into CaMV *35S* expression vectors to be tested in *N. benthamiana*. Infiltration of the candidates produced strong HR for both *Rpi-amr1c-2308* and *Rpi-amr1a-2308* indicating constitutive activity. *N. benthamiana* infiltrations were performed at 0.2 OD_{600}, leaves were imaged at 4 dpi.

4.2.6 – *Rpc2* and *Rpi-amr5* are functional in transgenic *S. lycopersicum*

Next, the function of *Rpi-amr5* and *Rpc2* was tested in *Solanum lycopersicum*, which can be infected by both *P. infestans* and *P. capsici*. Both genes were recloned into a novel USER compatible acceptor (pICSLUS0005OD) containing *SaNRC4a* promoter and terminator. This vector was used to investigate the function of the alleles when expressed at moderate levels, as opposed to high levels produced by the CaMV *35S* promoter. Constructs were transformed into the susceptible variety Moneymaker. Stable transformants were tested by drop-inoculation with either *P. capsici* or *P. infestans* zoospores. *Rpc2* transformants were found to be resistant to both pathogens, whilst *Rpi-amr5* transformants were only resistant to *P. infestans* (Fig. 4.9a, b). These results suggest that the absence of resistance conferred by *Rpi-amr5* is likely explained by allelic differences between *Rpi-amr5* and *Rpc2*, rather than their expression levels.

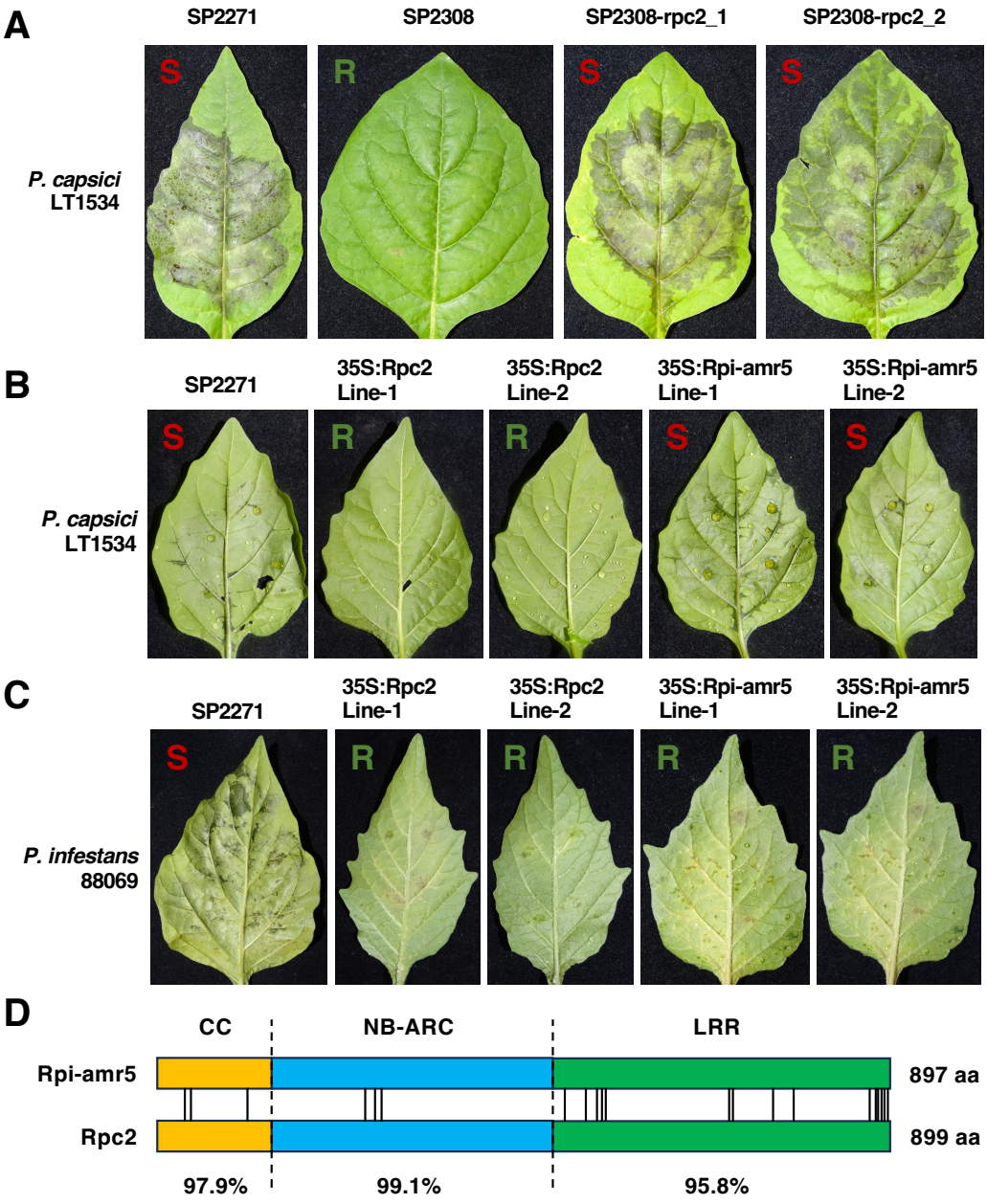

Figure 4.8. *Rpc2* is an allele of *Rpi-amr5* and confers resistance to both *P. infestans* and *P. capsici* in *S. americanum*. **(A)** CRISPR-induced knock out of *Rpc2* in SP2308 eliminates resistance to *P. capsici*. Biallelic *Rpc2* mutants have resistance equivalent to susceptible accession SP2271. Leaves were inoculated with 10 µl drops of *P. capsici* strain LT1534 at 20,000 spores ml^{-1} and imaged at 3 days post-inoculation. Two independent biallelic mutants are shown. **(B)** Overexpression of *Rpc2*, but not *Rpi-amr5*, elevates resistance to *P. capsici* in the susceptible *S. americanum* SP2271 background. Leaves were inoculated with 10 µl drops of *P. capsici* strain LT1534 at 20,000 spores ml^{-1} and imaged at 3 days post-inoculation. Two independent transgenic events are shown. **(C)** *Rpc2* overexpression elevates resistance to *P. infestans* in *S. americanum* accession SP2271. Leaves were inoculated with 10 µl drops of strain 88069 at a concentration of 20,000 spores ml^{-1}. Leaves were imaged at 5 days post-inoculation. **(D)** *Rpc2* and *Rpi-amr5* are alleles and show highly similar predicted amino acid sequences, the two NLRs have 97.4% amino acid identity. The positions of polymorphisms between the two predicted amino acid sequences are indicated.

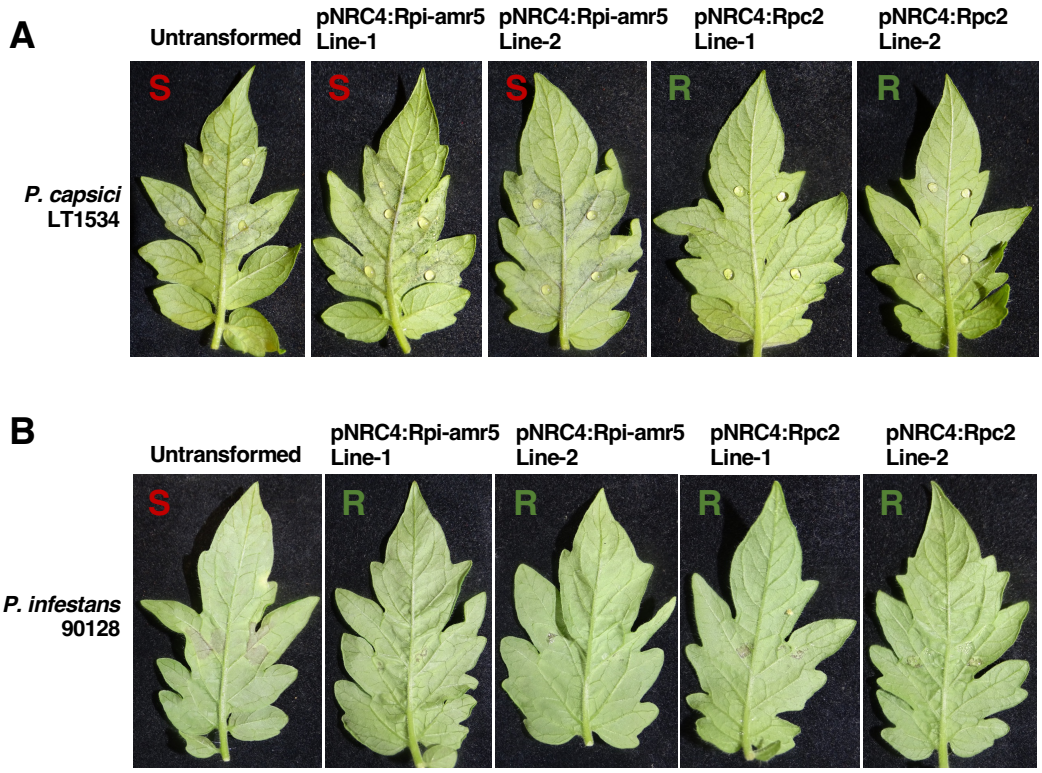

Figure 4.9. *Rpi-amr5* and *Rpc2* are functional in *S. lycopersicum* stable transformants. **(A)** *S. lycopersicum* (variety Moneymaker) lines expressing *Rpc2* under *SaNRC4a* regulatory elements are resistant to *P. capsici*, *Rpi-amr5* transgenic lines are no more resistant than the untransformed control. Two independent transgenic lines are shown for each construct. Leaves were inoculated with 10 µl drops of *P. capsici* strain LT1534 (10,000 spores ml^{-1}) and imaged at 3 days post-inoculation. **(B)** Transgenic *S. lycopersicum* expressing *Rpi-amr5,* or *Rpc2,* are resistant to *P. infestans*, the untransformed control is susceptible. Leaves were inoculated with *P. infestans* strain 90128 in 10 µl drops at a concentration of 20,000 spores ml^{-1}. Images were taken at 5 days post-inoculation.

4.2.7 – Neither *Rpc2* or *Rpi-amr5* confers strong resistance to *P. infestans* in transgenic *S. tuberosum*

Both *Rpi-amr5* and *Rpc2* confer resistance to *P. infestans* in *S. americanum* and *S. lycopersicum*. Therefore, transgenic *Solanum tuberosum* lines carrying *Rpi-amr5* or *Rpc2* under CaMV *35S* promoter were generated. For both constructs, 30 primary transformants were recovered and tested for resistance to *P. infestans*. Surprisingly, no tested plant showed any detectable gain of resistance relative to the untransformed control. Positive control lines carrying *Rpi-amr1* showed complete resistance to *P. infestans* (Fig. 4.10).

The reason for the lack of resistance in *S. tuberosum* is unclear. Resistance conferred by *Rpi-amr5* could be quantitative and insufficient for detectable resistance in *S. tuberosum*, since *P. infestans* is more virulent on *S. tuberosum*, and infection spread is faster than in either *S. lycopersicum* or susceptible *S. americanum* accessions. To investigate this in the future, *Rpi-amr5* could be co-delivered with other weaker resistance genes to test for elevated resistance. An alternative hypothesis is that there is less efficient signalling between Rpi-amr5 and potato NRC proteins, relative to *S. americanum* NRC alleles. However, why this signalling would work well for Rpi-amr1 but not for the closely related Rpi-amr5, is unclear.

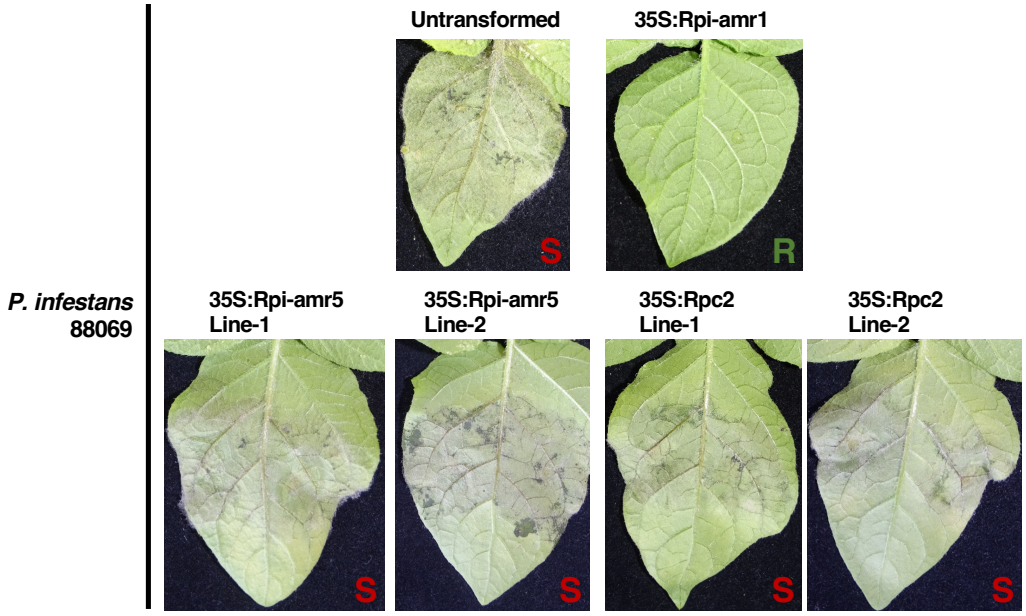

Figure 4.10. *Rpi-amr5* and *Rpc2* do not confer resistance in *S. tuberosum* stable transformants. Stable transgenic *S. tuberosum cv.* Maris Piper lines expressing either *35S:Rpi-amr5* and *35S:Rpc2* were produced. For each construct, 30 primary transgenic lines were screened, no transformant showed increased resistance to *P. infestans*. A transgenic line carrying *Rpi-amr1* was used as a control. Two representative independent transgenic lines for each construct are shown. Leaves were inoculated with 10 µl drops of *P. infestans* strain 88069 at 10,000 spores ml^{-1}. Leaves were photographed at 6 days post-inoculation.

4.2.8 – Co-expression of Rpi-amr5 with NbNRC2, but not SaNRC2, causes constitutive activity

Expression of *Rpi-amr5* or *Rpc2* under either CaMV *35S* or *SaNRC4a* promoters in *N. benthamiana* results in cell death (Fig. 4.11a). To enable screening of effector candidates in *N. benthamiana,* the cause of this effector-independent cell death was investigated. Both *Rpi-amr5* and *Rpc2* belong to the NRC-dependent NLR clade. NRC proteins are helper NLRs

through which cell death is activated after pathogen detection by sensor CC-NLRs (Ahn et al., 2023). *N. benthamiana* NRCs, which have not co-evolved with *S. americanum* sensor NLRs, may contribute to this constitutive activity. When *Rpi-amr5* was expressed in the *nrc234 N. benthamiana* line, no cell death was observed. Complementation with *35S:NbNRC2* restores constitutive cell death, while complementation with *35S:SaNRC2* does not (Fig. 4.11b). This discovery enabled the use of *35S:SaNRC2* and *nrc234 N. benthamiana* for screening candidate effectors.

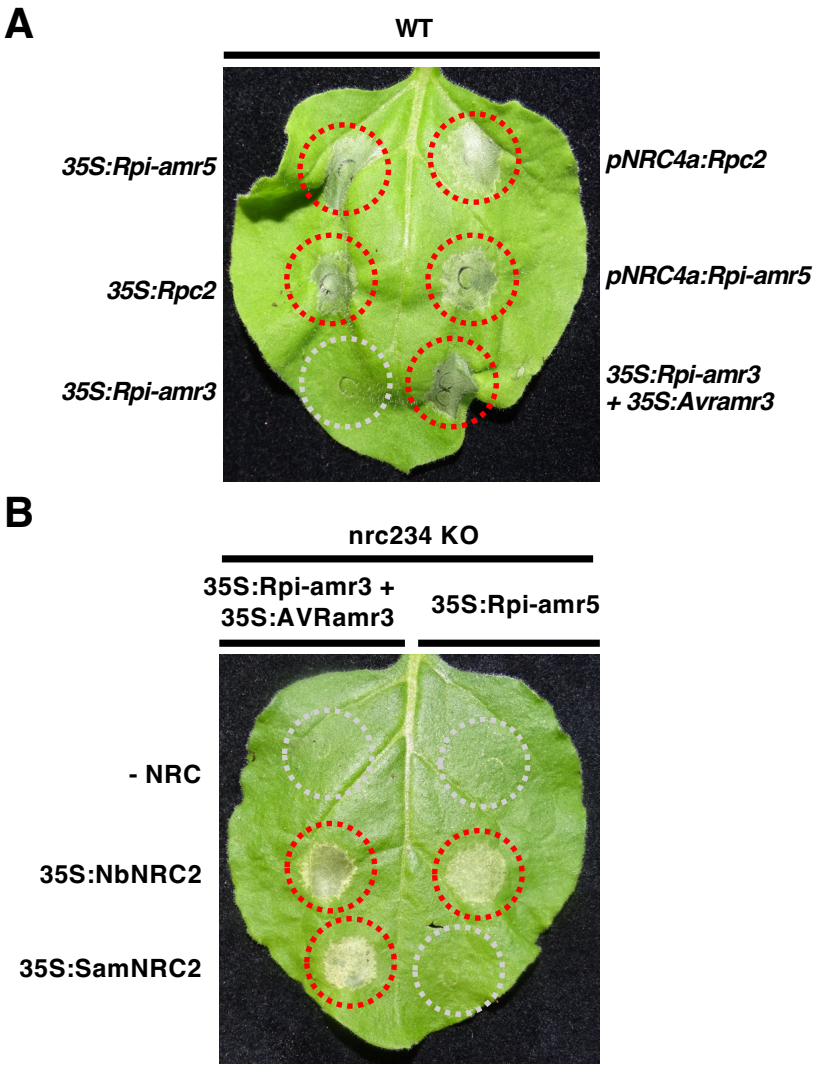

Figure 4.11. Constitutive activity of Rpi-amr5 in *N. benthamiana* is due to incompatibility with NbNRC alleles. (A) Rpi-amr5 and Rpc2 are autoactive in *N. benthamiana*. Infiltration of *Agrobacterium* strains expressing *Rpi-amr5* or *Rpc2* under either CaMV *35S* or *SaNRC4a* regulatory elements into WT *N. benthamiana* results in strong cell death after 3 days. Cell death is equivalent to effector-dependent activation of Rpi-amr3. *Agrobacterium* suspensions were infiltrated at 0.2 OD_{600}. **(B)** Absence of NRC helper NLRs abolishes constitutive activity of Rpi-amr5/Rpc2, complementation with *35S:NbNRC2*, but not *35S:SaNRC2*, restores constitutive activity. *Agrobacterium* strains were infiltrated at 0.2 OD_{600} and leaves were imaged at 3 dpi.

4.2.9 – Sa/NbNRC2 swaps reveals the NbNRC2 LRR domain to be responsible for the incompatibility with Rpi-amr5

Co-expression of *Rpi-amr5* with the *N. benthamiana* allele of *NRC2* leads to effector-independent cell death. This incompatibility implies that co-evolution is required to maintain appropriate interaction between sensors and helpers. Understanding the basis of this incompatibility could provide an insight into the interaction between these NLRs. To determine which polymorphisms between *NbNRC2* and *SaNRC2* are responsible, domain swaps were generated in which either the CC, NB-ARC or LRR domains were exchanged. Co-expression with *Rpi-amr3* and *Avramr3* in the *nrc234* KO line was used to test the functionality of these swaps. Several variants appeared to be non-functional, but others gave clear HR. Introduction of the NbNRC2 LRR domain into the SaNRC2 protein causes constitutive activity when co-expressed with Rpi-amr5 (Fig 4.12). While the reciprocal exchange was non-functional, the experiment suggests that the NbNRC2 LRR is responsible for incompatibility with Rpi-amr5.

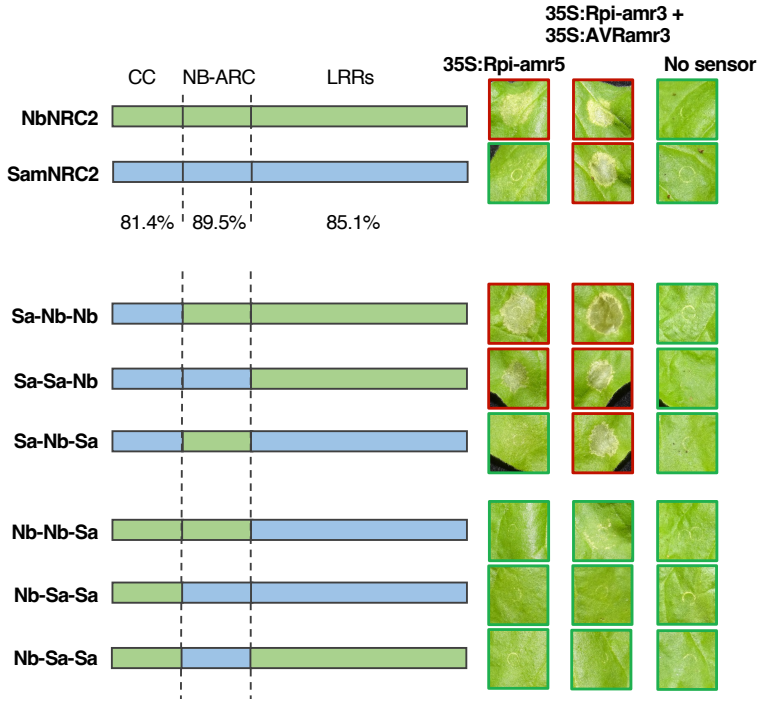

Figure 4.12. NbNRC2/SaNRC2 domain swaps implicate the NbNRC2-LRRs in effector-independent activation of Rpi-amr5. To determine which polymorphisms are responsible for incompatibility with Rpi-amr5, domain swaps between NbNRC2 and SaNRC2 was performed. Boundary positions were determined using an Alphafold model. Constructs were tested by transient expression in *nrc234* KO *N. benthamiana*. Helpers were co-expressed with either *Rpi-amr5,* or *Rpi-amr3* with *AVRamr3*. An additional infiltration lacking either sensor was used as a negative control to test for NRC autoactivation. Exchange of the *N. benthamiana* NRC2 LRRs into the *S. americanum* allele results in the gain of effector-independent activation when co-expressed with *Rpi-amr5*. *Agrobacterium* strains were infiltrated at 0.2 OD_{600} and leaves were imaged at 3 dpi.

Huang et al. (2023) studied the compatibility of Rpi-blb2 with alleles of NRC3. Rpi-blb2 can function with the tomato NRC3, but not the *N. benthamiana* allele. NbNRC3 compatibility with Rpi-blb2 can be established by point mutation of six residues in different interfaces across the NB-ARC and LRR domains. To test whether variation in these residues could be responsible for incompatibility of Rpi-amr5 with NbNRC2, the residues at these regions were compared. There is no variation between NbNRC2 and SaNRC2 at the exact positions identified by Huang et al. (2023), however, at two of these sites, nearby amino acids are polymorphic (Fig 4.13). This may suggest that additional regions are involved in the interaction between sensor and helper NLRs or that nearby polymorphism between SaNRC2 and NbNRC2 results in incompatibility at the previously identified sites. This finding demonstrates that the divergence of sensors and helpers not only can cause a loss of function, but also the loss of regulation and aberrant activation. Further analysis, through either further sequence exchange, or structural approaches, could dissect this.

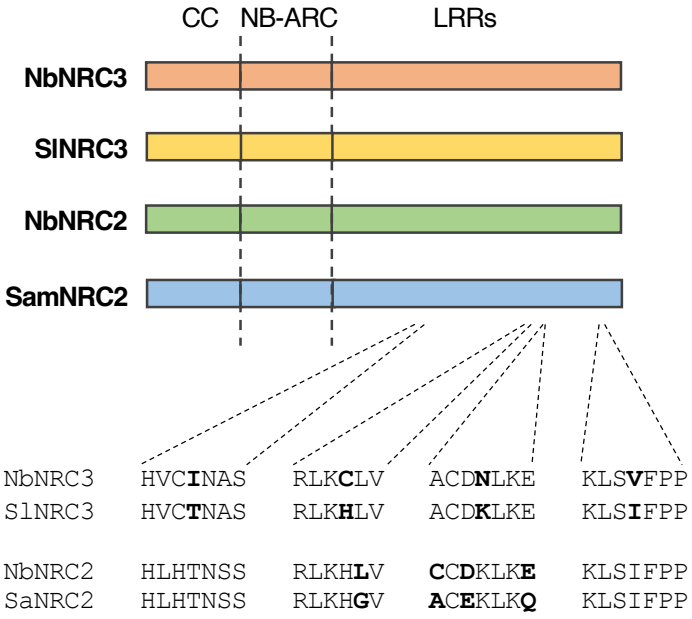

Figure 4.13. SaNRC2 and NbNRC2 are variable nearby to residues previously associated with sensor-incompatibility. In a previous publication, the sites responsible for the incompatibility between the Rpi-blb2 sensor NLR and NbNRC3 were identified using swaps with the compatible SlNRC3 (Huang et al. 2023). These sites and the surrounding residues were compared in the NbNRC2 and SaNRC2 LRRs. Polymorphic residues are indicated in bold. Polymorphisms between NRC3 alleles are non-variable between the NRC2 alleles, some surrounding residues are polymorphic within two of the four regions. Conceivably these residues may be associated with sensor-helper incompatibility observed between Rpi-amr5 and NbNRC2.

4.2.10 – Rpi-amr5 and Rpc2 both recognise PITG_16275 and PITG_09160 from *P. infestans*

Given the high similarity between *Rpi-amr5* and *Rpc2* alleles, it was hypothesised that they confer *P. infestans* resistance by recognising the same effector and that the susceptible accession SP2271 would be unable to recognise this effector. All available *S. americanum* accessions have been screened for recognition of 315 *P. infestans* effectors (Lin et al., 2023). These data were used to identify effectors recognised by SP2308 and SP2275, but not SP2271. Five effectors are recognised by SP2275 but not SP2271, 19 effectors are recognised by SP2308 but not SP2271. Of these effectors, two are recognised by both SP2275 and SP2308. These effectors were tested by transient expression in *nrc234 N. benthamiana* with *35S:SaNRC2,* and either *Rpi-amr5* or *Rpc2*. The effector encoded by the gene *PITG_16275*, is recognised by both *Rpi-amr5* and *Rpc2* (Fig. 4.14a).

To identify other *P. infestans* effectors that may be recognised, the bioinformatic tool Foldseek was used to perform a structural homology search (van Kempen et al., 2022). The search was performed against a library of predicted structures for *P. infestans*-secreted proteins (Seong and Krasileva, 2023). The predicted structure for PITG_16275 was used a query in this search (Fig. 4.14c). The output was inspected for hits with high Tm score, indicating good structural alignment, and a high bit score which is indicative of the length of the hit as well as the coverage of the query.

From this search, PITG_09160 was identified as a structural homologue of PITG_16275 (Fig. 4.14b, Fig. 4.14c). These effectors share 39.2% amino acid identity after the EER motif. Three more *P. infestans* effectors; PITG_06076, PITG_06059 and PITG_06074, were also identified. Previously published data shows that these three effectors are not expressed during infection (Lin et al., 2020). In transient expression assays, Rpi-amr5 and Rpc2 were found to recognise PITG_09160 and activate HR (Fig. 4.14a). We conclude that PITG_16275 and PITG_09160 are the elicitors of Rpi-amr5 and Rpc2 from *P. infestans*.

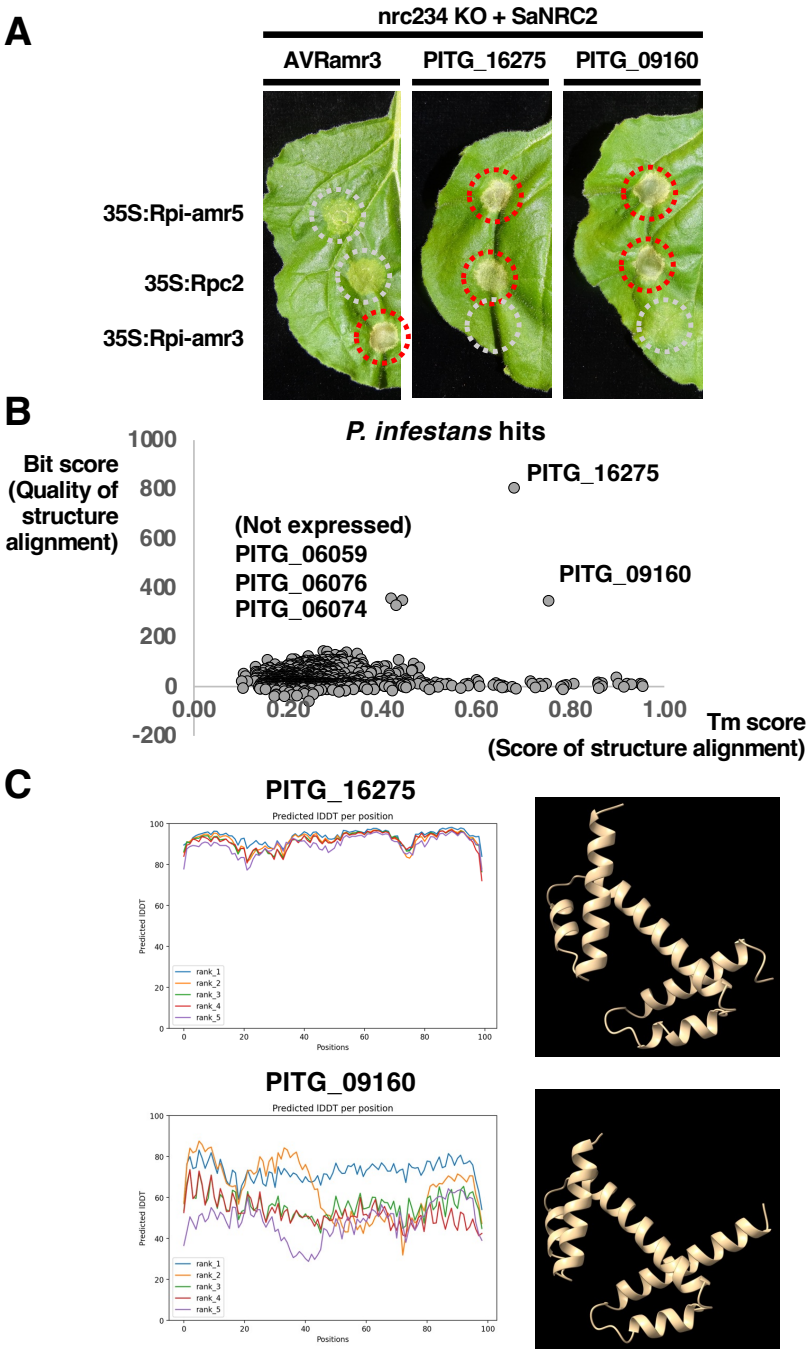

Figure 4.14. Rpi-amr5 and Rpc2 recognise at least two *P. infestans* effectors. (A) Rpi-amr5 and Rpc2 recognise PITG_09160 and PITG_16275. Co-expression of *SaNRC2*, with either *Rpi-amr1c* allele, and *PITG_09160* or *PITG_16275* results in effector-dependent hypersensitive response. Expression of these effectors with *Rpi-amr3* and *SaNRC2* does not result in cell death. *Agrobacterium* strains were infiltrated at 0.2 OD_{600} and leaves were imaged at 3 dpi. **(B)** *P. infestans* contains four additional effectors with predicted structural similarity. A Foldseek search was performed using a local database of *P. infestans* effector models (generated by Seong and Krasileva (2023)), PITG_16275 was used as an input. Each effector is represented by a data point in the plot. The hits with high Bit score and Tm score were inspected as possible structural homologues. **(C)** Alphafold was used to predict structures for both PITG_16275 and PITG_09160. For each model, the LDDT score at each position is shown.

4.2.11 – PITG_16275 recognition was independently mapped to the *Rpi-amr1* cluster

PITG_16275 and PITG_09160 have been identified as the elicitors of Rpi-amr5 and Rpc2. Of the 52 *S. americanum* accessions, 24 respond to PITG_16275. This response was independently mapped by postdoctoral researchers Dr Maheen Alam and Dr Xiao Lin. An F2 population was produced from a cross between SP2297, which responds to PITG_16275, and SP2271, which does not. This population segregates in a 3:1 (responsive: non-responsive) ratio and DNA from 74 responding plants and 33 non-responding plants was used for bulked segregant RenSeq. In the bulked segregant analysis, the *Rpi-amr1*/*Rpi-amr5*/*Rpc2* locus was found to co-segregate with resistance (Fig. 4.15a). In SP2297, the predicted Rpi-amr1c-2297 amino acid sequence is identical to the characterised Rpi-amr5 (Fig. 4.15b). Therefore, responsiveness to PITG_16275 in SP2297 is conferred by *Rpi-amr5*.

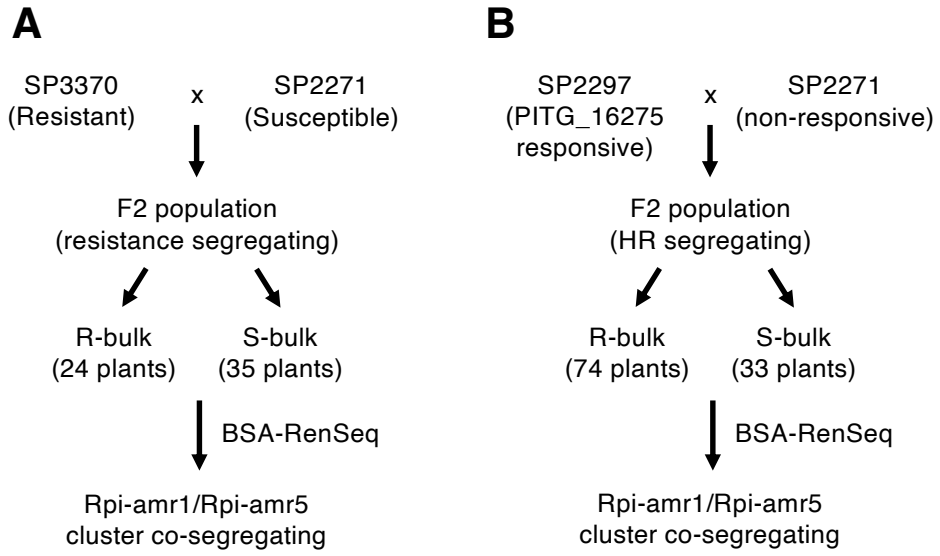

C

	Rpi-amr1e-...	Rpc-amr1c-...	Rpi-amr1c-...	Rpi-amr1c-...	Rpi-amr1c-...
Rpi-amr1e-2273		74.0%	74.1%	74.1%	74.1%
Rpc-amr1c-2308	74.0%		97.4%	97.4%	97.4%
Rpi-amr1c-2275	74.1%	97.4%		100%	100%
Rpi-amr1c-2297	74.1%	97.4%	100%		100%
Rpi-amr1c-3370	74.1%	97.4%	100%	100%	

Figure 4.15. Rpi-amr5 function in four accessions has been validated. (A) Resistance to *P. infestans* in the *S. americanum* accession SP3370 was mapped in an F2 population produced by crossing SP3370 with the susceptible accession SP2271. Bulked segregant analysis was used to position the resistance to the *Rpi-amr1*/*Rpi-amr5*/*Rpc2* locus. **(B)** Independently, recognition of PITG_16275 was mapped in an F2 population produced by crossing the responsive line SP2297 with the non-responsive line SP2271. Responsiveness to PITG_16275 segregates in a 3:1 ratio of responsive: non-responsive. Bulked segregant analysis was used to position the recognition on Chromosome 11 at the *Rpi-amr1*/*Rpi-amr5*/*Rpc2* cluster. The population screening and mapping was performed by Dr Maheen Alam and Dr Xiao Lin. **(C)**

Functionally validated *Rpi-amr1c* alleles encode NLRs with high amino acid identity. Heatmap of the percent identity of aligned amino acid sequence of these alleles. All four were independently mapped using either resistance to *P. infestans* (*Rpi-amr5*/*Rpi-amr1c-SP2275, Rpi-amr1c-SP3370*), resistance to *P. capsici* (*Rpc2*/*Rpi-amr1c-SP2308*), or recognition of PITG_16275 (*Rpi-amr1c-SP2297*).

4.2.12 – Homologues of PITG_16275 are found in several *Phytophthora* species, but not *P. capsici*

Rpi-amr5 and Rpc2 recognise two *P. infestans* effectors, which share sequence and structure similarity. BLAST against both the *P. capsici* genome and predicted proteome found no proteins with homology to PITG_16275 or PITG_09160. Therefore, a structural homology search was performed against a list of predicted effectors. Effectors were predicted based on the presence of a signal peptide, as well as EER and RXLR motifs. From the *P. capsici* proteome prediction, 356 SP-RXLR-EER proteins were identified. Alphafold prediction of these proteins was performed to assemble a library of predicted structures to use as a Foldseek database. However, no proteins are predicted to share high structural similarity to the recognised *P. infestans* proteins (Fig. 4.16a). Using this approach, homologues were identified in *P. palmivora*, *P. parasitica*, *P. megakarya* and *P. cactorum* by searching against public pdb databases built into Foldseek (Fig. 4.16b). The genes which encode proteins with the highest scoring hit from each species were synthesised and transiently expressed with *Rpi-amr5* and *Rpc2*. These effectors share between 38 and 60% amino acid identity to PITG_16275 (Fig. 4.17a, Fig. 4.17b).

Co-expression of the *P. megakarya*, *P. palmivora* and *P. parasitica* orthologues with *Rpi-amr5* caused strong cell death. For the *P. cactorum* orthologue, HR was very weak (Fig. 4.17c). While resistance to these species has not been tested, this experiment demonstrates that Rpi-amr5 and Rpc2 can recognise at least five *Phytophthora* species. Homologues of PITG_16275 are found across diverse *Phytophthora* species. Interestingly, many more PITG_16275 homologues were predicted in *P. palmivora* and *P. megakarya* (21 and 28) than in *P. parasitica*, *P. cactorum* or *P. infestans* (8, 2 and 5), suggesting there has been expansion of this effector group in these species.

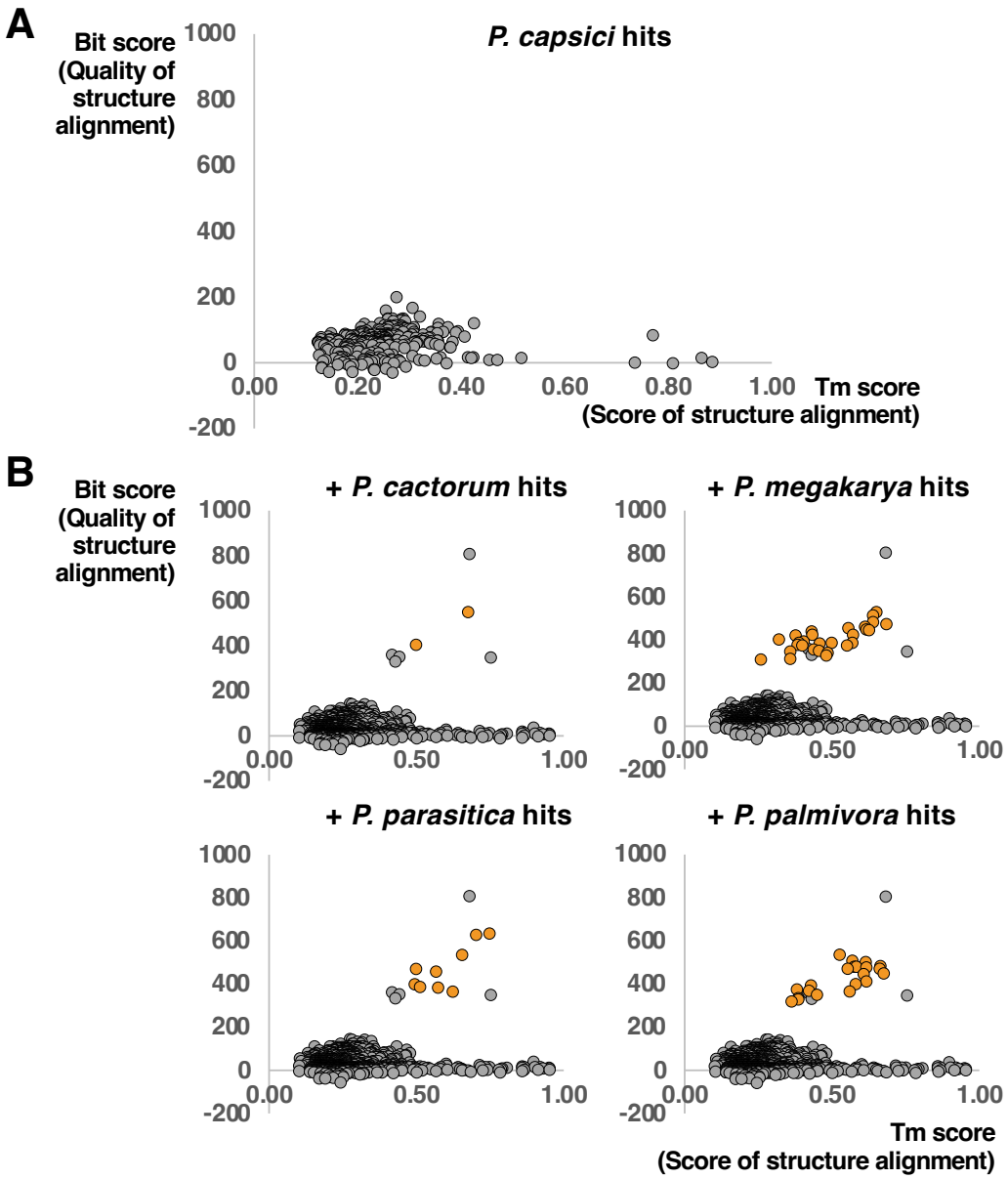

Figure 4.16. Many *Phytophthora* species share structural homologues of PITG_16275, but not *P. capsici*. (A) A Foldseek search was performed to identify structural homologues of PITG_16275 in *P. capsici*. Using Alphafold, the structures of 303 *P. capsici* SP-RXLR-EER effectors were predicted. The predicted structure of PITG_16275 was used as an input for the Foldseek search. The result is represented as a plot of the Tm score for each hit against the Bit score for each hit. No clear orthologues of PITG_16275 were identified. **(B)** Unlike *P. capsici*, structural homologues of PITG_16275 were identified in *P. cactorum*, *P. megakarya*, *P. parasitica* and *P. palmivora*. Searches were performed using the databases built into the Foldseek server. Proteins identified from each *Phytophthora* species are indicated in orange, their position within the plot from Figure 4.14b is shown.

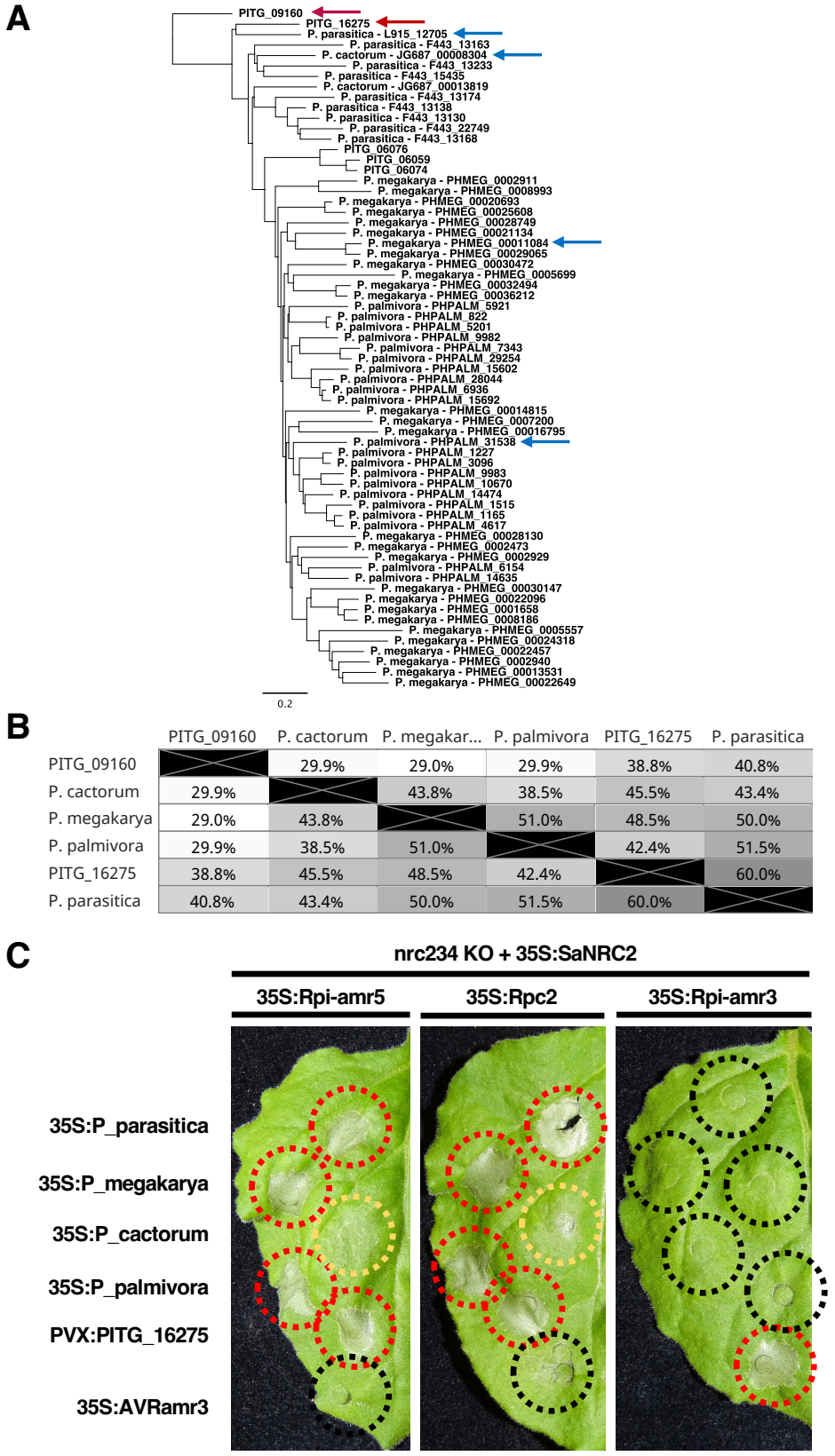

	PITG_09160	P. cactorum	P. megakar...	P. palmivora	PITG_16275	P. parasitica
PITG_09160		29.9%	29.0%	29.9%	38.8%	40.8%
P. cactorum	29.9%		43.8%	38.5%	45.5%	43.4%
P. megakarya	29.0%	43.8%		51.0%	48.5%	50.0%
P. palmivora	29.9%	38.5%	51.0%		42.4%	51.5%
PITG_16275	38.8%	45.5%	48.5%	42.4%		60.0%
P. parasitica	40.8%	43.4%	50.0%	51.5%	60.0%	

Figure 4.17. Rpi-amr5 and Rpc2 recognise PITG_16275 homologues from other *Phytophthora* species. (A) Orthologues of PITG_09160 and PITG_16275 are found in *P. megakarya* (28), *P. palmivora* (21), *P. parasitica* (8) and *P. cactorum* (2). An additional 3 homologous effectors are found in *P. infestans*. Orthologues were identified using NCBI BLAST and a Foldseek structural homology search. PITG_09160 and PITG_16275 are

indicated with red arrows. Cloned orthologues from *P. megakarya*, *P. palmivora*, *P. parasitica* and *P. cactorum* are indicated by blue arrows, these were selected based on the result of the Foldseek search. **(B)** Heatmap of the percent amino acid identity between the two recognised *P. infestans* effectors and the cloned orthologues from *P. megakarya*, *P. palmivora*, *P. parasitica* and *P. cactorum*. **(C)** Rpi-amr5 and Rpc2 can recognise PITG_16275 orthologues from *P. megakarya*, *P. palmivora*, *P. parasitica* and weakly recognise a *P. cactorum* orthologue. Effectors were co-expressed with sensor NLRs and SaNRC2 in the *N. benthamiana nrc234* KO line. *Agrobacterium* strains infiltrated at 0.3 OD_{600}, images were taken at 3 dpi.

4.2.13 – Three *P. capsici* effectors are recognised by both Rpi-amr5 and Rpc2

No *P. capsici* effectors with homology to PITG_16275 or PITG_09160 were identified using sequence or structural homology searches. Therefore, a library of 277 FLAG-tagged *P. capsici* RxLR effectors (and 80 additional allelic variants) was cloned using a combination of gene synthesis and PCR amplification from *P. capsici* gDNA (Fig. 4.18a). The cloning of this library was performed with Dr Xiao Lin and PhD student Li Long. Effectors were screened by transient expression in SP2308, SP2275 and SP2271. Effectors which elicit HR in SP2308 were screened for recognition by *Rpc2*/*Rpi-amr5* in *N. benthamiana*. Three *P. capsici* effectors are recognised by Rpc2: PcE144, PcE149 and PcE150. Surprisingly, Rpi-amr5 also demonstrated recognition of these effectors despite not being able to confer *P. capsici* resistance in *S. americanum* or *S. lycopersicum* (Fig. 4.18b).

The three recognised *P. capsici* effectors have high sequence similarity to each other (65.4-92.5% amino acid identity), but low identity to the recognised *P. infestans* effectors (10.4-15.9% amino acid identity). No orthologues of PcE144, PcE149 or PcE150 were identified in *P. infestans*, *P. parasitica*, *P. palmivora*, *P. megakarya* or *P. cactorum*.

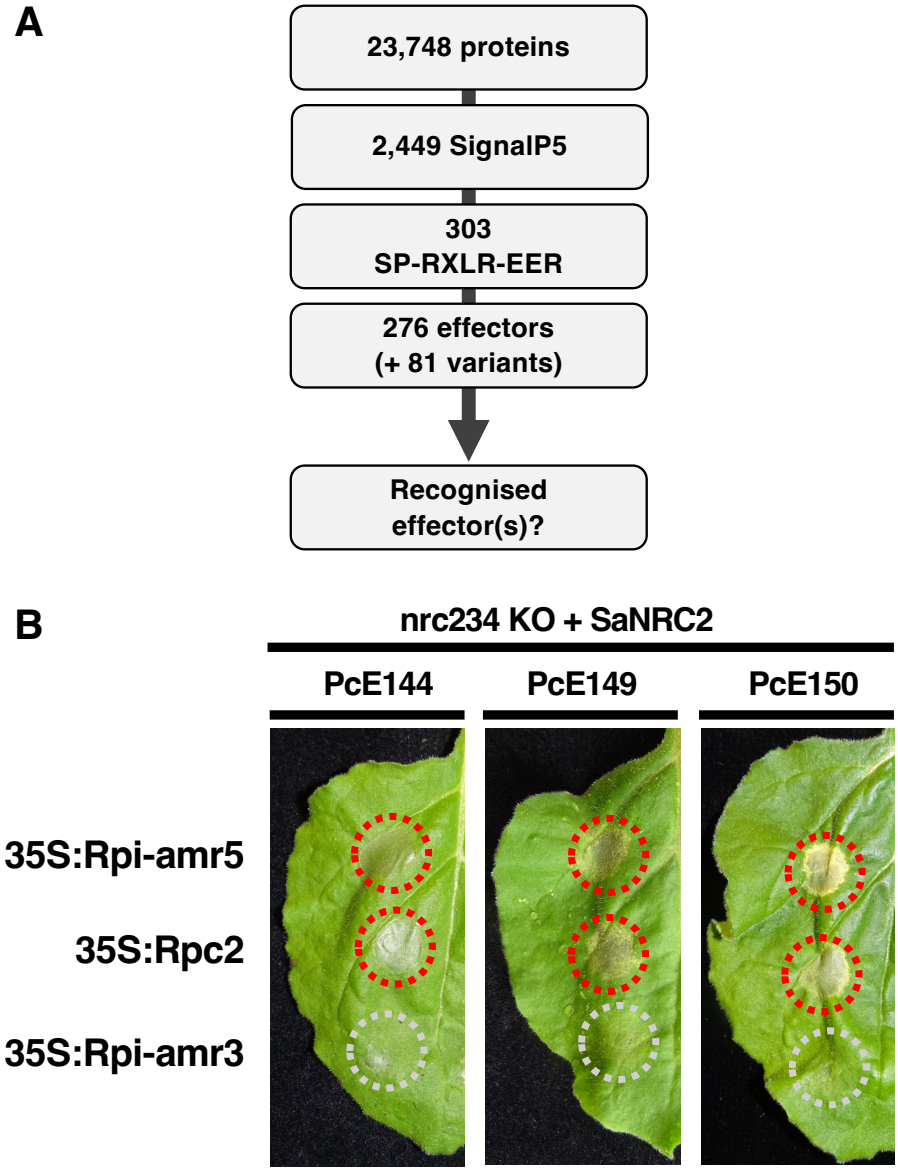

Figure 4.18. Rpi-amr5 and Rpc2 recognise at least three *P. capsici* effectors. (A) *P. capsici* effector identification pipeline. From the predicted proteome of *P. capsici* (Stajich et al., 2021), SP-RXLR-EER effectors were identified by filtering for the presence of a signal peptide, RXLR motif and EER motif. Of the resulting 303 predicted effectors, 276 were successfully cloned. Through cloning, 81 additional allelic variants were identified. **(B)** Rpi-amr5 and Rpc2 both recognise three *P. capsici* effectors: PcE144, PcE149 and PcE150. Expression of these effectors with SaNRC2 and Rpi-amr5 results in cell death. A similar response was seen upon expression with Rpc2. No HR was present when either PcE144, PcE149 or PcE150 were co-expressed with Rpi-amr3. All *Agrobacterium* strains were infiltrated at 0.2 OD_{600}. Leaves were imaged at 3 dpi.

4.2.14 – Rpi-amr5 and Rpc2 associate with their cognate effectors *in planta*

Five effectors elicit HR via Rpi-amr5 and Rpc2, two from *P. infestans* and three from *P. capsici*. These effectors have diverse length and amino acid sequence. To determine whether these effectors are recognised by direct association with the NLRs or via processing of a guarded or monitored protein, a split luciferase assay was used to test for association *in planta*. NLRs were tagged with the C-terminal luciferase fragment and effectors were tagged with the N-terminal luciferase fragment. The *nrc234 N. benthamiana* line was used to express NLR and elicitor constructs without causing cell death. Clear luminescence was observed with all five recognised effectors when expressed with either Rpi-amr5 or Rpc*2*. No signal was produced upon co-expression with Rpi-amr3. AVRamr3, which does not activate Rpi-amr5 or Rpc2, was used a control (Fig. 4.19). This suggests that despite the lack of similarity between the recognised effectors, they activate both Rpi-amr5 and Rpc2 through proximity to and association with the NLRs, rather than through modification of a host target or another indirect recognition model.

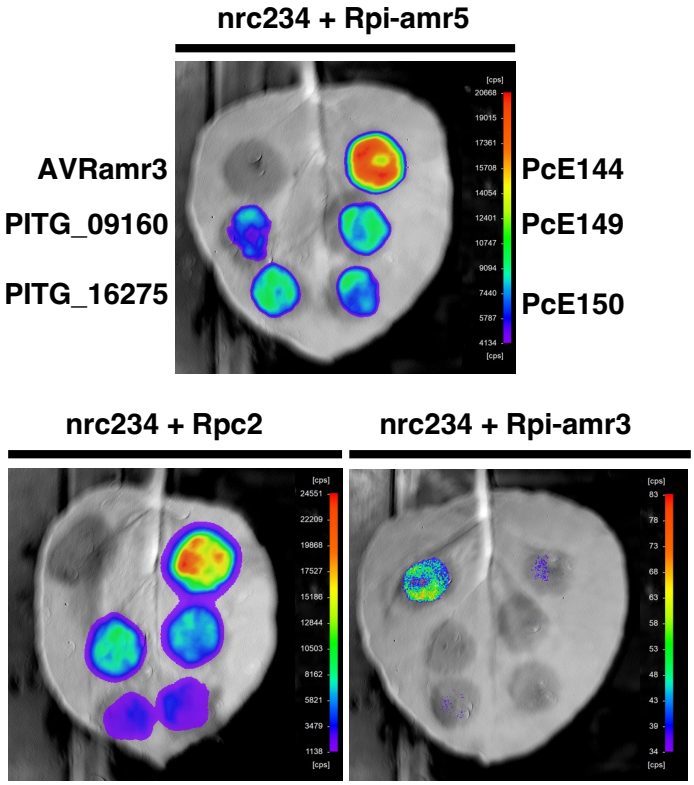

Figure 4.19. Rpi-amr5 and Rpc2 associate with their recognised effectors *in planta*. A split luciferase assay was used to test for *in planta* association between the five recognised effectors (PITG_09160, PITG_16275, PcE144, PcE149 and PcE150) and both Rpi-amr5 and Rpc2. Luminescence was observed when either Rpi-amr5 or Rpc2, but not Rpi-amr3, was co-expressed with the effectors. To avoid cell death, the assay was performed in the *nrc234* KO *N. benthamiana* line. Sensor NLRs were tagged with a C-terminal luciferase fragment, effectors were tagged with an N-terminal luciferase fragment.

Despite the low sequence similarity between the recognised *P. infestans* and *P. capsici* effectors (Fig. 4.20a), they could share a similar structure or a fold which is recognised by Rpi-amr5 and Rpc2. However, the fact that these *P. capsici* effectors were not identified in the previously described Foldseek homology search is inconsistent with this hypothesis. To investigate why, Alphafold models were inspected. Model quality was assessed using the LDDT (local distance difference test) score across the structure. For PITG_16275, a high-quality prediction was achieved (Fig. 4.20b). For PcE144, PcE149 and PcE150, the mean LDDT of the best model is below 65, indicating low confidence (Fig. 4.20c). While the models of these effectors are distinct from PITG_16275, no meaningful conclusions can be made due to their low confidence.

To try to gain further insight into the recognition of these effectors by Rpi-amr5, PITG_16275 truncation was performed. Four constructs were made to remove whole α-helices from the N-terminus and C-terminus, this was guided by the predicted structure (Fig. 4.21a, Fig. 4.21b). Removal of the N-terminal α-helix had no effect on HR, but further truncation resulted in a complete loss of recognition. Recognition was lost when PITG_16275 was truncated at the C-terminus (Fig. 4.21c). Validation of the expression of these truncations is ongoing, but this phenotype suggests that the recognition of PITG_16275 is dependent on the presence of most of the protein post-EER. Truncation of the 21 amino acids after the EER does not alter recognition by Rpi-amr5.

A

	P.cap_E144	P.cap_E149	P.cap_E150	PITG_09160	PITG_16275
P.cap_E144		65.4%	65.6%	10.4%	15.2%
P.cap_E149	65.4%		92.5%	11.8%	15.9%
P.cap_E150	65.6%	92.5%		11.8%	15.2%
PITG_09160	10.4%	11.8%	11.8%		39.2%
PITG_16275	15.2%	15.9%	15.2%	39.2%	

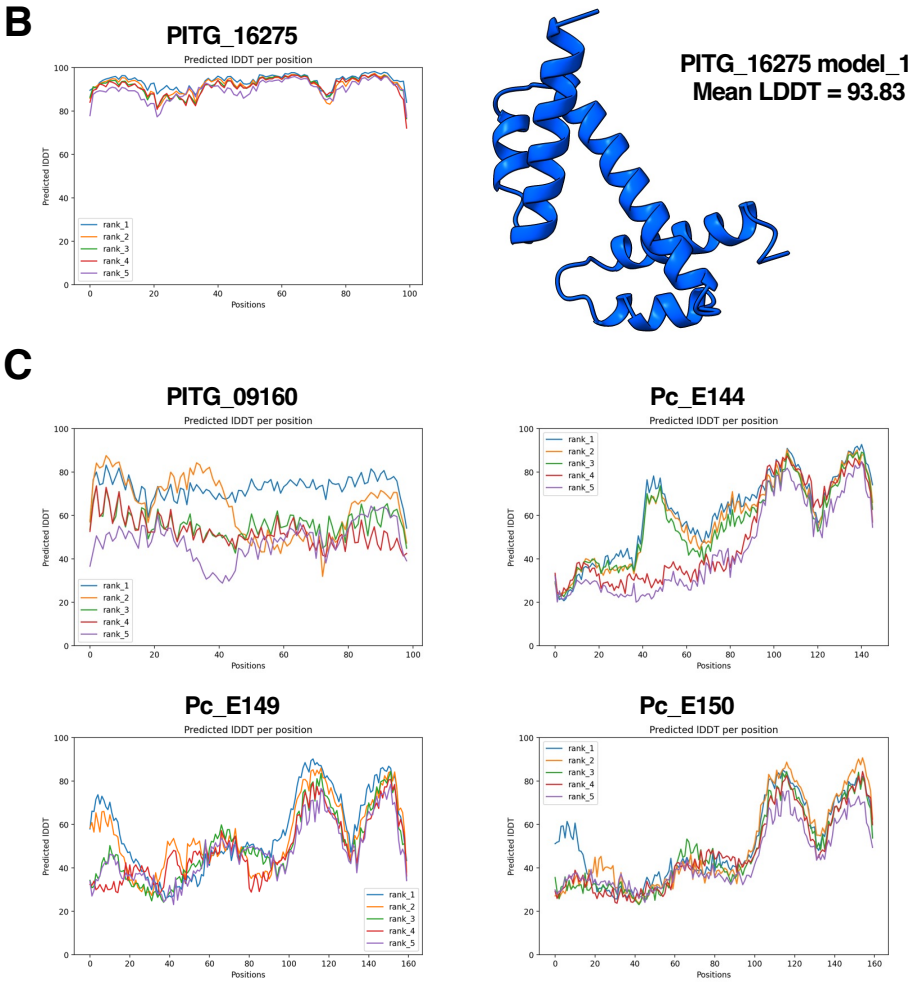

Figure 4.20. The identified elicitors of Rpi-amr5 and Rpc2 have low sequence similarity and poor structural prediction. (A) Heatmap showing the percent identity of the post-EER amino acid sequences for the five effectors recognised by Rpi-amr5 and Rpc2. PITG_09160 and PITG_16275, from *P. infestans*, have low sequence similarity to PcE144, PcE149 and PcE150, from *P. capsici*. **(B)** LDDT plot and structural prediction produced by Alphafold for the *P. infestans* effector PITG_16275. The sequence after the EER motif was used as an input. The mean LDDT score and structure for the best model is shown. **(C)** LDDT plots of Alphafold structural predictions of the four other elicitors of Rpi-amr5 and Rpc2. Low confidence models were produced, this can be seen by the low LDDT scores throughout the predicted models.

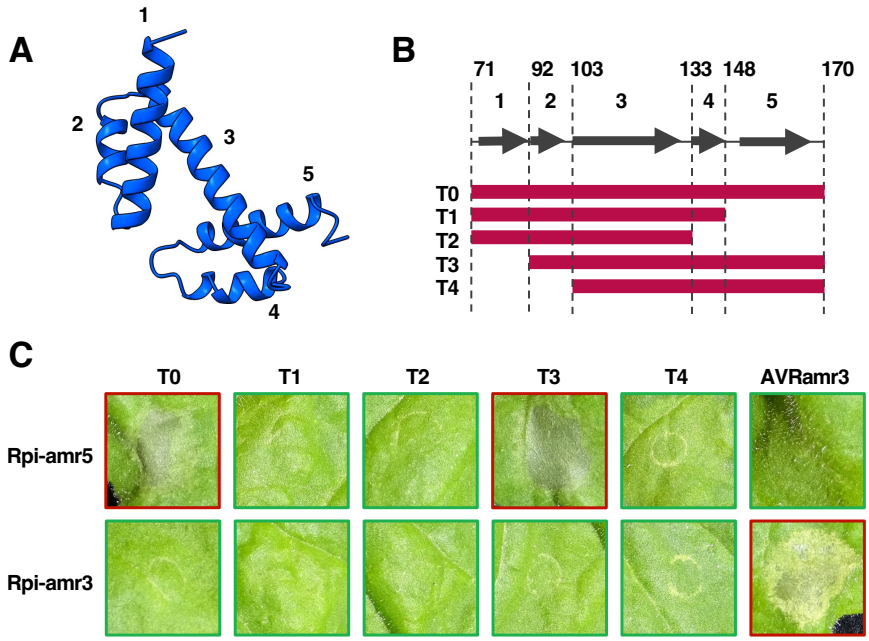

Figure 4.21. Truncation of the PITG_16275 N-terminal α-helix does not abolish recognition by Rpi-amr5. (A) The Alphafold model of PITG_16275 contains five predicted α-helices. **(B)** The position of five α-helices within the PITG_16275 amino acid sequence is represented. Five constructs containing truncated fragments of PITG_16275 were cloned, the amino acid position relative to the start of the protein is shown, T0 (the construct used in previous assays) starts immediately after the EER motif and is truncated at the signal peptide. Additional truncations (T1, T2, T3, T4) were made, removing individual predicted α-helices. **(C)** *Rpi-amr5* was co-expressed with truncations of PITG_16275 to identify which regions are dispensable for recognition by Rpi-amr5. Rpi-amr3 was used as a negative control in this experiment. All *Agrobacterium* strains were infiltrated at 0.3 OD_{600}. Pictures were taken at 3 dpi.

4.2.15 – Could Rpc2, but not Rpi-amr5, evade suppression by a *P. capsici* effector?

Rpi-amr5 and Rpc2 both recognise three *P. capsici* effectors. Given this, it is surprising that *Rpi-amr5* does not confer resistance to *P. capsici*. One hypothesis is that *P. capsici* can suppress Rpi-amr5, but Rpc2 evades this suppression. To test this, *P. capsici* effectors were co-expressed with Rpi-amr5 in wild-type *N. benthamiana* to test for suppression of Rpi-amr5-dependent cell death (Fig. 4.22a). So far, 90 effectors have been tested by this approach. One effector, PcE221, appeared to suppress constitutive activity of Rpi-amr5 but not that of Rpc2 or the AVRamr1-dependent cell death mediated by Rpi-amr1 (Fig. 4.22b). The potato cyst nematode effector SPRYSEC15 (SS15) was used as a positive control for suppression, this effector is capable of suppressing NRC2 through direct binding to its NB-ARC domain (Derevnina et al., 2021, Contreras et al., 2023a).

The suppression of Rpi-amr5 constitutive activity in wild-type *N. benthamiana* provided an explanation for the lack of *P. capsici* resistance conferred by this allele. However, this is not supported by the following experiments which suggest that PcE221 is not a true suppressor of Rpi-amr5. A similar suppression experiment was performed in SP2275 and SP2308. Expression of PITG_16275 caused strong HR in both SP2308 and SP2275, and neither PcE221 nor SS15 could suppress this (Fig. 4.22c). SS15 can suppress alleles of NRC1/2/3 (Contreras et al., 2023a), however, its ability to suppress NRCs from *S. americanum* has not been tested. This assay suggests that at least one allele escapes suppression. An alternative transient assay was performed in *nrc234 N. benthamiana*. Rpi-amr5, Rpc2 and Rpi-amr3 were transiently expressed with SaNRC2, their cognate effectors, and either PcE221, SS15 or an empty vector control. PcE221 appeared to have no effect on the effector-dependent cell death response of either Rpi-amr5 or Rpc2 (Fig. 4.22d).

The transient assays in *S. americanum* and *nrc234 N. benthamiana* suggest that PcE221 is not a true suppressor of Rpi-amr5. The reason for reduced constitutive activity of Rpi-amr5 upon co-expression with PcE221 in wild-type *N. benthamiana* is unclear. However, this experiment is not representative of effector-dependent activation, instead HR is due to incompatibility with NRC proteins. These experiments do not rule out that a *P. capsici* effector can suppress Rpi-amr5 and this will be assessed by evaluating the remaining *P. capsici* effectors.

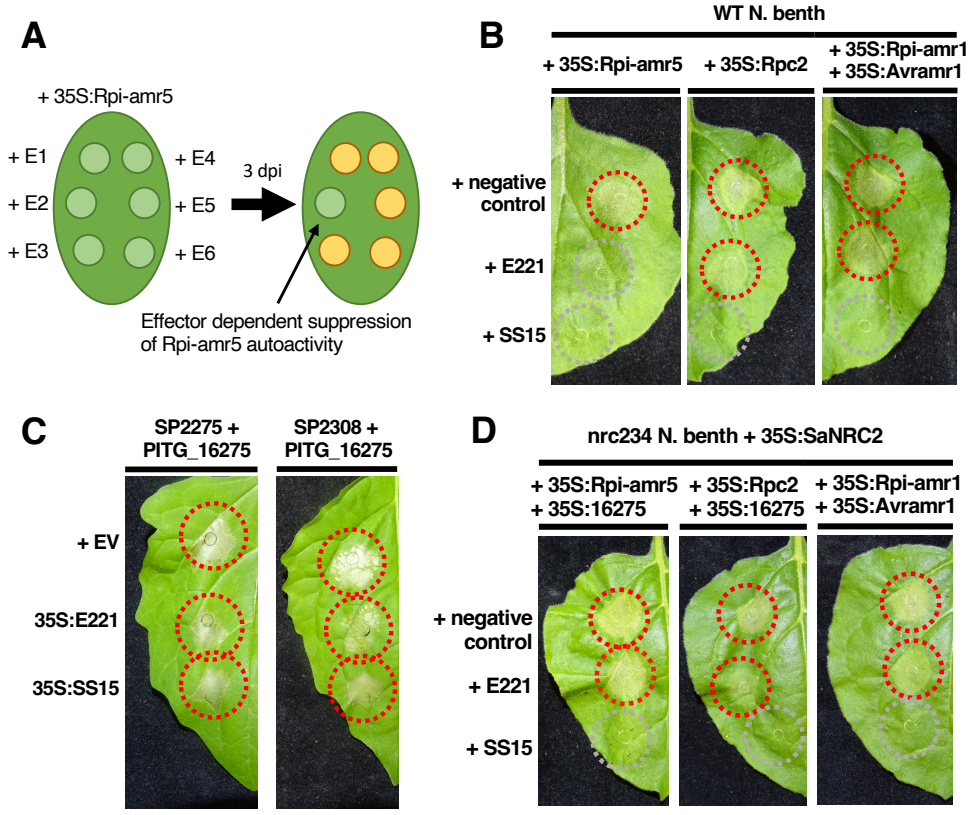

Figure 4.22. Screening for a *P. capsici* effector that suppresses Rpi-amr5, but not Rpc2. **(A)** An illustration representing the assay used to test the ability of *P. capsici* effectors to suppress the constitutive activity of Rpi-amr5 in WT *N. benthamiana*. An *A. tumefaciens* strain expressing Rpi-amr5 (at 0.1 OD_{600}), was co-infiltrated with candidate suppressors (at 1.0 OD_{600}), infiltrated sites were phenotyped at 3 dpi. **(B)** *P. capsici* PcE221 appeared to reduce the constitutive-activity of Rpi-amr5 in WT *N. benthamiana*. The constitutive-activity of Rpc2, and the effector-dependent activation of Rpi-amr1 did not appear to change. SS15, a nematode suppressor of NbNRC2 was used as a positive control for suppression of cell death, an empty vector was used as a negative control. **(C)** PcE221 does not suppress effector-dependent activation of Rpi-amr5 or Rpc2 in *S. americanum*. PITG_16275 was expressed in SP2275 and SP2308 leaves at 0.05 OD_{600} to activate Rpi-amr5 or Rpc2, respectively. PcE221, SS15 and an empty vector control were expressed to test for a loss of effector-dependent activation. No suppression was observed for any combination. **(D)** Effector-dependent activation of Rpi-amr5, Rpc2 and Rpi-amr1 was unaffected by addition of PcE221. The assay was performed in *nrc234* KO *N. benthamiana*, an *Agrobacterium* strain expressing SaNRC2 was included in all infiltrations. All *Agrobacterium* strains were at an OD_{600} of 0.1, except the suppressors where OD_{600} 1.0 was used.

4.2.16 – Structural prediction suggests that Rpi-amr5 and Rpc2 may differ in effector binding or recognition

An alternative explanation for this phenotype is that Rpc2 may bind to an additional effector or have a greater affinity to PcE144, PcE149 and PcE150. For this to be possible, surface-exposed polymorphisms on the concave surface of the LRRs would be expected. To investigate this, Alphafold was used to map the position of polymorphisms onto predicted Rpc2 and Rpi-amr5 structures. For both NLRs, the mean LDDT score for the top model is above 80, areas with low score include regions linking domains, the exterior of the LRR domain and a predicted post-LRR sequence (Fig. 4.23a). Interestingly, five polymorphic amino acids are positioned in a cluster on the concave surface of the LRRs (Fig. 4.23b). These polymorphisms could be related to effector binding and may enable additional recognition, or stronger recognition of effectors by Rpc2.

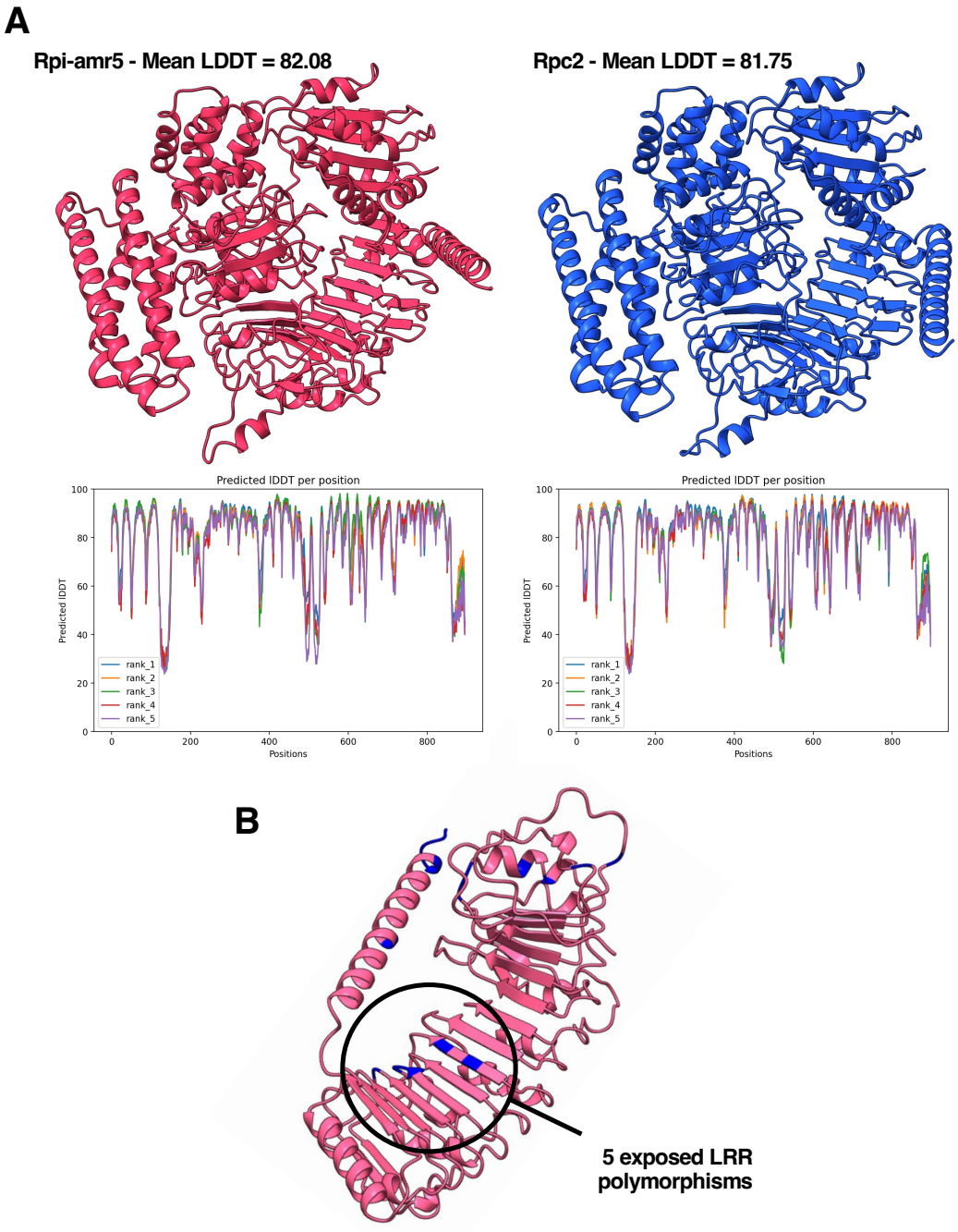

Figure 4.23. Rpi-amr5 and Rpc2 have similar predicted structures. (A) Alphafold was used to predict the structure of the full length Rpi-amr5 and Rpc2. The best scoring model for each prediction is shown, overall predicted quality of the model is estimated by the mean LDDT score shown. The LDDT score at each position of five generated models is also shown. The predicted structures for Rpi-amr5 and Rpc2 are highly similar. **(B)** Polymorphisms between Rpi-amr5 and Rpc2 are distributed across the LRR model. The predicted Rpc2 LRR model is shown, Rpi-amr5 polymorphisms are indicated in blue, several are predicted to be located on the concave surface of the LRRs.

4.2.17 – *Solanum* immune receptors convergently evolved recognition of *P. infestans* effectors

Rpi-amr5 and Rpc2 recognise PITG_09160 and PITG_16275. These effectors were previously described as core effectors of *P. infestans* and show little variation between strains (Yin et al., 2017). Effectoromics screens of other *Solanum* species against *P. infestans* effector libraries have been performed. Several *Solanaceae* species have been reported to respond to these effectors. PITG_16275 is recognised in an accession of *Solanum venturii* (Pais et al., 2018). Similarly, *Capsicum annuum* shows differential recognition of PITG_09160, 13 out of 42 tested accessions respond with HR (Lee et al., 2014). It is unlikely that there is a functional *Rpi-amr5* allele in either *S. venturii* or *C. annuum*. The most closely related NLR in *C. annuum* (cultivar CM334) has 62.3% amino acid identity to Rpi-amr5. Whilst there is no published *S. venturii* genome, available *S. tuberosum* (namely, the DM and RH accessions), *Solanum neorossii*, *Solanum bulbocastanum*, *Solanum chacoense* and *Solanum etuberosum* genomes were investigated for orthologues of *Rpi-amr5*. Complete orthologues were only identified in *S. chacoense* and *S. tuberosum* (RH). Respectively, these share 76.2% and 76.1% amino acid identity with Rpi-amr5. It is unlikely that the recognitions in *C. annuum* or *S. venturii* are due to *Rpi-amr5* orthologues. To support this, species closely related to *S. americanum* were investigated. In available data for the black nightshades *S. villosum and S. nigrum,* there is no complete *Rpi-amr1c* allele (discussed further in Chapter 5). Functional alleles of *Rpi-amr1* and *Rpi-amr3* have been identified in *S. nigrum*, but there are accessions that lack recognition of these effectors. *Rpi-amr5* may show similar variation between accessions.

Interestingly, there is additional non-Rpi-amr5 recognition of PITG_09160 within *S. americanum*. *rpi-amr5* and *rpc2* knock-out lines were screened for the loss of recognition of the five recognised effectors. SP2275 *rpi-amr5* lines showed loss of response to all effectors, however, SP2308 *rpc2* lines retained recognition of PITG_09160 as well as Pc_E149 and Pc_E150 (Fig. 4.24a). This suggests that there are additional receptors in SP2308 which detect these effectors. Other *S. americanum* accessions lacking functional *Rpi-amr5* alleles also respond to PITG_09160 (Fig. 4.24b). Altogether, these data suggest that multiple immune receptors within *S. americanum* and other *Solanaceae* species have convergently evolved multiple, distinct recognitions of PITG_09160 and PITG_16275.

A

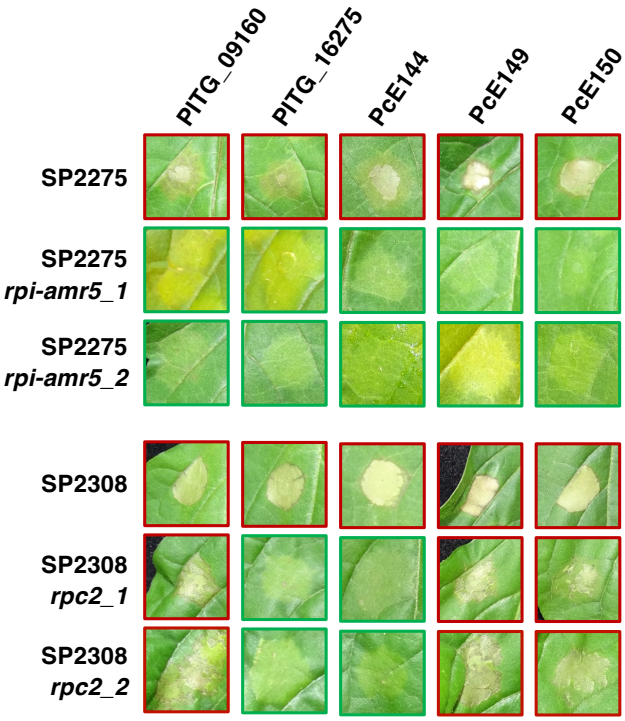

B

	16275	09160	PcE144	PcE149	PcE150	
SP2275	2	2	2	2	2	Complete Rpi-amr1c
SP2308	2	2	2	2	2	
SP1102	2	2	1	0	0	
SP2273	2	2	0	2	2	
SP3400	2	2	0	2	2	
SP2360	2	2	0	2	2	
SP2297	2	2	0	2	2	
SP1101	0	1.5	0	0	0	Frameshift/ premature stop
SP3409	0	1	0	?	0	
SP2307	0	1.5	1	1	0	
SP3406	0	0	0	0	0	
SP1032	0	1	0	1	2	
SP3399	0	2	0	0	2	
SP2272	0	1.5	0	0	0	
SP2298	0	1	0	0	0	
SP2300	0	1	0	0	0	
SP2271	0	2	0	0	0	No Rpi-amr1c

Figure 4.24. *S. americanum* contains additional Rpi-amr5/Rpc2-independent recognition of PITG_09160, but not PITG_16275. (A) SP2308 *rpc2* KO lines contain Rpc2-independent recognition of PITG_09160, PcE149 and PcE150. Infiltration of the five recognised effectors was performed in SP2275, SP2308 and CRISPR-induced *rpi-amr5*/*rpc2* KO mutants. Two independent mutant lines were screened for both SP2275 and SP2308. *Agrobacterium* strains were infiltrated at 0.3 OD_{600}, photographs were taken 5 dpi. **(B)** Response to PITG_16275 in *S. americanum* perfectly correlates with presence of a complete *Rpi-amr1c* allele. Response to PITG_09160 and other effectors does not always follow this pattern. Some accessions lacking an *Rpi-amr1c* allele respond to one of more of these effectors indicating the presence of Rpi-amr5/Rpc2-independent recognition. Strength of cell death is indicated from 0 (absence of HR) to 2 (strong HR). **Data in panel B is a summary of screening performed by PhD student Li Long.**

4.3 – Discussion:

4.3.1 – *Rpi-amr5* and *Rpc2* are *Rpi-amr1* paralogues which recognise five *Phytophthora* effectors

The *Phytophthora* genus contains a diverse range of plant pathogens, many of which are economically important. The late blight pathogen *P. infestans* remains a global threat to potato production and *P. capsici* causes disease on many *Solanum, Capsicum* and *Cucurbit* species. *S. americanum* is a non-host to *P. infestans*, but only two *S. americanum* accessions are resistant to *P. capsici.* Using map-based cloning and sequence capture, a novel *Rpi* gene from *S. americanum* was cloned. This gene, *Rpi-amr5,* is a paralogue of *Rpi-amr1* and encodes a CC-NLR. *Rpc2* is an allele of *Rpi-amr5* and shares 97.4% amino acid identity. Resistance to *P. infestans* was conferred in tomato by both genes, and resistance to *P. capsici* for *Rpc2*.

Surprisingly, both Rpi-amr5 and Rpc2 are constitutively active in *N. benthamiana*. This is NRC-dependent and not observed in *nrc234* KO lines. Constitutive activity was reconstituted by the expression of *35S:NbNRC2*, but not *35S:SaNRC2*. This suggests that cell death is due to incompatibility with *N. benthamiana* but not *S. americanum NRC* alleles. In a recent study, Foong-Jing et al. (2023) found that sensor NLRs may function poorly with helpers from diverged plant species. Our data suggests that this could not only appear as complete failure of a helper to "help" a sensor NLR from a distantly related genus, but also as an aberrant activation of helpers in an effector-independent manner. However, many *Solanum* NLRs can function with *N. benthamiana* helpers. The constitutive activity phenotype provides another facet of restricted taxonomic functionality which should be considered when transferring NLRs between species. This discovery enabled the screening of candidate effectors in *N. benthamiana nrc234* mutant line using *35S:SaNRC2*.

The ETI interactions of *P. infestans* with *S. americanum* were previously characterised using 'effectoromics' (Lin et al., 2023). By screening effectors recognised by SP2275 and SP2308, but not SP2271, PITG_16275 and PITG_09160 were identified as the *P. infestans* elicitors of Rpi-amr5 and Rpc2 (Fig. 4.25a). These effectors both share similar predicted structures despite only 39.2% amino acid identity after the EER motif. Using the protein structure homology search tool Foldseek, homologous effectors from *P. megakarya*, *P. parasitica* and *P. palmivora* were identified. At least one orthologue from each species activates HR when co-expressed with either *Rpi-amr5* or *Rpc2*. While only one orthologue from each species was tested, this effector family is highly expanded in *P. megakarya* and *P. palmivora*. The ability of Rpi-amr5 and Rpc2 to recognise additional orthologues from these species will be tested,

as will their ability to confer resistance to these pathogens. Surprisingly, no PITG_16275 orthologues were identified in *P. capsici*. To identify the recognised effector, a library of *P. capsici* RXLR effectors was generated and screened in *S. americanum*. Several effectors are recognised in both the resistant and susceptible accessions. In *N. benthamiana* transient assays, three *P. capsici* effectors are recognised by both Rpi-amr5 and Rpc2 (Fig. 4.25b), none of which have homologues in *P. infestans*, *P. parasitica*, *P. palmivora*, *P. megakarya* or *P. cactorum*.

4.3.2 – Why does *Rpi-amr5* not confer resistance to *P. capsici*?

Three *P. capsici* effectors were identified as elicitors of Rpc2, and surprisingly, Rpi-amr5 also recognises all of them in *N. benthamiana* transient assays. So far, it is unclear why *Rpi-amr5* does not confer visible *P. capsici* resistance. Experiments involving overexpression of each allele in *S. americanum* and *S. lycopersicum* demonstrate that this is not due to differences in expression levels of the two NLRs. Instead, allelic differences must be responsible. There are several hypotheses that could be explored. The simplest one is that another effector is recognised by Rpc2, but not Rpi-amr5 (Fig 4.25d). This effector may have been absent from the initial annotation or may not have been successfully cloned. Of the 303 predicted effectors, 27 were not cloned. Additional recognition of a non-RXLR effector could be possible. All cloned *Rpi* genes encoding NLRs function through recognition of RXLR effectors, but other effector types do exist. Cytoplasmic non-RXLR effectors from oomycetes are well documented. For example, ATR5 from *Hyaloperonospora arabidopsidis*. ATR5 is the elicitor of RPP5, an *A. thaliana* NLR. ATR5 contains many canonical effector features including a signal peptide, EER motif and WY/LWY motifs. However, instead of RXLR, ATR5 has a Gly-Arg-Val-Arg (GRVR) motif (Bailey et al., 2011, Kim et al., 2023). Similarly, ATR2, the elicitor of RPP2A and RPP2B, is a non-RXLR effector which carries a signal peptide, EER motif and WY domains (Kim et al., 2023). Wood et al. (2020) found that several oomycetes, including *P. capsici*, have many secreted proteins lacking an RXLR motif which still contain either an EER motif or WY domain. To address this, an expanded list of effectors was compiled. When predicted proteins were filtered for WY or LWY domains and a signal peptide, 34 previously unidentified effectors were found. This expanded search was performed with PhD student Yufei Li. These effectors will be cloned and tested in *S. americanum* to identify additional recognitions, prioritizing those most highly expressed. Several polymorphisms that map onto the concave surface of the LRRs support the potential for additional Rpc2-specific recognition. These polymorphisms could alter the binding capability of the NLR.

Alternatively, *Rpi-amr5* could confer quantitative resistance to *P. capsici,* which may not be detectable in detached leaf assays. *S. americanum* accessions which are susceptible to *P. infestans* in detached leaf assays are completely resistant in field conditions. *Rpi-amr5* could confer resistance that is weaker than the response conferred by *Rpc2*. Although direct interaction between the recognised effectors and the NLRs has not been confirmed, split luciferase assay suggests association *in planta*. Differences in affinity, or strength of binding could be responsible for the observed phenotypes. Previous studies have shown that binding strength can correlate with the cell death response. For instance, variants of the NLR RPP1 have demonstrated differential affinities for ATR1 variants, with stronger binding correlating with a heightened HR phenotype (Steinbrenner et al., 2015). Similarly, variants of PikP-1 and Pikh have been found to confer extended recognition of *Magnaporthe* effectors through enhanced affinity to additional effector variants (De la Concepcion et al., 2019, De la Concepcion et al., 2021).

Another important consideration is that effector recognition in this context is assessed through a transient assay, where each component is overexpressed. Very little is known about the expression patterns of these *P. capsici* effectors during actual plant infection. The gene annotation performed by Stajich et al. (2021), based on mRNA extracted from *P. capsici* tissue grown on solid media, leaves it unclear whether the three effectors recognised by Rpi-amr5 are expressed during plant infection.

Finally, the difference in resistance could be attributed to allele-specific suppression of Rpi-amr5 (Fig. 4.25c). In an assay where constitutive activity was used as a surrogate for effector-dependent activity, one effector appeared to reduce cell death. While this result was reproducible, subsequent experiments using effector-dependent activation produced contradictory results. While only a small number of cloned effectors have been tested in this assay, 267 cloned effectors remain untested. Suppression of NLR-dependent immunity has been demonstrated in multiple studies (Yin et al., 2017, Derevnina et al., 2021, Contreras et al., 2023a). This phenomenon could explain many instances where recognition does not correlate with resistance. For instance, Rpi-amr1 recognises a *P. capsici* orthologue of AVRamr1 but this does not translate into resistance in either *S. americanum* or transgenic *N. benthamiana*. Similarly, the *S. americanum* NLRs R02860 and R04373 recognise the *P. infestans* effectors PITG_02860 and PITG_04373, but they do not confer visible resistance. These NLRs may be suppressed, resulting in reduction or abolition of resistance. Understanding the nature of suppression could facilitate the engineering of resistant alleles that evade this suppression.

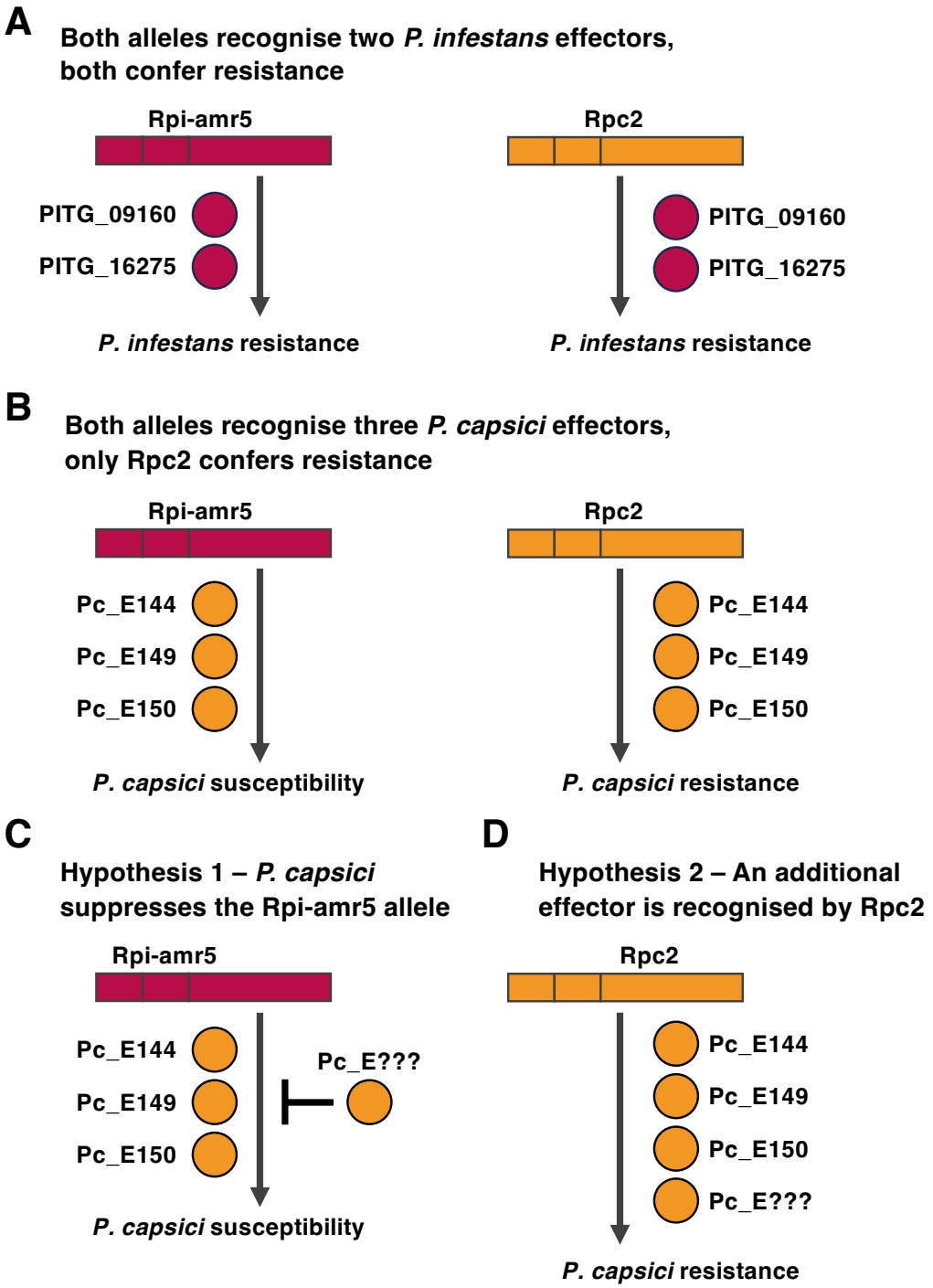

Figure 4.25. Why does *Rpi-amr5* not confer *P. capsici* resistance? (A) Rpi-amr5 and Rpc2 recognise two RXLR effectors from *P. infestans* (PITG_16275 and PITG_09160). Both confer resistance to *P. infestans*. **(B)** Rpi-amr5 and Rpc2 also recognise three effectors from *P. capsici* (PcE144, PcE149 and PcE150). Only *Rpc2* confers resistance to *P. capsici*. **(C)** One hypothesis to explain the lack of resistance to *P. capsici* conferred by *Rpi-amr5* is that another unidentified effector suppresses Rpi-amr5, but not Rpc2. **(D)** A second hypothesis is that Rpc2, but not Rpi-amr5, is able to recognise an additional unidentified effector from *P. capsici*. This recognition is required for resistance.

4.3.3 – *Solanaceae* have convergently evolved recognition of PITG_09160 and PITG_16275

In addition to Rpi-amr5 and Rpc2, another *S. americanum* receptor recognises PITG_09160. Response to PITG_09160 is lost in SP2275 *rpi-amr5* lines, but not SP2308 *rpc2* lines. This suggests that an additional recognition locus is present in SP2308. Other accessions lacking functional Rpi-amr5 alleles also respond to PITG_09160, supporting the hypothesis of the existence of an additional receptor. Furthermore, several instances of PITG_09160 and PITG_16275 recognition in other *Solanaceae* species have been reported. *Rpi-amr5* function is unlikely to be conserved in these species, suggesting the convergent evolution of receptors to recognise these effectors. Similarly, the recognition of *P. infestans* AVR2 has convergently evolved. AVR2 is recognised by both R2 and Rpi-mcq1 which respectively map to Chromosome 4 in *Solanum demissum* and Chromosome 9 in *Solanum mochiquense* (Aguilera-Galvez et al., 2018). Like AVR2, PITG_09160 and PITG_16275 may be important for virulence and pathogenicity of *P. infestans*. PITG_09160 has been shown to suppress AVR3a-dependent HR in potato (Yin et al., 2017). No function for PITG_16275 has been published, but it may have a similar function in supporting virulence of *P. infestans* through the suppression of immunity.

4.3.4 – Rpi-amr5 could provide an insight into the mechanism of multiple effector recognition

Rpi-amr5 and Rpc2 recognise diverse *Phytophthora* effectors. PITG_16275 orthologues from other *Phytophthora* species share low sequence identity but are still recognised. The three recognised *P. capsici* effectors are unrelated to PITG_16275. Further work is required to investigate the basis of this broad recognition. Multiple effector recognition is often achieved through an indirect mechanism, involving guarded proteins or integrated domains. This is exemplified in the ZAR1 CC-NLR and pseudokinase PBL2 decoy system, and the RPS4/RRS1-R TIR-NLR pair (Wang et al., 2015a, Sarris et al., 2015). Other instances of multiple recognition can be explained by a conserved effector structure, such as recognition of the homologous effectors HopQ1, XopQ and RipB by the *N. benthamiana* TIR-NLR ROQ1. We show that interaction of Rpi-amr5/Rpc2 with its five cognate effectors is most likely direct, but it remains unclear whether the effectors have conserved structures. Models produced by Alphafold are of low quality, so this must be determined experimentally.

The barley NLR MLA3 confers resistance to two phylogenetically distinct fungal pathogens, *Magnaporthe oryzae* and *Blumeria graminis*. The *M. oryzae* effector has been identified as

Pwl2, a MAX (*Magnaporthe* Avrs and ToxB-like) effector known to determine *M. oryzae* host range. Whilst the *B. graminis* effector AVR_{A3} has not been identified, the MAX effector family is absent from *B. graminis* suggesting it is distinct from Pwl2 (Brabham et al., 2023). Like MLA3, Rpi-amr5/Rpc2 could recognise multiple distinct protein structures. Studying the mechanism of multiple effector recognition in NLRs, such as Rpi-amr5/Rpc2 and MLA3, could aid the engineering of novel effector recognition or expansion of the recognition spectrum of cloned NLRs.

4.3.5 – Host and non-host resistance in *S. americanum* directly overlaps

Non-host resistance is a broad and complex phenomenon. As discussed by Panstruga and Moscou (2020), NLR-mediated immunity has roles in both host and non-host resistance. By cloning *Rpc2* and *Rpi-amr5*, the similarities between host and non-host resistance are highlighted. *S. americanum* is a non-host to *P. infestans*. Resistance to *P. capsici* is accession-specific and characteristic of host resistance. Despite these differences, resistance to these two pathogens directly overlaps. In one accession, resistance to *P. capsici* is due to a specific *Rpi* gene allele. Like Rpi-amr1 and Rpi-amr3, Rpi-amr5 is capable of recognising effectors from several other *Phytophthora* species. The presence of homologues of this effector across multiple species may suggest that loss of these effectors to evade recognition may be detrimental to pathogen virulence.

It is notable that *Rpi-amr5* and *Rpc2* are members of the *Rpi-amr1* gene cluster. In many *S. americanum* accessions *Rpi-amr1* and *Rpi-amr5* form a stack of resistance genes. This could contribute to the apparent durability of *Rpi-amr1* and explain why no tested *P. infestans* strains can evade recognition by Rpi-amr1. Moreover, SP2275 may contain additional resistance at this locus. *P. infestans* lesions on SP2275 *rpi-amr5* lines are visibly smaller than on SP2271, phenotypes shown in Figure 4.5b are at 10 days post-inoculation and are equivalent to 5 days post-inoculation in SP2271. It is unclear why this cluster has produced such a diverse recognition capacity against *Phytophthora* species. NLR clusters are known to be 'hotspots' for genetic diversity, and clustering is thought to facilitate diversification and evolution to counter rapidly evolving pathogens (Baggs et al., 2017, Richard et al., 2018). Such clusters often arise from tandem duplication, which promotes further diversification and recombination among paralogues (Yang et al., 2008, Van de Weyer et al., 2019). A well-known example is the *RPP8*/*RCY1*/*HRT* locus in Arabidopsis, where intragenic recombination has contributed to the evolution of genes that confer resistance downy mildew, turnip crinkle virus and cucumber mosaic virus, respectively (McDowell et al., 1998, Takahashi et al., 2002,

Cooley et al., 2000). At the *Rpi-amr1* locus, we have identified multiple novel recognitions of *Phytophthora* species. Further study of the diversity within *S. americanum* NLR clusters could provide insights into why this specific locus appears to be a 'hotspot' for new recognition specificities. This may be a consequence of greater variation within the *Rpi-amr1* cluster, when compared to other loci, or it could reflect an unknown characteristic of this NLR family that enables particularly effective resistance to *Phytophthora* species.

Similarly, it is intriguing why certain receptor classes are disproportionately implicated in resistance to specific pathogens. All NLRs encoded by *Rpi*-genes are CC-NLRs, although other uncloned or unpublished *Rpi* genes may encode other classes of NLR. *P. infestans* may be capable of strong suppression of TIR-NLR immunity. This could be either through inhibition of the RPW8-NLRs, or by targeting small molecules produced by activated TIR-NLR sensors. Understanding the molecular basis of this suppression could lead to engineering approaches that allow evasion of suppression.

4.3.6 – Have the major components of *S. americanum* NHR *to P. infestans* been cloned?

In the characterisation of *S. americanum* NHR to *P. infestans*, strong resistance in most accessions is conferred by *Rpi-amr1* and *Rpi-amr3*. Of the 46 accessions that resist *P. infestans* in detached leaf assays, only 2 lack either of these *R*-genes. Resistance in the remaining two accessions (SP2275 and SP3370) is attributed to *Rpi-amr5*. However, other weaker resistances do exist. An allele of *Rpi-amr4* which confers recognition of PITG_22825, is also found in SP2271 which is one of the most susceptible accessions. Despite this, the SP1102 allele of *Rpi-amr4* confers quantitative resistance in *N. benthamiana* transient assays (Lin et al., 2023). The NLRs R02860 and R04373, which recognise PITG_02860 and PITG_04373 respectively, do not appear to confer any resistance either in *S. americanum*, or when overexpressed in *N. benthamiana* (Lin et al., 2023).

There are at least three accessions which have novel and uncharacterised resistance to *P. infestans*, these are SP1101, SP2300 and SP2298. Resistance was identified through backcrossing to segregate away *Rpi-amr1*/*Rpi-amr3*, or by using CRISPR to mutate *Rpi-amr1*/*3* (this work is unpublished and was performed with Dr Sarah Pottinger, Dr Xiao Lin and Maria Sindalovskaya). In these instances, resistance is dominant but does not segregate clearly as a monogenic trait. *Rpi-amr1* and *Rpi-amr3* appear to be the major components of NHR and are supported by multiple weaker *R*-genes, including *Rpi-amr4* and *Rpi-amr5* (Fig. 4.26).

A further layer of resistance may be too quantitative to detect in laboratory detached leaf assays. Laboratory susceptible accessions are resistant in field conditions. These accessions can recognise numerous *P. infestans* effectors, for example, SP2271 responds to 25 effectors. These recognitions, individually or together, may contribute to resistance in the field, especially in suboptimal infection conditions and low inoculum levels. In laboratory conditions inoculum is much more concentrated and conditions are optimised to promote infection. For deployment in transgenic potato or tomato, genes conferring strong resistance are required. Stacking of multiple quantitative resistances would be less feasible and less desirable. Nevertheless, there is scientific interest in understanding the basis of these quantitative resistances.

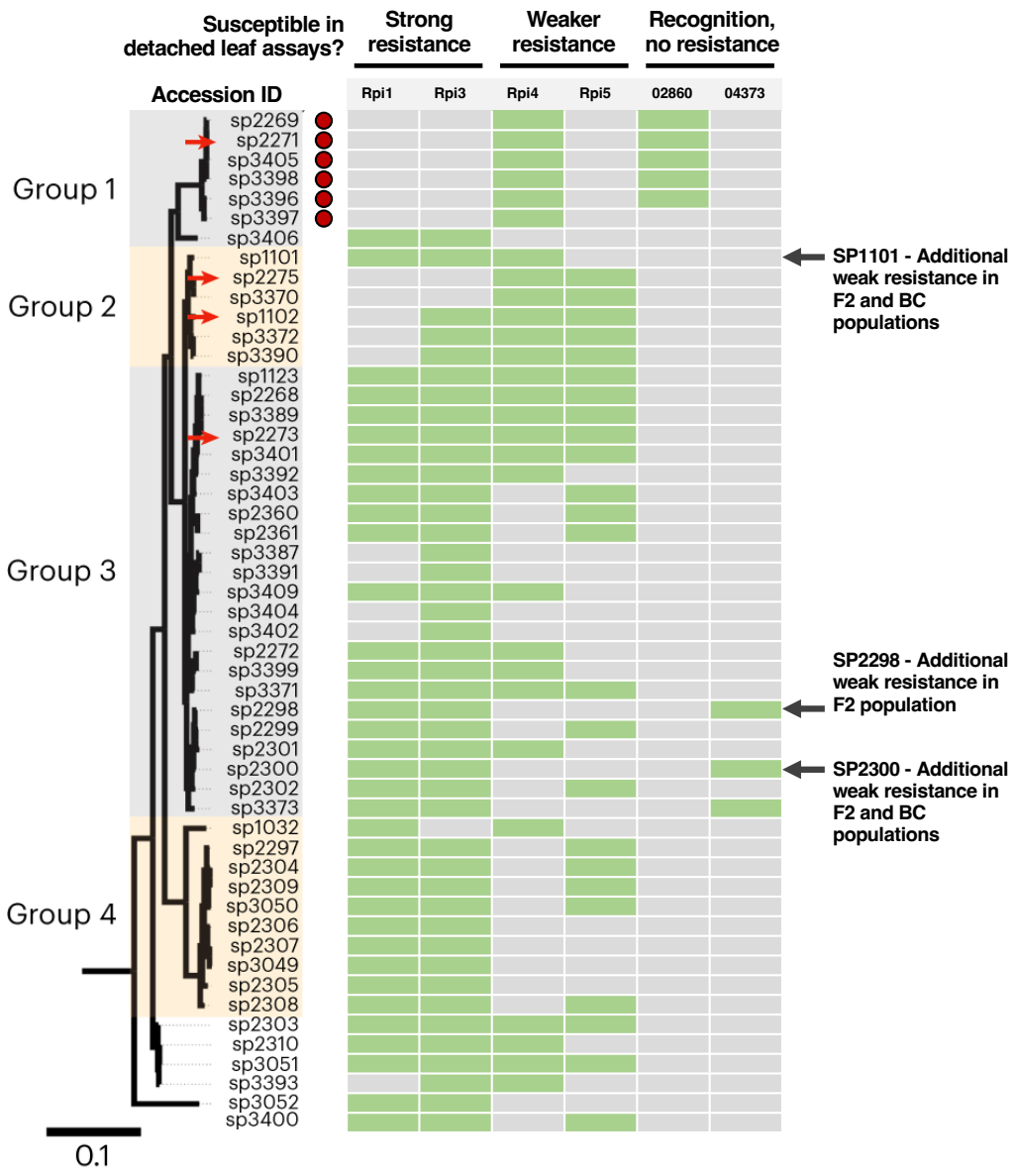

Figure 4.26. Distribution of cloned *Rpi* genes within *S. americanum* accessions. Figure showing the predicted *Rpi* gene repertoire of each of the 52 *S. americanum* accessions (*Rpi-amr1/3/4/5* are abbreviated to *Rpi1/3/4/5*). Accessions which are susceptible to *P. infestans* in detached leaf assays are indicated with red circles. In each accession, the presence of cloned *Rpi* genes is represented by green boxes, this was predicted by the response to the cloned effector (For *Rpi-amr5*, PITG_16275 is used as Rpi-amr5-independent recognition of PITG_09160 exists). Three accessions have an additional resistance factor identified in F2 or backcross populations. The phylogenetic tree is adapted from Lin et al. 2023, the reference accessions are indicated with red arrows.

Chapter 5: Characterising additional resistance to *P. capsici* in *Solanum* species

5.1 – Introduction

In the previous chapter, the first resistance gene against *Phytophthora capsici* was cloned. This gene, *Rpc2* (*RESISTANCE TO PHYTOPHTHORA CAPSICI 2*), is a paralogue of *Rpi-amr1* found in *Solanum americanum* accession SP2308. *Rpc2* encodes a CC-NLR that recognises at least three effectors from *P. capsici*. Within the *S. americanum* collection, a second *P. capsici* resistant accession was identified – SP1102, which contains novel resistance designated as *Rpc1*. In this chapter, *Rpc1* was mapped, and candidates were tested using VIGS and transient expression assays. While the resistance gene has not been cloned yet, it could provide an additional resource to confer *P. capsici* resistance in transgenic crops.

In addition to *S. americanum,* the black nightshade clade contains hexaploid species *Solanum nigrum* and *Solanum scabrum*, as well as the tetraploid species *Solanum villosum* (Särkinen et al., 2015, Särkinen et al., 2018). Accessions of these three species were also investigated for resistance to *P. capsici*. Two *S. villosum* accessions contain resistance which was demonstrated to be distinct from either *Rpc1* or *Rpc2*. However, complex inheritance hindered the mapping of these *S. villosum R*-genes.

The dissection of resistance to *P. capsici* in these species will provide insight into the genetic basis of resistance to *P. capsici*. Cloning of these *R*-genes will enable *P. capsici* resistant crops to be generated through *R*-gene stacking.

5.2 – Results

5.2.1 – *Rpc1* resistance maps to an *R*-gene cluster on Chromosome 10

Two *S. americanum* accessions with strong resistance to *P. capsici* have been identified: SP2308 and SP1102. Resistance in SP2308 is conferred by *Rpc2,* as described in Chapter 4. The novelty of SP1102 resistance was demonstrated through VIGS of the *Rpc2* cluster. Since the silencing of this cluster does not affect the resistance in SP1102, we conclude that factors distinct from *Rpc2* are responsible for the resistance (Fig. 4.6c).

In a biparental mapping population produced by crossing SP1102 to the susceptible accession SP2271, resistance segregates in a 3:1 ratio. Therefore, a single gene, which was named *Rpc1* (*RESISTANCE TO PHYTOPHTHORA CAPSICI 1*), is responsible for resistance. *Rpc1* was mapped to a cluster of NLR-encoding genes on Chromosome 10, and flanking markers were identified (Fig. 5.1a). The mapping of *Rpc1* was performed by Dr Kamil Witek and Dr Agnieszka Witek.

Following the whole-genome assembly and chromosome-level scaffolding of SP1102 (Lin et al., 2023), we could position the resistance-flanking markers and examine the *Rpc1* region. This 997 Kb interval contains a large cluster of NLR-encoding genes (Fig. 5.1a).

5.2.2 – *Rpc1* candidates encode homologues of the Rpi-chc1 and R1 NLRs

Within the *Rpc1* interval, there are 12 NLR-encoding genes. Alphabetical identifiers were given to distinguish each of these genes; *Rpc1a* to *Rpc1k,* and *Rpc1x* (Fig. 5.1a). *Rpc1x* was absent from the initial draft assemblies. This may have been caused by sequence collapse due to the high sequence identity between *Rpc1x* and the neighbouring paralogues. The *Rpc1* gene cluster has previously been associated with *Phytophthora* resistance. In *Solanum chacoense*, this cluster includes the potato late blight resistance gene *Rpi-chc1* (Monino-Lopez et al., 2021). An orthologue of *Rpi-chc1*, *R04373* in *S. americanum*, enables the recognition of the *Phytophthora infestans* effector PITG_04373 (Lin et al., 2023). To confirm that *Rpc1* candidates are *Rpi-chc1* orthologues, we aligned the NB-ARC sequences of the candidates with previously characterised NLRs and constructed a phylogenetic tree. Of the 12 NLRs in the cluster, 11 are Rpi-chc1 homologues. The remaining NLR falls into a clade with R1, an NLR from *Solanum demissum* which also confers late blight resistance (Fig. 5.1b, Table. 5.1).

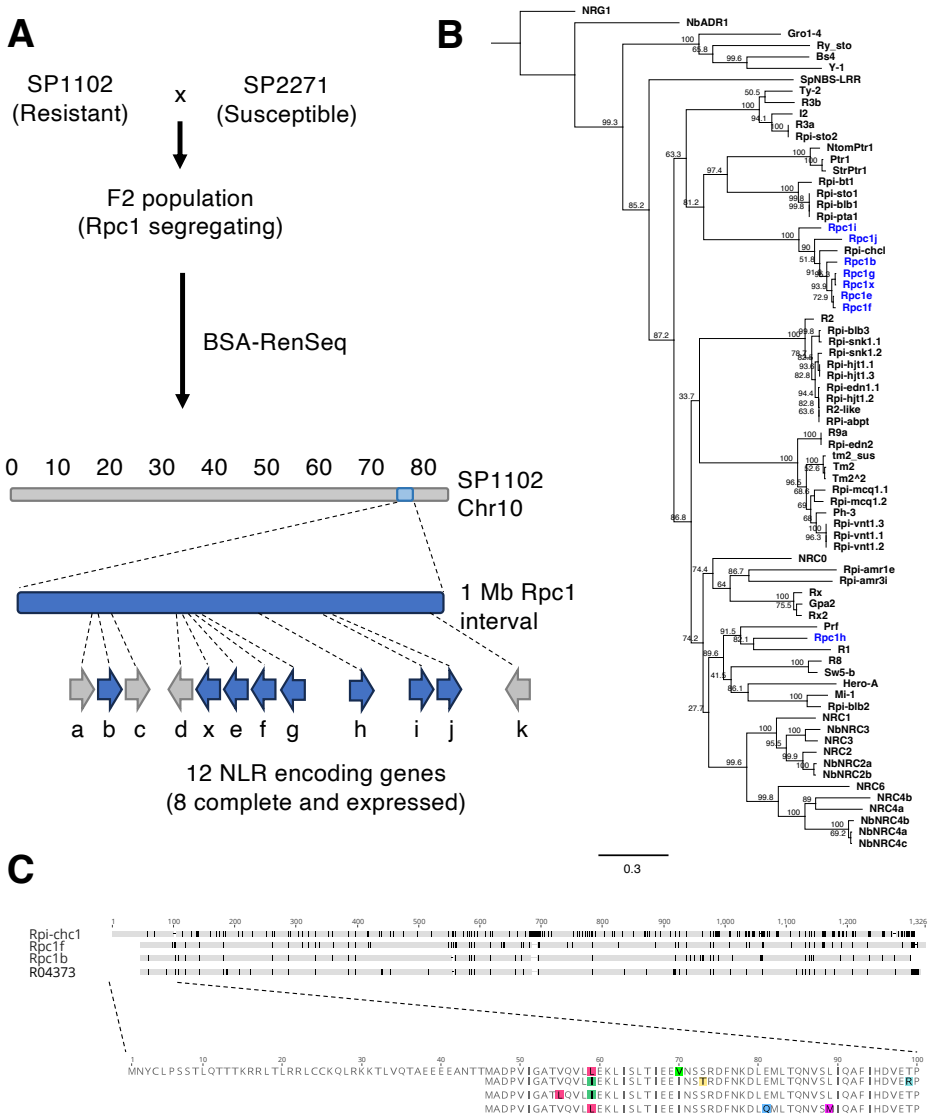

Figure 5.1. *Rpc1* maps to a cluster of NLR-encoding genes which contains homologues of *Rpi-chc1* and *R1*. (A) In an F2 population, produced from a cross between *P. capsici* resistant accession SP1102 and susceptible accession SP2271, *Rpc1* resistance segregates as a monogenic trait. Using the SP1102 reference genome, *Rpc1* was mapped to a cluster of NLR-encoding genes on Chromosome 10. *Rpc1* candidates are indicated in blue, other candidates either show no expression in SP1102, are found in other susceptible accessions, or lack canonical NLR domains. **(B)** A phylogenetic analysis of the NLRs in this cluster shows the closest characterised homologues of Rpc1 candidates. NB-ARC sequences of the eight complete and expressed NLRs within the *Rpc1* interval were aligned to a library of functionally characterised *Solanum*, *Nicotiana* and *Capsicum* NLRs. These NLR sequences were taken from the dataset compiled by (Kourelis et al., 2021). Rpc1 candidates are indicated in blue, most are orthologues of the *S. chacoense* NLR Rpi-chc1, and one candidate has homology to the *S. demissum* NLR R1. The support for each branch within the tree is indicated as a percentage determined from 1000 iterations. **(C)** Rpc1 candidates with homology to Rpi-chc1 have a truncated N-terminus compared to the orthologue from *S. chacoense*. To illustrate this, the predicted amino acid sequence of Rpc1b and Rpc1f is shown aligned to the published Rpi-chc1 and R04373 sequences. An expanded view of the first 100 amino acids of the alignment is shown.

Candidates were filtered using cDNA RenSeq data produced from SP1102 leaf tissue. Mapped reads were used to predict gene models and determine whether paralogues are expressed. Eight of the NLR-encoding genes within this cluster are expressed and encode complete NLRs (Table. 5.1). Interestingly, Rpi-chc1 homologues in *S. americanum* have a truncated N-terminal domain. Relative to the characterised Rpi-chc1, 45 amino acids are absent from the *S. americanum* NLRs (Fig. 5.1c). This is also observed in R04373, a characterised Rpi-chc1-like NLR from *S. americanum*.

Table 5.1. Seven NLR-encoding genes were identified as *Rpc1* candidates. *Rpc1* confers resistance to *P. capsici* in *S. americanum* accession SP1102. *Rpc1* maps to a cluster of NLR-encoding genes on Chromosome 10. This cluster contains 12 NLR-encoding genes which encode 1 R1-like and 11 Rpi-chc1-like NLRs. The ID, expression (determined using cDNA RenSeq of SP1102) and the closest functionally charactered homologue is shown. Expressed candidates encoding complete NLRs were tested in transient *N. benthamiana* assays. Each candidate was transiently expressed in whole leaves, which were subsequently assessed for increased resistance to *P. capsici* (see Figure 5.4). The result of the assay is indicated for each candidate.

NLR_ID	NLR clade	Expression in SP1102	Candidate notes	Transient gain of resistance assay in *N. benthamiana*
Rpc1a	Rpi-chc1	**No expression**	-	-
Rpc1b	Rpi-chc1	Expressed	-	**No visible resistance**
Rpc1c	Rpi-chc1	**No expression**	-	-
Rpc1d	Rpi-chc1	Expressed	**Premature stop in exon 1**	-
Rpc1e	Rpi-chc1	Expressed	-	**No visible resistance**
Rpc1f	Rpi-chc1	Expressed	-	**No visible resistance**
Rpc1g	Rpi-chc1	Expressed	-	**No visible resistance**
Rpc1h	R1	Expressed	-	-
Rpc1i	Rpi-chc1	Expressed	-	**No visible resistance**
Rpc1j	Rpi-chc1	Expressed	-	**No visible resistance**
Rpc1k	Rpi-chc1	Expressed	**Premature stop in exon 1**	-
Rpc1x	Rpi-chc1	Expressed	-	**No visible resistance**

5.2.3 – Silencing of the *Rpi-chc1* gene family compromises *P. capsici* resistance in SP1102

Eight NLR encoding genes were identified as *Rpc1* candidates. To determine whether *Rpc1* resistance is conferred by any of these genes, VIGS was used. A TRV2 construct containing a fragment of *Rpc1b*, which is highly conserved between paralogues, was used to silence the

Rpi-chc1 homologues. A separate TRV2 construct targeting the *R1* orthologue was also used. VIGS of the *Rpi-chc1* homologues compromises *Rpc1* resistance and produces a phenotype comparable to the susceptible SP2271 accession. Silencing of the *R1* orthologue had no effect on resistance (Fig. 5.2). These data show that *Rpc1* is encoded by a homologue of *Rpi-chc1*, with seven genes remaining as candidates.

While VIGS was an effective approach to demonstrate that *Rpi-chc1* orthologues are required for resistance, further dissection by gene silencing was hindered by high sequence similarity among all paralogues, five of these share over 94% identity within their CDS sequences (Fig. 5.3). Similarly, UTR and intron sequences are nearly identical across these paralogues, making it impossible to design paralogue-specific silencing constructs.

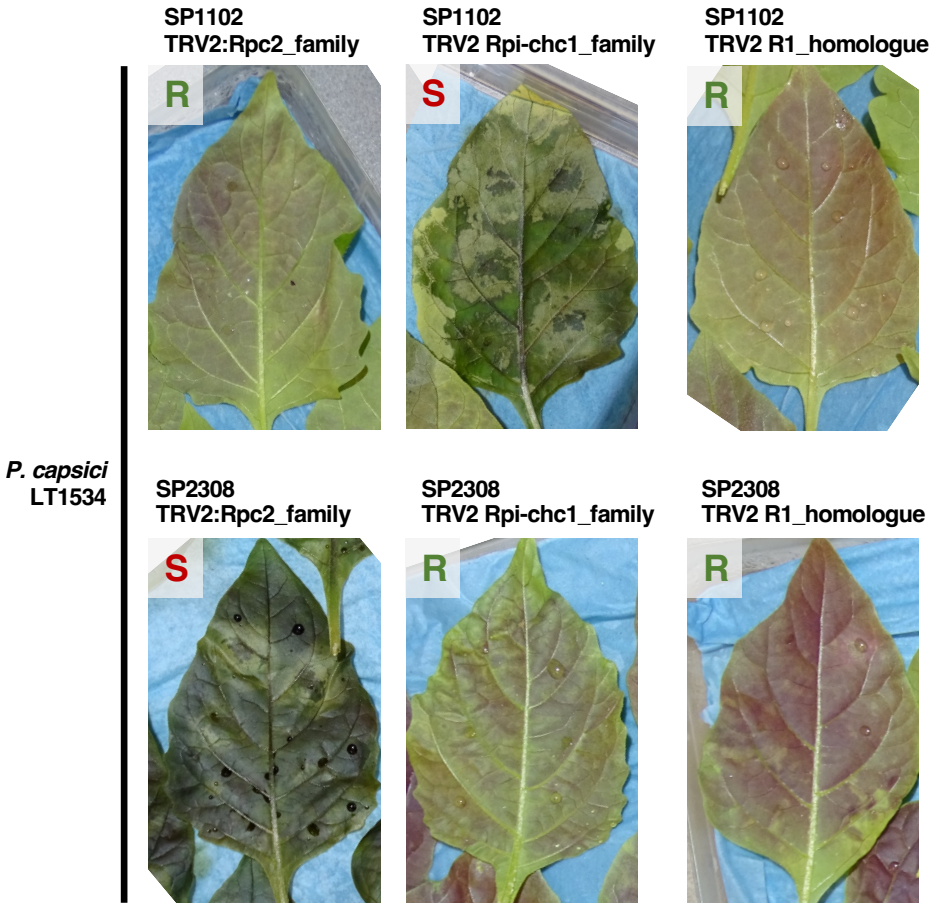

Figure 5.2. Silencing of *Rpi-chc1* homologues in SP1102 compromises resistance to *P. capsici*. VIGS of *Rpc1* candidates was performed in SP1102. Silencing of all *Rpi-chc1* homologues rendered SP1102 susceptible whereas targeting either the *Rpc2* cluster, or the *R1* homologue, did not affect resistance. SP2308 was used as a control in this experiment. In SP2308, silencing of *Rpc2* cluster reduces resistance but the silencing of either the *Rpi-chc1* cluster or *R1,* does not. Leaves were drop-inoculated with *P. capsici* strain LT1534 (10 µl drops at a concentration of 20,000 spores ml^{-1}) and imaged at 3 days post-inoculation.

	Rpc1f	Rpc1b	Rpc1e	Rpc1x	Rpc1g	Rpc1i	Rpc1j
Rpc1f		94.7%	94.6%	93.6%	94.4%	84.5%	83.3%
Rpc1b	94.7%		95.0%	95.2%	95.0%	84.1%	82.8%
Rpc1e	94.6%	95.0%		99.4%	99.4%	84.2%	82.7%
Rpc1x	93.6%	95.2%	99.4%		99.7%	84.3%	82.7%
Rpc1g	94.4%	95.0%	99.4%	99.7%		84.3%	82.7%
Rpc1i	84.5%	84.1%	84.2%	84.3%	84.3%		83.6%
Rpc1j	83.3%	82.8%	82.7%	82.7%	82.7%	83.6%	

Figure 5.3. Many *Rpc1* candidates share high sequence similarity. The figure shows a heatmap of the percent identity between the CDS sequences of *Rpc1* candidates. CDS sequences were determined using cDNA RenSeq data generated from SP1102 leaf tissue. Paralogue-specific silencing could not be performed due to the high sequence similarity between many paralogues.

5.2.4 – *Rpc1* candidates do not confer *P. capsici* resistance in transient *N. benthamiana* assays

Using VIGS, we demonstrated that the *Rpi-chc1* homologues are responsible for the *P. capsici* resistance in SP1102. Seven genes remained as candidates. In an initial test, transient gain-of-resistance assays were performed in *Nicotiana benthamiana*. Candidates were cloned into a CaMV *35S*-regulated binary vector and expressed in whole *N. benthamiana* leaves. Leaves were inoculated with *P. capsici* zoospores two days post-infiltration. None of the candidates appeared to elevate resistance in this assay (Fig. 5.4). Nevertheless, this experiment does not exclude these candidates, as either the experimental setup or the biology of *P. capsici* may prevent the observation of a qualitative increase in resistance. The rapid transition of *P. capsici* from biotrophy to necrotrophy may produce a more quantitative resistance phenotype in assays for *Rpc* genes compared to *Rpi* genes. Additionally, no positive control for *P. capsici* resistance is available, as the only cloned *P. capsici* resistance gene, *Rpc2*, is constitutively active in *N. benthamiana*. To address this, variation in the *N. benthamiana* assay could be tested by employing alternative inoculation methods, such as transferring media plugs containing *P. capsici* or directly applying hyphae. More robust phenotyping methods, like measuring lesion sizes and growth rates, could be implemented, they were initially omitted due to the assumption that a qualitative phenotype would be observed. Alternatively, *Rpc1* candidates may lack functionality in *N. benthamiana*, potentially due to the absence of an additional factor required for resistance. This is, however, considered unlikely, as the closely related NLRs Rpi-chc1 and R04373 are known to confer cell death function in *N. benthamiana*.

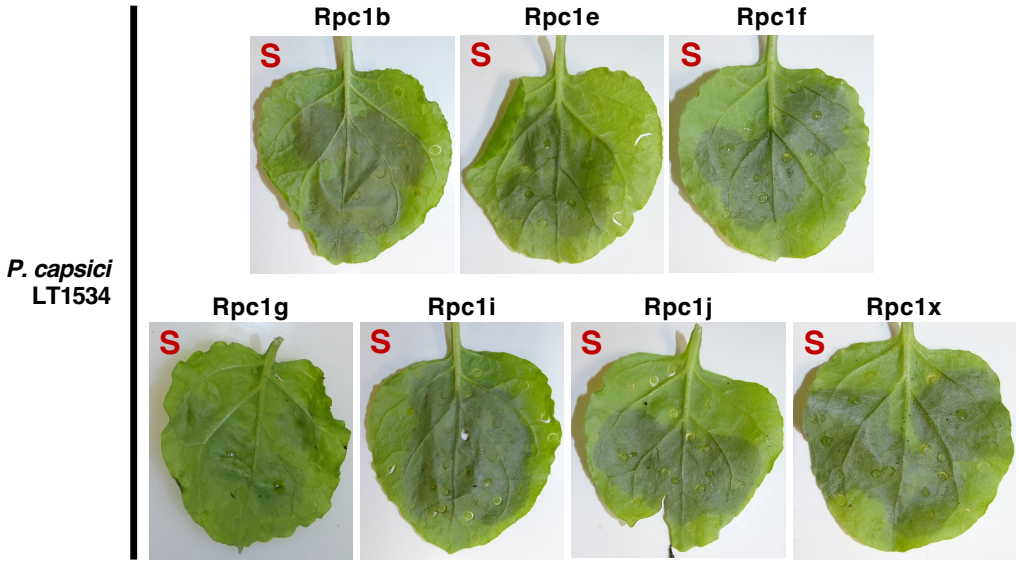

Figure 5.4. No *Rpc1* candidates confer resistance to *P. capsici* in an *N. benthamiana* transient assay. *Rpc1* candidates were tested in *N. benthamiana* transient assays. No candidate elevates resistance in this assay. *Agrobacterium* strains were infiltrated at an OD_{600} of 0.2. Two days post-infiltration leaves were detached and *P. capsici* inoculation was performed (10 µl drops at 10,000 spores ml^{-1}). Leaves were photographed at 6 days post-inoculation. There is no positive control available for this assay as there are no cloned *Rpc* genes that are not constitutively active in wild-type *N. benthamiana*.

5.2.5 – In an F2 population, recognition of PcE26 co-segregates with resistance to *P. capsici*

Since no gain of resistance was observed in the *N. benthamiana* transient assay, an alternative approach was adopted. We sought to identify the recognised effector to facilitate the testing of candidates in a cell death assay. The *P. capsici* effector library was screened against SP1102, SP2271, SP2275 and SP2308 as described in Chapter 4. The screening was performed by PhD student Li Long. Although SP1102 recognises many effectors, only recognition of PcE26 is unique to this accession.

As a candidate elicitor of Rpc1, PcE26 was screened in a small F2 population of 147 plants to determine whether recognition of this effector co-segregates with resistance. In this population, 37 susceptible segregants were identified, all of which lacked recognition of PcE26, while all resistant plants displayed recognition of the effector. This indicates a strong linkage between the recognition of PcE26 and *Rpc1*.

5.2.6 – *Rpc1* candidates do not confer recognition of PcE26 in *N. tabacum* transient assays

As PcE26 recognition appears to co-segregate with *Rpc1* in the F2 population, this effector may be the elicitor of Rpc1. Cell death assays in *Nicotiana tabacum* were used to test Rpc1 candidates for recognition of PcE26. Each candidate was co-expressed with either PcE26 or AVRamr3. No candidate showed autoactivity, and no HR was observed in any combination with PcE26 (Fig. 5.5). As previously discussed, the *Rpc1* candidates may lack functionality in *Nicotiana* species, potentially explaining the absence of cell death upon co-expression with PcE26. To address this, further experiments will be conducted to identify the gene, including repeating the HR assay in *S. americanum*, where *Rpc1* is known to be functional. Also, a combination of candidate genes may be required to recognise the effector. To test this, the assay will be performed with candidates expressed in multiple combinations.

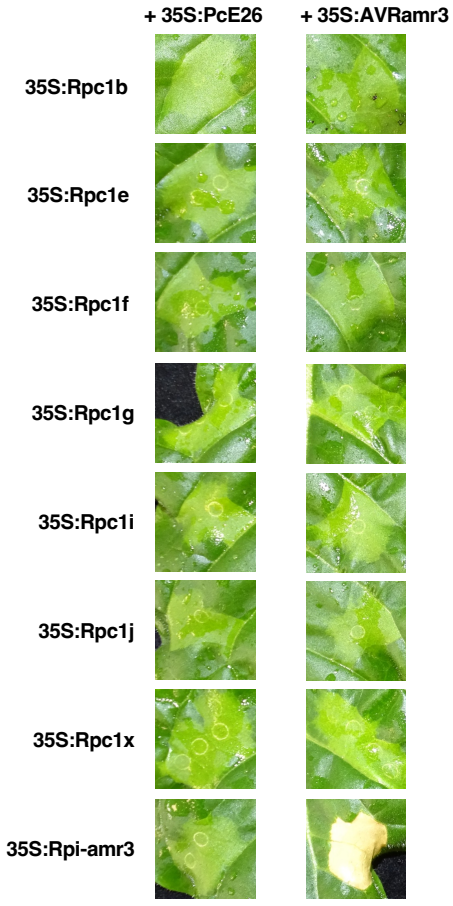

Figure 5.5. Co-expression of PcE26 with Rpc1 candidates in *N. tabacum* does not result in HR. In a small *S. americanum* F2 population, *Rpc1* was found to co-segregate with the recognition of PcE26. In an *N. tabacum* transient assay, Rpc1 candidates were co-expressed with PcE26 to determine if any paralogue can recognise this effector. No HR was observed for any combination with PcE26. Rpi-amr3 and AVRamr3 were used as controls in this assay. Each *Agrobacterium* strain was diluted to 0.2 OD_{600} before infiltration, leaves were imaged at 5 dpi.

5.2.7 – Two *S. villosum* accessions are highly resistant to *P. capsici*

Two novel *Rpc* genes from *S. americanum* have been mapped. In the screening process to identify resistant *S. americanum* accessions, other *Solanum* species from the black nightshade clade were also evaluated. This included the hexaploid species *S. nigrum* and *S. scabrum*, as well as the tetraploid species *S. villosum*. No resistant *S. scabrum* accessions were found, while ten *S. nigrum* accessions and two resistant *S. villosum* exhibited resistance to *P. capsici* (Fig. 5.6, Fig. 5.7a). We focused on *S. villosum*, as the hexaploid genetics of *S. nigrum* would significantly complicate the investigation of the resistance in this species.

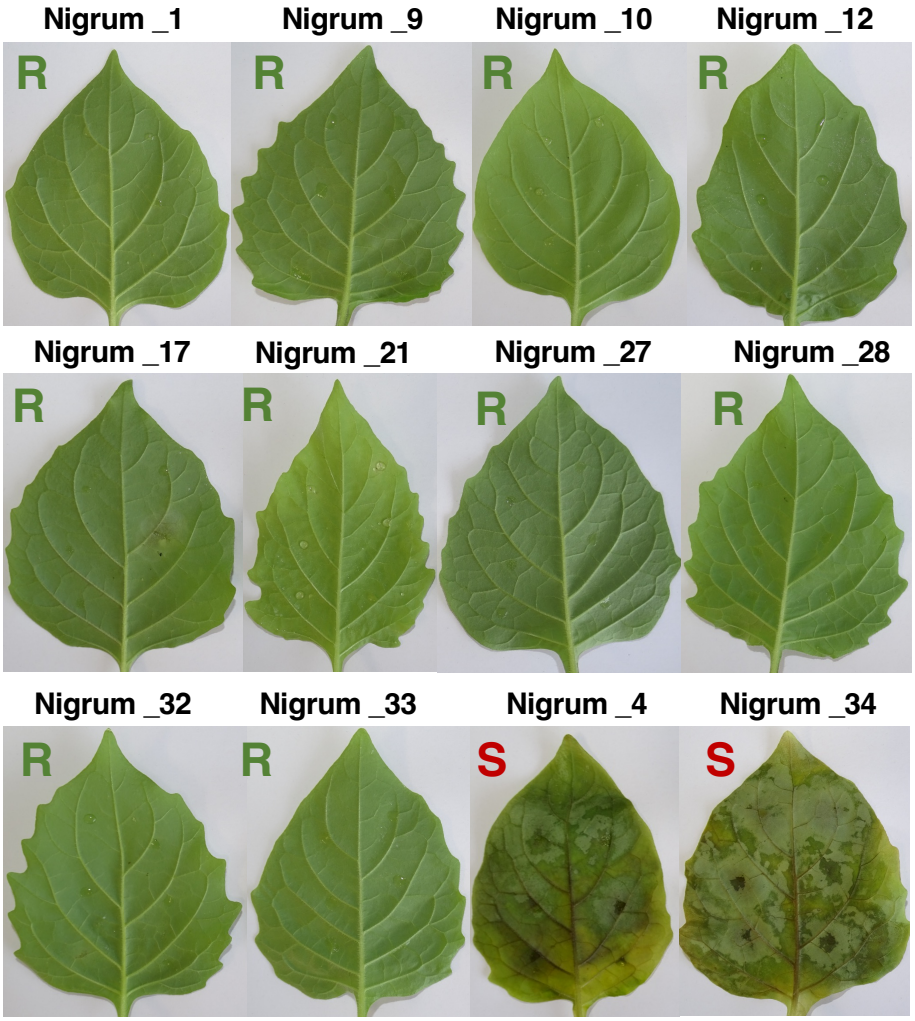

Figure 5.6. Several *S. nigrum* accessions resist *P. capsici* in detached leaf assays. Of the 30 accessions of *S. nigrum* which were assayed for resistance to *P. capsici* in detached leaf assays, 10 show resistance to *P. capsici*, all others are completely susceptible. The phenotypes of 10 resistant accessions and two susceptible examples, are shown. Leaves were inoculated with *P. capsici* zoospores (10 µl drops at a concentration of 10,000 spores ml^{-1}) and photographed 3 days post-inoculation.

S. villosum is believed to be an autotetraploid (Särkinen et al., 2018), although some reports suggest that chromosome segregation and inheritance may be more similar to that of an allotetraploid species (Sultana and Alam, 2007). Two *S. villosum* accessions (SP3057 and SP3065) are highly resistant to *P. capsici* (Fig. 5.7a). All other accessions are susceptible, as SP3059 was successfully crossed to both resistant lines it was chosen as the susceptible background for future work.

5.2.8 – Resistance of *S. villosum* to *P. capsici* is distinct from *Rpc1* and *Rpc2*

Although *S. villosum* and *S. americanum* are distinct species, it is possible that resistance genes are shared between them. Previous work demonstrated that functional orthologues of *S. americanum* late blight resistance genes are found in *S. nigrum* and *S. nigrescens*. *S. nigrum* orthologues of *Rpi-amr1* and *Rpi-amr3* show very high sequence similarity to the characterised *S. americanum* variants. These *S. nigrum* alleles are functional and confer recognition of AVRamr1 and AVRamr3; and resistance to *P. infestans* (Witek et al., 2021, Lin et al., 2022). Before characterising the *P. capsici* resistance in *S. villosum*, we demonstrated its novelty compared to both *Rpc1* and *Rpc2*.

SMRT RenSeq was performed on SP3057, SP3059 and SP3065 to identify *Rpc2* orthologues in these accessions. Notably, in the resistant accession SP3065, *Rpc2* includes a frameshift which leads to a premature stop within the NB-ARC. In SP3057, the assembled allele is incomplete and lacks the final exon resulting in the absence of the final 34 amino acids (Fig. 5.7c). While the final exon may just be missing from the assembly, the amino acid sequence of these alleles is less similar to the functional Rpc2 than several *S. americanum* alleles which do not confer *P. capsici* resistance (Fig. 5.7b). To confirm that *Rpc2* is non-functional in SP3057 and SP3065, Rpc2 elicitors identified in Chapter 4 were transiently expressed in these accessions. No hypersensitive response was observed for either PcE144, PcE149 or PcE150. Therefore, resistance in SP3057 and SP3065 is not due to *Rpc2* (Fig. 5.8a).

Finally, VIGS was used to confirm that *Rpc1* is not responsible for *P. capsici* resistance in *S. villosum*. Firstly, to show that VIGS is effective in *S. villosum,* a construct was used to silence the gene which encodes the magnesium-chelatase subunit ChIH. Clear bleaching of leaf tissue was observed confirming the efficacy of TRV-based VIGS in *S. villosum* (Fig. 5.8c). Silencing of the *Rpc1* and the *Rpc2* clusters separately or together did not affect resistance (Fig. 5.8b). Therefore, *S. villosum* resistance is distinct from *Rpc1* and *Rpc2*. If resistance in SP3065 and SP3057 is due to the action of NLRs, they are encoded by a different gene family.

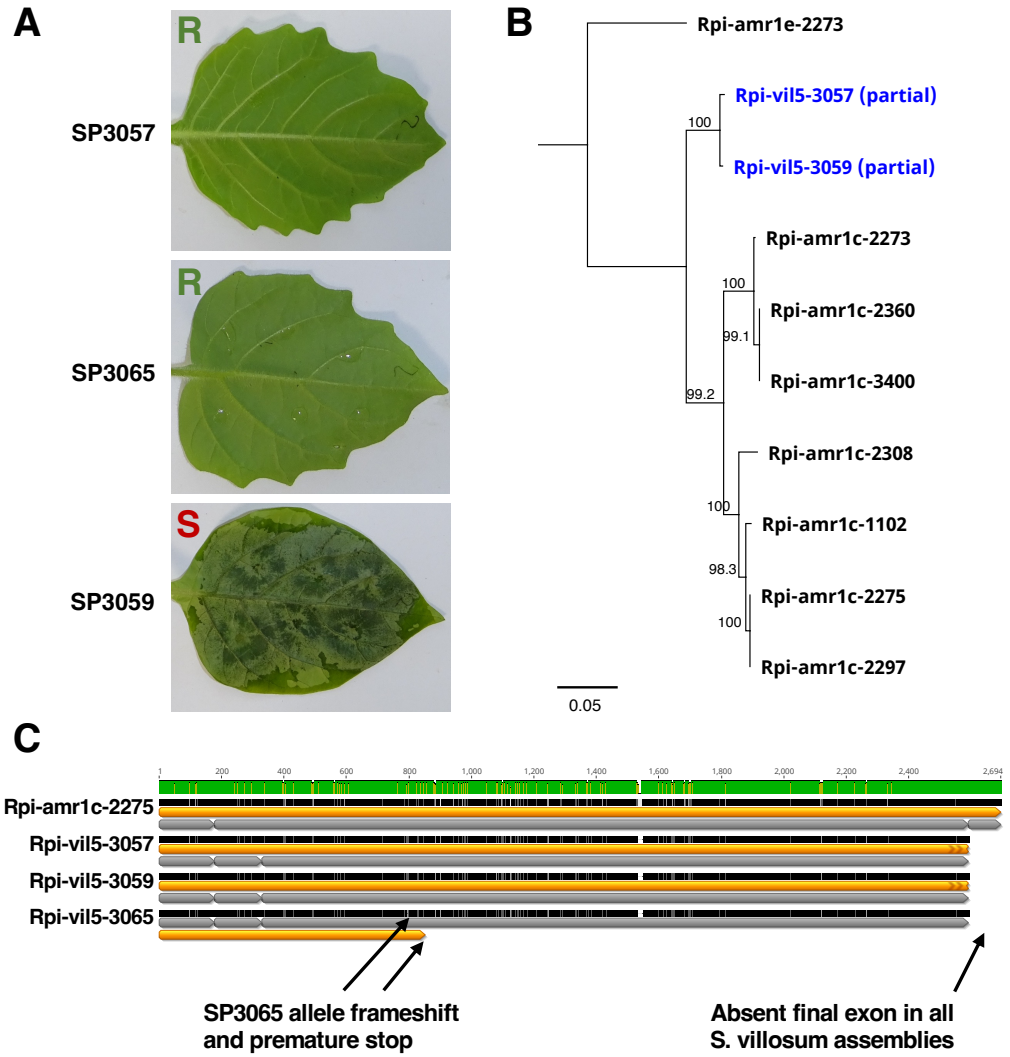

Figure 5.7. *S. villosum* contains novel resistance to *P. capsici*. **(A)** The *S. villosum* accessions SP3057 and SP3065 are highly resistant to *P. capsici*, SP3059 is susceptible. Leaves shown were inoculated with *P. capsici* zoospores (10 µl drops at a concentration of 10,000 spores ml^{-1}) and photographed 3 days post-inoculation. **(B)** SMRT RenSeq was used to identify the *Rpc2* alleles present in these three *S. villosum* accessions. Contigs identified were only partially covering the *Rpc2* gene, with the final exon being absent, or unassembled. The predicted proteins from these partial alleles are less related to Rpc2 (indicated as Rpi-amr1c-2308) than other alleles which do not confer *P. capsici* resistance. The phylogenetic tree was constructed by aligning the amino acid sequences of *S. americanum* and *S. villosum* Rpi-amr1c proteins. The tree is rooted using Rpi-amr1e-2273, the NLR from SP2273 characterised for *P. infestans* resistance. The support for each branch is indicated as a percentage determined from 1000 iterations. **(C)** *S. villosum* RenSeq assemblies do not contain a complete orthologue of *Rpi-amr5*/*Rpc2*. The predicted gene structures of the SP3057, SP3059 and SP3065 alleles are represented. In each of these assemblies, the final coding exon is absent. There is no functional *Rpi-amr5*/*Rpc2* orthologue in SP3065, a frameshift mutation results in a premature stop codon.

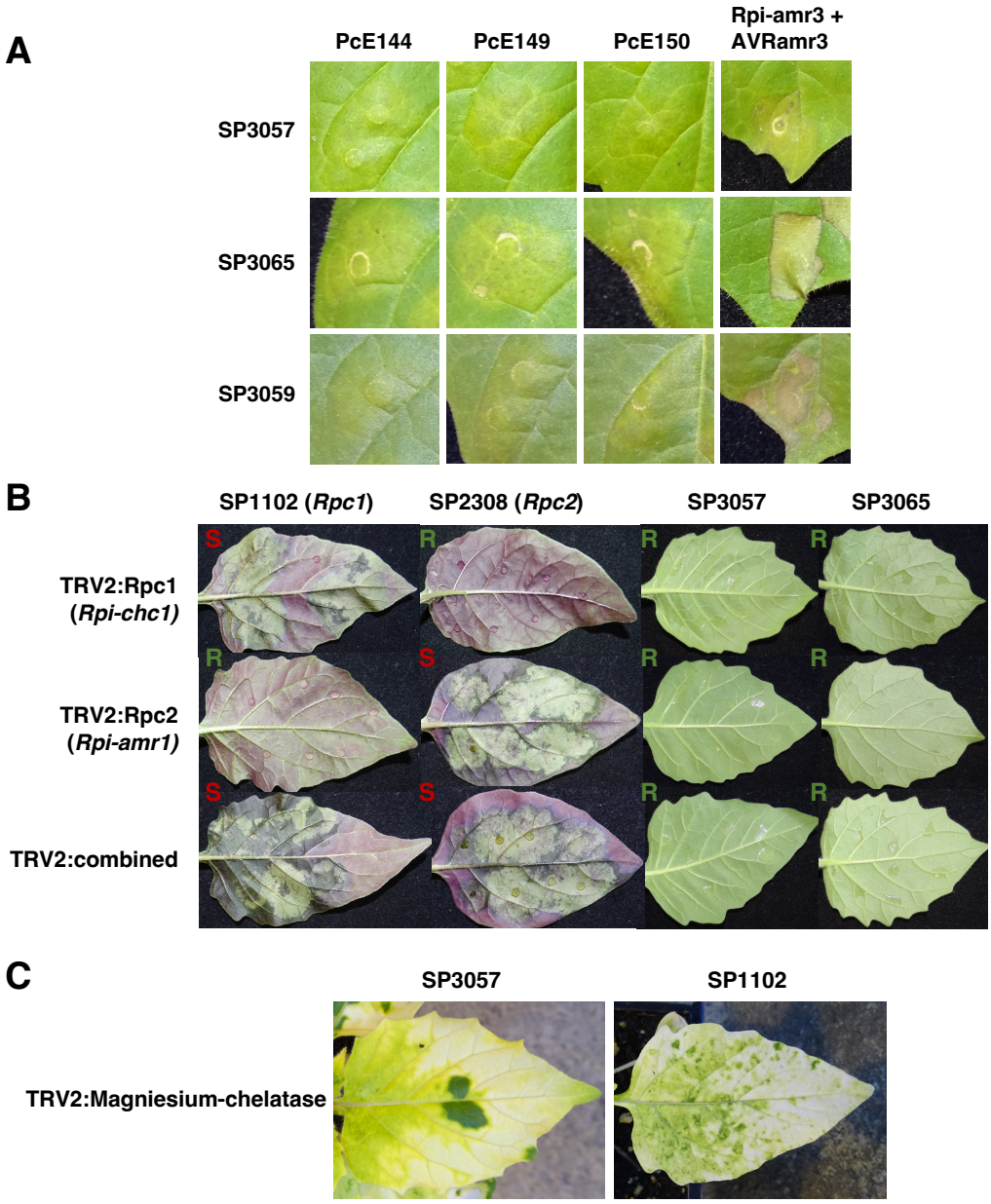

Figure 5.8. Resistance to *P. capsici* in *S. villosum* is not due to *Rpc2* or *Rpc1*. (A) *P. capsici* resistant *S. villosum* accessions do not respond to the elicitors of Rpc2. *Agrobacterium* suspensions were infiltrated at 0.3 OD_{600} and photographed at 5 dpi. Co-expression of Rpi-amr3 and AVRamr3 was used as a positive control for HR. **(B)** Resistance to *P. capsici* in *S. villosum* distinct from the *S. americanum Rpc* genes. VIGS was used to silence the *Rpc1* (*Rpi-chc1*) and *Rpc2* (*Rpi-amr1*) gene clusters. SP3057 and SP3065 both remain resistant after silencing of these clusters, both individually and combined. SP1102 (containing *Rpc1*) and SP2308 (containing *Rpc2*) were used as controls. Leaves were photographed 3 days post-inoculation with *P. capsici* zoospores (10 µl drops at a concentration of 10,000 spores ml^{-1}). **(C)** To confirm that *S. villosum* is amenable to gene silencing using the TRV system, silencing of the gene encoding magnesium-chelatase subunit ChIH was performed. Silencing with this construct produced clear tissue bleaching consistent with previously reported phenotypes. The performance of VIGS in *S. villosum* (SP3057 is shown) is comparable to *S. americanum* (SP1102 is shown).

5.2.9 – Resistance in *S. villosum* is not simply inherited and may be polygenic

The resistance in *S. villosum* accessions SP3057 and SP3065 is novel and previously uncharacterised. To investigate the nature of these resistances, biparental mapping populations were developed by crossing the resistant lines with the susceptible accession SP3059.

The F1 produced from crossing the resistant SP3057 to the susceptible SP3059 is highly resistant demonstrating that resistance is dominant (Fig. 5.9a, Fig. 5.9c). However, phenotyping of an F2 population revealed a segregation ratio inconsistent with patterns expected for a simple dominant and monogenic trait, in either a autotetraploid, allotetraploid or even diploid system. Of the 200 plants tested, 64 plants have strong resistance, while the remaining 116 plants showed complete susceptibility (Fig. 5.9a). The genetic basis of this resistance is unclear. The strong F1 resistance suggests that dosage is not a major factor in determining the phenotype, but the segregation suggests that multiple genes are required in combination to confer resistance.

Similarly, resistance from SP3065 is not conferred by a single dominant *R*-gene. F1 plants produced by crossing SP3065 (resistant) with SP3059 (susceptible) are completely susceptible (Fig. 5.9b, Fig. 5.9d). This phenotype suggested that resistance in SP3065 could be recessive or dosage-dependent. In an F2 population of 200 plants, 14 plants were found to be resistant, this is approximately a 1:15 ratio (resistant: susceptible). This suggests that the absence of 2 loci confers resistance if inheritance occurs in an allotetraploid manner (Fig. 5.9b).

P. capsici resistance in *S. villosum* appears to be polygenic and more complex than the resistance characterised in *S. americanum*. We cannot yet determine the nature of these resistances or the genes that control them. However, the resistance in SP3065 appears to be recessive. To confirm this model, backcrosses from the F1 to both parents should be performed. If two recessive resistance genes are present, then backcrossing to SP3065 should result in resistance in one-quarter of the progeny. In backcrosses to SP3059, susceptibility in all plants is expected.

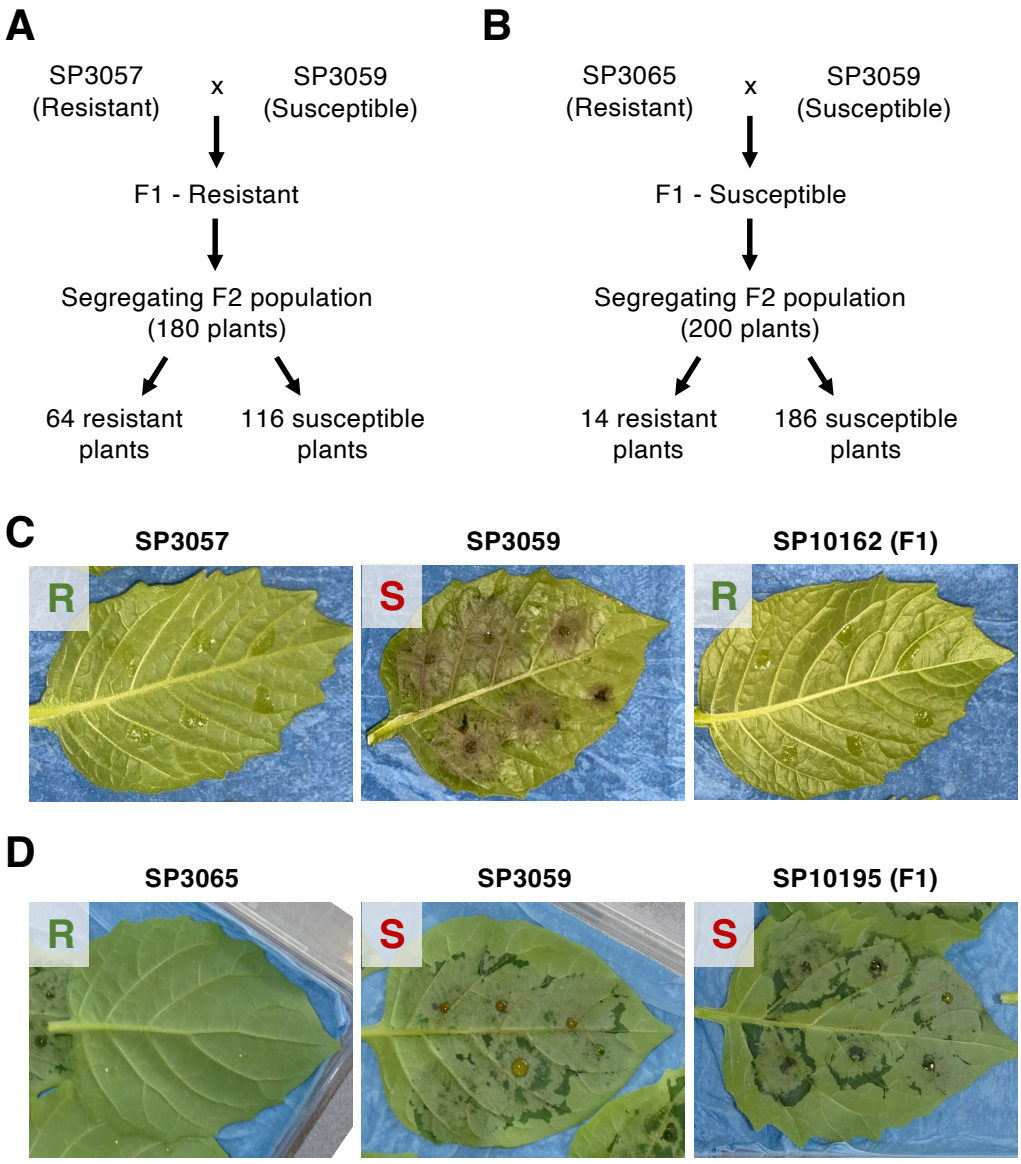

Figure 5.9. Inheritance of *P. capsici* resistance in *S. villosum* is complex and not monogenic. (A) Population structure used to characterise the resistance to *P. capsici* in the *S. villosum* accession SP3057. Resistance is dominant but does not segregate in a clear monogenic manner in an F2 population. **(B)** Crosses used to investigate the dominance and genes involved in the *P. capsici* resistance from SP3065. Progeny from the cross between SP3065 and SP3059 are susceptible suggesting that resistance is recessive or dosage-dependent. **(C)** The F1 (SP10162) produced from crossing SP3057 to SP3059 is highly resistant, the resistance in SP3057 is dominant. Leaves were inoculated with *P. capsici* zoospores (10,000 spores ml^{-1}) and photographed at 3 days post-inoculation. **(D)** The F1 (SP10195) produced by crossing SP3065 to SP3059 is susceptible, indicating a recessive or quantitative resistance.

5.3 – Discussion

5.3.1 – *Rpc1* confers novel resistance to *P. capsici* in *S. americanum*

In the previous chapter, the *Resistance to Phytophthora capsici (Rpc)* gene, *Rpc2,* was cloned from *S. americanum* accession SP2308. Here, resistance from another *S. americanum* accession was investigated. This resistance, named *Rpc1*, was mapped to a cluster of NLR-encoding genes on Chromosome 10 and was found to be an *Rpi-chc1* orthologue. However, no gene in this family confers resistance to *P. capsici* in an *N. benthamiana* transient assay.

In an alternative approach, the *P. capsici* effector library was screened and a candidate elicitor for Rpc1 was identified. This effector, PcE26, appears to co-segregate with resistance in an F2 population. Co-expression of this effector with Rpc1 candidates in *N. tabacum* did not result in HR. The reason for this is unclear. Although these NLRs may be non-functional in *N. benthamiana* and *N. tabacum*, it is unlikely as both Rpi-chc1 and R04373 are functional in *Nicotiana* species (Monino-Lopez et al., 2021, Lin et al., 2023). As the Rpi-chc1 family is not NRC-dependent, absence or incompatibility with *N. benthamiana* helper NLRs is also unlikely. It is possible that these *R*-genes cannot function individually, instead, one or more may be required in combination. Co-expression of multiple Rpc1 candidates with PcE26 could reveal a combination of genes required for recognition.

It is important to consider that the co-segregation of PcE26 recognition with *Rpc1* does not guarantee that this is the recognised effector. In the future, additional effectors will be cloned and tested in the *P. capsici* resistant *S. americanum* accessions in the same way as it was described in Chapter 4.

The characterisation of *Rpc1* highlights the similarities and differences between *S. americanum* resistance to *P. capsici*, and *P. infestans*. *Rpi-amr1*, *Rpi-amr3* and *Rpi-amr5*, which confer qualitative resistance to *P. infestans*, are widely distributed across the accessions. Resistance to *P. capsici* is much rarer and functional alleles of each gene are only found in individual accessions. *Rpc1* is an orthologue of *Rpi-chc1*, another *Phytophthora R*-gene which encodes a CC-NLR. So far, all investigated NLRs which recognise either *P. infestans* or *P. capsici*, are CC-NLRs.

5.3.2 – Additional *P. capsici* resistance exists in *Solanum villosum* and *Solanum nigrum*

Prior to the identification of *Rpc1* and *Rpc2*, there were no major characterised *R*-genes against *P. capsici*. This work demonstrates that NLR-mediated resistance against *P. capsici* can be effective, despite its rapid transition to necrotrophy. The resistance to *P. capsici* in two other species was briefly investigated. Resistant accessions of *S. nigrum and S. villosum* were identified, and resistance in *S. villosum* was pursued. The resistance to *P. capsici* in *S. villosum* is not due to either *Rpc1* or *Rpc2*. The novelty of this resistance was demonstrated through genomics, effector screening, and VIGS.

However, resistance in *S. villosum* accessions SP3057 and SP3065 appears to be less suitable for map-based cloning via a bulked segregant RenSeq approach, as the unknown nature of segregation in this species complicates mapping these resistances. While resistance in SP3057 is dominant, an unexpected segregation pattern was observed in an F2 population. Resistance may be dosage-dependent, or multiple genes may be required. Interestingly, resistance in accession SP3065 may be recessive. F1 plants, produced by crossing SP3065 to SP3059, are susceptible. While this has not yet been characterised through backcrossing, the molecular basis of a recessive resistance would be interesting to investigate further. If characterised this resistance could be utilised in agriculture through a gene-editing approach. Recessive resistance is often considered broader and more durable than dominant resistance. Many known recessive resistances involve the modification or removal of a host target required for infection (van Esse et al., 2020). The best-known example is the resistance conferred by loss-of-function allele of *mildew resistance locus o* (*mlo*). First characterised as providing resistance to powdery mildew in barley, *mlo*-based resistance has proven effective against powdery mildew pathogens in several *Cucurbitaceae*, *Brassicaceae* and *Solanaceae* species (Kusch and Panstruga, 2017). The recessive resistance in *S. villosum* could offer a similarly broad effect. Additionally, this resistance could be combined with characterised NLR-mediated resistance, such as *Rpc2*, to provide resistance with a multi-layered mode of action further enhancing durability.

5.3.3 – Prospects for deployment of *P. capsici* resistance from wild *Solanum* species

There is value in investigating the resistance in wild species. The transfer of multiple resistances into crop species could have great significance in agriculture. The approach of using cloned *R*-genes to elevate resistance to *P. infestans* in potato exemplifies the potential for deploying resistance to *P. capsici* (Jones et al., 2014, Ghislain et al., 2019).

A transgenic approach to develop *P. capsici* resistance in tomato, pepper or Cucurbits is limited by the availability of cloned *R*-genes. While nearly 50 *Rpi* genes have been cloned (Paluchowska et al., 2022), the only cloned *Rpc* gene is *Rpc2*. *P. infestans* remains a significant economic threat, with resistance-breaking strains evolving to evade many *Rpi* genes. Leveraging insights from non-host resistance in species like *Arabidopsis thaliana* (resistant to *Albugo candida*) and *Solanum americanum* (resistant to *P. infestans*), we can enhance durability by stacking multiple *Rpi* genes within the same genetic background. However, incorporating multiple *Rpi* genes into potato varieties is challenging, primarily due to the heterozygous, autotetraploid nature of potato genetics. Instead, the array of cloned *Rpi* genes provides the tools for developing durable resistance via a transgenic approach. Chapters 4 and 5 illustrate that resistance to *P. capsici* can be conferred by NLRs, and, though rare, variation for *P. capsici* resistance does exist. As additional *Rpc* genes are cloned, a similar strategy could be applied to enhance resistance in hosts of *P. capsici*. Nevertheless, as is often the case, a transgenic approach for elevating resistance is mostly limited by regulations rather than variation available to characterise.

Chapter 6: General discussion

6.1 – Summary of research progress

The goal of my thesis was to gain insight into the molecular and genetic basis of disease resistance in several *Solanum* species. I investigated resistance to three agriculturally important pathogens, and my findings advance the understanding of various aspects of plant-pathogen interactions, including resistance in the phloem, the basis of non-host resistance, and the interactions of sensor NLRs with their cognate effectors and helper NLRs.

In Chapter 3, I investigated resistance to potato leafroll virus (PLRV) in *Solanum tuberosum ssp. andigena* and cloned the resistance gene Rl_{adg}. Rl_{adg} encodes a TIR-NLR that recognises a serine protease which is essential for viral replication. The resistance conferred by this gene has the potential for broader use, for example, to elevate resistance to viral pathogens of sugar beet and oilseed rape. Rl_{adg} is the first NLR that has been found to confer resistance to a phloem-limited pathogen. This discovery demonstrates that NLR-mediated resistance can effectively control pathogens in the phloem.

The cloning of *Rpi-amr5* (Chapter 4), a paralogue of *Rpi-amr1*, builds upon previous work on the dissection of non-host resistance (NHR) against *Phytophthora infestans* in the wild species *Solanum americanum*. In line with previous findings, the recognition of RXLR effectors by CC-NLRs appears to be the main component of this NHR, though other potential sources cannot be discounted. Interestingly, a variant of *Rpi-amr5* was found to confer strong resistance to *Phytophthora capsici*. This gene, named *Rpc2*, is the first cloned *R*-gene against *P. capsici*. This discovery highlights that while host and non-host resistance are often described as being distinct, the mechanism behind these resistances can directly overlap. Two *P. infestans* effectors, and three *P. capsici* effectors are recognised by both NLRs. It is currently unclear why *Rpi-amr5* does not confer resistance to *P. capsici*.

In Chapter 5, resistance to *P. capsici* in several other *Solanum* accessions was investigated. *Rpc1*, from *S. americanum,* was mapped. Although not yet cloned, it was demonstrated that *Rpc1* is an orthologue of the late blight resistance gene *Rpi-chc1*. Using effectoromics, a candidate elicitor from *P. capsici* was identified.

In addition to the two *P. capsici*-resistant *S. americanum* accessions, resistance in two additional *Solanum* species was identified. Using cell death assays and VIGS, the resistance of two *Solanum villosum* accessions was shown to be distinct from *Rpc1* and *Rpc2*. The data presented in this thesis demonstrate that there are at least four *R*-genes against *P. capsici*. While only one has been cloned, there is potential for identifying additional *Rpc* genes and making *Rpc*-gene stacks to reduce the impact of *P. capsici*.

6.2 – What is the basis of non-host resistance to *P. infestans* in *S. americanum*?

While many *R*-genes have been identified and utilised in agriculture, pathogen races can evolve to overcome them by changing their effector repertoire. Research aimed at understanding the durability of some resistances has led to the conceptualisation of non-host resistance (NHR). NHR is defined as the ability of all accessions of a species to resist all isolates of a pathogen (Schulze-Lefert and Panstruga, 2011, Panstruga and Moscou, 2020). NHR can be studied through several approaches. Cevik et al. (2019) and Borhan et al. (2008) investigated the NHR of *A. thaliana* to *A. candida* using transgressive segregation to separate and clone individual *R*-genes. Laflamme et al. (2020) investigated NHR of *Arabidopsis* to non-host-adapted *Pseudomonas syringae* strains using a library of effectors transformed into the virulent *P. syringae pv. tomato* DC3000 strain.

In the NHR of *S. americanum* to *P. infestans*, all accessions are resistant in field conditions. To observe susceptibility, concentrated inoculum and conditions optimised for infection must be used. Additionally, an effectoromics approach was employed to screen for variation in the recognition of 315 RXLR effectors in all available accessions. Through these approaches, the major NLR components of this NHR have been identified: *Rpi-amr1*, *Rpi-amr3*, *Rpi-amr4,* and *Rpi-amr5* (Witek et al., 2016, Witek et al., 2021, Lin et al., 2023). All *S. americanum* accessions recognise numerous additional *P. infestans* effectors. Two of these 'recognition genes' have been identified, however, while they respond to transient overexpression of *P. infestans* effectors, they do not confer an observable resistance phenotype in detached leaf assays (Lin et al., 2023). As previously discussed in this thesis, the detached leaf assay is ideal for characterising qualitative resistance. These genes, and other recognition genes in *S. americanum*, may confer a quantitative increase in resistance to *P. infestans* that is not detectable in this assay. Nevertheless, these genes may still prove useful: when transferred together, they could have a cumulative effect. Although they may not produce a qualitative phenotype alone, these genes could support others, such as *Rpi-amr1* and *Rpi-amr3,* enhancing durability of these *Rpi* genes.

All cloned *Rpi* genes from *S. americanum* encode CC-NLRs, and Rpi-amr1, Rpi-amr3, Rpi-amr4 and Rpi-amr5 all belong to the NRC-dependent clade of NLRs. One current model for NHR in *S. americanum* is that multiple *Rpi* genes which encode NLRs are present in different combinations in each accession, and this results in durable resistance. This model is consistent with NHR of *A. thaliana* to *A. candida*, and NHR of barley and *Brachypodium distachyon* to wheat stripe rust (*Puccinia striiformis f.sp. tritici*) (Cevik et al., 2019, Dawson et al., 2016, Li et al., 2016, Gilbert et al., 2018). The nature of the recognised molecule is also likely to contribute to the durability of resistance. The *P. infestans* effectors recognised by Rpi-amr1, Rpi-amr3 and Rpi-amr5 are all found in multiple *Phytophthora* species. While the virulence function has not been characterised for all these proteins, their conservation across different species could suggest an important role during infection. This is also supported by the expansion of the PITG_16275 homologues in *P. megakarya* and *P. palmivora*, as these species contain 28 and 21 PITG_16275 homologues respectively.

The identification of *Rpc2* as an allele of *Rpi-amr5* also demonstrates that despite the proposed distinction between host and non-host resistance, the molecular basis of these resistances directly overlaps. It is likely that the only difference is the context of these resistances. In these instances, NHR is a polygenic species-wide phenomenon, whereas host resistance is accession-specific and monogenic.

6.3 – What are the next steps in dissecting *S. americanum* NHR?

While seven NLR-encoding *Rpi* genes have been cloned from *S. americanum*, there are other novel resistances present. Using CRISPR and backcrossing, additional resistance from three accessions has been identified. These resistances are dominant but do not segregate in a monogenic manner. Thus, similar to the field resistance of *S. americanum*, they may be associated with the cumulative effect of multiple loci. These loci could still confer recognition of RXLR effectors via NLR proteins. Twenty-five RXLR effectors are recognised by the laboratory susceptible accession SP2271, but only two of them have a corresponding *R*-gene cloned. To test whether the remaining recognitions contribute to field resistance, the responsible receptors could be sequentially identified and mutated. However, this approach would require the laborious development and phenotyping of populations for each recognition. Also, as three effector recognitions are non-variable between accessions, it is impossible to generate mapping populations for these recognitions. As an alternative approach, CRISPR could be utilised to remove recognitions concurrently. The coordinated

mutation of genes encoding the NRCs could be used to remove recognitions facilitated by NRC-dependent NLRs. Similarly, mutation of *EDS1* could reveal the role of any TIR-NLRs in mediating these recognitions.

Given the recent discovery that intracellular immunity functions through the potentiation of cell-surface immunity (Ngou et al., 2021, Yuan et al., 2021), it is striking that no LRR-RLPs, or LRR-RLKs have been found to confer resistance to *P. infestans* in *S. americanum*. The LRR-RLK PERU and the LRR-RLP ELR have been implicated in quantitative resistance to *P. infestans* in potato. These cell-surface receptors recognise Pep-13 and INF1 respectively (Torres Ascurra et al., 2023, Du et al., 2015a). While *S. americanum* does not contain *PERU* or *ELR* orthologues, other PRRs may contribute to the remaining uncharacterised resistance. Given the model of mutual potentiation between ETI and PTI, it seems unlikely that *S. americanum* lacks any cell surface immune receptors capable of recognising *P. infestans*. The absence of identified receptors may be due to a focus on mapping the strongest resistances, potentially creating a bias toward *R*-genes encoding NLR immune receptors. An alternative approach may help to clarify the role of PRRs in NHR of *S. americanum* to *P. infestans*. CRISPR-guided knock-out of cell-surface co-receptors including the SOMATIC EMBRYOGENESIS RECEPTOR-LIKE KINASES (SERKs) and SUPPRESSOR OF BIR1-1 (SOBIR1) could be used to investigate this possibility. SERKs, which include BAK1 (BRI1-ASSOCIATED RECEPTOR KINASE 1), are co-receptors with which PRRs heterodimerize to initiate the downstream signalling (Heese et al., 2007). SOBIR1 is an LRR-RLK which is required by LRR-RLPs, which lack a kinase domain, to activate the downstream signalling (Liebrand et al., 2013, Gust and Felix, 2014). By knocking out BAK1 and SOBIR1 in an *S. americanum* accession lacking any major *Rpi* genes, the role of LRR-RLPs and LRR-RLKs in field resistance to *P. infestans* could be determined.

However, there are two limitations to this approach. Firstly, resistance may not be controlled by TIR-NLRs, NRC-dependent CC-NLRs, or PRRs. Instead, resistance may be due to NRC-independent NLRs like Rpi-chc1 or Rpi-vnt1. Secondly, resistance could be partially non-receptor-mediated. For example, effectors that promote virulence on one species may interact less well with the orthologous host target in another species (McLellan et al., 2022).

6.4 – Characterising the interactions between sensor and helper NLRs

Since the identification of the NRC class of helper NLRs, our understanding of their role in plant immunity has rapidly advanced. Unlike RPW8-NLRs and RLK co-receptors, the NRCs often have partial genetic redundancy: many sensor NLRs can function through several NRCs. This has been described as an 'NLR network' (Wu et al., 2016, Wu et al., 2017). Recent structural analysis of NRCs has revealed a model in which NRCs exist in a homodimer as their resting state. It was predicted that the activated sensor disrupts this, causing the release of primed monomers, which then oligomerise into a resistosome structure. In the case of NRC4, an activated hexameric resistosome has been characterised (Liu et al., 2023, Muniyandi et al., 2023).

While these studies have characterised the resting state and the activated resistosome structures of NRCs, the 'missing link' in the characterisation of the NRC signalling is the signal transduction between the sensor and the helper. While the exact interaction interface has not been identified, it has been demonstrated that the NB-domain of sensors is the minimal unit required to activate helper NLRs (Contreras et al., 2023b, Rairdan et al., 2008). Huang et al. (2023) observed that divergence between the tomato and *N. benthamiana* NRC3 proteins within the NB-ARC and LRR domains resulted in a loss of compatibility of the *N. benthamiana* NRC3 with the sensor Rpi-blb2. Together, these data suggest that upon effector detection, sensor NLRs undergo a conformational change which exposes the NB-domain, which interacts with the helper NRC. Possibly, NRC's NB-ARC and LRR domains are involved in this interaction. Here, the *S. americanum* sensor NLR Rpi-amr5 was found to be constitutively active when co-expressed with the *N. benthamiana* NRC2, but not with the *S. americanum* orthologue. Polymorphisms within the LRR domains of these two NRC2 proteins are responsible for this phenotype. These data suggest that there is some interaction between the sensor and helper NLRs prior to the detection of the effector.

The constitutive activity of Rpi-amr5 in *N. benthamiana* also highlights a novel aspect of restricted taxonomic functionality (RTF). RTF is the absence of NLR function outside of certain species, or taxonomic groups (Tai et al., 1999). For NRC-dependent CC-NLRs, it has been proposed that co-transfer with a helper NLR could overcome RTF (Ahn et al., 2023). As helpers and sensors have co-evolved together, alleles from different species may be diverged and incompatible. While the outcome of the RTF phenomenon can be a complete absence of activity, it can also manifest in an aberrant ectopic activation of the immune response.

6.5 – Approaches to overcome a lack of natural host resistance to pathogens

An issue which is often discussed in plant breeding is a lack of natural diversity for resistance in host species. For many pathogens, there are no reported *R*-genes. To overcome this, several approaches can be taken. The simplest strategy to overcome a lack of host resistance is to search for diversity in other species. One success is the identification and transfer of late blight resistance genes from wild potato relatives into *S. tuberosum*, such as *Rpi-chc1* from *Solanum chacoense* and *Rpi-vnt1* from *Solanum venturii* (Monino-Lopez et al., 2021, Foster et al., 2009, Jones et al., 2014).

By identifying the elicitors of these *R*-proteins, we can understand the breadth of their recognition and discover resistance to additional pathogens. For instance, the PVY and PLRV resistance genes Ry_{sto} and Rl_{adg} also confer recognition of the *Brassica* viruses TuMV and TuYV. It is unlikely that these *R*-genes are necessary for resistance to TuMV and TuYV in *S. stoloniferum* or *S. tuberosum*, as these viruses and plant species have not co-evolved. Instead, resistance to these non-adapted pathogens is a consequence of homology between pathogen proteins. Although this approach has not been attempted, it would be possible to actively search for resistance in a host species of a related pathogen, where recognition may be a consequence of co-evolution with related pathogens.

Furthermore, characterised receptor-effector pairs could be utilised as a scaffold to develop novel recognition. This approach, described by Zdrzałek et al. (2023) as the 'resurfacing' of LRR domains, involves the specific modification of the LRRs to alter the effector binding capacity. This was demonstrated by Tamborski et al. (2022), who modified the recognition capacity of the wheat NLR Sr50. Wild-type Sr50 confers resistance to wheat stem rust through recognition of the effector AvrSr50. Modification of the Sr50 LRRs was used to establish recognition of the AvrSr50-related effector AvrSr35. Advances in structural modelling mean that the changes required to create or enhance recognitions can be predicted without prior structural studies. By discovering new NLR and effector pairs and characterising their interaction, the repertoire of available scaffolds expands. Rl_{adg} directly recognises the serine proteases from poleroviruses, but not enamovirus proteases that share a similar predicted structure. Structure-guided modification of Rl_{adg} could expand recognition to enamoviruses as well. Similarly, the modification of this NLR could allow tailoring alleles for maximisation of affinity with each recognised polerovirus protease.

An ambitious alternative to exploring natural diversity is to generate novel recognitions via a completely synthetic approach. This was recently exemplified by Kourelis et al. (2023) who utilised an immune receptor-nanobody fusion system to develop a novel immune receptor. To achieve this, the Pik-1/Pik-2 NLR pair from rice was used. Pik-1 contains an HMA integrated domain which detects the *M. oryzae* effector AVR-Pik. To design a Pik-1 NLR capable of recognising GFP, the HMA domain was exchanged for a camelid-derived GFP nanobody. This 'Pikobody' NLR can trigger an immune response in *N. benthamiana* when challenged with a GFP-expressing clone of potato virus X. This approach utilised knowledge of the molecular basis of plant immunity, and the paired NLR-ID system, to develop a novel approach to generate an immune response. In theory, Pikobodies which recognise any protein could be produced, provided that a nanobody can be generated. It is important to consider that while this method enabled the generation of a novel recognition, the performance of resistance is dependent on the same factors as unmodified NLRs. Effectors must be translocated into the plant cell in a high enough dosage for the detection, and the delivery must happen at the infection stage where recognition of those effectors would result in resistance. Additionally, Pikobodies will still be vulnerable to suppression by pathogens. To ensure durability, alternative 'chassis' should be used to prevent the simultaneous suppression of the Pik-1-derived NLRs. The limitation of this approach will be in public acceptance and regulations, as it can only be achieved using transgenics and relies on the use of a protein derived from an animal system.

6.6 – Modification of host proteins and immune receptors can prevent susceptibility

Pathogen effectors manipulate the host to promote infection. Understanding the molecular basis of this process will enable engineering for resistance. McLellan et al. (2022) demonstrate that the diversification of host targets between host and non-host species can result in a loss of vulnerability to pathogen effectors. Expression of the *A. thaliana* protein PUB33 in *N. benthamiana* and potato reduces the rate of infection by *P. infestans*. Specific modification of the potato PUB33 orthologue could reproduce a similar phenotype. Through a similar approach, understanding how pathogens suppress immune receptors and downstream signalling will enable the engineering of resistance. *Phytophthora* effectors suppress both NRC helper NLRs and individual sensor NLRs (Derevnina et al., 2021, Yin et al., 2017).

Allele-specific suppression could explain the absence of *P. capsici* resistance conferred by Rpi-amr5. While both variants recognise three *P. capsici* effectors, Rpi-amr5 does not confer *P. capsici* resistance, whereas Rpc2 does. *P. capsici* may be capable of suppressing Rpi-amr5, but not Rpc2. In this instance, the resistant allele exists and is available to use. If this

phenomenon is widespread, other suppressed recognitions could be engineered to produce resistance. For example, Rpi-amr1 can recognise the *P. capsici* orthologue of AVRamr1, but no *Rpi-amr1* allele has been shown to confer resistance to *P. capsici*. If this is due to the action of a suppressor, a *P. capsici*-resistant allele could be engineered.

Conversely, evasion of immune suppression may result in a quantitative effect rather than a qualitative one. There are several examples of immune suppressors that appear to have a minimal effect on resistance. The NLRs R3a and Rpi-blb2 confer resistance to *P. infestans* despite cell death suppression by the effectors PITG_09160 and PITG_15278 (Derevnina et al., 2021, Yin et al., 2017). Similarly, the *N. benthamiana* helper NLRs NRC2 and NRC3 are suppressed by the *P. infestans* effector AVRcap1b (Derevnina et al., 2021). Despite this, the NRC2/NRC3-dependent Rpi-amr1, still confers resistance in *N. benthamiana* (Witek et al., 2021).

6.7 – Summary and outlook

The project aimed to develop an understanding of the genetic and molecular basis of resistance in several *Solanum* species. Through the characterisation of this resistance, three novel *R*-genes have been cloned.

Rl_{adg} encodes a TIR-NLR that recognises serine proteases from the phloem-limited poleroviruses. Many of these viruses will become increasingly prevalent as the warming climate extends the range of aphid vectors. The recognition spectrum of this NLR could be expanded further and enable the recognition of other structurally similar serine proteases found in related viruses.

Throughout this project, our understanding of the basis of non-host resistance to *P. infestans* in *S. americanum* has improved. So far, all cloned components of this NHR encode CC-NLRs that recognise RXLR effectors. *Rpi-amr1*, *Rpi-amr3* and *Rpi-amr5* also confer recognition of multiple *Phytophthora* species which may indicate that the elicitors are conserved and contribute to virulence. NHR to *P. infestans* was also found to directly overlap with host resistance to *P. capsici*. *Rpc2*, an allele of *Rpi-amr5*, confers strong accession-specific resistance to *P. capsici*. These data also provide the foundation for further studies including characterisation of the interaction between sensor and helper NLRs, the basis of multiple effector recognition, and the mechanism of immune suppression by *P. capsici*.

Bibliography

ADACHI, H., CONTRERAS, M. P., HARANT, A., WU, C. H., DEREVNINA, L., SAKAI, T., DUGGAN, C., MORATTO, E., BOZKURT, T. O., MAQBOOL, A., WIN, J. & KAMOUN, S. 2019. An N-terminal motif in NLR immune receptors is functionally conserved across distantly related plant species. *Elife,* 8.

AGUILERA-GALVEZ, C., CHAMPOURET, N., RIETMAN, H., LIN, X., WOUTERS, D., CHU, Z., JONES, J. D. G., VOSSEN, J. H., VISSER, R. G. F., WOLTERS, P. J. & VLEESHOUWERS, V. 2018. Two different R gene loci co-evolved with Avr2 of Phytophthora infestans and confer distinct resistance specificities in potato. *Stud Mycol,* 89**,** 105-115.

AHN, H.-K., LIN, X., OLAVE-ACHURY, A. C., DEREVNINA, L., CONTRERAS, M. P., KOURELIS, J., WU, C.-H., KAMOUN, S. & JONES, J. D. G. 2023. Effector-dependent activation and oligomerization of plant NRC class helper NLRs by sensor NLR immune receptors Rpi-amr3 and Rpi-amr1. *The EMBO Journal,* 42**,** e111484.

ANDIKA, I. B., WEI, S., CAO, C., SALAIPETH, L., KONDO, H. & SUN, L. 2017. Phytopathogenic fungus hosts a plant virus: A naturally occurring cross-kingdom viral infection. *Proceedings of the National Academy of Sciences,* 114**,** 12267-12272.

ANDOLFO, G., JUPE, F., WITEK, K., ETHERINGTON, G. J., ERCOLANO, M. R. & JONES, J. D. G. 2014. Defining the full tomato NB-LRR resistance gene repertoire using genomic and cDNA RenSeq. *Bmc Plant Biology,* 14.

ANDRET-LINK, P., SCHMITT-KEICHINGER, C., DEMANGEAT, G., KOMAR, V. & FUCHS, M. 2004. The specific transmission of Grapevine fanleaf virus by its nematode vector Xiphinema index is solely determined by the viral coat protein. *Virology,* 320**,** 12-22.

AXTELL, M. J. & STASKAWICZ, B. J. 2003. Initiation of RPS2-Specified Disease Resistance in Arabidopsis Is Coupled to the AvrRpt2-Directed Elimination of RIN4. *Cell,* 112**,** 369-377.

BAGGS, E., DAGDAS, G. & KRASILEVA, K. V. 2017. NLR diversity, helpers and integrated domains: making sense of the NLR IDentity. *Current Opinion in Plant Biology,* 38**,** 59-67.

BAGGS, E., MONROE, J. G., THANKI, A. S., O'GRADY, R., SCHUDOMA, C., HAERTY, W. & KRASILEVA, K. V. 2020. Convergent Loss of an EDS1/PAD4 Signaling Pathway in Several Plant Lineages Reveals Co-evolved Components of Plant Immunity and Drought Response. *The Plant Cell***,** tpc.00903.2019.

BAILEY, K., ÇEVIK, V., HOLTON, N., BYRNE-RICHARDSON, J., SOHN, K. H., COATES, M., WOODS-TÖR, A., AKSOY, H. M., HUGHES, L., BAXTER, L., JONES, J. D. G., BEYNON, J., HOLUB, E. B. & TÖR, M. 2011. Molecular Cloning of ATR5Emoy2 from Hyaloperonospora arabidopsidis, an Avirulence Determinant That Triggers RPP5-Mediated Defense in Arabidopsis. *Molecular Plant-Microbe Interactions®,* 24**,** 827-838.

BAKKER, E. G., TOOMAJIAN, C., KREITMAN, M. & BERGELSON, J. 2006. A Genome-Wide Survey of R Gene Polymorphisms in Arabidopsis. *The Plant Cell,* 18**,** 1803-1818.

BARCHENGER, D. W., LAMOUR, K. H. & BOSLAND, P. W. 2018. Challenges and Strategies for Breeding Resistance in Capsicum annuum to the Multifarious Pathogen, Phytophthora capsici. *Front Plant Sci,* 9**,** 628.
BARKER, H. 1987. Invasion of Non-phloem Tissue in Nicotiana clevelandii by Potato Leafroll Luteovirus Is Enhanced in Plants also Infected with Potato Y Potyvirus. *Journal of General Virology,* 68**,** 1223-1227.
BASS, C. & FIELD, L. M. 2018. Neonicotinoids. *Curr Biol,* 28**,** R772-r773.
BEAKES, G. W., GLOCKLING, S. L. & SEKIMOTO, S. 2012. The evolutionary phylogeny of the oomycete "fungi". *Protoplasma,* 249**,** 3-19.
BEBBER, D. P., RAMOTOWSKI, M. A. T. & GURR, S. J. 2013. Crop pests and pathogens move polewards in a warming world. *Nature Climate Change,* 3**,** 985-988.
BETTGENHAEUSER, J., GARDINER, M., SPANNER, R., GREEN, P., HERNANDEZ-PINZON, I., HUBBARD, A., AYLIFFE, M. & MOSCOU, M. J. 2018. The genetic architecture of colonization resistance in Brachypodium distachyon to non-adapted stripe rust (Puccinia striiformis) isolates. *PLoS Genet,* 14**,** e1007637.
BETTGENHAEUSER, J., GILBERT, B., AYLIFFE, M. & MOSCOU, M. J. 2014. Nonhost resistance to rust pathogens - a continuation of continua. *Front Plant Sci,* 5**,** 664.
BHULLAR, N. K., ZHANG, Z., WICKER, T. & KELLER, B. 2010. Wheat gene bank accessions as a source of new alleles of the powdery mildew resistance gene Pm3: a large scale allele mining project. *BMC Plant Biology,* 10**,** 88.
BI, G., SU, M., LI, N., LIANG, Y., DANG, S., XU, J., HU, M., WANG, J., ZOU, M., DENG, Y., LI, Q., HUANG, S., LI, J., CHAI, J., HE, K., CHEN, Y.-H. & ZHOU, J.-M. 2021. The ZAR1 resistosome is a calcium-permeable channel triggering plant immune signaling. *Cell,* 184**,** 3528-3541.e12.
BI, Y., HU, J., CUI, X., SHAO, J., LU, X., MENG, Q. & LIU, X. 2014. Sexual reproduction increases the possibility that Phytophthora capsici will develop resistance to dimethomorph in China. *Plant Pathology,* 63**,** 1365-1373.
BIAŁAS, A., LANGNER, T., HARANT, A., CONTRERAS, M. P., STEVENSON, C. E., LAWSON, D. M., SKLENAR, J., KELLNER, R., MOSCOU, M. J., TERAUCHI, R., BANFIELD, M. J. & KAMOUN, S. 2021. Two NLR immune receptors acquired high-affinity binding to a fungal effector through convergent evolution of their integrated domain. *Elife,* 10.
BITTNER-EDDY, P. D., CRUTE, I. R., HOLUB, E. B. & BEYNON, J. L. 2000. RPP13 is a simple locus in Arabidopsis thaliana for alleles that specify downy mildew resistance to different avirulence determinants in Peronospora parasitica. *Plant J,* 21**,** 177-88.
BJORNSON, M., KAJALA, K., ZIPFEL, C. & DING, P. 2020. Low-cost and High-throughput RNA-seq Library Preparation for Illumina Sequencing from Plant Tissue. *Bio-protocol,* 10**,** e3799.
BONARDI, V., TANG, S., STALLMANN, A., ROBERTS, M., CHERKIS, K. & DANGL, J. L. 2011. Expanded functions for a family of plant intracellular immune receptors beyond specific recognition of pathogen effectors. *Proc Natl Acad Sci U S A,* 108**,** 16463-8.
BORHAN, M. H., GUNN, N., COOPER, A., GULDEN, S., TÖR, M., RIMMER, S. R. & HOLUB, E. B. 2008. WRR4 Encodes a TIR-NB-LRR Protein That Confers Broad-

Spectrum White Rust Resistance in Arabidopsis thaliana to Four Physiological Races of Albugo candida. *Molecular Plant-Microbe Interactions®,* 21**,** 757-768.

BOURRAS, S., KUNZ, L., XUE, M., PRAZ, C. R., MÜLLER, M. C., KÄLIN, C., SCHLÄFLI, M., ACKERMANN, P., FLÜCKIGER, S., PARLANGE, F., MENARDO, F., SCHAEFER, L. K., BEN-DAVID, R., ROFFLER, S., OBERHAENSLI, S., WIDRIG, V., LINDNER, S., ISAKSSON, J., WICKER, T., YU, D. & KELLER, B. 2019. The AvrPm3-Pm3 effector-NLR interactions control both race-specific resistance and host-specificity of cereal mildews on wheat. *Nature Communications,* 10**,** 2292.

BOURRAS, S., MCNALLY, K. E., BEN-DAVID, R., PARLANGE, F., ROFFLER, S., PRAZ, C. R., OBERHAENSLI, S., MENARDO, F., STIRNWEIS, D., FRENKEL, Z., SCHAEFER, L. K., FLÜCKIGER, S., TREIER, G., HERREN, G., KOROL, A. B., WICKER, T. & KELLER, B. 2015. Multiple Avirulence Loci and Allele-Specific Effector Recognition Control the Pm3 Race-Specific Resistance of Wheat to Powdery Mildew. *The Plant Cell,* 27**,** 2991-3012.

BRABHAM, H. J., GÓMEZ DE LA CRUZ, D., WERE, V., SHIMIZU, M., SAITOH, H., HERNÁNDEZ-PINZÓN, I., GREEN, P., LORANG, J., FUJISAKI, K., SATO, K., MOLNÁR, I., ŠIMKOVÁ, H., DOLEŽEL, J., RUSSELL, J., TAYLOR, J., SMOKER, M., GUPTA, Y. K., WOLPERT, T., TALBOT, N. J., TERAUCHI, R. & MOSCOU, M. J. 2023. Barley MLA3 recognizes the host-specificity effector Pwl2 from Magnaporthe oryzae. *The Plant Cell*.

BRASIER, C., SCANU, B., COOKE, D. & JUNG, T. 2022. Phytophthora: an ancient, historic, biologically and structurally cohesive and evolutionarily successful generic concept in need of preservation. *IMA Fungus,* 13**,** 12.

BRASIER, C. M. 2001. Rapid Evolution of Introduced Plant Pathogens via Interspecific Hybridization: Hybridization is leading to rapid evolution of Dutch elm disease and other fungal plant pathogens. *BioScience,* 51**,** 123-133.

BRASIER, C. M. 2008. The biosecurity threat to the UK and global environment from international trade in plants. *Plant Pathology,* 57**,** 792-808.

BROWN, J. K. M. & TELLIER, A. 2011. Plant-Parasite Coevolution: Bridging the Gap between Genetics and Ecology. *Annual Review of Phytopathology,* 49**,** 345-367.

BURCH-SMITH, T. M., SCHIFF, M., CAPLAN, J. L., TSAO, J., CZYMMEK, K. & DINESH-KUMAR, S. P. 2007. A Novel Role for the TIR Domain in Association with Pathogen-Derived Elicitors. *PLOS Biology,* 5**,** e68.

CAO, Y., KÜMMEL, F., LOGEMANN, E., GEBAUER, J. M., LAWSON, A. W., YU, D., UTHOFF, M., KELLER, B., JIRSCHITZKA, J., BAUMANN, U., TSUDA, K., CHAI, J. & SCHULZE-LEFERT, P. 2023. Structural polymorphisms within a common powdery mildew effector scaffold as a driver of coevolution with cereal immune receptors. *Proceedings of the National Academy of Sciences,* 120**,** e2307604120.

CARNEIRO, O. L. G., RIBEIRO, S., MOREIRA, C. M., GUEDES, M. L., LYRA, D. H. & PINTO, C. 2017. Introgression of the Rl(adg) allele of resistance to potato leafroll virus in Solanum tuberosum L. *Crop Breeding and Applied Biotechnology,* 17**,** 242-249.

CASTEL, B., NGOU, P.-M., CEVIK, V., REDKAR, A., KIM, D.-S., YANG, Y., DING, P. & JONES, J. D. G. 2019. Diverse NLR immune receptors activate defence via the RPW8-NLR NRG1. *New Phytologist,* 222**,** 966-980.

CESARI, S., BERNOUX, M., MONCUQUET, P., KROJ, T. & DODDS, P. 2014. A novel conserved mechanism for plant NLR protein pairs: the 'integrated decoy' hypothesis. *Frontiers in Plant Science,* 5.

CESARI, S., THILLIEZ, G., RIBOT, C., CHALVON, V., MICHEL, C., JAUNEAU, A., RIVAS, S., ALAUX, L., KANZAKI, H., OKUYAMA, Y., MOREL, J.-B., FOURNIER, E., THARREAU, D., TERAUCHI, R. & KROJ, T. 2013. The Rice Resistance Protein Pair RGA4/RGA5 Recognizes the Magnaporthe oryzae Effectors AVR-Pia and AVR1-CO39 by Direct Binding *The Plant Cell,* 25**,** 1463-1481.

CEVIK, V., BOUTROT, F., APEL, W., ROBERT-SEILANIANTZ, A., FURZER, O. J., REDKAR, A., CASTEL, B., KOVER, P. X., PRINCE, D. C., HOLUB, E. B. & JONES, J. D. G. 2019. Transgressive segregation reveals mechanisms of Arabidopsis immunity to Brassica-infecting races of white rust Albugo candida. *Proceedings of the National Academy of Sciences,* 116**,** 2767.

CHEN, J., UPADHYAYA, N. M., ORTIZ, D., SPERSCHNEIDER, J., LI, F., BOUTON, C., BREEN, S., DONG, C., XU, B., ZHANG, X., MAGO, R., NEWELL, K., XIA, X., BERNOUX, M., TAYLOR, J. M., STEFFENSON, B., JIN, Y., ZHANG, P., KANYUKA, K., FIGUEROA, M., ELLIS, J. G., PARK, R. F. & DODDS, P. N. 2017. Loss of AvrSr50 by somatic exchange in stem rust leads to virulence for Sr50 resistance in wheat. *Science,* 358**,** 1607-1610.

CHEN, Y., LIU, Z. & HALTERMAN, D. A. 2012. Molecular Determinants of Resistance Activation and Suppression by Phytophthora infestans Effector IPI-O. *PLOS Pathogens,* 8**,** e1002595.

CHEN, Z., LIU, F., ZENG, M., WANG, L., LIU, H., SUN, Y., WANG, L., ZHANG, Z., CHEN, Z., XU, Y., ZHANG, M., XIA, Y., YE, W., DONG, S., GOVERS, F., WANG, Y. & WANG, Y. 2023. Convergent evolution of immune receptors underpins distinct elicitin recognition in closely related Solanaceous plants. *The Plant Cell,* 35**,** 1186-1201.

CLEMENTE, T. 2006. Nicotiana (Nicotiana tobaccum, Nicotiana benthamiana). *In:* WANG, K. (ed.) *Agrobacterium Protocols.* Totowa, NJ: Humana Press.

COLLIER, S. M., HAMEL, L.-P. & MOFFETT, P. 2011. Cell Death Mediated by the N-Terminal Domains of a Unique and Highly Conserved Class of NB-LRR Protein. *Molecular Plant-Microbe Interactions®,* 24**,** 918-931.

COLON, I. T., EIJLANDER, R., BUDDING, D. J., VAN IJZENDOORN, M. T., PIETERS, M. M. J. & HOOGENDOORN, J. 1992. Resistance to potato late blight (Phytophthora infestans (Mont.) de Bary) in Solanum nigrum, S. villosum and their sexual hybrids with S. tuberosum and S. demissum. *Euphytica,* 66**,** 55-64.

CONTRERAS, M. P., PAI, H., SELVARAJ, M., TOGHANI, A., LAWSON, D. M., TUMTAS, Y., DUGGAN, C., YUEN, E. L. H., STEVENSON, C. E. M., HARANT, A., MAQBOOL, A., WU, C. H., BOZKURT, T. O., KAMOUN, S. & DEREVNINA, L. 2023a. Resurrection of plant disease resistance proteins via helper NLR bioengineering. *Sci Adv,* 9**,** eadg3861.

CONTRERAS, M. P., PAI, H., THOMPSON, R., CLAEYS, J., ADACHI, H. & KAMOUN, S. 2023b. The nucleotide binding domain of NRC-dependent disease resistance

proteins is sufficient to activate downstream helper NLR oligomerization and immune signaling. *bioRxiv*, 2023.11.30.569466.
CONTRERAS, M. P., PAI, H., TUMTAS, Y., DUGGAN, C., YUEN, E. L. H., CRUCES, A. V., KOURELIS, J., AHN, H. K., LEE, K. T., WU, C. H., BOZKURT, T. O., DEREVNINA, L. & KAMOUN, S. 2023c. Sensor NLR immune proteins activate oligomerization of their NRC helpers in response to plant pathogens. *Embo j,* 42, e111519.
COOLEY, M. B., PATHIRANA, S., WU, H. J., KACHROO, P. & KLESSIG, D. F. 2000. Members of the Arabidopsis HRT/RPP8 family of resistance genes confer resistance to both viral and oomycete pathogens. *Plant Cell,* 12, 663-76.
COOPER, A. J., LATUNDE-DADA, A. O., WOODS-TÖR, A., LYNN, J., LUCAS, J. A., CRUTE, I. R. & HOLUB, E. B. 2008. Basic Compatibility of Albugo candida in Arabidopsis thaliana and Brassica juncea Causes Broad-Spectrum Suppression of Innate Immunity. *Molecular Plant-Microbe Interactions®,* 21, 745-756.
COWAN, G., MACFARLANE, S. & TORRANCE, L. 2023. A new simple and effective method for PLRV infection to screen for virus resistance in potato. *J Virol Methods,* 315, 114691.
DANGL, J. L. & JONES, J. D. G. 2001. Plant pathogens and integrated defence responses to infection. *Nature,* 411, 826-833.
DAWSON, A. M., FERGUSON, J. N., GARDINER, M., GREEN, P., HUBBARD, A. & MOSCOU, M. J. 2016. Isolation and fine mapping of Rps6: an intermediate host resistance gene in barley to wheat stripe rust. *Theor Appl Genet,* 129, 831-843.
DE LA CONCEPCION, J. C., FRANCESCHETTI, M., MACLEAN, D., TERAUCHI, R., KAMOUN, S. & BANFIELD, M. J. 2019. Protein engineering expands the effector recognition profile of a rice NLR immune receptor. *eLife,* 8, e47713.
DE LA CONCEPCION, J. C., MAIDMENT, J. H. R., LONGYA, A., XIAO, G., FRANCESCHETTI, M. & BANFIELD, M. J. 2021. The allelic rice immune receptor Pikh confers extended resistance to strains of the blast fungus through a single polymorphism in the effector binding interface. *PLOS Pathogens,* 17, e1009368.
DEREVNINA, L., CONTRERAS, M. P., ADACHI, H., UPSON, J., VERGARA CRUCES, A., XIE, R., SKŁENAR, J., MENKE, F. L. H., MUGFORD, S. T., MACLEAN, D., MA, W., HOGENHOUT, S. A., GOVERSE, A., MAQBOOL, A., WU, C.-H. & KAMOUN, S. 2021. Plant pathogens convergently evolved to counteract redundant nodes of an NLR immune receptor network. *PLOS Biology,* 19, e3001136.
DOENCH, J. G., FUSI, N., SULLENDER, M., HEGDE, M., VAIMBERG, E. W., DONOVAN, K. F., SMITH, I., TOTHOVA, Z., WILEN, C., ORCHARD, R., VIRGIN, H. W., LISTGARTEN, J. & ROOT, D. E. 2016. Optimized sgRNA design to maximize activity and minimize off-target effects of CRISPR-Cas9. *Nat Biotechnol,* 34, 184-191.
DU, J., VERZAUX, E., CHAPARRO-GARCIA, A., BIJSTERBOSCH, G., KEIZER, L. C. P., ZHOU, J., LIEBRAND, T. W. H., XIE, C., GOVERS, F., ROBATZEK, S., VAN DER VOSSEN, E. A. G., JACOBSEN, E., VISSER, R. G. F., KAMOUN, S. & VLEESHOUWERS, V. G. A. A. 2015a. Elicitin recognition confers enhanced resistance to Phytophthora infestans in potato. *Nature Plants,* 1, 15034.

DU, Y., MPINA, M. H., BIRCH, P. R., BOUWMEESTER, K. & GOVERS, F. 2015b. Phytophthora infestans RXLR Effector AVR1 Interacts with Exocyst Component Sec5 to Manipulate Plant Immunity. *Plant Physiol,* 169**,** 1975-90.
DUGGAN, C., TUMTAS, Y. & BOZKURT, T. O. 2021. A golden-gate compatible TRV2 virus induced gene silencing (VIGS) vector. *Zenodo*.
ELLIS, J. G., LAWRENCE, G. J., LUCK, J. E. & DODDS, P. N. 1999. Identification of regions in alleles of the flax rust resistance gene L that determine differences in gene-for-gene specificity. *Plant Cell,* 11**,** 495-506.
ERNST, K., KUMAR, A., KRISELEIT, D., KLOOS, D. U., PHILLIPS, M. S. & GANAL, M. W. 2002. The broad-spectrum potato cyst nematode resistance gene (Hero) from tomato is the only member of a large gene family of NBS-LRR genes with an unusual amino acid repeat in the LRR region. *Plant J,* 31**,** 127-36.
ESAU, K. & HOEFERT, L. L. 1972. Development of infection with beet western yellows virus in the sugarbeet. *Virology,* 48**,** 724-738.
FARNHAM, G. & BAULCOMBE, D. C. 2006. Artificial evolution extends the spectrum of viruses that are targeted by a disease-resistance gene from potato. *Proceedings of the National Academy of Sciences,* 103**,** 18828-18833.
FAUSTIN, B., LARTIGUE, L., BRUEY, J.-M., LUCIANO, F., SERGIENKO, E., BAILLY-MAITRE, B., VOLKMANN, N., HANEIN, D., ROUILLER, I. & REED, J. C. 2007. Reconstituted NALP1 Inflammasome Reveals Two-Step Mechanism of Caspase-1 Activation. *Molecular Cell,* 25**,** 713-724.
FAWKE, S., DOUMANE, M. & SCHORNACK, S. 2015. Oomycete Interactions with Plants: Infection Strategies and Resistance Principles. *Microbiology and Molecular Biology Reviews,* 79**,** 263-280.
FEEHAN, J. M., WANG, J., SUN, X., CHOI, J., AHN, H.-K., NGOU, B. P. M., PARKER, J. E. & JONES, J. D. G. 2023. Oligomerization of a plant helper NLR requires cell-surface and intracellular immune receptor activation. *Proceedings of the National Academy of Sciences,* 120**,** e2210406120.
FILLATTI, J. J., KISER, J., ROSE, R. & COMAI, L. 1987. Efficient Transfer of a Glyphosate Tolerance Gene into Tomato Using a Binary Agrobacterium Tumefaciens Vector. *Bio/Technology,* 5**,** 726-730.
FLOR, H. H. 1942. Inheritance of pathogenicity in Melampsora lini. 32**,** 653–669 pp.
FOONG-JING, G., CHING-YI, H., LIDA, D. & CHIH-HANG, W. 2023. NRC immune receptor networks show diversified hierarchical genetic architecture across plant lineages. *bioRxiv***,** 2023.10.25.563953.
FOSTER, S. J., PARK, T. H., PEL, M., BRIGNETI, G., SLIWKA, J., JAGGER, L., VAN DER VOSSEN, E. & JONES, J. D. 2009. Rpi-vnt1.1, a Tm-2(2) homolog from Solanum venturii, confers resistance to potato late blight. *Mol Plant Microbe Interact,* 22**,** 589-600.
FRY, W. 2008. Phytophthora infestans: the plant (and R gene) destroyer. *Mol Plant Pathol,* 9**,** 385-402.
GAYATHRI, P., SATHESHKUMAR, P. S., PRASAD, K., NAIR, S., SAVITHRI, H. S. & MURTHY, M. R. N. 2006. Crystal structure of the serine protease domain of Sesbania mosaic virus polyprotein and mutational analysis of residues forming the S1-binding pocket. *Virology,* 346**,** 440-451.

GEU-FLORES, F., NOUR-ELDIN, H. H., NIELSEN, M. T. & HALKIER, B. A. 2007. USER fusion: a rapid and efficient method for simultaneous fusion and cloning of multiple PCR products. *Nucleic Acids Res,* 35**,** e55.

GHISLAIN, M., BYARUGABA, A. A., MAGEMBE, E., NJOROGE, A., RIVERA, C., ROMAN, M. L., TOVAR, J. C., GAMBOA, S., FORBES, G. A., KREUZE, J. F., BAREKYE, A. & KIGGUNDU, A. 2019. Stacking three late blight resistance genes from wild species directly into African highland potato varieties confers complete field resistance to local blight races. *Plant Biotechnol J,* 17**,** 1119-1129.

GILBERT, B., BETTGENHAEUSER, J., UPADHYAYA, N., SOLIVERES, M., SINGH, D., PARK, R. F., MOSCOU, M. J. & AYLIFFE, M. 2018. Components of Brachypodium distachyon resistance to nonadapted wheat stripe rust pathogens are simply inherited. *PLOS Genetics,* 14**,** e1007636.

GILROY, E. M., BREEN, S., WHISSON, S. C., SQUIRES, J., HEIN, I., KACZMAREK, M., TURNBULL, D., BOEVINK, P. C., LOKOSSOU, A., CANO, L. M., MORALES, J., AVROVA, A. O., PRITCHARD, L., RANDALL, E., LEES, A., GOVERS, F., VAN WEST, P., KAMOUN, S., VLEESHOUWERS, V. G. A. A., COOKE, D. E. L. & BIRCH, P. R. J. 2011. Presence/absence, differential expression and sequence polymorphisms between PiAVR2 and PiAVR2-like in Phytophthora infestans determine virulence on R2 plants. *New Phytologist,* 191**,** 763-776.

GLADIEUX, P., OOSTERHOUT, C. V., FAIRHEAD, S., JOUET, A., ORTIZ, D., RAVEL, S., SHRESTHA, R.-K., FROUIN, J., HE, X., ZHU, Y., MOREL, J.-B., HUANG, H., KROJ, T. & JONES, J. D. G. 2022. Extensive immune receptor repertoire diversity in disease-resistant rice landraces. *bioRxiv***,** 2022.12.05.519081.

GRECH-BARAN, M., WITEK, K., JONES, J. D. & HENNIG, J. 2019. Coat protein of conserved structure from multiple potyviruses triggers Rysto-mediated immunity. *Molecular Plant-Microbe Interactions,* 32**,** 68-68.

GRECH-BARAN, M., WITEK, K., POZNAŃSKI, J. T., GRUPA-URBAŃSKA, A., MALINOWSKI, T., LICHOCKA, M., JONES, J. D. G. & HENNIG, J. 2022. The Rysto immune receptor recognises a broadly conserved feature of potyviral coat proteins. *New Phytologist,* 235**,** 1179-1195.

GREER, S. F., HACKENBERG, D., GEGAS, V., MITROUSIA, G., EDWARDS, D., BATLEY, J., TEAKLE, G. R., BARKER, G. C. & WALSH, J. A. 2021. Quantitative Trait Locus Mapping of Resistance to Turnip Yellows Virus in Brassica rapa and Brassica oleracea and Introgression of These Resistances by Resynthesis Into Allotetraploid Plants for Deployment in Brassica napus. *Front Plant Sci,* 12**,** 781385.

GUST, A. A. & FELIX, G. 2014. Receptor like proteins associate with SOBIR1-type of adaptors to form bimolecular receptor kinases. *Curr Opin Plant Biol,* 21**,** 104-111.

HAAS, B. J., KAMOUN, S., ZODY, M. C., JIANG, R. H., HANDSAKER, R. E., CANO, L. M., GRABHERR, M., KODIRA, C. D., RAFFAELE, S., TORTO-ALALIBO, T., BOZKURT, T. O., AH-FONG, A. M., ALVARADO, L., ANDERSON, V. L., ARMSTRONG, M. R., AVROVA, A., BAXTER, L., BEYNON, J., BOEVINK, P. C., BOLLMANN, S. R., BOS, J. I., BULONE, V., CAI, G., CAKIR, C., CARRINGTON, J. C., CHAWNER, M., CONTI, L., COSTANZO, S., EWAN, R., FAHLGREN, N., FISCHBACH, M. A., FUGELSTAD, J., GILROY, E. M., GNERRE, S., GREEN, P. J., GRENVILLE-BRIGGS, L. J., GRIFFITH, J., GRÜNWALD, N. J., HORN, K., HORNER, N. R., HU, C. H.,

HUITEMA, E., JEONG, D. H., JONES, A. M., JONES, J. D., JONES, R. W., KARLSSON, E. K., KUNJETI, S. G., LAMOUR, K., LIU, Z., MA, L., MACLEAN, D., CHIBUCOS, M. C., MCDONALD, H., MCWALTERS, J., MEIJER, H. J., MORGAN, W., MORRIS, P. F., MUNRO, C. A., O'NEILL, K., OSPINA-GIRALDO, M., PINZÓN, A., PRITCHARD, L., RAMSAHOYE, B., REN, Q., RESTREPO, S., ROY, S., SADANANDOM, A., SAVIDOR, A., SCHORNACK, S., SCHWARTZ, D. C., SCHUMANN, U. D., SCHWESSINGER, B., SEYER, L., SHARPE, T., SILVAR, C., SONG, J., STUDHOLME, D. J., SYKES, S., THINES, M., VAN DE VONDERVOORT, P. J., PHUNTUMART, V., WAWRA, S., WEIDE, R., WIN, J., YOUNG, C., ZHOU, S., FRY, W., MEYERS, B. C., VAN WEST, P., RISTAINO, J., GOVERS, F., BIRCH, P. R., WHISSON, S. C., JUDELSON, H. S. & NUSBAUM, C. 2009. Genome sequence and analysis of the Irish potato famine pathogen Phytophthora infestans. *Nature,* 461**,** 393-8.

HACKENBERG, D., ASARE-BEDIAKO, E., BAKER, A., WALLEY, P., JENNER, C., GREER, S., BRAMHAM, L., BATLEY, J., EDWARDS, D., DELOURME, R., BARKER, G., TEAKLE, G. & WALSH, J. 2020. Identification and QTL mapping of resistance to Turnip yellows virus (TuYV) in oilseed rape, Brassica napus. *Theoretical and Applied Genetics,* 133**,** 383-393.

HAMEED, A., IQBAL, Z., ASAD, S. & MANSOOR, S. 2014. Detection of Multiple Potato Viruses in the Field Suggests Synergistic Interactions among Potato Viruses in Pakistan. *Plant Pathol J,* 30**,** 407-15.

HARDIGAN, M. A., CRISOVAN, E., HAMILTON, J. P., KIM, J., LAIMBEER, P., LEISNER, C. P., MANRIQUE-CARPINTERO, N. C., NEWTON, L., PHAM, G. M., VAILLANCOURT, B., YANG, X., ZENG, Z., DOUCHES, D. S., JIANG, J., VEILLEUX, R. E. & BUELL, C. R. 2016. Genome Reduction Uncovers a Large Dispensable Genome and Adaptive Role for Copy Number Variation in Asexually Propagated Solanum tuberosum. *Plant Cell,* 28**,** 388-405.

HARRIS, C. J., SLOOTWEG, E. J., GOVERSE, A. & BAULCOMBE, D. C. 2013. Stepwise artificial evolution of a plant disease resistance gene. *Proceedings of the National Academy of Sciences,* 110**,** 21189-21194.

HAVERKORT, A. J., STRUIK, P. C., VISSER, R. G. F. & JACOBSEN, E. 2009. Applied Biotechnology to Combat Late Blight in Potato Caused by Phytophthora Infestans. *Potato Research,* 52**,** 249-264.

HE, J., YE, W., CHOI, D. S., WU, B., ZHAI, Y., GUO, B., DUAN, S., WANG, Y., GAN, J., MA, W. & MA, J. 2019. Structural analysis of Phytophthora suppressor of RNA silencing 2 (PSR2) reveals a conserved modular fold contributing to virulence. *Proc Natl Acad Sci U S A,* 116**,** 8054-8059.

HEESE, A., HANN, D. R., GIMENEZ-IBANEZ, S., JONES, A. M., HE, K., LI, J., SCHROEDER, J. I., PECK, S. C. & RATHJEN, J. P. 2007. The receptor-like kinase SERK3/BAK1 is a central regulator of innate immunity in plants. *Proc Natl Acad Sci U S A,* 104**,** 12217-22.

HEMMING, D., BELL, J., COLLIER, R., DUNBAR, T., DUNSTONE, N., EVERATT, M., EYRE, D., KAYE, N., KORYCINSKA, A., PICKUP, J. & SCAIFE, A. A. 2022. Likelihood of Extreme Early Flight of Myzus persicae (Hemiptera: Aphididae) Across the UK. *Journal of Economic Entomology,* 115**,** 1342-1349.

HOLM, L., LAIHO, A., TÖRÖNEN, P. & SALGADO, M. 2023. DALI shines a light on remote homologs: One hundred discoveries. *Protein Science,* 32**,** e4519.

HU, J., DIAO, Y., ZHOU, Y., LIN, D., BI, Y., PANG, Z., TROUT FRYXELL, R., LIU, X. & LAMOUR, K. 2013. Loss of Heterozygosity Drives Clonal Diversity of Phytophthora capsici in China. *PLOS ONE,* 8**,** e82691.

HUANG, C.-Y., HUANG, Y.-S., SUGIHARA, Y., WANG, H.-Y., HUANG, L.-T., LOPEZ-AGUDELO, J. C., CHEN, Y.-F., LIN, K.-Y., CHIANG, B.-J., TOGHANI, A., KOURELIS, J., DEREVNINA, L. & WU, C.-H. 2023. Functional divergence shaped the network architecture of plant immune receptors. *bioRxiv***,** 2023.12.12.571219.

HUANG, S., JIA, A., SONG, W., HESSLER, G., MENG, Y., SUN, Y., XU, L., LAESSLE, H., JIRSCHITZKA, J., MA, S., XIAO, Y., YU, D., HOU, J., LIU, R., SUN, H., LIU, X., HAN, Z., CHANG, J., PARKER, J. E. & CHAI, J. 2022. Identification and receptor mechanism of TIR-catalyzed small molecules in plant immunity. *Science,* 377**,** eabq3297.

JACOB, P., KIM, N. H., WU, F., EL-KASMI, F., CHI, Y., WALTON, W. G., FURZER, O. J., LIETZAN, A. D., SUNIL, S., KEMPTHORN, K., REDINBO, M. R., PEI, Z.-M., WAN, L. & DANGL, J. L. 2021. Plant "helper" immune receptors are Ca2+-permeable nonselective cation channels. *Science,* 373**,** 420-425.

JIA, A., HUANG, S., MA, S., CHANG, X., HAN, Z. & CHAI, J. 2023. TIR-catalyzed nucleotide signaling molecules in plant defense. *Current Opinion in Plant Biology,* 73**,** 102334.

JINGWEI, L., WANG, B., SONG, X.-M., WANG, R., CHEN, L., ZHANG, H., HAMBORG, Z. & WANG, Q. 2013. Potato leafroll virus (PLRV) and Potato virus Y (PVY) influence vegetative growth, physiological metabolism, and microtuber production of in vitro-grown shoots of potato (Solanum tuberosum L.). *Plant Cell, Tissue and Organ Culture (PCTOC),* 114.

JOHAL, G. S. & BRIGGS, S. P. 1992. Reductase activity encoded by the HM1 disease resistance gene in maize. *Science,* 258**,** 985-7.

JONES, J. D. G. & DANGL, J. L. 2006. The plant immune system. *Nature,* 444**,** 323-329.

JONES, J. D. G., WITEK, K., VERWEIJ, W., JUPE, F., COOKE, D., DORLING, S., TOMLINSON, L., SMOKER, M., PERKINS, S. & FOSTER, S. 2014. Elevating crop disease resistance with cloned genes. *Philosophical Transactions of the Royal Society B-Biological Sciences,* 369.

JONES, R. A. C. 2021. Global Plant Virus Disease Pandemics and Epidemics. *Plants (Basel),* 10.

JUERGENS, M., PAETSCH, C., KRÄMER, I., ZAHN, M., RABENSTEIN, F., SCHONDELMAIER, J., SCHLIEPHAKE, E., SNOWDON, R., FRIEDT, W. & ORDON, F. 2010. Genetic analyses of the host-pathogen system Turnip yellows virus (TuYV)-rapeseed (Brassica napus L.) and development of molecular markers for TuYV-resistance. *Theor Appl Genet,* 120**,** 735-44.

JUPE, F., PRITCHARD, L., ETHERINGTON, G. J., MACKENZIE, K., COCK, P. J., WRIGHT, F., SHARMA, S. K., BOLSER, D., BRYAN, G. J., JONES, J. D. & HEIN, I. 2012. Identification and localisation of the NB-LRR gene family within the potato genome. *BMC Genomics,* 13**,** 75.

JUPE, F., WITEK, K., VERWEIJ, W., SLIWKA, J., PRITCHARD, L., ETHERINGTON, G. J., MACLEAN, D., COCK, P. J., LEGGETT, R. M., BRYAN, G. J., CARDLE, L., HEIN, I. & JONES, J. D. G. 2013a. Resistance gene enrichment sequencing (RenSeq)

enables reannotation of the NB-LRR gene family from sequenced plant genomes and rapid mapping of resistance loci in segregating populations. *Plant Journal,* 76**,** 530-544.

JUPE, J., STAM, R., HOWDEN, A. J. M., MORRIS, J. A., ZHANG, R., HEDLEY, P. E. & HUITEMA, E. 2013b. Phytophthora capsici-tomato interaction features dramatic shifts in gene expression associated with a hemi-biotrophic lifestyle. *Genome Biology,* 14**,** R63.

KARASOV, T. L., KNISKERN, J. M., GAO, L., DEYOUNG, B. J., DING, J., DUBIELLA, U., LASTRA, R. O., NALLU, S., ROUX, F., INNES, R. W., BARRETT, L. G., HUDSON, R. R. & BERGELSON, J. 2014. The long-term maintenance of a resistance polymorphism through diffuse interactions. *Nature,* 512**,** 436-440.

KARKI, H. S., ABDULLAH, S., CHEN, Y. & HALTERMAN, D. A. 2021. Natural Genetic Diversity in the Potato Resistance Gene RB Confers Suppression Avoidance from Phytophthora Effector IPI-O4. *Molecular Plant-Microbe Interactions®,* 34**,** 1048-1056.

KAY, S., BOCH, J. & BONAS, U. 2005. Characterization of AvrBs3-Like Effectors from a Brassicaceae Pathogen Reveals Virulence and Avirulence Activities and a Protein with a Novel Repeat Architecture. *Molecular Plant-Microbe Interactions®,* 18**,** 838-848.

KIM, D., LANGMEAD, B. & SALZBERG, S. L. 2015. HISAT: a fast spliced aligner with low memory requirements. *Nature methods,* 12**,** 357-360.

KIM, D. S., WOODS-TÖR, A., CEVIK, V., FURZER, O. J., LI, Y., MA, W., TÖR, M. & JONES, J. D. G. 2023. ATR2Cala2 from Arabidopsis-infecting downy mildew requires 4 TIR-NLR immune receptors for full recognition. *bioRxiv***,** 2023.04.25.538220.

KOENIG, D., HAGMANN, J., LI, R., BEMM, F., SLOTTE, T., NEUFFER, B., WRIGHT, S. I. & WEIGEL, D. 2019. Long-term balancing selection drives evolution of immunity genes in Capsella. *eLife,* 8**,** e43606.

KOLMOGOROV, M., YUAN, J., LIN, Y. & PEVZNER, P. A. 2019. Assembly of long, error-prone reads using repeat graphs. *Nature Biotechnology,* 37**,** 540-546.

KONDRÁK, M., KOPP, A., URI, C., SÓS-HEGEDŰS, A., CSÁKVÁRI, E., SCHILLER, M., BARTA, E., CERNÁK, I., POLGÁR, Z., TALLER, J. & BÁNFALVI, Z. 2020. Mapping and DNA sequence characterisation of the Rysto locus conferring extreme virus resistance to potato cultivar 'White Lady'. *PloS one,* 15**,** e0224534-e0224534.

KOURELIS, J., MARCHAL, C., POSBEYIKIAN, A., HARANT, A. & KAMOUN, S. 2023. NLR immune receptor–nanobody fusions confer plant disease resistance. *Science,* 379**,** 934-939.

KOURELIS, J., SAKAI, T., ADACHI, H. & KAMOUN, S. 2021. RefPlantNLR is a comprehensive collection of experimentally validated plant disease resistance proteins from the NLR family. *PLOS Biology,* 19**,** e3001124.

KOURELIS, J. & VAN DER HOORN, R. A. L. 2018. Defended to the Nines: 25 Years of Resistance Gene Cloning Identifies Nine Mechanisms for R Protein Function. *Plant Cell,* 30**,** 285-299.

KRASILEVA, K. V., DAHLBECK, D. & STASKAWICZ, B. J. 2010. Activation of an Arabidopsis resistance protein is specified by the in planta association of its

leucine-rich repeat domain with the cognate oomycete effector. *Plant Cell,* 22**,** 2444-58.

KUANG, H., WEI, F., MARANO, M. R., WIRTZ, U., WANG, X., LIU, J., SHUM, W. P., ZABORSKY, J., TALLON, L. J., RENSINK, W., LOBST, S., ZHANG, P., TORNQVIST, C. E., TEK, A., BAMBERG, J., HELGESON, J., FRY, W., YOU, F., LUO, M. C., JIANG, J., ROBIN BUELL, C. & BAKER, B. 2005. The R1 resistance gene cluster contains three groups of independently evolving, type I R1 homologues and shows substantial structural variation among haplotypes of Solanum demissum. *Plant J,* 44**,** 37-51.

KUSCH, S. & PANSTRUGA, R. 2017. mlo-Based Resistance: An Apparently Universal "Weapon" to Defeat Powdery Mildew Disease. *Molecular Plant-Microbe Interactions®,* 30**,** 179-189.

KVITKO, B. H., PARK, D. H., VELÁSQUEZ, A. C., WEI, C. F., RUSSELL, A. B., MARTIN, G. B., SCHNEIDER, D. J. & COLLMER, A. 2009. Deletions in the repertoire of Pseudomonas syringae pv. tomato DC3000 type III secretion effector genes reveal functional overlap among effectors. *PLoS Pathog,* 5**,** e1000388.

LAFLAMME, B., DILLON, M. M., MARTEL, A., ALMEIDA, R. N. D., DESVEAUX, D. & GUTTMAN, D. S. 2020. The pan-genome effector-triggered immunity landscape of a host-pathogen interaction. *Science,* 367**,** 763-768.

LAMOUR, K. H. & HAUSBECK, M. K. 2000. Mefenoxam Insensitivity and the Sexual Stage of Phytophthora capsici in Michigan Cucurbit Fields. *Phytopathology®,* 90**,** 396-400.

LAMOUR, K. H. & HAUSBECK, M. K. 2002. The Spatiotemporal Genetic Structure of Phytophthora capsici in Michigan and Implications for Disease Management. *Phytopathology,* 92**,** 681-4.

LAMOUR, K. H., MUDGE, J., GOBENA, D., HURTADO-GONZALES, O. P., SCHMUTZ, J., KUO, A., MILLER, N. A., RICE, B. J., RAFFAELE, S., CANO, L. M., BHARTI, A. K., DONAHOO, R. S., FINLEY, S., HUITEMA, E., HULVEY, J., PLATT, D., SALAMOV, A., SAVIDOR, A., SHARMA, R., STAM, R., STOREY, D., THINES, M., WIN, J., HAAS, B. J., DINWIDDIE, D. L., JENKINS, J., KNIGHT, J. R., AFFOURTIT, J. P., HAN, C. S., CHERTKOV, O., LINDQUIST, E. A., DETTER, C., GRIGORIEV, I. V., KAMOUN, S. & KINGSMORE, S. F. 2012a. Genome Sequencing and Mapping Reveal Loss of Heterozygosity as a Mechanism for Rapid Adaptation in the Vegetable Pathogen Phytophthora capsici. *Molecular Plant-Microbe Interactions®,* 25**,** 1350-1360.

LAMOUR, K. H., STAM, R., JUPE, J. & HUITEMA, E. 2012b. The oomycete broad-host-range pathogen Phytophthora capsici. *Molecular Plant Pathology,* 13**,** 329-337.

LEE, E. S., HEO, J., BANG, W. Y., CHOUGULE, K. M., WAMINAL, N. E., HONG, N. T., KIM, M. J., BEAK, H. K., KIM, Y. J., PRIATAMA, R. A., JANG, J. I., CHA, K. I., SON, S. H., RAJENDRAN, S., CHOO, Y.-K., BAE, J. H., KIM, C. M., LEE, Y. K., BAE, S., JONES, J. D. G., SOHN, K. H., LEE, J., KIM, H. H., HONG, J. C., WARE, D., KIM, K. & PARK, S. J. 2023. Engineering homoeologs provide a fine scale for quantitative traits in polyploid. *Plant Biotechnology Journal,* 21**,** 2458-2472.

LEE, H.-A., KIM, S.-Y., OH, S.-K., YEOM, S.-I., KIM, S.-B., KIM, M.-S., KAMOUN, S. & CHOI, D. 2014. Multiple recognition of RXLR effectors is associated with

nonhost resistance of pepper against Phytophthora infestans. *New Phytologist,* 203**,** 926-938.
LEE, H.-A., LEE, H.-Y., SEO, E., LEE, J., KIM, S.-B., OH, S., CHOI, E., CHOI, E., LEE, S. E. & CHOI, D. 2017. Current Understandings of Plant Nonhost Resistance. *Molecular Plant-Microbe Interactions®,* 30**,** 5-15.
LEE, S., WHITAKER, V. M. & HUTTON, S. F. 2016. Mini Review: Potential Applications of Non-host Resistance for Crop Improvement. *Frontiers in Plant Science,* 7**,** 6.
LEFEUVRE, P., MARTIN, D. P., ELENA, S. F., SHEPHERD, D. N., ROUMAGNAC, P. & VARSANI, A. 2019. Evolution and ecology of plant viruses. *Nature Reviews Microbiology,* 17**,** 632-644.
LEWIS, J. D., LEE, A. H.-Y., HASSAN, J. A., WAN, J., HURLEY, B., JHINGREE, J. R., WANG, P. W., LO, T., YOUN, J.-Y., GUTTMAN, D. S. & DESVEAUX, D. 2013. The Arabidopsis ZED1 pseudokinase is required for ZAR1-mediated immunity induced by the Pseudomonas syringae type III effector HopZ1a. *Proceedings of the National Academy of Sciences,* 110**,** 18722-18727.
LI, F., UPADHYAYA, N. M., SPERSCHNEIDER, J., MATNY, O., NGUYEN-PHUC, H., MAGO, R., RALEY, C., MILLER, M. E., SILVERSTEIN, K. A. T., HENNINGSEN, E., HIRSCH, C. D., VISSER, B., PRETORIUS, Z. A., STEFFENSON, B. J., SCHWESSINGER, B., DODDS, P. N. & FIGUEROA, M. 2019. Emergence of the Ug99 lineage of the wheat stem rust pathogen through somatic hybridisation. *Nat Commun,* 10**,** 5068.
LI, K., HEGARTY, J., ZHANG, C., WAN, A., WU, J., GUEDIRA, G. B., CHEN, X., MUÑOZ-AMATRIAÍN, M., FU, D. & DUBCOVSKY, J. 2016. Fine mapping of barley locus Rps6 conferring resistance to wheat stripe rust. *Theor Appl Genet,* 129**,** 845-859.
LI, Q., WANG, J., BAI, T., ZHANG, M., JIA, Y., SHEN, D., ZHANG, M. & DOU, D. 2020. A Phytophthora capsici effector suppresses plant immunity via interaction with EDS1. *Molecular Plant Pathology*.
LIEBRAND, T. W. H., VAN DEN BERG, G. C. M., ZHANG, Z., SMIT, P., CORDEWENER, J. H. G., AMERICA, A. H. P., SKLENAR, J., JONES, A. M. E., TAMELING, W. I. L., ROBATZEK, S., THOMMA, B. P. H. J. & JOOSTEN, M. H. A. J. 2013. Receptor-like kinase SOBIR1/EVR interacts with receptor-like proteins in plant immunity against fungal infection. *Proceedings of the National Academy of Sciences,* 110**,** 10010-10015.
LIN, X., JIA, Y., HEAL, R., PROKCHORCHIK, M., SINDALOVSKAYA, M., OLAVE-ACHURY, A., MAKECHEMU, M., FAIRHEAD, S., NOUREEN, A., HEO, J., WITEK, K., SMOKER, M., TAYLOR, J., SHRESTHA, R.-K., LEE, Y., ZHANG, C., PARK, S. J., SOHN, K. H., HUANG, S. & JONES, J. D. G. 2023. Solanum americanum genome-assisted discovery of immune receptors that detect potato late blight pathogen effectors. *Nature Genetics,* 55**,** 1579-1588.
LIN, X., OLAVE-ACHURY, A., HEAL, R., PAIS, M., WITEK, K., AHN, H.-K., ZHAO, H., BHANVADIA, S., KARKI, H. S., SONG, T., WU, C.-H., ADACHI, H., KAMOUN, S., VLEESHOUWERS, V. G. A. A. & JONES, J. D. G. 2022. A potato late blight resistance gene protects against multiple Phytophthora species by recognizing a broadly conserved RXLR-WY effector. *Molecular Plant,* 15**,** 1457-1469.

LIN, X., SONG, T., FAIRHEAD, S., WITEK, K., JOUET, A., JUPE, F., WITEK, A. I., KARKI, H. S., VLEESHOUWERS, V. G. A. A., HEIN, I. & JONES, J. D. G. 2020. Identification of Avramr1 from Phytophthora infestans using long read and cDNA pathogen-enrichment sequencing (PenSeq). *Molecular Plant Pathology,* 21**,** 1502-1512.

LIPKA, U., FUCHS, R. & LIPKA, V. 2008. Arabidopsis non-host resistance to powdery mildews. *Current Opinion in Plant Biology,* 11**,** 404-411.

LIU, F., YANG, Z., WANG, C., MARTIN, R., QIAO, W., CARETTE, J. E., LUAN, S., NOGALES, E. & STASKAWICZ, B. 2023. The activated plant NRC4 immune receptor forms a hexameric resistosome. *bioRxiv*.

LIU, Y., ZENG, Z., ZHANG, Y. M., LI, Q., JIANG, X. M., JIANG, Z., TANG, J. H., CHEN, D., WANG, Q., CHEN, J. Q. & SHAO, Z. Q. 2021. An angiosperm NLR Atlas reveals that NLR gene reduction is associated with ecological specialization and signal transduction component deletion. *Mol Plant,* 14**,** 2015-2031.

LU, X., KRACHER, B., SAUR, I. M. L., BAUER, S., ELLWOOD, S. R., WISE, R., YAENO, T., MAEKAWA, T. & SCHULZE-LEFERT, P. 2016. Allelic barley MLA immune receptors recognize sequence-unrelated avirulence effectors of the powdery mildew pathogen. *Proceedings of the National Academy of Sciences,* 113**,** E6486-E6495.

LÜDKE, D., SAKAI, T., KOURELIS, J., TOGHANI, A., ADACHI, H., POSBEYIKIAN, A., FRIJTERS, R., PAI, H., HARANT, A., ERNST, K., GANAL, M., VERHAGE, A., WU, C.-H. & KAMOUN, S. 2023. A root-specific NLR network confers resistance to plant parasitic nematodes. *bioRxiv***,** 2023.12.14.571630.

LUO, M., XIE, L., CHAKRABORTY, S., WANG, A., MATNY, O., JUGOVICH, M., KOLMER, J. A., RICHARDSON, T., BHATT, D., HOQUE, M., PATPOUR, M., SØRENSEN, C., ORTIZ, D., DODDS, P., STEUERNAGEL, B., WULFF, B. B. H., UPADHYAYA, N. M., MAGO, R., PERIYANNAN, S., LAGUDAH, E., FREEDMAN, R., LYNNE REUBER, T., STEFFENSON, B. J. & AYLIFFE, M. 2021. A five-transgene cassette confers broad-spectrum resistance to a fungal rust pathogen in wheat. *Nat Biotechnol,* 39**,** 561-566.

MA, S., LAPIN, D., LIU, L., SUN, Y., SONG, W., ZHANG, X., LOGEMANN, E., YU, D., WANG, J., JIRSCHITZKA, J., HAN, Z., SCHULZE-LEFERT, P., PARKER, J. E. & CHAI, J. 2020. Direct pathogen-induced assembly of an NLR immune receptor complex to form a holoenzyme. *Science,* 370**,** eabe3069.

MACKEY, D., BELKHADIR, Y., ALONSO, J. M., ECKER, J. R. & DANGL, J. L. 2003. Arabidopsis RIN4 Is a Target of the Type III Virulence Effector AvrRpt2 and Modulates RPS2-Mediated Resistance. *Cell,* 112**,** 379-389.

MACKEY, D., HOLT, B. F., WIIG, A. & DANGL, J. L. 2002. RIN4 Interacts with Pseudomonas syringae Type III Effector Molecules and Is Required for RPM1-Mediated Resistance in Arabidopsis. *Cell,* 108**,** 743-754.

MACLEOD, K., GREER, S. F., BRAMHAM, L. E., PIMENTA, R. J. G., NELLIST, C. F., HACKENBURG, D., TEAKLE, G. R., BARKER, G. C. & WALSH, J. A. 2023. A review of sources of resistance to turnip yellows virus (TuYV) in Brassica species. *Annals of Applied Biology,* 183**,** 200-208.

MACQUEEN, A., SUN, X. & BERGELSON, J. 2016. Genetic architecture and pleiotropy shape costs of Rps2-mediated resistance in Arabidopsis thaliana. *Nature Plants,* 2**,** 16110.

MAEKAWA, T., KRACHER, B., VERNALDI, S., VER LOREN VAN THEMAAT, E. & SCHULZE-LEFERT, P. 2012. Conservation of NLR-triggered immunity across plant lineages. *Proceedings of the National Academy of Sciences,* 109**,** 20119-20123.

MAIDMENT, J. H. R., SHIMIZU, M., BENTHAM, A. R., VERA, S., FRANCESCHETTI, M., LONGYA, A., STEVENSON, C. E. M., DE LA CONCEPCION, J. C., BIAŁAS, A., KAMOUN, S., TERAUCHI, R. & BANFIELD, M. J. 2023. Effector target-guided engineering of an integrated domain expands the disease resistance profile of a rice NLR immune receptor. *eLife,* 12**,** e81123.

MANN, K. S. & SANFAÇON, H. 2019. Expanding Repertoire of Plant Positive-Strand RNA Virus Proteases. *Viruses,* 11.

MARCHAL, C., ZHANG, J., ZHANG, P., FENWICK, P., STEUERNAGEL, B., ADAMSKI, N. M., BOYD, L., MCINTOSH, R., WULFF, B. B. H., BERRY, S., LAGUDAH, E. & UAUY, C. 2018. BED-domain-containing immune receptors confer diverse resistance spectra to yellow rust. *Nature Plants,* 4**,** 662-668.

MARTEL, A., LAFLAMME, B., SETO, D., BASTEDO, D. P., DILLON, M. M., ALMEIDA, R. N. D., GUTTMAN, D. S. & DESVEAUX, D. 2020. Immunodiversity of the Arabidopsis ZAR1 NLR Is Conveyed by Receptor-Like Cytoplasmic Kinase Sensors. *Frontiers in Plant Science,* 11.

MARTIN, R., QI, T., ZHANG, H., LIU, F., KING, M., TOTH, C., NOGALES, E. & STASKAWICZ, B. J. 2020. Structure of the activated ROQ1 resistosome directly recognizing the pathogen effector XopQ. *Science,* 370**,** eabd9993.

MCDOWELL, J. M., DHANDAYDHAM, M., LONG, T. A., AARTS, M. G., GOFF, S., HOLUB, E. B. & DANGL, J. L. 1998. Intragenic recombination and diversifying selection contribute to the evolution of downy mildew resistance at the RPP8 locus of Arabidopsis. *Plant Cell,* 10**,** 1861-74.

MCLELLAN, H., HARVEY, S. E., STEINBRENNER, J., ARMSTRONG, M. R., HE, Q., CLEWES, R., PRITCHARD, L., WANG, W., WANG, S., NUSSBAUMER, T., DOHAI, B., LUO, Q., KUMARI, P., DUAN, H., ROBERTS, A., BOEVINK, P. C., NEUMANN, C., CHAMPOURET, N., HEIN, I., FALTER-BRAUN, P., BEYNON, J., DENBY, K. & BIRCH, P. R. J. 2022. Exploiting breakdown in nonhost effector–target interactions to boost host disease resistance. *Proceedings of the National Academy of Sciences,* 119**,** e2114064119.

MENARDO, F., PRAZ, C. R., WYDER, S., BEN-DAVID, R., BOURRAS, S., MATSUMAE, H., MCNALLY, K. E., PARLANGE, F., RIBA, A., ROFFLER, S., SCHAEFER, L. K., SHIMIZU, K. K., VALENTI, L., ZBINDEN, H., WICKER, T. & KELLER, B. 2016. Hybridization of powdery mildew strains gives rise to pathogens on novel agricultural crop species. *Nature Genetics,* 48**,** 201-205.

MICHELMORE, R. W. & MEYERS, B. C. 1998. Clusters of resistance genes in plants evolve by divergent selection and a birth-and-death process. *Genome Res,* 8**,** 1113-30.

MIHOVILOVICH, E., ALARCON, L., PEREZ, A. L., ALVARADO, J., ARELLANO, C. & BONIERBALE, M. 2007. High levels of heritable resistance to Potato leafroll virus (PLRV) in Solanum tuberosum subsp andigena. *Crop Science,* 47**,** 1091-1103.

MONDAL, S., WENNINGER, E. J., HUTCHINSON, P. J. S., WHITWORTH, J. L., SHRESTHA, D., EIGENBRODE, S. D., BOSQUE-PEREZ, N. A. & SNYDER, W. E.

2017. Responses of Aphid Vectors of Potato leaf roll virus to Potato Varieties. *Plant Dis,* 101**,** 1812-1818.

MONINO-LOPEZ, D., NIJENHUIS, M., KODDE, L., KAMOUN, S., SALEHIAN, H., SCHENTSNYI, K., STAM, R., LOKOSSOU, A., ABD-EL-HALIEM, A., VISSER, R. G. F. & VOSSEN, J. H. 2021. Allelic variants of the NLR protein Rpi-chc1 differentially recognize members of the Phytophthora infestans PexRD12/31 effector superfamily through the leucine-rich repeat domain. *The Plant Journal,* 107**,** 182-197.

MOON, H., PANDEY, A., YOON, H., CHOI, S., JEON, H., PROKCHORCHIK, M., JUNG, G., WITEK, K., VALLS, M., MCCANN, H. C., KIM, M. S., JONES, J. D. G., SEGONZAC, C. & SOHN, K. H. 2021. Identification of RipAZ1 as an avirulence determinant of Ralstonia solanacearum in Solanum americanum. *Mol Plant Pathol,* 22**,** 317-333.

MUNDT, C. C. 2018. Pyramiding for Resistance Durability: Theory and Practice. *Phytopathology®,* 108**,** 792-802.

MUNIYANDI, S., AMIRALI, T., HSUAN, P., YU, S., JIORGOS, K., ENOCH LOK HIM, Y., TARHAN, I., HE, Z., RONGRONG, X., ABBAS, M., JUAN CARLOS DE LA, C., MARK, J. B., LIDA, D., BENJAMIN, P., DAVID, M. L., TOLGA, O. B., CHIH-HANG, W., SOPHIEN, K. & MAURICIO, P. C. 2023. Activation of plant immunity through conversion of a helper NLR homodimer into a resistosome. *bioRxiv***,** 2023.12.17.572070.

NGOU, B. P. M., AHN, H.-K., DING, P. & JONES, J. D. G. 2021. Mutual potentiation of plant immunity by cell-surface and intracellular receptors. *Nature,* 592**,** 110-115.

NGOU, B. P. M., DING, P. & JONES, J. D. G. 2022a. Thirty years of resistance: Zig-zag through the plant immune system. *The Plant Cell,* 34**,** 1447-1478.

NGOU, B. P. M., HEAL, R., WYLER, M., SCHMID, M. W. & JONES, J. D. G. 2022b. Concerted expansion and contraction of immune receptor gene repertoires in plant genomes. *Nature Plants,* 8**,** 1146-1152.

NIKS, R. E. & MARCEL, T. C. 2009. Nonhost and basal resistance: how to explain specificity? *New Phytologist,* 182**,** 817-828.

NURKIYANOVA, K. M., RYABOV, E. V., COMMANDEUR, U., DUNCAN, G. H., CANTO, T., GRAY, S. M., MAYO, M. A. & TALIANSKY, M. E. 2000. Tagging potato leafroll virus with the jellyfish green fluorescent protein gene. *J Gen Virol,* 81**,** 617-26.

NÜRNBERGER, T. & LIPKA, V. 2005. Non-host resistance in plants: new insights into an old phenomenon. *Molecular Plant Pathology,* 6**,** 335-345.

OH, S., KIM, S., PARK, H.-J., KIM, M.-S., SEO, M.-K., WU, C.-H., LEE, H.-A., KIM, H.-S., KAMOUN, S. & CHOI, D. 2023. Nucleotide-binding leucine-rich repeat network underlies nonhost resistance of pepper against the Irish potato famine pathogen Phytophthora infestans. *Plant Biotechnology Journal,* 21**,** 1361-1372.

OVCHINNIKOVA, A., KRYLOVA, E., GAVRILENKO, T., SMEKALOVA, T., ZHUK, M., KNAPP, S. & SPOONER, D. M. 2011. Taxonomy of cultivated potatoes (Solanum section Petota: Solanaceae). *Botanical Journal of the Linnean Society,* 165**,** 107-155.

PAIS, M., YOSHIDA, K., GIANNAKOPOULOU, A., PEL, M. A., CANO, L. M., OLIVA, R. F., WITEK, K., LINDQVIST-KREUZE, H., VLEESHOUWERS, V. G. A. A. & KAMOUN, S. 2018. Gene expression polymorphism underpins evasion of host immunity in an asexual lineage of the Irish potato famine pathogen. *BMC Evolutionary Biology,* 18**,** 93.

PALUCHOWSKA, P., ŚLIWKA, J. & YIN, Z. 2022. Late blight resistance genes in potato breeding. *Planta,* 255**,** 127.

PANSTRUGA, R. & MOSCOU, M. J. 2020. What is the Molecular Basis of Nonhost Resistance? *Molecular Plant-Microbe Interactions®,* 33**,** 1253-1264.

PARLEVLIET, J. E. & ZADOKS, J. C. 1977. The integrated concept of disease resistance: A new view including horizontal and vertical resistance in plants. *Euphytica,* 26**,** 5-21.

PARNISKE, M., HAMMOND-KOSACK, K. E., GOLSTEIN, C., THOMAS, C. M., JONES, D. A., HARRISON, K., WULFF, B. B. H. & JONES, J. D. G. 1997. Novel Disease Resistance Specificities Result from Sequence Exchange between Tandemly Repeated Genes at the Cf-4/9 Locus of Tomato. *Cell,* 91**,** 821-832.

PEART, J. R., MESTRE, P., LU, R., MALCUIT, I. & BAULCOMBE, D. C. 2005. NRG1, a CC-NB-LRR Protein, together with N, a TIR-NB-LRR Protein, Mediates Resistance against Tobacco Mosaic Virus. *Current Biology,* 15**,** 968-973.

PRINCE, D. C., RALLAPALLI, G., XU, D. Y., SCHOONBEEK, H. J., CEVIK, V., ASAI, S., KEMEN, E., CRUZ-MIRELES, N., KEMEN, A., BELHAJ, K., SCHORNACK, S., KAMOUN, S., HOLUB, E. B., HALKIER, B. A. & JONES, J. D. G. 2017. Albugo-imposed changes to tryptophanderived antimicrobial metabolite biosynthesis may contribute to suppression of non- host resistance to Phytophthora infestans in Arabidopsis thaliana. *Bmc Biology,* 15**,** 22.

QUESADA-OCAMPO, L. M., GRANKE, L. L., MERCIER, M. R., OLSEN, J. & HAUSBECK, M. K. 2011. Investigating the Genetic Structure of Phytophthora capsici Populations. *Phytopathology®,* 101**,** 1061-1073.

RAIRDAN, G. J., COLLIER, S. M., SACCO, M. A., BALDWIN, T. T., BOETTRICH, T. & MOFFETT, P. 2008. The Coiled-Coil and Nucleotide Binding Domains of the Potato Rx Disease Resistance Protein Function in Pathogen Recognition and Signaling *The Plant Cell,* 20**,** 739-751.

RICHARD, M. M. S., GRATIAS, A., MEYERS, B. C. & GEFFROY, V. 2018. Molecular mechanisms that limit the costs of NLR-mediated resistance in plants. *Molecular Plant Pathology,* 19**,** 2516-2523.

SADOWY, E., JUSZCZUK, M., DAVID, C., GRONENBORN, B. & HULANICKA, M. D. 2001. Mutational analysis of the proteinase function of Potato leafroll virus. *J Gen Virol,* 82**,** 1517-1527.

SAKAI, T., MARTINEZ-ANAYA, C., CONTRERAS, M. P., KAMOUN, S., WU, C.-H. & ADACHI, H. 2023. The NRC0 gene cluster of sensor and helper NLR immune receptors is functionally conserved across asterid plants
. *bioRxiv***,** 2023.10.23.563533.

SALTOS, L. A., MONTEROS-ALTAMIRANO, Á., REIS, A. & GARCÉS-FIALLOS, F. R. 2022. Phytophthora capsici: the diseases it causes and management strategies to produce healthier vegetable crops. *Horticultura Brasileira,* 40.

SANOGO, S. & JI, P. 2012. Integrated management of Phytophthora capsici on solanaceous and cucurbitaceous crops: current status, gaps in knowledge and research needs. *Canadian Journal of Plant Pathology,* 34**,** 479-492.

SANOGO, S., LAMOUR, K., KOUSIK, S., LOZADA, D. N., PARADA ROJAS, C. H., QUESADA-OCAMPO, L., WYENANDT, C. A., BABADOOST, M., HAUSBECK, M. K., HANSEN, Z., ALI, E., MCGRATH, M., HU, J., CROSBY, K. & MILLER, S. A. 2022. Phytophthora capsici, 100 Years Later: Research Mile Markers from 1922 to 2022. *Phytopathology*.

SÄRKINEN, T., BARBOZA, G. E. & KNAPP, S. 2015. True Black nightshades: Phylogeny and delimitation of the Morelloid clade of Solanum. *TAXON,* 64**,** 945-958.

SÄRKINEN, T., POCZAI, P., BARBOZA, G. E., VAN DER WEERDEN, G. M., BADEN, M. & KNAPP, S. 2018. A revision of the Old World Black Nightshades (Morelloid clade of Solanum L., Solanaceae). *PhytoKeys***,** 1-223.

SARRIS, P. F., CEVIK, V., DAGDAS, G., JONES, J. D. G. & KRASILEVA, K. V. 2016. Comparative analysis of plant immune receptor architectures uncovers host proteins likely targeted by pathogens. *BMC Biology,* 14**,** 8.

SARRIS, P. F., DUXBURY, Z., HUH, S. U., MA, Y., SEGONZAC, C., SKLENAR, J., DERBYSHIRE, P., CEVIK, V., RALLAPALLI, G., SAUCET, S. B., WIRTHMUELLER, L., MENKE, F. L. H., SOHN, K. H. & JONES, J. D. G. 2015. A Plant Immune Receptor Detects Pathogen Effectors that Target WRKY Transcription Factors. *Cell,* 161**,** 1089-1100.

SAUR, I. M. L., PANSTRUGA, R. & SCHULZE-LEFERT, P. 2021. NOD-like receptor-mediated plant immunity: from structure to cell death. *Nature Reviews Immunology,* 21**,** 305-318.

SAVARY, S., WILLOCQUET, L., PETHYBRIDGE, S. J., ESKER, P., MCROBERTS, N. & NELSON, A. 2019. The global burden of pathogens and pests on major food crops. *Nature Ecology & Evolution,* 3**,** 430-439.

SAVENKOV, E. I. & VALKONEN, J. P. T. 2001. Potyviral Helper-Component Proteinase Expressed in Transgenic Plants Enhances Titers of Potato Leaf Roll Virus but Does Not Alleviate Its Phloem Limitation. *Virology,* 283**,** 285-293.

SCHORNACK, S., BALLVORA, A., GÜRLEBECK, D., PEART, J., GANAL, M., BAKER, B., BONAS, U. & LAHAYE, T. 2004. The tomato resistance protein Bs4 is a predicted non-nuclear TIR-NB-LRR protein that mediates defense responses to severely truncated derivatives of AvrBs4 and overexpressed AvrBs3. *The Plant Journal,* 37**,** 46-60.

SCHORNACK, S., PETER, K., BONAS, U. & LAHAYE, T. 2005. Expression levels of avrBs3-like genes affect recognition specificity in tomato Bs4- but not in pepper Bs3-mediated perception. *Mol Plant Microbe Interact,* 18**,** 1215-25.

SCHULTINK, A., QI, T., BALLY, J. & STASKAWICZ, B. 2019. Using forward genetics in Nicotiana benthamiana to uncover the immune signaling pathway mediating recognition of the Xanthomonas perforans effector XopJ4. *New Phytologist,* 221**,** 1001-1009.

SCHULTINK, A., QI, T., LEE, A., STEINBRENNER, A. D. & STASKAWICZ, B. 2017. Roq1 mediates recognition of the Xanthomonas and Pseudomonas effector proteins XopQ and HopQ1. *The Plant Journal,* 92**,** 787-795.

SCHULZE-LEFERT, P. & PANSTRUGA, R. 2011. A molecular evolutionary concept connecting nonhost resistance, pathogen host range, and pathogen speciation. *Trends Plant Sci,* 16**,** 117-25.

SCHWARTZ, A. R., MORBITZER, R., LAHAYE, T. & STASKAWICZ, B. J. 2017. TALE-induced bHLH transcription factors that activate a pectate lyase contribute to water soaking in bacterial spot of tomato. *Proc Natl Acad Sci U S A,* 114**,** E897-e903.

SEEHOLZER, S., TSUCHIMATSU, T., JORDAN, T., BIERI, S., PAJONK, S., YANG, W., JAHOOR, A., SHIMIZU, K. K., KELLER, B. & SCHULZE-LEFERT, P. 2010. Diversity at the Mla powdery mildew resistance locus from cultivated barley reveals sites of positive selection. *Mol Plant Microbe Interact,* 23**,** 497-509.

SEO, E., KIM, S., YEOM, S. I. & CHOI, D. 2016. Genome-Wide Comparative Analyses Reveal the Dynamic Evolution of Nucleotide-Binding Leucine-Rich Repeat Gene Family among Solanaceae Plants. *Front Plant Sci,* 7**,** 1205.

SEONG, K. & KRASILEVA, K. V. 2023. Prediction of effector protein structures from fungal phytopathogens enables evolutionary analyses. *Nature Microbiology,* 8**,** 174-187.

SEONG, K., SEO, E., WITEK, K., LI, M. & STASKAWICZ, B. 2020. Evolution of NLR resistance genes with noncanonical N-terminal domains in wild tomato species. *New Phytologist,* 227**,** 1530-1543.

SHEPARDSON, S., ESAU, K. & MCCRUM, R. 1980. Ultrastructure of potato leaf phloem infected with potato leafroll virus. *Virology,* 105**,** 379-392.

SHI, X., XIONG, Y., ZHANG, K., ZHANG, Y., ZHANG, J., ZHANG, L., XIAO, Y., WANG, G. L. & LIU, W. 2023. The ANIP1-OsWRKY62 module regulates both basal defense and Pi9-mediated immunity against Magnaporthe oryzae in rice. *Mol Plant,* 16**,** 739-755.

SINDHU, A., CHINTAMANANI, S., BRANDT, A. S., ZANIS, M., SCOFIELD, S. R. & JOHAL, G. S. 2008. A guardian of grasses: specific origin and conservation of a unique disease-resistance gene in the grass lineage. *Proc Natl Acad Sci U S A,* 105**,** 1762-7.

SOBCZAK, M., AVROVA, A., JUPOWICZ, J., PHILLIPS, M., ERNST, K. & KUMAR, A. 2005. Characterization of Susceptibility and Resistance Responses to Potato Cyst Nematode (Globodera spp.) Infection of Tomato Lines in the Absence and Presence of the Broad-Spectrum Nematode Resistance Hero Gene. *Molecular plant-microbe interactions : MPMI,* 18**,** 158-68.

SOHN, K. H., ZHANG, Y. & JONES, J. D. G. 2009. The Pseudomonas syringae effector protein, AvrRPS4, requires in planta processing and the KRVY domain to function. *The Plant Journal,* 57**,** 1079-1091.

STAAL, J., KALIFF, M., DEWAELE, E., PERSSON, M. & DIXELIUS, C. 2008. RLM3, a TIR domain encoding gene involved in broad-range immunity of Arabidopsis to necrotrophic fungal pathogens. *The Plant Journal,* 55**,** 188-200.

STAHL, E. A., DWYER, G., MAURICIO, R., KREITMAN, M. & BERGELSON, J. 1999. Dynamics of disease resistance polymorphism at the Rpm1 locus of Arabidopsis. *Nature,* 400**,** 667-671.

STAJICH, J. E., VU, A. L., JUDELSON, H. S., VOGEL, G. M., GORE, M. A., CARLSON, M. O., DEVITT, N., JACOBI, J., MUDGE, J., LAMOUR, K. H. & SMART, C. D. 2021. High-Quality Reference Genome Sequence for the Oomycete Vegetable

Pathogen Phytophthora capsici Strain LT1534. *Microbiology Resource Announcements,* 10**,** 10.1128/mra.00295-21.
STEINBRENNER, A. D., GORITSCHNIG, S. & STASKAWICZ, B. J. 2015. Recognition and Activation Domains Contribute to Allele-Specific Responses of an Arabidopsis NLR Receptor to an Oomycete Effector Protein. *PLOS Pathogens,* 11**,** e1004665.
STEUERNAGEL, B., JUPE, F., WITEK, K., JONES, J. D. G. & WULFF, B. B. H. 2015. NLR-parser: rapid annotation of plant NLR complements. *Bioinformatics,* 31**,** 1665-1667.
STRUGALA, R., DELVENTHAL, R. & SCHAFFRATH, U. 2015. An organ-specific view on non-host resistance. *Front Plant Sci,* 6**,** 526.
STUKENBROCK, E. H. 2016. The Role of Hybridization in the Evolution and Emergence of New Fungal Plant Pathogens. *Phytopathology,* 106**,** 104-12.
SULTANA, S. & ALAM, S. 2007. Differential Fluorescent Chromosome Banding of Solanum nigrum L. and Solanum villosum L. from Bangladesh. *Cytologia - CYTOLOGIA TOKYO,* 72**,** 213-219.
SUTHERLAND, C. A., PRIGOZHIN, D. M., MONROE, J. G. & KRASILEVA, K. V. 2023. High intraspecies allelic diversity in Arabidopsis NLR immune receptors is associated with distinct genomic and epigenomic features. *bioRxiv*.
TAI, T. H., DAHLBECK, D., CLARK, E. T., GAJIWALA, P., PASION, R., WHALEN, M. C., STALL, R. E. & STASKAWICZ, B. J. 1999. Expression of the Bs2 pepper gene confers resistance to bacterial spot disease in tomato. *Proceedings of the National Academy of Sciences,* 96**,** 14153-14158.
TAKAHASHI, H., MILLER, J., NOZAKI, Y., TAKEDA, M., SHAH, J., HASE, S., IKEGAMI, M., EHARA, Y. & DINESH-KUMAR, S. P. 2002. RCY1, an Arabidopsis thaliana RPP8/HRT family resistance gene, conferring resistance to cucumber mosaic virus requires salicylic acid, ethylene and a novel signal transduction mechanism. *Plant J,* 32**,** 655-67.
TAKKEN, F. L., ALBRECHT, M. & TAMELING, W. I. 2006. Resistance proteins: molecular switches of plant defence. *Curr Opin Plant Biol,* 9**,** 383-90.
TAMADA, T. & KONDO, H. 2013. Biological and genetic diversity of plasmodiophorid-transmitted viruses and their vectors. *Journal of General Plant Pathology,* 79**,** 307-320.
TAMBORSKI, J., SEONG, K., LIU, F., STASKAWICZ, B. & KRASILEVA, K., V. 2022. Engineering of Sr33 and Sr50 plant immune receptors to alter recognition specificity and autoactivity. *bioRxiv***,** 2022.03.05.483131.
TAMELING, W. I. L., VOSSEN, J. H., ALBRECHT, M., LENGAUER, T., BERDEN, J. A., HARING, M. A., CORNELISSEN, B. J. C. & TAKKEN, F. L. W. 2006. Mutations in the NB-ARC Domain of I-2 That Impair ATP Hydrolysis Cause Autoactivation. *Plant Physiology,* 140**,** 1233-1245.
TANG, B., FENG, L., HULIN, M. T., DING, P. & MA, W. 2023. Cell-type-specific responses to fungal infection in plants revealed by single-cell transcriptomics. *Cell Host Microbe,* 31**,** 1732-1747.e5.
TARR, D. E. & ALEXANDER, H. M. 2009. TIR-NBS-LRR genes are rare in monocots: evidence from diverse monocot orders. *BMC Res Notes,* 2**,** 197.
TENTHOREY, J. L., HALOUPEK, N., LÓPEZ-BLANCO, J. R., GROB, P., ADAMSON, E., HARTENIAN, E., LIND, N. A., BOURGEOIS, N. M., CHACÓN, P., NOGALES, E. &

VANCE, R. E. 2017. The structural basis of flagellin detection by NAIP5: A strategy to limit pathogen immune evasion. *Science,* 358**,** 888-893.
TERAUCHI, R. & YOSHIDA, K. 2010. Towards population genomics of effector–effector target interactions. *New Phytologist,* 187**,** 929-939.
THILLIEZ, G. J. A., ARMSTRONG, M. R., LIM, T. Y., BAKER, K., JOUET, A., WARD, B., VAN OOSTERHOUT, C., JONES, J. D. G., HUITEMA, E., BIRCH, P. R. J. & HEIN, I. 2019. Pathogen enrichment sequencing (PenSeq) enables population genomic studies in oomycetes. *New Phytologist,* 221**,** 1634-1648.
THORDAL-CHRISTENSEN, H., BIRCH, P. R. J., SPANU, P. D. & PANSTRUGA, R. 2018. Why did filamentous plant pathogens evolve the potential to secrete hundreds of effectors to enable disease? *Mol Plant Pathol,* 19**,** 781-785.
TIAN, D., TRAW, M. B., CHEN, J. Q., KREITMAN, M. & BERGELSON, J. 2003. Fitness costs of R-gene-mediated resistance in Arabidopsis thaliana. *Nature,* 423**,** 74-77.
TORRES ASCURRA, Y. C., ZHANG, L., TOGHANI, A., HUA, C., RANGEGOWDA, N. J., POSBEYIKIAN, A., PAI, H., LIN, X., WOLTERS, P. J., WOUTERS, D., DE BLOK, R., STEIGENGA, N., PAILLART, M. J. M., VISSER, R. G. F., KAMOUN, S., NÜRNBERGER, T. & VLEESHOUWERS, V. G. A. A. 2023. Functional diversification of a wild potato immune receptor at its center of origin. *Science,* 381**,** 891-897.
TURNBULL, D., WANG, H., BREEN, S., MALEC, M., NAQVI, S., YANG, L., WELSH, L., HEMSLEY, P., ZHENDONG, T., BRUNNER, F., GILROY, E. M. & BIRCH, P. R. J. 2019. AVR2 Targets BSL Family Members, Which Act as Susceptibility Factors to Suppress Host Immunity. *Plant Physiology,* 180**,** 571-581.
VAN DE WEYER, A.-L., MONTEIRO, F., FURZER, O. J., NISHIMURA, M. T., CEVIK, V., WITEK, K., JONES, J. D. G., DANGL, J. L., WEIGEL, D. & BEMM, F. 2019. A Species-Wide Inventory of NLR Genes and Alleles in Arabidopsis thaliana. *Cell,* 178**,** 1260-1272.e14.
VAN DER BIEZEN, E. A. & JONES, J. D. G. 1998. The NB-ARC domain: a novel signalling motif shared by plant resistance gene products and regulators of cell death in animals. *Current Biology,* 8**,** R226-R228.
VAN DER VOSSEN, E. A., GROS, J., SIKKEMA, A., MUSKENS, M., WOUTERS, D., WOLTERS, P., PEREIRA, A. & ALLEFS, S. 2005. The Rpi-blb2 gene from Solanum bulbocastanum is an Mi-1 gene homolog conferring broad-spectrum late blight resistance in potato. *Plant J,* 44**,** 208-22.
VAN ESSE, H. P., REUBER, T. L. & VAN DER DOES, D. 2020. Genetic modification to improve disease resistance in crops. *New Phytologist,* 225**,** 70-86.
VAN KEMPEN, M., KIM, S. S., TUMESCHEIT, C., MIRDITA, M., GILCHRIST, C. L. M., SÖDING, J. & STEINEGGER, M. 2022. Foldseek: fast and accurate protein structure search. *bioRxiv***,** 2022.02.07.479398.
VEGA-ARREGUIN, J. C., SHIMADA-BELTRAN, H., SEVILLANO-SERRANO, J. & MOFFETT, P. 2017. Non-host Plant Resistance against Phytophthora capsici Is Mediated in Part by Members of the I2 R Gene Family in Nicotiana spp. *Frontiers in Plant Science,* 8**,** 11.
VEGA-SÁNCHEZ, M. E., ERSELIUS, L. J., RODRIGUEZ, A. M., BASTIDAS, O., HOHL, H. R., OJIAMBO, P. S., MUKALAZI, J., VERMEULEN, T., FRY, W. E. & FORBES, G. A. 2000. Host adaptation to potato and tomato within the US−1 clonal

lineage of Phytophthora infestans in Uganda and Kenya. *Plant Pathology,* 49**,** 531-539.
VELASQUEZ, A. C., MIHOVILOVICH, E. & BONIERBALE, M. 2007. Genetic characterization and mapping of major gene resistance to potato leafroll virus in Solanumtuberosum ssp. andigena. *Theor Appl Genet,* 114**,** 1051-8.
VERCAUTEREN, A., BOUTET, X., D'HONDT, L., VAN BOCKSTAELE, E., MAES, M., LEUS, L., CHANDELIER, A. & HEUNGENS, K. 2011. Aberrant genome size and instability of Phytophthora ramorum oospore progenies. *Fungal Genetics and Biology,* 48**,** 537-543.
VLEESHOUWERS, V. G., RAFFAELE, S., VOSSEN, J. H., CHAMPOURET, N., OLIVA, R., SEGRETIN, M. E., RIETMAN, H., CANO, L. M., LOKOSSOU, A., KESSEL, G., PEL, M. A. & KAMOUN, S. 2011. Understanding and exploiting late blight resistance in the age of effectors. *Annu Rev Phytopathol,* 49**,** 507-31.
WANG, G., ROUX, B., FENG, F., GUY, E., LI, L., LI, N., ZHANG, X., LAUTIER, M., JARDINAUD, M. F., CHABANNES, M., ARLAT, M., CHEN, S., HE, C., NOËL, L. D. & ZHOU, J. M. 2015a. The Decoy Substrate of a Pathogen Effector and a Pseudokinase Specify Pathogen-Induced Modified-Self Recognition and Immunity in Plants. *Cell Host Microbe,* 18**,** 285-95.
WANG, H., OLIVEIRA-GARCIA, E., BOEVINK, P. C., TALBOT, N. J., BIRCH, P. R. J. & VALENT, B. 2023a. Filamentous pathogen effectors enter plant cells via endocytosis. *Trends in Plant Science,* 28**,** 1214-1217.
WANG, H., WANG, S., WANG, W., XU, L., WELSH, L. R. J., GIERLINSKI, M., WHISSON, S. C., HEMSLEY, P. A., BOEVINK, P. C. & BIRCH, P. R. J. 2023b. Uptake of oomycete RXLR effectors into host cells by clathrin-mediated endocytosis. *The Plant Cell,* 35**,** 2504-2526.
WANG, J., HU, M., WANG, J., QI, J., HAN, Z., WANG, G., QI, Y., WANG, H. W., ZHOU, J. M. & CHAI, J. 2019a. Reconstitution and structure of a plant NLR resistosome conferring immunity. *Science,* 364.
WANG, J., WANG, J., HU, M., WU, S., QI, J., WANG, G., HAN, Z., QI, Y., GAO, N., WANG, H. W., ZHOU, J. M. & CHAI, J. 2019b. Ligand-triggered allosteric ADP release primes a plant NLR complex. *Science,* 364.
WANG, K.-D., DUGHBAJ, M. A., NGUYEN, T. T. V., NGUYEN, T. Q. Y., OZA, S., VALDEZ, K., ANDA, P., WALTZ, J. & SACCO, M. A. 2023c. Systematic mutagenesis of Polerovirus protein P0 reveals distinct and overlapping amino acid functions in Nicotiana glutinosa. *Virology,* 578**,** 24-34.
WANG, K.-D., EMPLEO, R., NGUYEN, T. T. V., MOFFETT, P. & SACCO, M. A. 2015b. Elicitation of hypersensitive responses in Nicotiana glutinosa by the suppressor of RNA silencing protein P0 from poleroviruses. *Molecular Plant Pathology,* 16**,** 435-448.
WANG, M.-Y., CHEN, J.-B., WU, R., GUO, H.-L., CHEN, Y., LI, Z.-J., WEI, L.-Y., LIU, C., HE, S.-F., DU, M.-D., GUO, Y.-L., PENG, Y.-L., JONES, J. D. G., WEIGEL, D., HUANG, J.-H. & ZHU, W.-S. 2023d. The plant immune receptor SNC1 monitors helper NLRs targeted by a bacterial effector. *Cell Host & Microbe,* 31**,** 1792-1803.e7.
WANG, S., VETUKURI, R. R., KUSHWAHA, S. K., HEDLEY, P. E., MORRIS, J., STUDHOLME, D. J., WELSH, L. R. J., BOEVINK, P. C., BIRCH, P. R. J. & WHISSON, S. C. 2021. Haustorium formation and a distinct biotrophic

transcriptome characterize infection of Nicotiana benthamiana by the tree pathogen Phytophthora kernoviae. *Molecular Plant Pathology,* 22**,** 954-968.
WANG, S., WELSH, L., THORPE, P., WHISSON, S. C., BOEVINK, P. C. & BIRCH, P. R. J. 2018. The Phytophthora infestans Haustorium Is a Site for Secretion of Diverse Classes of Infection-Associated Proteins. *mBio,* 9.
WAWRA, S., TRUSCH, F., MATENA, A., APOSTOLAKIS, K., LINNE, U., ZHUKOV, I., STANEK, J., KOŹMIŃSKI, W., DAVIDSON, I., SECOMBES, C. J., BAYER, P. & VAN WEST, P. 2017. The RxLR Motif of the Host Targeting Effector AVR3a of Phytophthora infestans Is Cleaved before Secretion. *Plant Cell,* 29**,** 1184-1195.
WEI, H. L., CHAKRAVARTHY, S., MATHIEU, J., HELMANN, T. C., STODGHILL, P., SWINGLE, B., MARTIN, G. B. & COLLMER, A. 2015. Pseudomonas syringae pv. tomato DC3000 Type III Secretion Effector Polymutants Reveal an Interplay between HopAD1 and AvrPtoB. *Cell Host Microbe,* 17**,** 752-62.
WHISSON, S. C., BOEVINK, P. C., MOLELEKI, L., AVROVA, A. O., MORALES, J. G., GILROY, E. M., ARMSTRONG, M. R., GROUFFAUD, S., VAN WEST, P., CHAPMAN, S., HEIN, I., TOTH, I. K., PRITCHARD, L. & BIRCH, P. R. J. 2007. A translocation signal for delivery of oomycete effector proteins into host plant cells. *Nature,* 450**,** 115-118.
WITEK, K., JUPE, F., WITEK, A. I., BAKER, D., CLARK, M. D. & JONES, J. D. G. 2016. Accelerated cloning of a potato late blight-resistance gene using RenSeq and SMRT sequencing. *Nature Biotechnology,* 34**,** 656-660.
WITEK, K., LIN, X., KARKI, H. S., JUPE, F., WITEK, A. I., STEUERNAGEL, B., STAM, R., VAN OOSTERHOUT, C., FAIRHEAD, S., HEAL, R., COCKER, J. M., BHANVADIA, S., BARRETT, W., WU, C. H., ADACHI, H., SONG, T., KAMOUN, S., VLEESHOUWERS, V., TOMLINSON, L., WULFF, B. B. H. & JONES, J. D. G. 2021. A complex resistance locus in Solanum americanum recognizes a conserved Phytophthora effector. *Nat Plants,* 7**,** 198-208.
WOOD, K. J., NUR, M., GIL, J., FLETCHER, K., LAKEMAN, K., GANN, D., GOTHBERG, A., KHUU, T., KOPETZKY, J., NAQVI, S., PANDYA, A., ZHANG, C., MAISONNEUVE, B., PEL, M. & MICHELMORE, R. 2020. Effector prediction and characterization in the oomycete pathogen Bremia lactucae reveal host-recognized WY domain proteins that lack the canonical RXLR motif. *PLOS Pathogens,* 16**,** e1009012.
WORLD HEALTH ORGANIZATION 2022. *The State of Food Security and Nutrition in the World 2022: Repurposing food and agricultural policies to make healthy diets more affordable*, Food & Agriculture Org.
WU, C.-H. & DEREVNINA, L. 2023. The battle within: How pathogen effectors suppress NLR-mediated immunity. *Current Opinion in Plant Biology,* 74**,** 102396.
WU, C. H., ABD-EL-HALIEM, A., BOZKURT, T. O., BELHAJ, K., TERAUCHI, R., VOSSEN, J. H. & KAMOUN, S. 2017. NLR network mediates immunity to diverse plant pathogens. *Proc Natl Acad Sci U S A,* 114**,** 8113-8118.
WU, C. H., BELHAJ, K., BOZKURT, T. O., BIRK, M. S. & KAMOUN, S. 2016. Helper NLR proteins NRC2a/b and NRC3 but not NRC1 are required for Pto-mediated cell death and resistance in Nicotiana benthamiana. *New Phytol,* 209**,** 1344-52.

WU, Y., LI, D., HU, Y., LI, H., RAMSTEIN, G. P., ZHOU, S., ZHANG, X., BAO, Z., ZHANG, Y., SONG, B., ZHOU, Y., ZHOU, Y., GAGNON, E., SÄRKINEN, T., KNAPP, S., ZHANG, C., STÄDLER, T., BUCKLER, E. S. & HUANG, S. 2023. Phylogenomic discovery of deleterious mutations facilitates hybrid potato breeding. *Cell,* 186**,** 2313-2328.e15.

YAN, X., TANG, B., RYDER, L. S., MACLEAN, D., WERE, V. M., ESEOLA, A. B., CRUZ-MIRELES, N., MA, W., FOSTER, A. J., OSÉS-RUIZ, M. & TALBOT, N. J. 2023. The transcriptional landscape of plant infection by the rice blast fungus Magnaporthe oryzae reveals distinct families of temporally co-regulated and structurally conserved effectors. *The Plant Cell,* 35**,** 1360-1385.

YANG, S., ZHANG, X., YUE, J.-X., TIAN, D. & CHEN, J.-Q. 2008. Recent duplications dominate NBS-encoding gene expansion in two woody species. *Molecular Genetics and Genomics,* 280**,** 187-198.

YIN, J., GU, B., HUANG, G., TIAN, Y., QUAN, J., LINDQVIST-KREUZE, H. & SHAN, W. 2017. Conserved RXLR Effector Genes of Phytophthora infestans Expressed at the Early Stage of Potato Infection Are Suppressive to Host Defense. *Front Plant Sci,* 8**,** 2155.

YOSHIDA, K., SCHUENEMANN, V. J., CANO, L. M., PAIS, M., MISHRA, B., SHARMA, R., LANZ, C., MARTIN, F. N., KAMOUN, S., KRAUSE, J., THINES, M., WEIGEL, D. & BURBANO, H. A. 2013. The rise and fall of the Phytophthora infestans lineage that triggered the Irish potato famine. *Elife,* 2**,** e00731.

YUAN, M., JIANG, Z., BI, G., NOMURA, K., LIU, M., WANG, Y., CAI, B., ZHOU, J.-M., HE, S. Y. & XIN, X.-F. 2021. Pattern-recognition receptors are required for NLR-mediated plant immunity. *Nature,* 592**,** 105-109.

ZADOKS, J. C. 2008. The Potato Murrain on the European Continent and the Revolutions of 1848. *Potato Research,* 51**,** 5-45.

ZDRZAŁEK, R., STONE, C., DE LA CONCEPCION, J. C., BANFIELD, M. J. & BENTHAM, A. R. 2023. Pathways to engineering plant intracellular NLR immune receptors. *Current Opinion in Plant Biology,* 74**,** 102380.

ZHAI, K., DENG, Y., LIANG, D., TANG, J., LIU, J., YAN, B., YIN, X., LIN, H., CHEN, F., YANG, D., XIE, Z., LIU, J.-Y., LI, Q., ZHANG, L. & HE, Z. 2019. RRM Transcription Factors Interact with NLRs and Regulate Broad-Spectrum Blast Resistance in Rice. *Molecular Cell,* 74**,** 996-1009.e7.

ZHAI, K., LIANG, D., LI, H., JIAO, F., YAN, B., LIU, J., LEI, Z., HUANG, L., GONG, X., WANG, X., MIAO, J., WANG, Y., LIU, J. Y., ZHANG, L., WANG, E., DENG, Y., WEN, C. K., GUO, H., HAN, B. & HE, Z. 2022. NLRs guard metabolism to coordinate pattern- and effector-triggered immunity. *Nature,* 601**,** 245-251.

ZHANG, P., JIA, Y., SHI, J., CHEN, C., YE, W., WANG, Y., MA, W. & QIAO, Y. 2019. The WY domain in the Phytophthora effector PSR1 is required for infection and RNA silencing suppression activity. *New Phytologist,* 223**,** 839-852.

ZHAO, T., RUI, L., LI, J., NISHIMURA, M. T., VOGEL, J. P., LIU, N., LIU, S., ZHAO, Y., DANGL, J. L. & TANG, D. 2015. A Truncated NLR Protein, TIR-NBS2, Is Required for Activated Defense Responses in the exo70B1 Mutant. *PLOS Genetics,* 11**,** e1004945.

ZHAO, Y.-B., LIU, M.-X., CHEN, T.-T., MA, X., LI, Z.-K., ZHENG, Z., ZHENG, S.-R., CHEN, L., LI, Y.-Z., TANG, L.-R., CHEN, Q., WANG, P. & OUYANG, S. 2022. Pathogen

effector AvrSr35 triggers Sr35 resistosome assembly via a direct recognition mechanism. *Science Advances,* 8**,** eabq5108.

ZHENG, X., MCLELLAN, H., FRAITURE, M., LIU, X., BOEVINK, P. C., GILROY, E. M., CHEN, Y., KANDEL, K., SESSA, G., BIRCH, P. R. & BRUNNER, F. 2014. Functionally redundant RXLR effectors from Phytophthora infestans act at different steps to suppress early flg22-triggered immunity. *PLoS Pathog,* 10**,** e1004057.

ZIMNOCH-GUZOWSKA, E., LEBECKA, R., KRYSZCZUK, A., MACIEJEWSKA, U., SZCZERBAKOWA, A. & WIELGAT, B. 2003. Resistance to Phytophthora infestans in somatic hybrids of Solanum nigrum L. and diploid potato. *Theoretical and Applied Genetics,* 107**,** 43-48.

Appendices

Appendix 1. PLRV sequences used in this project. The names and accession numbers for each of the 22 PLRV genomic sequences used in this chapter. The table also contains the URL to access each of these sequences.

Strain ID	Accession number	Link
Potato leafroll virus strain Zim13	AF453388.1	https://www.ncbi.nlm.nih.gov/nuccore/18656700
Potato leafroll virus strain OP	AF453389.1	https://www.ncbi.nlm.nih.gov/nuccore/AF453389.1
Potato leafroll virus strain Noir	AF453390.1	https://www.ncbi.nlm.nih.gov/nuccore/AF453390.1
Potato leafroll virus strain Fr1	AF453391.1	https://www.ncbi.nlm.nih.gov/nuccore/AF453391.1
Potato leafroll virus strain CU87	AF453393.1	https://www.ncbi.nlm.nih.gov/nuccore/AF453393.1
Potato leafroll virus strain 14.2	AF453394.1	https://www.ncbi.nlm.nih.gov/nuccore/AF453394.1
Potato leafroll virus isolate JPI-1	JQ420901.1	https://www.ncbi.nlm.nih.gov/nuccore/JQ420901.1
Potato leafroll virus isolate OTNI-2	JQ420904.1	https://www.ncbi.nlm.nih.gov/nuccore/JQ420904.1
Potato leafroll virus isolate PLRV-IM	KC456052.1	https://www.ncbi.nlm.nih.gov/nuccore/KC456052.1
Potato leafroll virus isolate PLRV-HB	KC456053.1	https://www.ncbi.nlm.nih.gov/nuccore/KC456053.1
Potato leafroll virus isolate PLRV-YN	KC456054.1	https://www.ncbi.nlm.nih.gov/nuccore/KC456054.1
Potato leafroll virus	KP090166.1	https://www.ncbi.nlm.nih.gov/nuccore/KP090166.1
Potato leafroll virus strain GAF318-4.2	KU586454.1	https://www.ncbi.nlm.nih.gov/nuccore/KU586454.1
Potato leafroll virus strain GAF318-8	KU586455.1	https://www.ncbi.nlm.nih.gov/nuccore/KU586455.1
Potato leafroll virus strain GAF318-13	KU586456.1	https://www.ncbi.nlm.nih.gov/nuccore/KU586456.1
Potato leafroll virus isolate Antioquia	KX712226.1	https://www.ncbi.nlm.nih.gov/nuccore/KX712226.1
Potato leafroll virus isolate PLRV-AR	KY856831.1	https://www.ncbi.nlm.nih.gov/nuccore/KY856831.1
Potato leafroll virus isolate EP	MF062487.1	https://www.ncbi.nlm.nih.gov/nuccore/MF062487.1
Potato leafroll virus isolate PLRV165	MG356502.1	https://www.ncbi.nlm.nih.gov/nuccore/MG356502.1
Potato leafroll virus isolate PLRV184	MG356504.1	https://www.ncbi.nlm.nih.gov/nuccore/MG356504.1
Potato leafroll virus isolate PLV-W13-136	MH937415.1	https://www.ncbi.nlm.nih.gov/nuccore/MH937415.1
Potato leafroll virus isolate Antioquia/May4	MK613996.1	https://www.ncbi.nlm.nih.gov/nuccore/MK613996.1

Appendix 2. Polerovirus genomes used in this project. The names, abbreviations, and accession numbers for each of the 9 polerovirus genomes used in this chapter. The table also contains the URL to access each of these sequences. PLRV strains are not included but are shown in Appendix 1.

Strain ID	Abbreviated to	Accession number	Accessible from
Beet mild yellowing virus isolate IPP	BMYV	DQ132996.1	https://www.ncbi.nlm.nih.gov/nuccore/DQ132996
Cucurbit aphid-borne yellows virus	CaBYV	EU000535.1	https://www.ncbi.nlm.nih.gov/nuccore/EU000535
Pepper vein yellows virus isolate HN	PeVYV	KP326573.1	https://www.ncbi.nlm.nih.gov/nuccore/KP326573
Turnip yellows virus isolate Landkreis Meissen_17	TuYV	MN497810.1	https://www.ncbi.nlm.nih.gov/nuccore/MN497810.1
Chickpea chlorotic stunt virus	CpCSV	NC_008249.1	https://www.ncbi.nlm.nih.gov/nuccore/NC_008249
Wheat yellow dwarf virus-GPV	WYDV	NC_012931.1	https://www.ncbi.nlm.nih.gov/nuccore/NC_012931
Cotton leafroll dwarf virus	CLRDV	NC_014545.1	https://www.ncbi.nlm.nih.gov/nuccore/NC_014545
Maize yellow dwarf virus-RMV	MYDV	NC_021484.1	https://www.ncbi.nlm.nih.gov/nuccore/NC_021484
Tobacco virus 2	TV2	NC_034265.1	https://www.ncbi.nlm.nih.gov/nuccore/NC_034265

Appendix 3. Enamovirus sequences used in this chapter. The names, accession numbers and abbreviations used in the thesis for each of the enamovirus genomic sequences used in this chapter. The table also contains the URL to access each of these sequences.

Strain ID	Abbreviated to	Accession number	Accessible from
Grapevine enamovirus-1 isolate SE-BR	GEV-1	NC_034836.1	https://www.ncbi.nlm.nih.gov/nuccore/NC_034836.1
Citrus vein enation virus, isolate VE-1	CVEV	NC_021564.1	https://www.ncbi.nlm.nih.gov/nuccore/NC_021564
Pea enation mosaic virus-1	PEMV	NC_003629.1	https://www.ncbi.nlm.nih.gov/nuccore/NC_003629

Appendix 4. *Solanum villosum* accessions used in this project. Nine *S. villosum* accessions were available to use in this project. IPK (IPK, Gatersleben Germany).

Seed packet ID	Collected from	Original ID	Resistant to *P. capsici*?
SP3056	IPK	SOLA 261	Susceptible
SP3057	IPK	SOLA 262	Resistant
SP3058	IPK	SOLA 273	Susceptible
SP3059	IPK	SOLA 264	Susceptible
SP3060	IPK	SOLA 267	Susceptible
SP3061	IPK	SOLA 270	Susceptible
SP3062	IPK	SOLA 273	Susceptible
SP3063	IPK	SOLA 274	Susceptible
SP3065	IPK	SOLA 405	Resistant

Appendix 5. *Solanum scabrum* accessions used in this project. Four *S. scabrum* accessions were available to use in this project. IPK (IPK, Gatersleben Germany).

Seed packet ID	Collected from	Original ID	Resistant to *P. capsici*?
SP3066	IPK	SOLA 28	Susceptible
SP3067	IPK	SOLA 201	Susceptible
SP3068	IPK	SOLA 283	Susceptible
SP3069	IPK	SOLA 402	Susceptible